Enzo Silvestri
Alessandro Muda
Davide Orlandi

Ultrasound Anatomy of Lower Limb Muscles

A Practical Guide

Foreword by
Nicola Maffulli

Springer

Ultrasound Anatomy of Lower Limb Muscles

Enzo Silvestri • Alessandro Muda
Davide Orlandi

Ultrasound Anatomy of Lower Limb Muscles

A Practical Guide

Foreword by Nicola Maffulli

Springer

Enzo Silvestri
Struttura Complessa di Diagnostica per Immagini ed Ecografia Interventistica
Ospedale Evangelico Internazionale
Genoa
Italy

Davide Orlandi
Dipartimento di Radiologia
Università degli studi di Genova
Genoa
Italy

Alessandro Muda
Dipartimento di Radiologia
IRCCS Ospedale San Martino IST
Genoa
Italy

ISBN 978-3-319-09479-3 ISBN 978-3-319-09480-9 (eBook)
DOI 10.1007/978-3-319-09480-9
Springer Cham Heidelberg New York Dordrecht London

Library of Congress Control Number: 2014954746

Printed on acid-free paper

Springer is part of Springer Science+Business Media (www.springer.com)

Foreword

The principles of musculoskeletal medicine have been established centuries ago, and serve us well. The 'look, feel move' paradigm is engrained in our psyche. It allows us to be efficient and effective, and guides accurate diagnosis and appropriate management. Nevertheless, to be accurate and effective, at times we need to extend the reach of our senses, and make sure that we have more objective elements to formulate a diagnosis, and to objectively assess whether our proposed management is working.

Ultrasonography has come to the forefront in the last few years: it is non-invasive, it is widely available, it has reached a level of image quality and a sophistication in techniques that allows a resolution of less that 2 mm, and it is relatively cheap. It has been criticised for being operator-dependent. This is partially true, but standardisation of imaging techniques and of reporting styles minimizes this latter concern. Health care professionals need to be trained in ultrasonography: it requires time, and to become experienced, errors have to be made, and cherished. Therefore, Drs. Silvestri, Muda, and Orlandi should be congratulated for several reasons: they have had the foresight of putting together a text which can be used as baseline for reference and teaching; they have succeeded in recruiting a whole series of authors who are at the forefront in this field; and, last but not least, they have produced for themselves perpetual work: advances in this field will require themselves and their authors to continue to update their knowledge, and put it forward to the readers.

I expect that my own copy will be well thumbed: one never ends learning in our field, and *Ultrasound Anatomy of Lower Limb Muscles: A Practical Guide* makes it topical and pleasant.

Enjoy it!

London, UK N. Maffulli

Contents

Part III Leg Muscles

Part IV Sectional Anatomical Tables

Part I

Basic Principles of Muscles Ultrasound

US Basic Principles

1

Silvia Perugin Bernardi, Alice Arcidiacono, and Enzo Silvestri

Ultrasonography (US) is a well-established tomographic technique capable of providing a real-time representation of each human body structure, including moving structures.

US clinical applications are continuously increasing thanks to its high sensitivity and image resolution, quickness, safety, portability and cost-effectiveness.

In the past decade, US become the referential imaging modality in the first-level study of the soft-tissue components of the musculoskeletal system. Recent technological innovations improved image quality, reducing artefacts, and made possible the precise and accurate evaluation of almost all soft-tissue structures. Rapid advances in transducer technology (broadband and high-definition probes), development of tissue harmonic imaging (THI) systems, new dedicated software and reconstruction algorithms (compound imaging, steering-based imaging, extended field-of-view imaging, three-dimensional imaging, sonoelastography), together with the possibility of a dynamic analysis of tendinous and muscular structures, resulted in increased diagnostic performances and opened new field of applications in the musculoskeletal area of interest.

In particular, the extended field-of-view imaging has overcome one of the main disadvantages of linear-array probes: the limited extension of the field-of-view (FOV often <4 cm wide) in imaging the soft tissues of the musculoskeletal system. With these transducers, displaying the full extent of a lesion and showing its relationship with adjacent anatomical structures on a single image may be problematic: this creates inadequate reproduction of the full lesion with consequent difficulties for colleagues when reading the US images. Extended field-of-view technology uses specific image registration analysis to track probe motion and reconstruct a large composite image during real-time scanning over long distances and curved body surfaces without using external positional devices. After selecting a scanning plane of interest, the examiner slides the linear probe along the skin surface in the direction of the scan plane while monitoring the image on the screen. During lateral probe motion, there is an advancing real-time portion of the image and a static portion, which displays what has been scanned. Especially in the evaluation of the musculoskeletal system,

S. Perugin Bernardi • A. Arcidiacono
Dipartimento di Radiologia,
Università degli studi di Genova, Genoa, Italy
e-mail: silvia.perugin@gmail.com;
alice.arcidiacono@hotmail.com

E. Silvestri (✉)
Struttura Complessa di Diagnostica per Immagini ed Ecografia Interventistica, Ospedale Evangelico Internazionale, Genoa, Italy
e-mail: silvi.enzo@gmail.com

E. Silvestri et al., *Ultrasound Anatomy of Lower Limb Muscles: A Practical Guide*,
DOI 10.1007/978-3-319-09480-9_1, © Springer International Publishing Switzerland 2015

extended field-of-view technique is an important diagnostic tool because it provides a panoramic representation of a lot of abnormalities such as large fluid collections, muscle injuries and tumours, in association with the appropriate landmarks (joints, tendons and muscles) which may even be remote from the structure of interest.

In addition, it is important to highlight that US imaging has acquired a central role, not only in diagnostic phase, but also as an important guide for therapeutic manoeuvres such as biopsies of soft-tissue masses (avoiding nerves and vessels), articular and periarticular infiltrative procedures, drainage of fluid collections and muscular haematomas.

As US examination is relatively operator dependent, it presumes a good knowledge of the physical principles on which it bases on and the technical properties of the available equipment.

Focus On

Sound waves are mechanical pressure waves, produced by a disturbance source, that induce vibration of the particles of the material. Each particle swings, moving small distances from its rest position, so the vibrational energy is propagated from particle to particle as a wave travelling through the medium. On the basis of their relationship to the propagation direction of energy, sound waves are classified as being longitudinal or transverse waves, if the particles vibrate in the same direction or perpendicular to the propagation, respectively. Longitudinal waves are typically observed in soft tissues and liquids; the compact bone is the only tissue capable of supporting transverse sound waves.

1.1 Ultrasound Wave Properties

Ultrasonography is based on the use of acoustic waves belong to the ultrasounds band. Ultrasounds are sounds possessing high frequencies, considerably higher than the human hearing range (>20 kHz).

Ultrasound waves propagate in the human body thanks to the elastic forces existing between the adjacent molecules of the encountered structures, as compression and rarefaction bands (Fig.1.1).

It is important to know the parameters characterizing an ultrasound wave: amplitude, frequency, wavelength, period, velocity, power and intensity (Table 1.1).

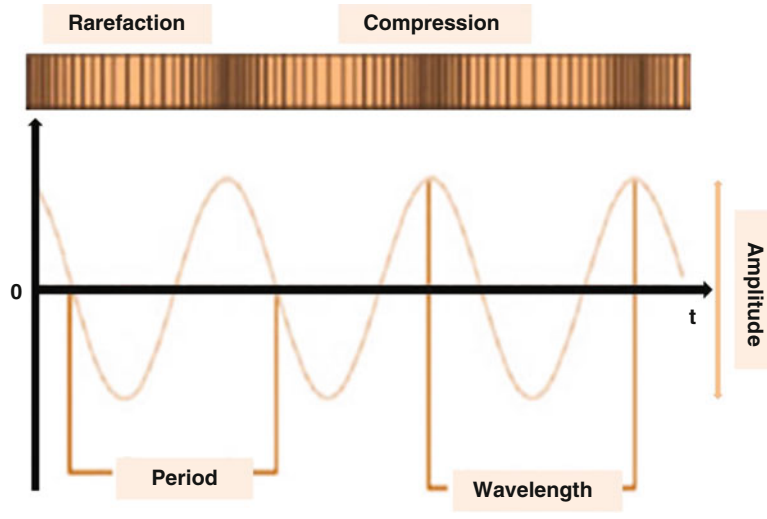

Fig. 1.1 The graphic demonstrates the oscillatory behaviour of the ultrasound waves propagating in tissues

Table 1.1 Main parameters that characterize an ultrasound wave

Amplitude (A)	The maximum pressure value reached during the compression phase
Frequency (ϒ)	The number of cycles per unit of time (complete oscillations that each particle undergoes each second). Frequencies employed in diagnostic ultrasonography range from 1.5 to 20 MHz and sometimes higher. The high frequency of ultrasound waves is correlated to a very low wavelength; this properties guarantee the production of thin beam, well collimated, with a small divergence
Wavelength (λ)	The spatial interval in which each oscillatory phenomenon is reproduced. It is inversely proportional to frequency and influences the spatial resolution of the US image: the smaller the wavelength (corresponding to high frequency), the higher the spatial resolution; the greater the wavelength (corresponding to low frequency), the lower the spatial resolution
Period (†)	The time interval in which each oscillatory phenomenon is reproduced
Velocity (v)	Depends on the physical properties of the propagation medium. It varies in relation with tissue elasticity and density. Acoustic velocity is greater in rigid or less compressible materials, such as the bone and metals, lower in air, water and soft tissues. The mean velocity in soft tissue (excluding the bone and air) is 1,540 m/s, the reference value used by manufacturers in the calibration of internal distance measurements
Power (P)	The total amount of energy passing through a surface per unit time (Watts)
Intensity (I)	The strength of an ultrasound wave; it is the energy per unit area per unit time (Watts per square centimetre). Intensity changes depending on the width of the ultrasound beam; in focused beams, it is the greatest at the focus where the beam width is the narrowest

1.2 Interactions Between US and Anatomical Structures

In ultrasonography, high-frequency sound waves are generated and transmitted through the body by a transducer. When the US beam runs into a tissue target, some of its energy is reflected back to the transducer as a returning echo, and some is deflected and continues its propagation into tissues. The transducer is responsible for both the production of the US beam and the detection of the returning echoes; it behave as an antenna that converts electrical pulses into the transmitted sound waves and receives the reflected and scattered ultrasound waves, converting them back into electrical signals, and then encoded into images.

Travelling through the body, a sound wave is subjected to varying phenomena that contribute to US image formation: attenuation, absorption, reflection, diffusion, refraction and divergence.

Attenuation: it is the continuous loss of acoustic energy (intensity) that the US beam undergoes running into tissues. It is usually expressed in units of decibels per centimetre and correlated to the US frequency (MHz) and the distance travelled (cm): the higher the frequency and the distance, the greater the attenuation. For this reason, although high-frequency US allow a better image resolution, the US beam is more attenuated. This fact has an important practical implication: high-frequency linear-array probes (7–13 MHz) are used for the study of superficial structures (tendons, muscles, ligaments); low-frequency curved-array probes (2.5-5 MHz) are utilized for deep organs evaluation. The main causes of attenuation are absorption, reflection, refraction, diffusion and divergence.

Absorption: it is the greatest cause of attenuation. The acoustic energy is transferred from the US beam to tissues and transformed into heat. The amount of absorption depends on US beam frequency and intrinsic characteristics of the medium (low in liquids, intermediate in soft tissues, high in bones and air).

Reflection: whenever the US beam encounters an interface between two materials with different acoustic impedance, some of the energy is reflected (reflection), and the remainder is transmitted deviated through the interface (refraction) (Fig. 1.2). The direction of the reflected wave (returning echo) depends on the orientation of sound wave relative to the surface: the angle of reflection equals the angle of incidence. The amplitude of the echo is directly correlated to (a) the orientation of the US beam to the reflecting

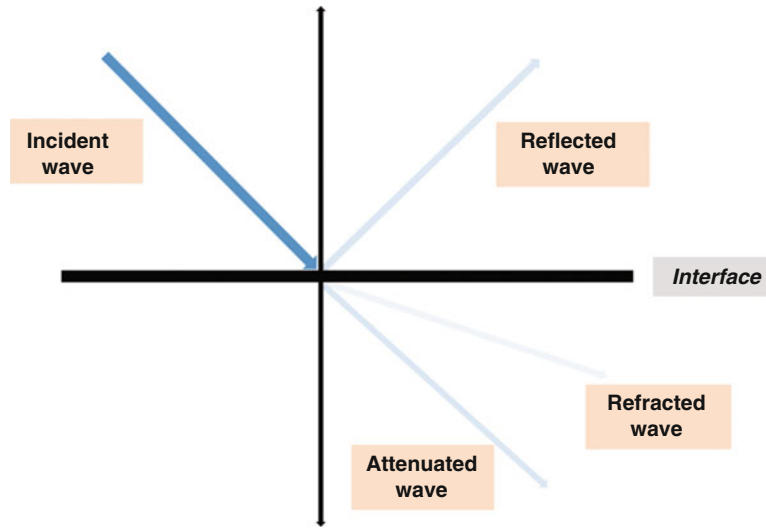

Fig. 1.2 Scheme of the physical phenomena contributing to US image formation

surface (reflection is the greatest when the US beam is perpendicular to the surface (angle of incidence = zero), so producing the strongest detected echoes in clinical sonograms (*specular reflection*)) and (b) the relative difference in acoustic impedance between the tissues on either side of the interface (acoustic impedance is an intrinsic property of tissues which expresses their resistance to the passage of the US beam (expressed in units of Rayls = kilograms per square metre per second)). The greater the difference in acoustic impedance between two materials, the stronger will be the intensity of the returning echo. Reflection can be either *specular* or *diffuse*, depending on the interface characteristics. When the interface is represented by a wide, smooth and homogeneous surface (diaphragm, vessel wall), the reflection is specular or mirror-like; when the interface shows a small, irregular and rough surface (parenchymal organs), the reflected wave will be diffuse.

Diffusion: it is the scattering of the reflected US beam in all directions (Fig. 1.2). It is typical of the parenchymal tissues, in which sound is scattered by the many cell and tissue elements that function as multiple interfaces.

Refraction: It is the deviation of the transmitted beam from the incident beam direction. It increases as the angle of incidence is not perpendicular to the surface.

Divergence: if the US beam is not focused, it tends to diverge distally with consequent reduction of the depth resolution.

1.3 Images Formation

Ultrasonographic images are obtained with a pulse-echo type of measurement.

The transducer is an essential element of US equipments. It is composed by a number of assembled crystals that are excited by electrical pulses (*reverse piezoelectric effect* – applying an electric field to crystals causes their mechanical oscillations). Based on the pulse-echo principle occurring with piezoelectric crystals, US transducers convert electricity (electrical energy) into sound (mechanical energy).

The US waves, sent from the transducer, propagate through tissues and then return reflected as echoes to the transducer. Those returning echoes are then converted back into electrical pulses by the transducer crystals (*piezoelectric effect* – converts mechanical energy, due to crystal deformation, into electrical energy) and are further processed in order to form the ultrasound image presented on the screen.

The US beam is considered a combination of multiple thin beams produced by each crystal assembled in the transducer, with a linear or

curved disposition. Currently, transducers contain a range of ultrasound frequencies (bandwidth) instead of a single fundamental frequency.

The generation of US images requires a complicated acquisition and display of ultrasound pulse-echo data. The broadband transducer generates a sequential series of focused beams all in the same plane (scan plane). Each set of target data from a single pulse transmission is placed in the image, as acquired along a line. All tissues in the scan plane are interrogated by these beams, and each real-time image frame is composed of a set of parallel or sector lines representing the positions of the interrogating beams in the patient. Computer algorithms are used to fill in between the image lines so that the image appears continuous.

When the transmitted US pulse encounters internal tissue targets, part of its energy is deflected (reflected or scattered) back to the transducer (the echo). Because pulse-echo imaging techniques employ the same transducer for both sending and receiving US pulses, only echoes travelling in the direction of the transducer have any chance of being detected.

The main pulse-echo parameters used in the formation of images include echo amplitude and target spatial position. Echo amplitude is encoded into shades of grey (greyscale imaging), with the lighter shades representing higher amplitude echoes.

The depth of the target along the direction of the beam is accurately calculated from a pulse time-of-flight measurement. Assuming US propagation velocity is fairly constant from tissue to tissue (1,540 m/s), the time between beam transmission and echo reception is used to determine the exact internal spatial location of all tissue targets.

Two important parameters representing image quality are as follows:

Spatial resolution refers to the capability to distinguish two adjacent points, along the axis of the beam (*axial resolution*) or in a plane perpendicular to the axis of the beam (*lateral resolution*).

Temporal resolution represents the capability of the US equipment to show anatomical structures in real time. It is related with the pulse repetition frequency (PRF) and with the frame (number of encoded images per unit time).

Visualization Systems

- Amplitude mode (*A-mode*): it is the simplest form of display. It is a diagram in which echo amplitude is shown according to tissue depth (echo time of flight).
- Time-motion mode (*TM-mode*): echoes returning from moving structures are displayed depending on the time. It is used in cardiac US evaluation.
- Brightness mode (*B-mode*): it is a greyscale tomographic imaging.

1.4 Artefacts

Image artefacts (errors in image display) are common in clinical ultrasonography and can cause confusion for the interpreting physician. Some artefacts occur secondary to improper scanning technique; others are unavoidable because they are correlated to the physical characteristic of the US beam.

A detailed description of US artefacts lies outside the aim of our handbook. However, the knowledge of artefacts often encountered in US soft-tissue evaluation is essential to improve diagnostic performance.

Anisotropy is the intrinsic property of some anatomical structures to modify their reflecting capability in respect to the US beam angle of incidence. If the US beam not perpendicularly encounters linear structures, such as muscles, tendons and ligaments, the reflection is not specular so the returning echoes have low intensity: the structure wrongly appears more hypoechoic (the artefact results with a loss of echogenicity in structure) (Fig. 1.3). The ability to recognize and correct anisotropy artefacts is important for image quality improvement and optimal patient care.

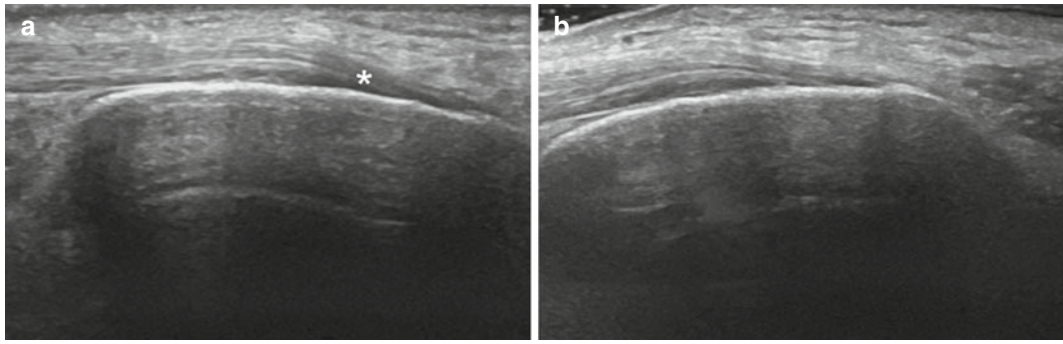

Fig. 1.3 US longitudinal scan of the distal insertion of the Achilles tendon onto the calcaneus. (**a**) With the US beam obliquely oriented, the tendon loses its echogenicity simulating a focal lesion (*). (**b**) The correct insonation of the tendon, with the US beam perpendicular to it, allows to appreciate its normal fibrillar hyperechoic echotexture

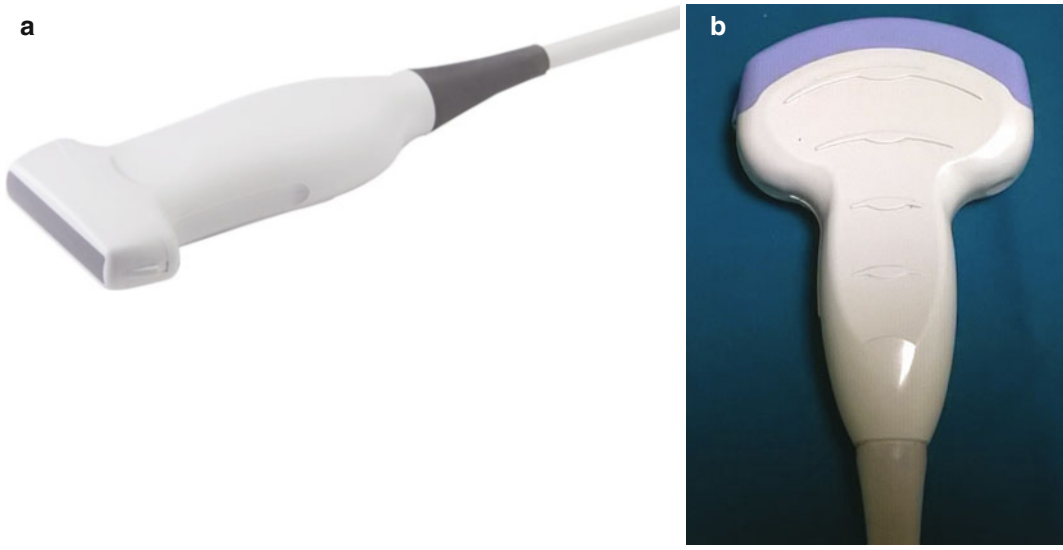

Fig. 1.4 (**a**) Linear-array probe (5–12 MHz). (**b**) Convex-array probe (2–5 MHz)

1.5 US Equipment: Hands On

Good technical skills are essential in order to extract the maximum amount of information that can be obtained with the equipment while avoiding the numerous pitfalls and artefacts of US imaging modality. Some important parameters can be adjusted before and during US examination in order to improve image quality and diagnostic performances.

1. *Probe selection*: high-frequency linear-array probes, operating with frequencies of 10 MHz or more, are mandatory for a precise evaluation of the soft tissues of the musculoskeletal system (Fig. 1.4). The main properties of broadband transducers are summarized in Table 1.2.

Table 1.2 Different features of US transducers

	Linear-array transducer	Curved-array transducer
Bandwidth (MHz)	7–13	2.5–5
US beam attenuation	↑	↓
US beam penetration in depth	↓	↑
Clinical application	Superficial tissues	Deep organs
Image resolution	↑ spatial resolution ↑definition	↓ spatial resolution

2. *US beam focusing*: it determines the number and pattern of focal zones (zone in which the width and thickness of the US beam is reduced in order to increase contrast and spatial resolution). The focal depth can be changed dynamically during the examination.
3. *Gain adjustment*: it optimizes echoes intensity at different levels of depth.
4. *Zoom*: it better visualizes small and thin structures.
5. *Dynamic range adjustment*: it sets the contrast resolution. High values of the dynamic range allow for the visualization of very low-intensity echoes, reducing the contrast resolution; so the dynamic range must be reduced in order to enhance the contrast resolution.

Different features of US transducers are presented in Table 1.2.

Suggested Reading

Feldman MK, Sanjeev K, Blackwood MS (2009) US artifacts. RadioGraphics 29:1179–1189

Goldstein A (1993) Overview of the physics of US. RathoGraphics; 13:701–704

Martinoli C, Bianchi S (2007) Ultrasound of the musculoskeletal system. Springer, New York

Ziskin MC (1993) Fundamental physics of ultrasound and its propagation in tissue. Radiographics 13: 705–709

Doppler Technologies and Ultrasound Elastography

2

Riccardo Sartoris and Alessandro Muda

2.1 Doppler Imaging

Doppler imaging is an established ultrasonographic method employed for the accurate non-invasive evaluation of the blood flow. As the name implies, US Doppler technique uses the *Doppler effect* to assess how blood flows through the major blood vessels.

Focus On

The *Doppler effect* is based on an essential principle: the sound frequency of a target changes as the target travels towards or away from a point of reference. Since the blood red cells can be considered moving targets, this effect is used to obtain information about the blood flow. In particular, when the US beam, produced by the probe, is transmitted into a vessel, the frequency of the received wave is different from that of the transmitted wave because the source (red cells) moves relative to the given receiver (probe). The change of frequency detected between the transmitted and the received US frequency is named "Doppler shift". The received US frequency would be higher if the direction is towards the receiver, lower if the direction is opposite.

The equation which describes this phenomenon is as follows:

$$\mathrm{Dn} = 2vf \cos\ q/c$$

- Dn: Doppler shift
- v: velocity of the blood (red cells)
- f: frequency of the incident wave
- q: angle between the direction of the movement and the direction of the US beam
- c: acoustic velocity

This equation allows the measurement of an important parameter, the velocity of the blood flow.

The Doppler shift of the moving blood red cells is continuously monitored to produce the Doppler signal; it is in the audible range and can thus be heard. The resulting sound is distinct and provides feedback to the operator.

US Doppler imaging allows to perform the following:

- *Qualitative analysis:* evaluating the presence, site and direction of the blood flow

R. Sartoris
Dipartimento di Radiologia,
Università degli studi di Genova, Genoa, Italy
e-mail: riccardo.sartoris@hotmail.it

A. Muda (✉)
Dipartimento di Radiologia,
IRCCS Ospedale San Martino IST, Genoa, Italy
e-mail: alessandro.muda@tiscali.it

E. Silvestri et al., *Ultrasound Anatomy of Lower Limb Muscles: A Practical Guide*,
DOI 10.1007/978-3-319-09480-9_2,

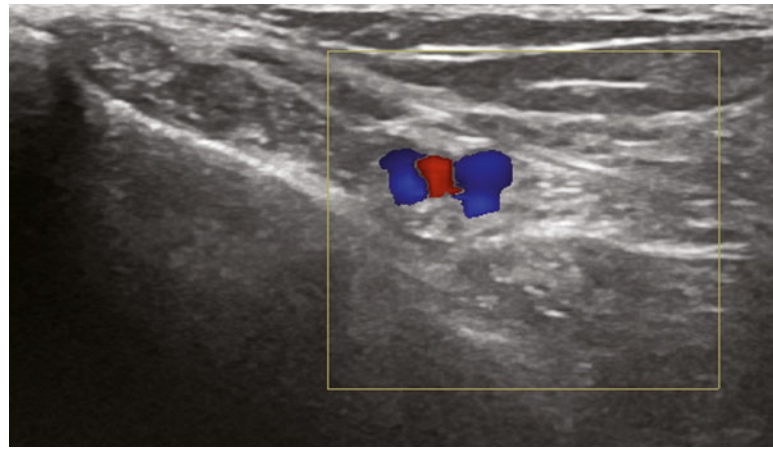

Fig. 2.1 Colour Doppler imaging shows the posterior tibial artery (*red*) and veins (*blue*) at the level of the medial malleolus. Especially in imaging soft tissues, identifying neurovascular bundles with US colour Doppler technique can be very useful to correctly localize tendinous and muscular structures

- *Quantitative analysis:* evaluating flow velocity and flow rate
- *Semiquantitative analysis:* evaluating the spectrum of the waves frequencies

Four main systems are developed to measure the velocity of the blood flow: continuous-wave Doppler, pulsed-wave Doppler, colour Doppler and power Doppler.

Continuous-Wave Doppler (CW-Doppler): It uses two separate crystals: one to emit and one to receive US beams continuously. This infinite pulse repetition rate allows insufficient time for the first pulse to return to the probe before the next is emitted. Consequently, the US machine cannot determine which sound pulse was frequency shifted and, therefore, cannot precisely define the location of the moving target. In conclusion, this technique enables the measurement of high-velocity blood flow, but the depth from which the returning echoes originate cannot be evaluated.

Pulsed-Wave Doppler (PW-Doppler): It uses the same crystal to emit and receive signals. The probe produces US beams in pulses, alternating the transmission and reception of the US beam. One important advantage of pulsed Doppler systems is their ability to provide Doppler shift data selectively from a small segment along the US beam, referred to as the "sample volume". The position of the sample volume is decided by the operator. When the US beam is transmitted into tissues, it travels for a given time until it is reflected by a moving red cell; then, it returns to the probe over the same time interval but at a shifted frequency. Calculating the total transit time, the US machine is able to measure the distance of the sample volume ("reflector"). In respect to the CW-Doppler, PW-Doppler is able to evaluate the depth from which the returning echoes originate, displaying an ultrasound image and waveform; however, it cannot correctly depict higher velocities (blood flow velocity measurements are limited to the physiologic range, usually around 1.5 m/s).

Aliasing phenomena are an artefact that happens with PW-Doppler when the blood flow velocity is too high and causes an error in frequency measurement. When the interval of the US pulses, expressed by the US machine as pulse repetition frequency (PRF, number of pulses within 1 s), is too long relative to the velocity of the blood flow, it will not be possible to determine the direction of blood flow. In particular, aliasing occurs when the velocity is more than one half of the PRF; in this case velocities above, this limit will be displayed on the tracing opposite to the true direction of blood flow. To correct for aliasing, the operator can increase the PRF or increase the angle between the US beam and the flow direction towards perpendicularity.

Colour Doppler: It is an ultrasound system in which the energy of the returning echoes is displayed as an assigned colour; by convention, echoes representing flow towards the probe are seen as shades of red, and the US machine displays coloured blood flow superimposed on a greyscale image, thus allowing simultaneous visualization of anatomy and flow dynamics (Fig. 2.1).

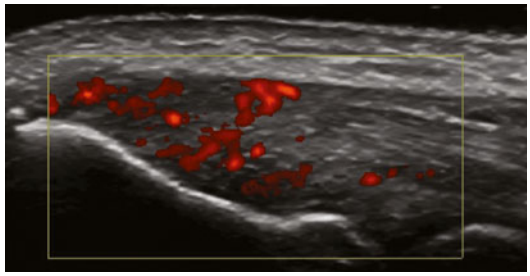

Fig. 2.2 Power Doppler imaging demonstrates the presence of tendinous hyperaemia

To optimize the colour Doppler evaluation, it is crucial to set the US beam at an optimal angulation <60° in respect to the vessel, basing on the physical Doppler equation (cos 90° = 0).

Power Doppler: It is a type of colour Doppler, more sensitive to blood flow compared with conventional colour Doppler; it shows small vessels and slow flow rates, indeed it is most commonly used to evaluate blood flow through vessels within solid organs. Power Doppler assigns a colour to blood flow regardless of direction (Fig. 2.2).

As the main interest is in detecting low-velocity microvascular flow in soft tissue imaging, power Doppler is generally preferred to colour Doppler, and although on new ultrasound machines, the difference is often negligible.

Power Doppler is extremely sensitive to the movement of the probe, which produces a flash artefact. It is important to optimally adjust the colour gain for Doppler imaging to avoid artefact if the setting is too sensitive and for false-negative flow if sensitivity is too low. Power-Doppler should be optimized while the probe is not in contact with patient's skin. The gain should be set at maximum level and then decreased up to the disappearance of all artefact. Further, it is important to set low wall filters (WF) and pulse repetition frequency (PRF) between 700 and 1,000 Hz in order to better evaluate low-velocity blood flows.

Combining with greyscale ultrasound, colour and power Doppler imaging allow unique real-time evaluation of the regional blood flow, enabling a wide range of applications for the evaluation of soft tissues. At first, these systems can be used to confirm that an anechoic structure is a blood vessel and to confirm the presence of the blood flow. Often blood vessels are used in musculoskeletal imaging as anatomical landmarks.

Increased blood flow on colour or power Doppler imaging may occur with greater perfusion, inflammation and neo-vascularity. For example, increased muscle perfusion can be physiologically seen after physical exercise.

Colour and power Doppler are very helpful in detecting inflammatory diseases. They also enable the differentiation between complex fluids and a mass or synovitis; the former typically has no internal flow, and the latter may show increased flow. After treatment for inflammatory diseases, such as arthritis, colour and power Doppler imaging can show interval decrease in flow, which would indicate a positive response.

When a mass is identified, increased blood flow may suggest neo-vascularity, possibly related to malignancy. Although the finding is nonspecific, a neoplasm without flow is more likely to be benign, and malignant tumours usually demonstrate increased flow and irregular vessels.

Colour and power Doppler findings represent a useful tool also for the quick assessment of vascular anomalies and post-traumatic vascular lesions.

It is also important to use colour Doppler imaging during a biopsy to ensure that major vessels are avoided.

2.2 Ultrasound Elastography

Ultrasound elastography (EUS) is a recently developed ultrasound-based method, which allows for qualitative visual or quantitative measurements of the mechanical properties of tissues. It is based on the general principle that mechanical stress applied to tissue causes changes within it, which depend on the elastic properties of tissue. Since disease alters the biomechanical properties of muscles and tendons, US elastography has been recently employed in clinical practice for research in biomechanics of the musculoskeletal system.

Two main forms of elastography are currently used in clinical practice, though other important implementations are to be expected.

The first is known as *strain elastography* (SE) (also described as compression elastography,

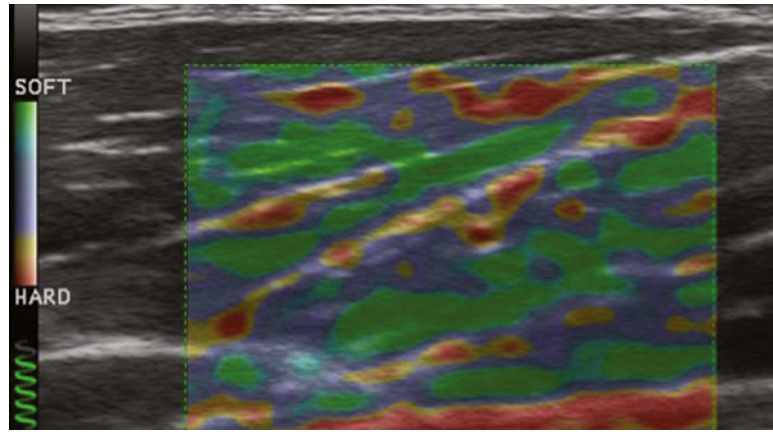

Fig. 2.3 Real-time elastography. Applying manual compression with the probe, the ultrasonograph shows soft structures in *green* and hard structures in *red* (qualitative measurement)

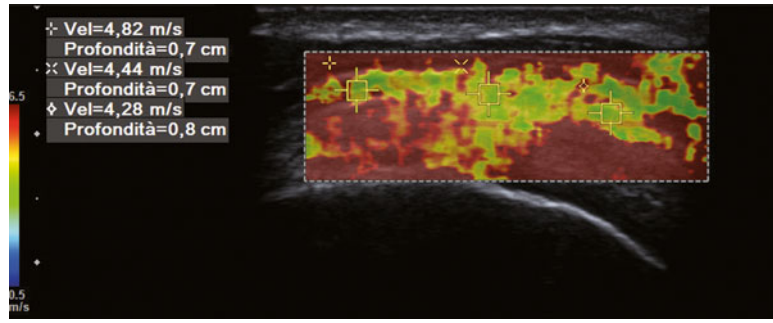

Fig. 2.4 ARFI elastography (share wave) of the gluteal insertion onto the greater trochanter. Note the quantitative measurements on the left of the image

sonoelastography and real-time elastography). The soft tissue deformation (which is the strain) is produced by an external palpation manually applied with the probe, and it is assessed by following the way the speckle in the image moves, usually with a tracking algorithm working on the radio-frequency data. Then, the data are used to form an image that is coded in colour or greyscale to show the pattern of strain, which is inversely related to tissue stiffness and can be subjectively assessed (Fig. 2.3).

The second typology, currently implemented, is *shear wave elastography* (SWE). Shear waves may not be familiar to clinical readers, but they frequently occur in human soft tissues. Shear waves are transverse waves rapidly attenuated by tissue (i.e. the particle movement is across the direction of travel); they travel much more slowly (between 1 and 10 m/s), and they are not supported by liquids of low viscosity. Shear waves are produced by any mechanical disturbance and occur naturally from muscular movements as well as being induced by the ultrasound systems used to measure their speed. A useful way to generate shear waves is to use acoustic radiation force: tiny displacements in soft tissue set up (shear waves) that travel sideways away from the "pushing" ultrasound beam. Though the amplitude of the resulting shear waves is minute (a few microns' displacement), they can be detected by conventional ultrasound using tracking algorithms (Fig. 2.4).

The recent introduction of EUS into commercially available ultrasound systems has driven research activity towards the potential clinical applications of this new technique also in the musculoskeletal system, such as the early detection of degenerative changes in tendinosis and the evaluation of elastic changes in muscular pathology (strain injuries).

In practice, elastography could be considered as an extension of conventional ultrasonography, in the same way as Doppler is integrated into clinical practice.

Suggested Reading

Arda K, Ciledag N, Aktas E, Kadri Arıbas B, Köse K (2011) Quantitative assessment of normal soft-tissue elasticity using shear-wave ultrasound elastography. AJR 197(3):532–536

Kot Wing BC, Zhi Jie Z, Chun Lee AW, Fong Leung VY, Ngor Fu S (2012) Elastic modulus of muscle and tendon with shear wave ultrasound elastography: variations with different technical settings. PLoS One 7(8):e44448

Martinoli C, Bianchi S (2007) Ultrasound of the musculoskeletal system. Springer, Berlin/New York

O' Neill J (2008) Musculoskeletal ultrasound: anatomy and technique. Springer, New York

Pavčec Z, Žokalj I, Saghir H, Pal A, Roić G (2006) Doppler ultrasound in the diagnosis and follow-up of the muscle rupture and an arteriovenous fistula of the thigh in 12 year boy. Radiol Oncol 40(4):211–215

Wells PN, Liang H-D (2011) Medical ultrasound: imaging of soft tissue strain and elasticity. J R Soc Interface 8:1521–1549

Normal Anatomy and Biomechanics

3

Davide Orlandi and Silvia Perugin Bernardi

3.1 Normal Anatomy

Muscle architecture refers to the macroscopic organization of the muscle fibers and has a great influence on muscle function.

The skeletal muscle consists of several *muscle fibers*, muscle cells that are considered the unit of contraction.

Muscle fibers are long and cylindrically shaped, with many nuclei, and are grouped into bundles (*fascicles*) separated by fibroadipose septa (*perimysium*). The *endomysium* is a thin connective tissue, deriving from the perimysium, which separates individual muscle fibers from each other. The whole muscle is enclosed in a fascial sheath known as *epimysium*.

The muscle fibers, the *epimysium* and the *perimysium*, could converge in strong and wide connective tissue terminal structures (*aponeurosis*), in *fasciae* or directly in *tendons* (Fig. 3.1).

Muscle fibers are classified by their histologic appearance, rapidity of contraction, and ability to bear fatigue (Table 3.1).

Slow-twitch or type I fibers have a small diameter, are invested by a rich capillary network, and appear red for the presence of a large amount of oxygen-binding protein (*myoglobin*). These type I fibers are resistant to fatigue, relying on oxidative metabolism for energy, and are better suited for continuous contractions over a long time.

On the other hand, *fast-twitch or type II fibers* have a larger diameter and can be further divided into the following:

- *Type IIa*: these fibers have a fast contraction speed and can use aerobic as well as anaerobic energy sources. These fibers contain a large number of mitochondria and myoglobin and are more prone to fatigue than type IIb fibers, but less than type I fibers. These fibers are a hybrid of type I and II fibers.
- *Type IIb*: these fibers have an extremely fast contraction speed, creating very forceful muscle contractions resulting in short, fast bursts of power and rapid fatigue. Unlike IIa fibers, they can only use anaerobic energy sources and contains a poor capillary network and a fewer myoglobin. Therefore, these fibers are

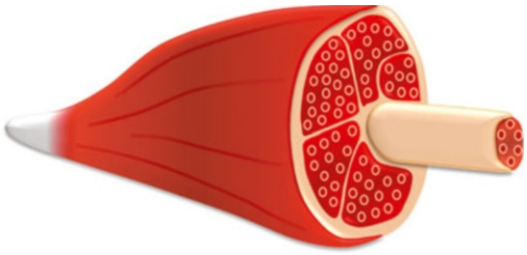

Fig. 3.1 Drawing showing skeletal muscle basic architecture

D. Orlandi (✉) • S. Perugin Bernardi
Dipartimento di Radiologia,
Università degli studi di Genova, Genoa, Italy
e-mail: my.davideorlandi@gmail.com;
silvia.perugin@gmail.com

E. Silvestri et al., *Ultrasound Anatomy of Lower Limb Muscles: A Practical Guide*,
DOI 10.1007/978-3-319-09480-9_3,

Table 3.1 Muscle fiber classification

	Fiber type I	Fiber type IIa	Fiber type IIb
Mytochondria	Many	Many	Few
Capillaries	Many	Many	Few
Myoglobin content	High	High	Low
Glycogen content	Low	Low	High
ATPase activity	Low	High	High
Contraction velocity	Slow	Fast	Fast
Fiber diameter	Small	Intermediate	Large
Rate of fatigue	Slow	Intermediate	Fast

known as white fibers and are more easily fatigable.

Each muscle has a different percentage of type I and type II fibers, but the proportion varies depending on the usual action of the muscle.

Muscle *vascularity* is provided by primary arteries, which runs along the long axis of the muscle and gives origin to feeding arteries that course obliquely toward the *epimysium*.

The feeding arteries account for as much as 30–50 % of the total resistance to muscle blood flow; indeed, they represent a relevant site for blood flow control proximally to muscle microcirculation.

A network of secondary arteriolar branches originates from the feeding arteries. Arterioles enter the perimysium and travel perpendicularly to the muscle fibers axis until giving origin to terminal branches that penetrates the *perimysium* and branching immediately into numerous capillaries that travels parallel to the muscle fibers in the *endomysium*.

The group of capillaries perfused by a terminal arteriole represents the microvascular unit: the smallest functional unit for blood flow regulation in the skeletal muscle. As previously mentioned, the density and the number of capillary networks are greater in oxidative muscles (red fibers).

The arrangement of venules and veins follows the course described for the arterioles and arteries.

The microscopic capillary exchanges between arteries and veins occur throughout the *endomysium* that surround the single muscle fibers.

According to the number of vascular pedicles, muscles are classified into five types:

- Type I: these muscles have a single vascular pedicle (e.g., tensor fasciae latae and gastrocnemius).
- Type II: these muscles have a single dominant vascular pedicle and numerous minor vascular pedicles (e.g., gracilis).
- Type III: these muscles have two different vascular pedicles that originate from different arteries (e.g., rectus abdominis and gluteus maximus).
- Type IV: these muscles have numerous minor vascular pedicles that should not supply the entire muscle alone (e.g., tibialis anterior and sartorius).
- Type V: these muscles have a single dominant pedicle and several secondary segmental pedicles (e.g., latissimus dorsi and pectoralis minor).

3.2 Biomechanics

Muscle tendon unit (*MTU*) is responsible for muscle contraction followed or not by joint movement and represents a crucial entity from a biomechanical point of view.

There are three main types of *muscle contraction* (Fig. 3.2):

- Isometric
- Isotonic – concentric
- Isotonic – eccentric

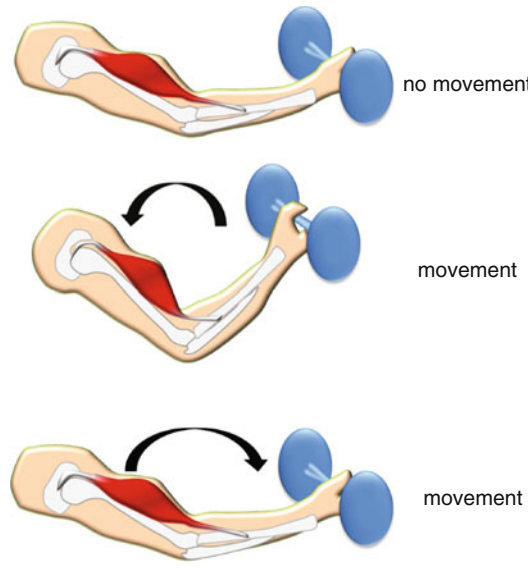

Fig. 3.2 Drawing showing the three main types of muscle contraction

3.2.1 Isometric Contraction

Isometric contraction occurs when the muscle develops tension to overcome a resistance but without any change in length, so the muscle attachments remain at the same distance apart.

This occurs, for example, when carrying an object in front of you and your muscles are contracting to hold the object at the same level.

The amount of force that a muscle is able to produce during an isometric contraction depends on the length of the muscle at the point of contraction.

3.2.2 Isotonic Contraction

Isotonic contraction occurs when the muscle length changes as it contracts, causing movement, and the tension in the muscle remains constant generating force at the musculotendinous junction.

- *Concentric*: in concentric contraction, the muscle shortens while generating force. This occurs when the force generated by the muscle exceeds the load opposing its contraction: an example is bending the elbow from straight to fully flexed, causing a concentric contraction of the biceps brachii muscle.
- *Eccentric*: in eccentric contraction, the muscle develops tension and, at the same time, elongates in order to overcome a resistance. The force generated is insufficient to overcome the external load, and the muscle fibers lengthen under contractile tension.

This movement is the opposite of concentric contraction and occurs when the muscle lengthens as it contracts. This usually involves the control or deceleration of a movement being initiated by the eccentric muscle agonist.

3.2.3 Muscle Fiber Arrangement

Knowledge of the *geometric arrangement* of muscle fibers is therefore important when studying muscle functions and the resultant joint actions: the muscle architecture considerably affects the manner in which muscle force is transmitted to tendons and bones.

Fiber arrangement is unique in every muscle, but, according to the shape and fascicular architecture, the muscles (Fig. 3.3; Table 3.2) can be classified into the following:

- *Parallel fasciculi*: the fibers lie in the longitudinal axis of the muscle belly and are arranged along the line of muscle force action.
- We can find this arrangement in quadrilateral (e.g., thyrohyoid), strip-like (e.g., sternohyoid and sartorius), strip-like with tendinous intersections (e.g., rectus abdominis), and fusiform (e.g., biceps brachii, digastric) muscles. The range of movement in such muscles is very wide.
- *Convergent fasciculi*: the muscular fibers converge on the point of insertion to maximize the contraction power.

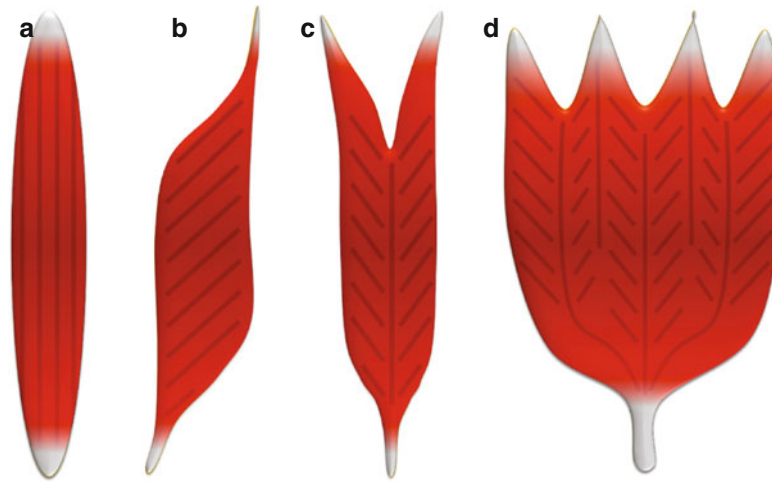

Fig. 3.3 Drawing showing the geometrical arrangement of muscle fibers. (**a**) Parallel fasciculi; (**b**) unipennate; (**c**) bipennate; (**d**) multipennate

Table 3.2 Examples of internal biomechanical properties of the main muscles

	Muscle	Fiber arrangement
Thigh	Sartorius	Strip like with parallel fasciculi
	Rectus femoris	Bipennate (inner); unipennate (outer)
	Adductor longus	Triangular with convergent fasciculi
	Adductor magnus	Cruciate muscle
	Biceps femoris	Bipennate
Leg	Peroneus longus	Bipennate
	Soleus	Bipennate
	Tibialis posterior	Unipennate
	Flexor hallucis longus	Bipennate
	Tibialis anterior	Circumpennate
	Extensor digitorum longus	Unipennate

This orientation is found in triangular (e.g., adductor longus) and fan-shaped (e.g., temporalis) muscles.

- *Spiral or twisted fasciculi*: spiral or twisted fibers are found in trapezius, pectoralis major, latissimus dorsi, and supinator.
- *Cruciate muscles*: fibers are crossed lying superficial and deep (e.g., sternocleidomastoid, masseter, and adductor magnus).
- *Sphincteric fasciculi*: fibers surround an opening or orifice (e.g., orbicularis oculi and orbicularis oris).
- *Pennate fasciculi*: fibers have a feather-like orientation. This arrangement makes the muscle more powerful, although the range of movement is reduced.

  The pennate muscles may be:
  - *Unipennate* when fibers have a linear origin and have a half feather shape (e.g., flexor pollicis longus, extensor digitorum longus, peroneus tertius, palmar interosseous)
  - *Bipennate* when the fascicles continue in a unique central tendon (e.g., rectus femoris, dorsal interosseous, peroneus longus, flexor hallucis longus)
  - *Multipennate* when multiple tendinous septa extend into the origin and the insertion (e.g., subscapularis, deltoid)

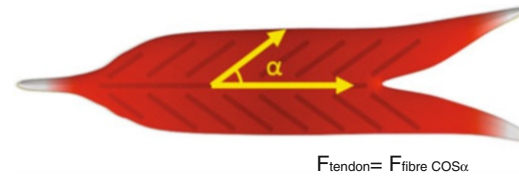

Fig. 3.4 Drawing showing pennation angle. Muscle strength is directly related to fiber strength and pennation angle cosine

  - *Circumpennate* when fibers from a cylindrical wall converge to a central tendon (e.g., tibialis anterior)

In the pennate muscles, the tendons present two parts: the internal (known also as aponeurosis) and the external one.

In pennate muscles, the most important architectural and biomechanical parameters are the fiber length, the muscle physiological cross-sectional area, and the pennation angle.

The *pennation angle* (PA), as showed in Fig. 3.4, is the angle between the direction of muscle fibers and the line of force action represented by the external tendon or the aponeurosis (internal tendon).

In different muscles, it varies from 0° to 30°. The angle increases with muscle hypertrophy and during muscle contraction. Ultrasound imaging could be easily used to determinate the PA and to evaluate the dynamic change of the PA during contraction.

The *physiological cross-sectional area* is the area of the cross section of a muscle perpendicular to its fibers, generally at its largest point.

Muscles may consist of a single muscle belly or more heads with different origins and a single common tendon insertion such as the biceps brachii which presents two heads and triceps brachii which presents three heads.

3.2.4 Aponeurosis and Fasciae

Another important anatomical structures are the *aponeurosis* and the *fasciae.* Aponeurosis is a term used to define the thick connective lamina inserting into the muscles and transmitting tensile forces to fasciae, joints, bones, and muscles themselves.

Fasciae should be defined as connective tissue bundles composed mostly by collagen fibers (but characterized by a different architecture if compared to tendons and aponeurosis). Fasciae could envelope vessels, nerves, and lymphatics, composing the neurovascular bundles.

Superficial fasciae merge with the deep layer of the derma, intertwined with the subcutaneous fatty tissue, and represent a peripheral envelope for the muscular structures.

Deep fasciae (or muscular fasciae) represent important anatomical structure, and a proper knowledge of such entities is mandatory performing US examination of muscles. They are well represented in the lower limb, where they course deep among muscle bellies furnishing a strong attachment to the bone and transmitting the tensile forces to it. An example of this setting is the iliotibial tract which is a thick widening of the deep femoral fascia of the thigh transmitting the force generated by the tensor fasciae latae and gluteus maximus muscles to the femur and tibia; another important example is the deep transverse fascia in the leg which separates the soleus from the deeper flexor muscles. Fasciae arrangement often delineates actual muscular compartments: this must be considered particularly in the presence of intermuscular fluid.

Suggested Reading

Aggeloussis N, Giannakou E, Albracht K, Arampatzis A (2010) Reproducibility of fascicle length and pennation angle of gastrocnemius medialis in human gait in vivo. Gait Posture 31:73–77

Englund EK, Elder CP, Xu Q, Ding Z, Damon BM (2011) Combined diffusion and strain tensor MRI reveals a heterogeneous, planar pattern of strain development during isometric muscle contraction. Am J Physiol Regul Integr Comp Physiol 300:R1079–R1090

Fukunaga T, Kawakami Y, Kuno S, Funato K, Fukashiro S (1997) Muscle architecture and function in humans. J Biomech 30:457–463

Ito M, Kawakami Y, Ichinose Y, Fukashiro S, Fukunaga T (1998) Nonisometric behavior of fascicles during isometric contractions of a human muscle. J Appl Physiol 85:1230–1235

Lieber RL (2002) Skeletal muscle structure, function, and plasticity. Lippincott Williams & Wilkins, Philadelphia

Maganaris CN, Baltzopoulos V, Sargeant AJ (2002) Repeated contractions alter the geometry of human skeletal muscle. J Appl Physiol 93:2089–2094

Perona P, Malik J (1990) Scale-space and edge detection using anisotropic diffusion. IEEE Trans Pattern Anal Mach Intell 12:629–639

Shi J, Zheng Y, Huang Q, Chen X (2008) Relationships among continuous sonomyography, electromyography and torque generated by normal upper arm muscles during isometric contraction. IEEE Trans Biomed Eng 55:1191–1198

White DCS, Thorson J (1975) The kinetics of muscle contraction. Pergamon Press, Oxford/New York

Ultrasound Basic Anatomy

4

Riccardo Sartoris and Enzo Silvestri

4.1 US Basic Anatomy

In the last decade, ultrasound (US) technology has had a very fast development with improvements in transducer technology, image resolution, software implementations and hardware developing. These changes together with the opportunity to perform a dynamic examination have widely improved the use of US in musculoskeletal field.

Muscle US is a convenient, non-invasive and real-time technique able to visualize normal and pathological muscle tissues.

Selection of the *proper transducer* and US parameters is an important aspect of muscle ultrasonography and depends on the depth and size of the examined structure.

For superficial muscles, high-frequency (*7–15 MHz*) linear transducers are most useful and provide a good balance between tissues penetration and resolution; however, a correct examination of deeper structures sometimes requires lower-frequency convex transducers (*3–10 MHz*).

R. Sartoris
Dipartimento di Radiologia,
Università degli studi di Genova, Genova, Italy
e-mail: riccardo.sartoris@hotmail.it

E. Silvestri (✉)
Struttura Complessa di Diagnostica per Immagini ed Ecografia Interventistica, Ospedale Evangelico Internazionale, Genova, Italy
e-mail: silvi.enzo@gmail.com

The sonographer's grip on the transducer is particularly important in soft-tissue ultrasound because fine and precise movements of the transducer are often required. The transducer should be held firmly with the ulnar aspect of the hand against the patient's body in order to stabilize it.

Patient lies on the examination bed in a suitable and comfortable position for the evaluation of the region of interest. Remember to always start the muscle examination in complete relaxation.

Frequently, it could be helpful to examine the contralateral side of the patient's body to make a comparative examination, thus highlighting also subtle alterations.

4.2 US Muscles Appearance

US muscles appearance is predominately hypoechoic with hyperechoic septations: muscle bundles are hypoechoic in comparison to subcutaneous fat and are separated by the hyperechogenic fibroadipose perimysium septa (Fig. 4.1).

In *short axis*, muscle tissue appears as dots and short lines producing a "starry sky" appearance (Fig. 4.2).

In *longitudinal section*, the hyperechoic structures, represented by fibroadipose septa, appear as parallel lines that gives rise to fusiform or pennate appearance (semipennate, unipennate, bipennate, multipennate).

In normal subjects, the *epimysium* surrounding the muscle appears as a highly reflective

E. Silvestri et al., *Ultrasound Anatomy of Lower Limb Muscles: A Practical Guide*,
DOI 10.1007/978-3-319-09480-9_4, © Springer International Publishing Switzerland 2015

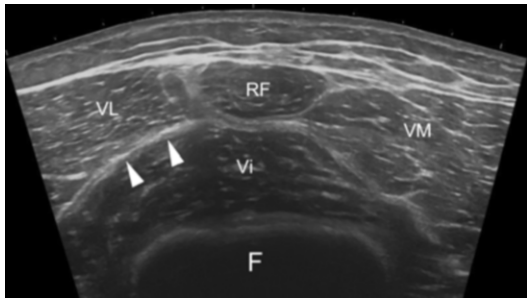

Fig. 4.1 Extended-field-of-view US scan showing thigh muscles and fasciae (*arrowheads*) appearance. *RF* rectus femoris, *VL* vastus lateralis, *VM* vastus medialis, *Vi*, vastus intermedius, *F* femur

structure; the bone, if visualized, appears as a bright echo, representing the cortex, with an anechoic bone shadow.

The intramuscular tendon and the aponeurosis appear as highly hyperechoic linear structures within the muscle; the musculotendinous junction, which varies in size from muscle to muscle, is seen as a hyperechoic fibrillar structure merging with the muscle belly (Figs. 4.3 and 4.4).

The fascia appears as a brightly echogenic fibrillar structure that delineates the muscle from subcutaneous tissue, and it is a very important

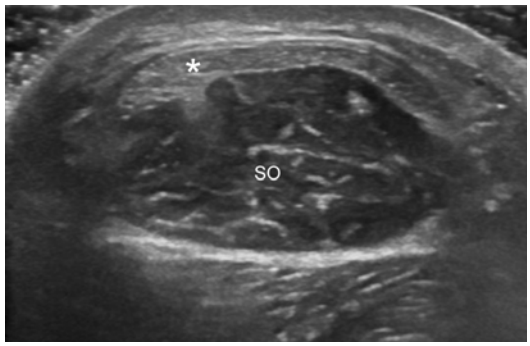

Fig. 4.2 US scan of the posterior leg showing soleus muscle (*SO*) internal architecture and, superficially, the forming Achilles tendon (*)

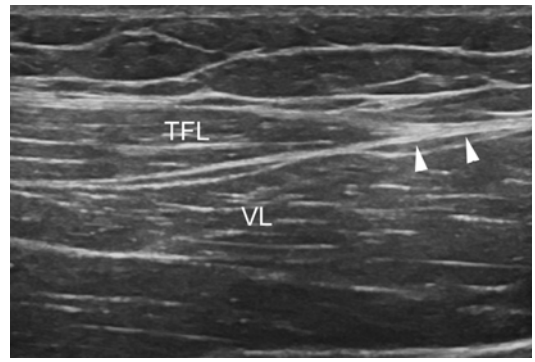

Fig. 4.3 US scan of the thigh showing the tensor fasciae latae (*TFL*) muscle and its aponeurosis (*arrowheads*). *VL* vastus lateralis muscle

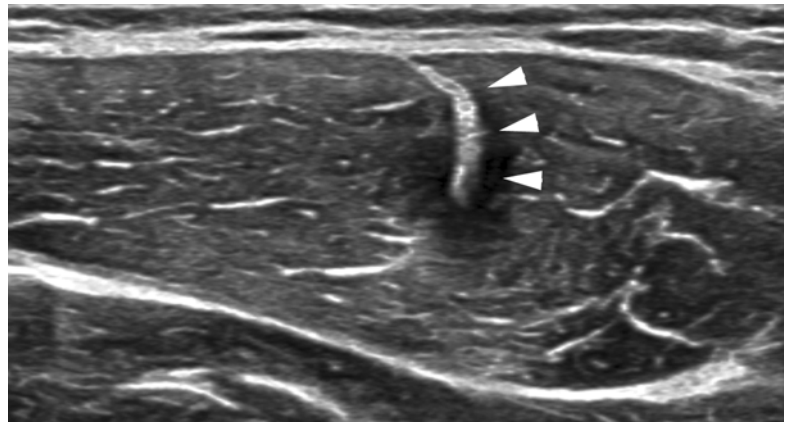

Fig. 4.4 US scan of the rectus femoris muscle showing indirect tendon appearance (*arrowheads*)

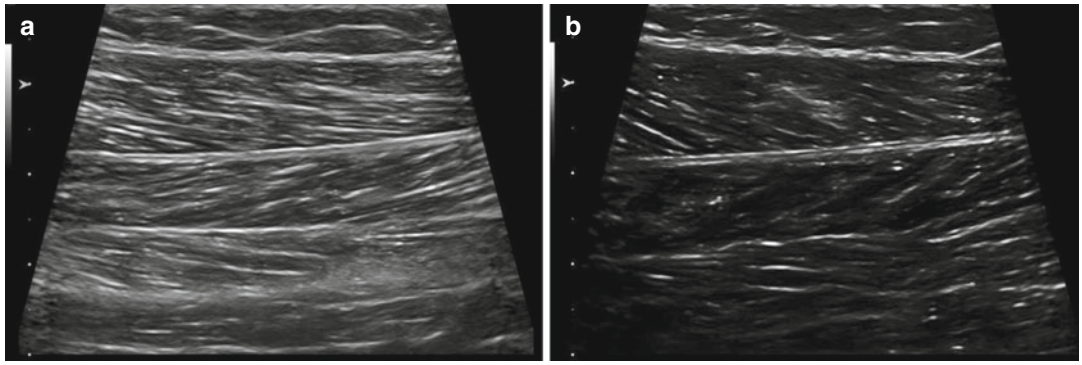

Fig. 4.5 US scan of medial gastrocnemius muscle showing correct insonation (**a**) and anisotropy artefacts (**b**)

landmark in order to distinguish the examined muscle from the adjacent ones.

Structure and appearance of skeletal muscles change with ageing. In addition to age-related muscle mass reduction, muscle quality changes include increased adipose tissue accumulation and water content within muscle that appear highly hyperechoic.

Muscle disuse results in altered composition and increased intramuscular fat accumulation. This condition is accompanied by a severe loss of muscle strength.

The examiner should pay attention to evaluate muscles with a correct angle of incidence of the US beam to avoid *anisotropy* artefacts. When the US beam is not perpendicular, the muscle shows a loss of echogenicity in structure (Fig. 4.5).

Because muscle tears and hematomas may appear hypoechoic, it is important to properly move or angle the transducer to prevent anisotropy as the cause of focal hypoechogenicity.

4.3 Extended Field of View (eFOV)

Extended field of view is a US imaging technique that could be very useful to obtain a panoramic view of the examined muscle, also highlighting its relationship with the adjacent ones. It requires deep knowledge of the anatomy and high manual skills as musculoskeletal sonographer to carefully depict the structures of interest (Fig. 4.6).

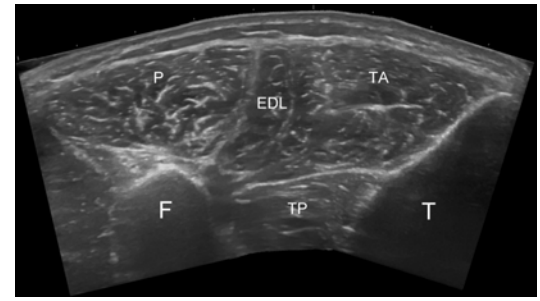

Fig. 4.6 Extended-field-of-view (eFOV) US scan of anterior leg compartment muscles. *TA* tibialis anterior muscle, *EDL* extensor digitorum longus muscle, *P* peroneal muscles, *TP* tibialis posterior muscle, *T* tibia, *F* fibula

Suggested Reading

Blazevich AJ, Gill ND, Zhou S (2006) Intra-and intermuscular variation in human quadriceps femoris architecture assessed in vivo. J Anat 209:289–310

Cady EB, Gardener JE, Edwards RH (1983) Ultrasonic tissue characterisation of skeletal muscle. Eur J Clin Invest 13:469–473

Campbell SE, Adler R, Sofka CM (2005) Ultrasound of muscle abnormalities. Ultrasound Q 21:87–94

Martinoli C, Bianchi S (2007) Ultrasound of the musculoskeletal system. Springer, Berlin/New York

Narici MV, Maganaris CN, Reeves ND, Capodaglio P (2003) Effect of aging on human muscle architecture. J Appl Physiol 95:2229–2234

O' Neill J (2008) Musculoskeletal ultrasound: anatomy and technique. Springer, New York

Peetrons P (2002) Ultrasound of muscles. Eur Radiol 12:35–43

Pillen S (2010) Skeletal muscle ultrasound. Eur J Transl Myol 1(4):145–155

Pillen S, Tak R, Lammens M, Verrijp K, Arts I, Zwarts M, Van Engelen B, Verrips A (2009) Skeletal muscle ultrasound: correlation between fibrous tissue and echo intensity. Ultrasound Med Biol 35:443–446

Rana M, Hamarneh G, Wakeling JM (2009) Automated tracking of muscle fascicle orientation in B-mode ultrasound images. J Biomech 42:2068–2073

Reimers K, Reimers CD, Wagner S, Paetzke I, Pongratz DE (1993) Skeletal muscle sonography: a correlative study of echogenicity and morphology. J Ultrasound Med 12:73–77

Zhao H, Zhang LQ (2011) Automatic tracking of muscle fascicles in ultrasound images using localized radon transform. IEEE Trans Biomed Eng 58:2094–2101

Zhou Y, Zheng YP (2008) Estimation of muscle fiber orientation in ultrasound images using revoting hough transform (RVHT). Ultrasound Med Biol 34: 1474–1481

Zhou Y, Zheng YP (2011) Longitudinal enhancement of the hyperechoic regions in ultrasonography of muscles using a Gabor filter bank approach: a preparation for semi-automatic muscle fiber orientation estimation. Ultrasound Med Biol 37:665–673

Muscles Dynamic US Analysis

5

Davide Orlandi, Angelo Corazza, and Piero Gatto

5.1 Dynamic Evaluation

With the patient in a comfortable position, the US exam should be started with the evaluation of the muscle *at rest* (Fig. 5.1a). Then the examiner continues the US exam with the first dynamic manoeuvre: the direct compression of the muscle with the probe helps to assess muscle thickness and also the elastic properties of the muscle fibres under compression. Further, in case of injury the compression could be helpful to squeeze muscular bundles and evaluate post-traumatic intramuscular fluid collection or subfascial haematoma, properly defining its content and extent.

Recently, direct compression could be performed both by means of grey scale US and sonoelastography, as explained below.

Then continue with the US evaluation during *active, passive and forced contraction* (Fig. 5.1b–d).

In particular, active contraction delineates the dynamic structural changes of the muscle-tendon-bone chain and its behaviour in case of pathology. Passive contraction applied by the operator helps to better evaluate the relationship between the adjacent anatomical structures during motion.

Forced contraction of a muscle and/or a muscular group, performed against appropriate resistance applied by the operator, could be very useful to highlight the presence of subtle tears. This latter dynamic evaluation reproduces the physiologic muscular dynamic during motion; indeed, it could be helpful also for the assessment of the stability of the healing tissue after fibres injury.

During forced contraction evaluation, a second operator could be necessary. Usually, in elite athletes, these functional tests are provided by the team medical doctor that assists the US examination.

A list of the most common dynamic manoeuvres, which could be performed during US examination, is illustrated in Table 5.1.

5.2 Architectural Features

As described above, US is able to evaluate muscular *architectural features*, such as *pennation angle*, *fibre orientation*, *fascicle length*, *fascicle curvature* and *muscle thickness*. These parameters correlate with force generation and are used in the evaluation of training in several types of sport. Therefore a proper application of muscle

D. Orlandi (✉) • A. Corazza
Dipartimento di Radiologia,
Università degli studi di Genova, Genova, Italy
e-mail: my.davideorlandi@gmail.com;
angelcoraz@libero.it

P. Gatto
Dipartimento di Ortopedia e Traumatologia,
IRCCS-AOU San Martino IST, Genova, Italy

Genoa CFC, Genoa, Italy

E. Silvestri et al., *Ultrasound Anatomy of Lower Limb Muscles: A Practical Guide*,
DOI 10.1007/978-3-319-09480-9_5, © Springer International Publishing Switzerland 2015

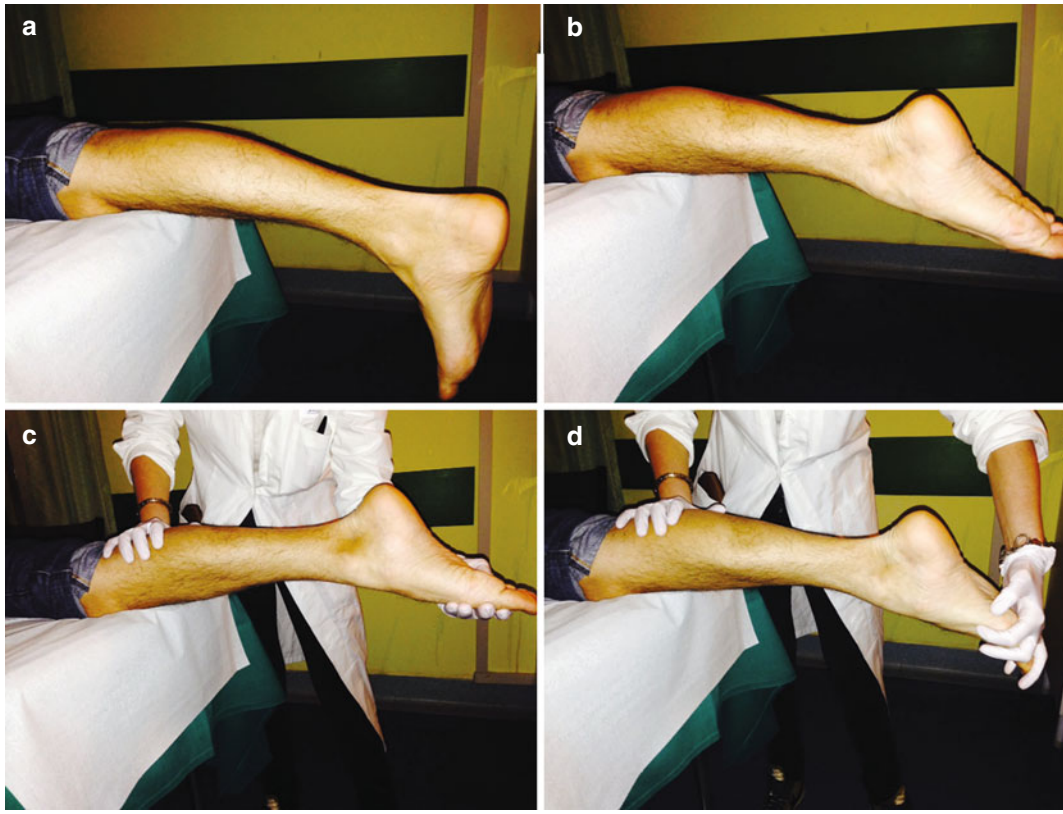

Fig. 5.1 Lower leg (**a**) dynamic evaluation during active, passive and forced contraction (**b–d**)

Table 5.1 List of the most common dynamic manoeuvres

Muscle	Patient decubitus	Patient action	Operator manoeuvre
Tensor fasciae latae	Supine; hands holding the table	Hip abduction, flexion and medial rotation	The hand pushes the anterolateral aspect of the leg, in the direction of the extension and adduction (not apply rotator force vectors)
Iliopsoas	Supine; leg extended with slight abduction and lateral rotation	Hip flexion	One hand fixes the contralateral side of the hip pushing down the contralateral iliac crest The other hand pushes the anteromedial aspect of the leg in the direction of hip extension and slight abduction
Gluteus maximus	Prone; knee 90° flexed	Hip extension with flexed knee	One hand fixes the hip pushing down the iliac crest The other hand pushes the posterior thigh in the direction of hip flexion
Gluteus medius (and minimus)	Contralateral decubitus; leg extended	Hip abduction	One hand fixes the hip in neutral position The other hand pushes the leg in the direction of the hip adduction and slight flexion (slight extension for the minimus)
Femoral quadriceps	Seated with leg 90°over the edge of the table; hands holding the table edge	Knee extension	One hand under the thigh just cranial to the knee The other hand holds the calf cranial to the ankle and pushes it in the direction of leg flexion (not apply rotator force vectors)

Table 5.1 (continued)

Muscle	Patient decubitus	Patient action	Operator manoeuvre
Adductors	Supine in frog leg position	Hip adduction	One hand fixes the hip The other hand pushes the medial aspect of the distal thigh, in the direction of the abduction
Lateral hamstring (biceps femoris)	Prone; leg extended	Knee flexion with medial rotation of the thigh and, consequently of the leg	The hand holds the leg just cranial to the ankle and pushes it in the direction of the leg extension (not operate rotator force vectors)
Medial hamstrings (semitendinosus and semimembranosus)	Prone; leg extended	Knee flexion with lateral rotation of the thigh and consequently of the leg	The hand holds the leg just cranial to the ankle and pushes it in the direction of the leg extension (not operate rotator vectors)
Peroneal	Supine with internal rotation of the ankle	Foot eversion and plantar flexion	One hand holds the leg cranial to the ankle The other hand pushes the inferolateral aspect of the foot in the direction of the inversion of the foot and dorsiflexion of the ankle
Tibialis posterior	Supine with leg in lateral rotation	Foot inversion with plantar flexion of the ankle	One hand holds the calf just cranial to the ankle The other hand pushes the inferomedial aspect of the foot in the direction of the eversion of the foot and dorsiflexion of the ankle
Tibialis anterior	Supine	Ankle dorsiflexion and foot inversion (without hallucis extension)	One hand holds the calf just cranial to the ankle The other hand pushes the dorsimedial aspect of the foot in the direction of plantar flexion of the ankle and foot eversion
Plantar flexors (gastrocnemius)	Prone; leg extended and foot over the edge of the table	Plantar flexion of the ankle	One hand holds the forefoot and opposes plantar flexion The other hand holds the calcaneus and opposes to its cranial traction
Soleus (specific)	Prone; knee 90° flexed	Plantar flexion of the ankle	One hand holds the calf cranial to the ankle The other hand pushes the calcaneus caudally, in the direction of the ankle dorsiflexion (without inversion and/or eversion of the foot)

ultrasound is based on training regimes evaluation (force versus duration), effects of overuse, strain and sports injuries.

An important tip for the examiner is to evaluate these parameters also on the contralateral muscle to make a comparison.

Pennation angle and *physiological cross-sectional area* are important determinants of the maximum contraction force (maximal isometric contraction), while muscle fibre length is related to the speed of contraction.

As previously described, the muscle strength is directly proportional to the cosine of the pennation angle, so muscular strength and aerobic work increase with the increase of the pennation angle up to 90° when the force becomes zero (cos 90 = 0).

Cross-sectional area is a direct measurement of muscle size and could evaluate the muscular hypertrophy or hypotrophy. This architectural parameter is better evaluated in US axial scan (Fig. 5.2).

Muscular thickness, *fibre length* and *pennation angle* could be evaluated on a longitudinal US scan.

Muscle thickness could be measured in transversal or longitudinal images as the distance between the superficial and the deep fascia at the widest distance (Fig. 5.3).

The *pennation angle* (fascicle angles) is defined as the angle between fascicles, and aponeurosis is also measured on longitudinal plane (Fig. 5.4).

After the measurement in relaxed state, muscle fibres could be evaluated during contraction, appearing more hypoechoic and with a greater cross-sectional area (Fig. 5.5).

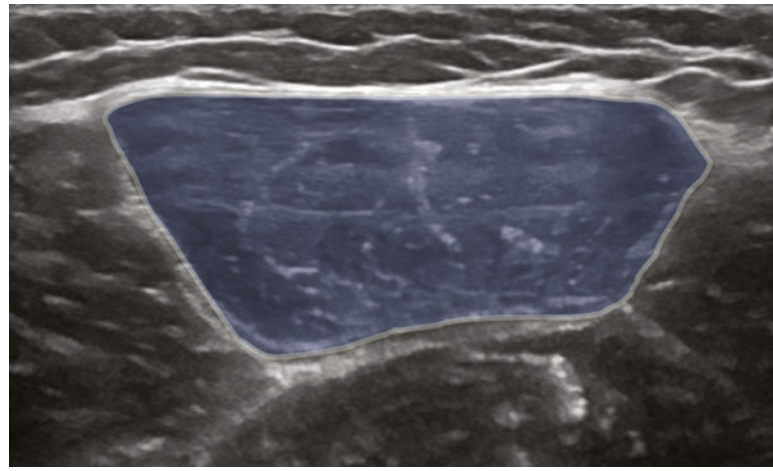

Fig. 5.2 US axial scan showing the cross-sectional area of rectus femoris muscle during contraction

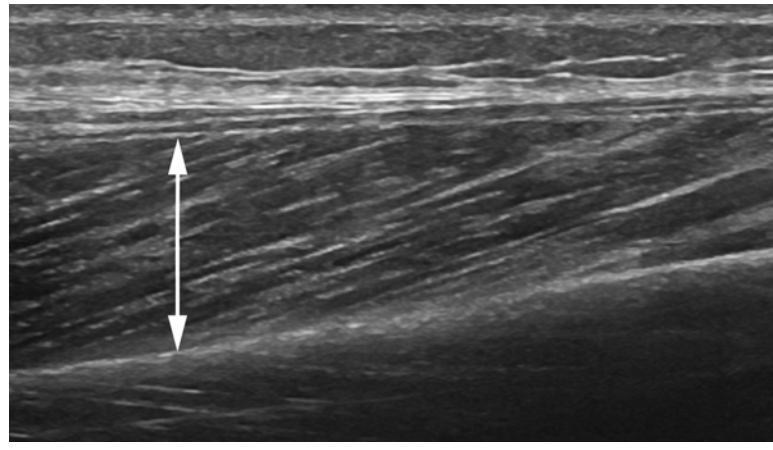

Fig. 5.3 US longitudinal scan showing the muscular thickness (*double-headed arrow*) of peroneus longus muscle at rest

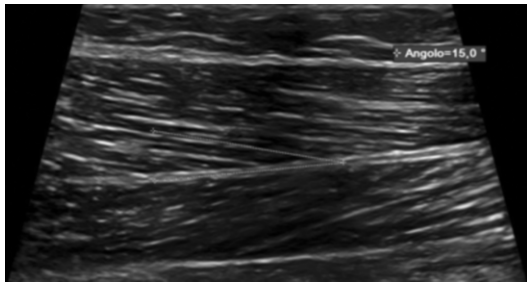

Fig. 5.4 US longitudinal scan showing the pennation angle (*dashed line*) of medial gastrocnemius muscle at rest

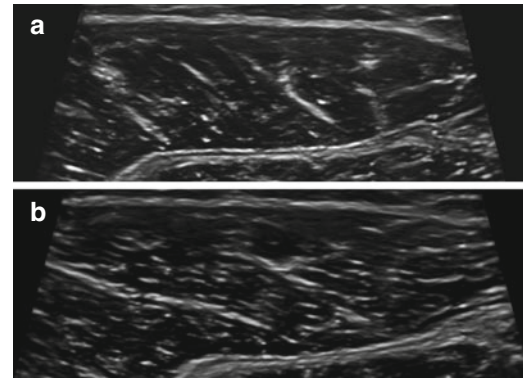

Fig. 5.5 US axial scan showing the cross-sectional area of medial gastrocnemius muscle at rest (**a**) and during active contraction (**b**)

Proceeding in the dynamic US scan on a longitudinal plane, *the fascicle lengths* are shorter than in the rest condition and the *muscular thickness* and the *pennation angle* significantly increase (Fig. 5.6).

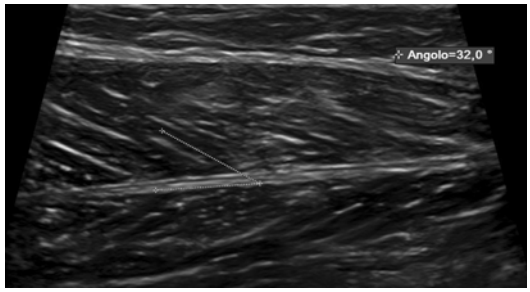

Fig. 5.6 US longitudinal scan showing the increment of the pennation angle (*dashed line*) of medial gastrocnemius muscle during active contraction

Therefore US could be used to measure the changes in muscle thickness, muscle fibre pennation angle, muscle fascicle length and muscle size during static and dynamic conditions.

5.3 Lower Limb Muscles Dynamic Manoeuvres

The table 5.1 reports specific dynamic manoeuvres developed for the assessment of the corresponding muscle or muscular group during active contraction. Further, the operator should progressively oppose resistance to the specific requested action to assess the tensile force during isometric contraction (Table 5.1 and Fig. 5.7).

Fig. 5.7 Examples of dynamic manoeuvres for the lower limb evaluation. Quadriceps muscles evaluation (**a**); adductor muscles evaluation (**b**); hamstring muscles evaluation (**c**); sural triceps muscles evaluation (**d**)

Suggested Reading

Bianchi S, Martinoli C, Abdelwahab IF, Derchi LE, Damiani S (1998) Sonographic evaluation of tears of the gastrocnemius medial head ("tennis leg"). J Ultrasound Med 17:157–162

Farris DJ, Sawicki GS (2012) Human medial gastrocnemius force–velocity behavior shifts with locomotion speed and gait. Proc Natl Acad Sci 109:977–982

Fukunaga T, Ichinose Y, Ito M, Kawakami Y, Fukashiro S (1997) Determination of fascicle length and pennation in a contracting human muscle in vivo. J Appl Physiol 82:354–358

Manal K, Roberts DP, Buchanan TS (2008) Can pennation angles be predicted from EMGs for the primary ankle plantar and dorsiflexors during isometric contractions? J Biomech 41:2492–2497

Martinoli C, Bianchi S (2007) Ultrasound of the musculoskeletal system. Springer, Berlin

Miyoshi T, Kihara T, Koyama H, Yamamoto SI, Komeda T (2009) Automatic detection method of muscle fiber movement as revealed by ultrasound images. Med Eng Phys 31:558–564

O' Neill J (2008) Musculoskeletal ultrasound: anatomy and technique. Springer, New York

Shi J, Zheng Y, Chen X, Huang Q (2007) Measurement of muscle fatigue with sonomyography: dimensional change of muscles detected from ultrasound images. Med Eng Phys 29:472–479

Zheng YP, Chan M, Shi J, Chen X, Huang QH (2006) Sonomyography: monitoring morphological changes of forearm muscles in actions with the feasibility for the control of powered prosthesis. Med Eng Phys 28:405–415

Zhou Y, Li J-Z, Zhou G, Zheng Y-P (2012) Dynamic measurement of pennation angle of gastrocnemius muscles during contractions based on ultrasound imaging. Biomed Eng Online 11:63. http://www.biomedical-engineering-online.com/content/11/1/63

Muscle Injuries: Pathophysiology and New Classification Models

6

Nicola Maffulli, Angelo Del Buono, and Enzo Silvestri

6.1 Anatomy and Biomechanics

Muscle lesions, a high percentage of all acute sports injuries, are frequent in high-demand athletes. Hamstrings, rectus femoris, and medial head of the gastrocnemius are the most commonly involved. They all contain a great percentage of type II fibers, a pennate architecture, and cross two joints and are injured during the eccentric phase of muscle contraction. This chapter describes pathophysiology of acute muscle injuries and, specifically, acute strains. These lesions have a significant impact on the athletes and their teams, but it is often difficult to predict short-term outcome and long-term prognosis. Predisposing factors and mechanisms of injury are described, and a new model of classification is showed. The object is to aid in the prevention, proper diagnosis, and management of these lesions.

6.2 Muscle Injury Classification

Acute injuries may result from direct and indirect trauma. When the insult to the muscle is direct, it produces a contusion at the point of contact; if the injury is indirect, without any contact, some myofibers are disrupted. Indirect injuries are passive or active. Specifically, passive injuries are the result of tensile overstretching forces without contraction; active lesions occur after eccentric overloads on the muscle. Contusions and strains account for more than 90 % of all sports-related skeletal muscle injuries, and lacerations are uncommon. Contusions occur in contact or combat sports after application of large compressive forces on the muscle. Muscle strains, very common in sprinters and jumpers, usually arise from an indirect trauma, from application of excessive tensile forces. Lacerations, rare in athletes, arise from direct blunt trauma to the epimysium and underlying muscles.

In *grade I injury (strain)*, the lesion involves a few muscle fibers, swelling and discomfort are complained, and strength and function are minimally impaired. US findings are often normal, with evidence of some perifascial fluid

N. Maffulli (✉)
Department of Musculoskeletal Disorders, University of Salerno, Salerno, Italy

Centre for Sports and Exercise Medicine, Barts and The London School of Medicine and Dentistry, Mile End Hospital, 275 Bancroft Road, London E1 4DG, UK
e-mail: n.maffulli@qmul.ac.uk

A. Del Buono
Department of Orthopaedic and Trauma Surgery, Ospedale Sant'Anna, San Fermo della Battaglia (Como), Como, Italy

E. Silvestri
Struttura Complessa di Diagnostica per Immagini ed Ecografia Interventistica, Ospedale Evangelico Internazionale, Genoa, Italy
e-mail: silvi.enzo@gmail.com

E. Silvestri et al., *Ultrasound Anatomy of Lower Limb Muscles: A Practical Guide*,
DOI 10.1007/978-3-319-09480-9_6,

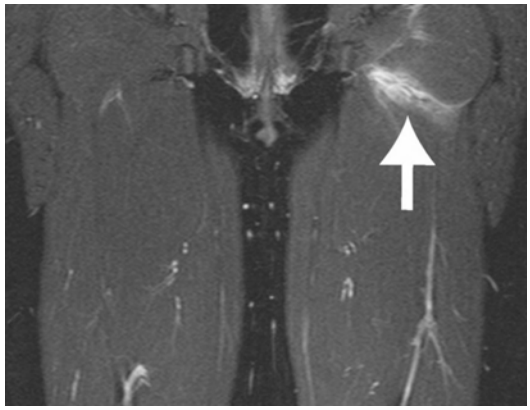

Fig. 6.1 Image of feathery edema-like pattern: intramuscular high signal (*arrow*), with no discernible muscle fiber disruption

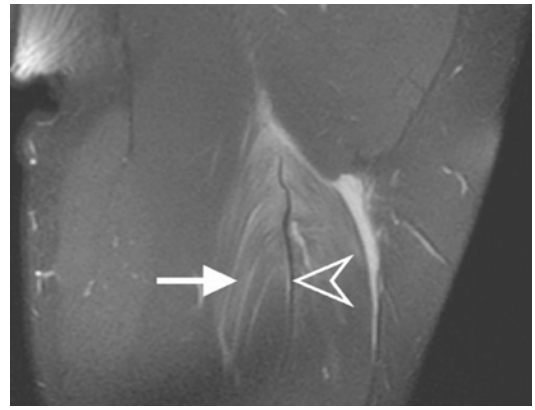

Fig. 6.2 Edema and hemorrhage of the muscle (*arrow*) or MTJ (*arrowhead*) extended to the fascial planes

in almost 50 % of the patients. At MR imaging, a classic "feathery" edema-like pattern may appear on fluid-sensitive sequences. Some fluid may appear in the central portion of the tendon and along the perifascial intermuscular region, without discernible disruption of muscle fibers or architectural distortion (Fig. 6.1).

In grade II Injury, a partial tear is macroscopically evident, with some continuity of fibers at the injury site. Less than one third of fibers are torn in low-grade injuries, from one third to two thirds in moderate ones, and more than two thirds in high-grade injuries. Muscle strength and high-speed/high-resistance athletic activities are impaired, with marked loss of muscle function. At US, muscle fibers are discontinuous, the disruption site is hypervascularized, and echogenicity is altered in and around the lesion. At MRI, appearance varies with both the acuity and the severity of the partial tear, changes are time dependent, and edema and hemorrhage of the muscle or MTJ may extend along the fascial planes, between muscle groups (Fig. 6.2). MRI can sometimes be predictive of the time high performance athletes will be away from play.

A grade III injury is a complete tear. At US and MR imaging, these injuries show complete discontinuity of muscle fibers, hematoma, and retraction of the muscle ends (Fig. 6.3). Clinically, muscle function is lost. When extensive edema and hemorrhage fill the defect between the torn edges, it is difficult to distinguish partial from complete tears, whereas real-time dynamic US imaging may be helpful.

Fig 6.3 Grade III tear. Muscle fibers are completely interrupted (*blue arrows*) with evidence of associated hematoma (*red arrow*) and muscle edema (*arrowheads*)

6.3 Predisposing Factors

Traumatic muscle injuries vary on the directions and angle movements of forces applied. Contusions, strains, or lacerations may be distinguished. Contusions and strains account for

more than 90 % of all sports-related skeletal muscle injuries, and lacerations are uncommon. Contusions occur in contact or combat sports after application of large compressive forces on the muscle. Muscle strains, very common in sprinters and jumpers, usually arise from an indirect trauma, from application of excessive tensile forces. Muscle lacerations, rare in athletes, arise from direct blunt trauma to the epimysium and underlying muscles.

Three types of muscle are at possible risk for injury:

1. *Two-joint muscles*. In such instance, the motion at one joint may increase the passive tension of the muscle and lead to an overstretch injury.
2. *Muscles contracting eccentrically*. Concentric and eccentric contractions are normally performed in functional activities. Specifically, eccentric contractions, common in the deceleration phase of activity, may induce acute strains by producing specific tensions which lead to myofiber overload injury.
3. *Muscles with a higher percentage of type II fibers*. These are fast-twitch muscles, in which speed of contraction produced is greater than in other muscles, predisposing a muscle to injury. The fact that most of the muscle action involved in running and sprinting is eccentric, muscle strains most often occur in sprinters or "speed athletes." In these sports, the muscles more susceptible to be strained are the hamstrings, gastrocnemius, quadriceps, hip flexors, hip adductors, erector spinae, deltoid, and rotator cuff.

The coordination and balance between agonist and antagonist muscles has to be taken into account. Specifically, flexibility imbalances between agonists and antagonists may predispose to injury. Flexible muscles are most likely to be injured. A previous injury makes more vulnerable to re-injury, justifying that sprinters with recent hamstring injuries have tighter and weaker hamstrings than uninjured those.

When rehabilitation is inadequate, strength, flexibility, and endurance may not be completely restored before return to activity. Therefore, residual weakness and impairment may predispose the muscle to a new injury. From the assumption that cold or tight muscles are more predisposed to muscular strain, proper stretching exercises and warm-up may prevent muscular injury. After warm-up, muscle elongation before failure is increased. In addition, since warm muscles (40 °C) are less stiff than cold (25 °C) muscles, warm-up may prevent and enhance performance.

6.4 Structural Changes

The most vulnerable site for an indirect strain injury is the musculotendinous junction, the weakest link within the muscle tendon unit. In eccentric muscle actions, when muscle tension increases suddenly, the damage may occur in the area beneath the epimysium and the site of muscle attachment to the periosteum. In fascial injuries, common in the medial calf and biceps femoris, differential contractions of adjacent muscle bellies may produce aponeurotic distraction injuries. Hamstring strain muscle injuries, the most widely studied, typically occur in the region of the MTJ, a transition zone organized in a system of highly folded membranes, designed to increase the junctional surface area and dissipate energy (Fig. 6.4). The region adjacent to the MTJ is more susceptible to injury than any

Fig. 6.4 US-guided hamstrings MTJ fluid aspiration. This transition zone is organized in a system of highly folded membranes, designed to increase the junctional surface area and dissipate energy

other component of the muscle unit, independently from type and direction of applied forces and muscle architecture. In this area, even a minor strain, by inducing an incomplete disruption, evident only at microscopy, may weaken it and predispose to further injury. Disruptions in the fibers cause biochemical changes both from direct injury to the fibers and from the inflammatory reaction.

6.5 Biochemical Changes

Serum creatine kinase (CK) and lactate dehydrogenase (LDH) enzyme levels are used to indirectly assess muscle damage following eccentric exercise. These biochemical markers are released after the insult. In addition, inflammatory reactions occur. Acute inflammation is designed to protect, localize, and remove injurious agents from the body and promote healing and repair. Chemical inflammatory mediators are present in acute muscular strain, such as histamine, serotonin, bradykinin, and prostaglandin. The capillary membrane permeability is increased, blood vessel diameter is changed, and pain receptors are stimulated. As consequence, the accumulation of proteins and transudate in the interstitial space produces edema. Therefore, swelling, heat, redness, and pain of inflammation are due to biochemical changes stimulated by chemical mediators. Inflammatory reaction and edema at 1–2 days after a stretch-induced muscular injury. The acute phase of inflammation lasts up to 3–4 days after the initial insult. Proliferation of fibroblasts, increased collagen production, and degradation of mature collagen weaken the tissue. In this way, stretching the tissue induces progressive irritation and limitation, up to predisposing to chronic muscle strains. When the inflammatory phase subsides, repair is started, for 2–3 weeks. Specifically, capillary growth and fibroblast activity to form immature collagen are promoted. This immature collagen is easily injured if overstressed. The final stage of healing is maturation and remodeling of collagen, occurring from 2 to 3 weeks after the insult, until patients are pain-free. In the healing phase, if fibers are not properly stressed, surrounding adhesions and scar resilient to remodeling may be formed.

6.6 Treatment of Acute Strains

Management varies on the severity of the injury, the natural healing process of the body, and the response of the tissue to new demands.

The overall goal is to assist and respect the body with its natural healing process. Therefore, the athletic trainer must not return the athlete to activity too soon. Two to three weeks of restricted activity are necessary to allow collagen formation and prevent re-injury.

Inflammatory Phase. Rest, ice, compression, and elevation (RICE) are indicated for at least 48 h. Rest protects the injured tissue, but immobilization may be detrimental to healing and uninjured tissues. Ice slows the inflammatory process and decreases pain and muscle spasm; compression and elevation reduce edema. Crutches are also recommended. When the inflammation subsides, passive range of motion (ROM) and gentle mobilization should be initiated to maintain soft tissue and joint integrity. Submaximal isometric muscle sets may be used at multiple angles to maintain strength and keep the developing scar tissue mobile. Aggressive stretching and strengthening should be avoided. Electrical stimulation and pulsed ultrasound should be used during both the inflammatory and repair phases to reduce pain and edema.

Repair Phase. The inflammatory and repair phases overlap during the first week after injury. An early accelerated rehabilitation program may prolong the inflammatory phase and lead to chronic muscle strain. When collagen is formed, it must be appropriately stressed in the normal lines of tension. Signs of inflammation (pain, swelling, redness, warmth) are signs of tissue overstress and allow to assess the rehabilitation program. Frequency, intensity, and duration of exercises are altered to allow for healing and to prevent inflammation for the next 1–2 weeks.

Cold may be beneficial initially to allow for pain-free exercise and aid in the formation of the scar tissue. Gentle, pain-free stretching and pain-free submaximal isometrics can be incorporated into contract-relax techniques to help align collagen fibers. A cardiovascular conditioning program should be incorporated for any athlete not capable of full athletic participation.

Maturation and Remodeling Phase. When collagen is mature, tension should be applied in the line of normal stresses to remodel properly. This stage presents at about 2–3 weeks after injury and is characterized by (1) the absence of inflammation; (2) full, pain-free ROM; and (3) pain after tissue resistance (passive ROM). The athlete is progressed as tolerated with limited participation in his/her sport. More vigorous stretching, closed- and open-chain strengthening, cardiovascular training, and sport-specific activities are allowed. Muscles must be stressed and overloaded in the manner in which they are used functionally, following the principle of specificity. Specifically, type of contraction (eccentric vs concentric), metabolism (aerobic vs anaerobic), and functional pattern (diagonal vs cardinal plane) of the muscle should be respected. Eccentric exercise is functional in most athletic activities, develops greater tension than concentric exercise, and may be more comfortable in the early stages of rehabilitation.

Proprioceptive and endurance training are used in the advanced stages of rehabilitation. After the athlete has regained full, pain-free active ROM and over 90 % strength bilaterally, full participation is allowed. Maintenance programs should be continued to avoid any dysfunctional adaptation or compensation.

6.7 Prevention of Acute Strains

Prevention of acute muscular strains implies adequate preseason screening of flexibility and strength balances in major joints (knee, shoulder, and ankle). Flexibility, strength, endurance, and proprioception should be also assessed. Adequate agonist/antagonist ratios for strength and flexibility should be attained for major muscle groups, and muscles must be strengthened in the mode in which they are used functionally. Warm-up and stretching before activity are recommended. Specifically, active warm-up such as jogging or biking should be helpful before specific muscle stretching, especially in two joint muscles at high risk for strain, muscles with high percentages of fast-twitch fibers (hamstrings, gastrocnemius, quadriceps, biceps), and those with high incidence of strain (hip flexors, hip adductors, erector spinae, rotator cuff). Muscles which contract eccentrically or decelerate in functional high-speed activities, such as the posterior rotator cuff in throwing athletes or the hamstrings in sprinters, should be stretched for 15–20 s and repeated four times.

6.8 New Concepts

We have proposed a recent anatomic classification of acute muscles strain injuries. We propose to distinguish muscular, MTJ (proximal and distal), and tendon injuries (proximal and distal). Considering the anatomy, muscular lesions can be further classified as intramuscular, myofascial, myofascial/perifascial, musculotendinous, or a combination. With regard to the site of injury, we classify muscular injuries as proximal, middle, and distal. The severity of the muscular and musculotendinous injuries is classified according to a 3-grade classification system from MRI and US.

Conclusion

Clinical assessment, site of injury, and pathophysiology can all provide prognostic information regarding convalescence and recovery time following an acute muscle strain injury. The anatomical system we proposed must be assessed with multiple joints to determine its utility. Well-planned, appropriately powered clinical research should be performed to determine whether the classification system put forward in the present chapter can be applied in clinical practice and be of greater value than current systems.

Suggested Reading

Askling CM, Tengvar M, Saartok T, Thorstensson A (2007) Acute first-time hamstring strains during high-speed running: a longitudinal study including clinical and magnetic resonance imaging findings. Am J Sports Med 35:197–206

Bach BR Jr, Warren RF, Wickiewicz TL (1987) Triceps rupture. A case report and literature review. Am J Sports Med 15:285–289

Best TM (1995) Muscle-tendon injuries in young athletes. Clin Sports Med 14:669–686

Chan O, Del Buono A, Best TM, Maffulli N (2012) Acute muscle strain injuries: a proposed new classification system. Knee Surg Sports Traumatol Arthrosc 20:2356–2362

Crisco JJ, Jokl P, Heinen GT, Connell MD, Panjabi MM (1994) A muscle contusion injury model. Biomechanics, physiology, and histology. Am J Sports Med 22:702–710

El-Khoury GY, Brandser EA, Kathol MH, Tearse DS, Callaghan JJ (1996) Imaging of muscle injuries. Skeletal Radiol 25:3–11

Friden J, Sjostrom M, Ekblom B (1983) Myofibrillar damage following intense eccentric exercise in man. Int J Sports Med 4:170–176

Garrett WE (1990) Jr. Muscle strain injuries: clinical and basic aspects. Med Sci Sports Exerc 22:436–443

Garrett WE (1996) Muscle strain injuries. Am J Sports Med 24:S2–S8

Garrett WE Jr, Rich FR, Nikolaou PK, Vogler JB 3rd (1989) Computed tomography of hamstring muscle strains. Med Sci Sports Exerc 21:506–514

Jarvinen MJ, Lehto MU (1993) The effects of early mobilisation and immobilisation on the healing process following muscle injuries. Sports Med 15:78–89

Jarvinen TA, Jarvinen TL, Kaariainen M, Kalimo H, Jarvinen M (2005) Muscle injuries: biology and treatment. Am J Sports Med 33:745–764

Kneeland JP (1997) MR imaging of muscle and tendon injury. Eur J Radiol 25:198–208

Koh ES, McNally EG (2007) Ultrasound of skeletal muscle injury. Semin Musculoskelet Radiol 11:162–173

Koulouris G, Connell D (2005) Hamstring muscle complex: an imaging review. Radiographics 25:571–586

Lee JC, Healy J (2004) Sonography of lower limb muscle injury. AJR Am J Roentgenol 182:341–351

Malliaropoulos N, Isinkaye T, Tsitas K, Maffulli N (2011) Reinjury after acute posterior thigh muscle injuries in elite track and field athletes. Am J Sports Med 39:304–310

Nikolaou PK, Macdonald BL, Glisson RR, Seaber AV, Garrett WE (1987) Biomechanical and histological evaluation of muscle after controlled strain injury. Am J Sports Med 15:9–14

Noonan TJ, Best TM, Seaber AV, Garrett WE (1993) Thermal effects on skeletal muscle tensile behavior. Am J Sports Med 21:517–522

Page P (1995) Pathophysiology of acute exercise-induced muscular injury: clinical implications. J Athl Train 30:29–34

Stauber WT (1989) Eccentric action of muscles: physiology, injury, and adaptation. Exerc Sport Sci Rev 17:157–185

Strickler T, Malone T, Garrett WE (1990) The effects of passive warming on muscle injury. Am J Sports Med 18:141–145

Taylor DC, Dalton JD Jr, Seaber AV, Garrett WE (1993) Experimental muscle strain injury. Early functional and structural deficits and the increased risk for reinjury. Am J Sports Med 21:190–194

Part II

Thigh Muscles

Sartorius and Tensor Fasciae Latae

7

Davide Orlandi, Enzo Silvestri,
and Luca Maria Sconfienza

7.1 Sartorius

7.1.1 Anatomy Key Points

The *sartorius muscle* is the longest muscle in the human body. It is a long, thin strip-like muscle that runs down all the length of the thigh (Fig. 7.1).

Its upper portion forms the lateral border of the femoral triangle (Scarpa's triangle) (Fig. 8.2).

The sartorius muscle arises from the anterior-superior iliac spine (ASIS) as well as from the notch just below the ASIS and then travels inferomedially crossing the upper third of the thigh.

It descends behind the medial condyle of the femur and inserts on the inner tibial tuberosity via an aponeurotic expansion that covers the tendons of the gracilis and semitendinosus muscles forming the *pes anserinus* (Fig. 10.14).

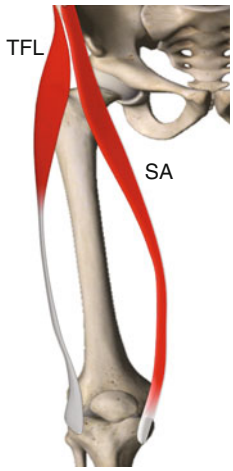

Fig. 7.1 Anatomical scheme of tensor fasciae latae (*TFL*) and sartorius (*SA*) muscles

D. Orlandi (✉)
Dipartimento di Radiologia,
Università degli studi di Genova, Genoa, Italy
e-mail: my.davideorlandi@gmail.com

E. Silvestri
Struttura Complessa di Diagnostica per Immagini ed Ecografia Interventistica, Ospedale Evangelico Internazionale, Genoa, Italy
e-mail: silvi.enzo@gmail.com

L.M. Sconfienza
Unità di radiologia, IRCCS Policlinico San Donato, Milan, Italy

Dipartimento di scienze biomediche per la salute, Università degli studi di Milano, Milan, Italy
e-mail: io@lucasconfienza.it

E. Silvestri et al., *Ultrasound Anatomy of Lower Limb Muscles: A Practical Guide*,
DOI 10.1007/978-3-319-09480-9_7,

The sartorius lies superficially to vastus intermedius, vastus lateralis and adductor longus muscles, and in its entire course, the muscle is covered by a duplication of the fascia lata.

The sartorius muscle innervation is supplied by the superficial branch of the femoral nerve, which is responsible for both sensory and motor components.

The blood supply comes from the muscular branches of the femoral artery.

The sartorius muscle is a two-joint muscle and moves both the hip and knee joint. Its main function is flexion, adduction and lateral rotation of the hip also helping the knee flexion and inward rotation.

7.1.2 Ultrasound Examination Technique

Start the examination of the sartorius muscle with the patient supine, with the lower limb in a neutral position. Then palpate the anterior-superior iliac spine (ASIS), which can be considered an important bony landmark for US examination (Fig. 7.2).

Place the transducer in an axial plane on the ASIS and visualize the two short tendons of the *sartorius* (medial) and the *tensor fasciae latae* (lateral) in a sagittal plane. In this scan plane, it is possible to identify the typical 'pseudothyroid' aspect with the hyperechoic cortical band between the two proximal insertions of the *sartorius* (medial) and *tensor fasciae latae* (lateral) muscles that present a hyperechoic fibrillar structure (Fig. 7.3).

Rotate the probe by 90° to evaluate the insertion on the ASIS in the longitudinal plane (Fig. 7.4).

Then shift the probe downwards following the sartorius muscle belly: this is the only muscle that can be seen superficially to rectus femoris, directing medially towards the medial thigh (Fig. 7.5).

Fig. 7.2 Lower limb position to evaluate the sartorius muscle

The sartorius muscle presents a typical triangular shape and lies superficially just under the fascia and the subcutaneous tissues.

Evaluate the myotendinous junction on axial and longitudinal plane (Figs. 7.6 and 7.7).

Then swipe the transducer distally on an axial scan to reach the distal insertion of the sartorius tendon on the anteromedial surface of the superior aspect of the tibial shaft (Fig. 7.8).

Turn the probe by 90° to evaluate the distal attachment of sartorius tendon on its long axis (Fig. 7.9).

Remember that the femoral vascular bundle is located in strict relationship with the sartorius muscle, representing an important landmark

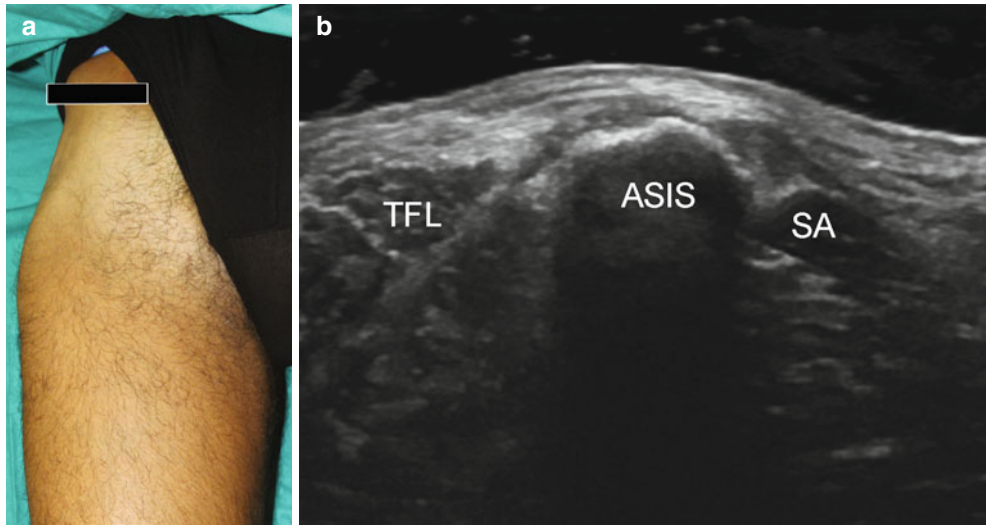

Fig 7.3 (**a**) Probe position for ASIS (anterior-superior iliac spine) evaluation on the axial plane. (**b**) US axial scan at ASIS level: note the proximal insertion of sartorius (*SA*) and tensor fasciae latae (*TFL*) muscles

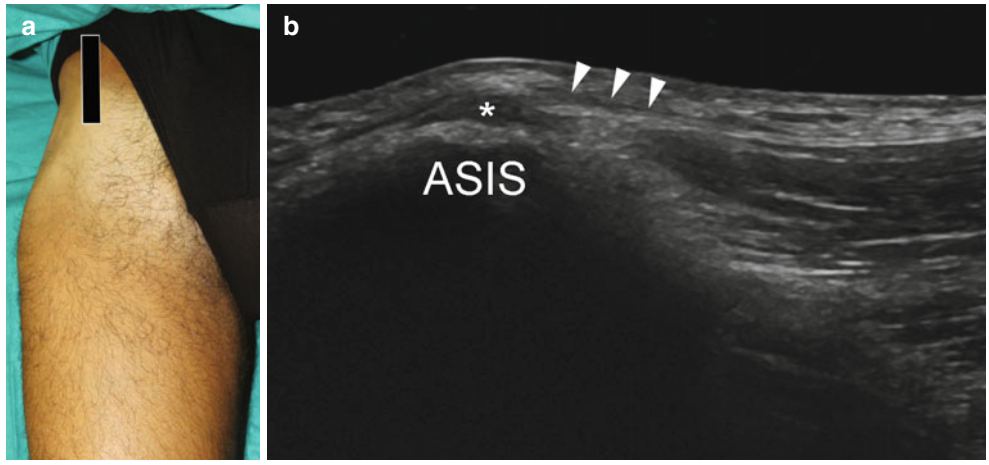

Fig 7.4 (**a**) Probe position for ASIS (anterior-superior iliac spine) evaluation on the longitudinal plane. (**b**) US longitudinal scan at ASIS level: note the proximal insertion (*) of sartorius and its myotendinous junction (*arrowheads*)

during its examination at the middle third of the thigh.

At this level the sartorius, the vastus medialis and the adductor magnus muscles delimitate the medial, anterolateral and posteromedial aspect of the Hunter's canal, respectively (Fig. 7.10).

Finally replace the transducer on the ASIS, medially to the attachment of the inguinal ligament, to identify the lateral femoral cutaneous nerve. This nerve can be seen as a small fasciculate structure crossing the lateral end of the inguinal ligament.

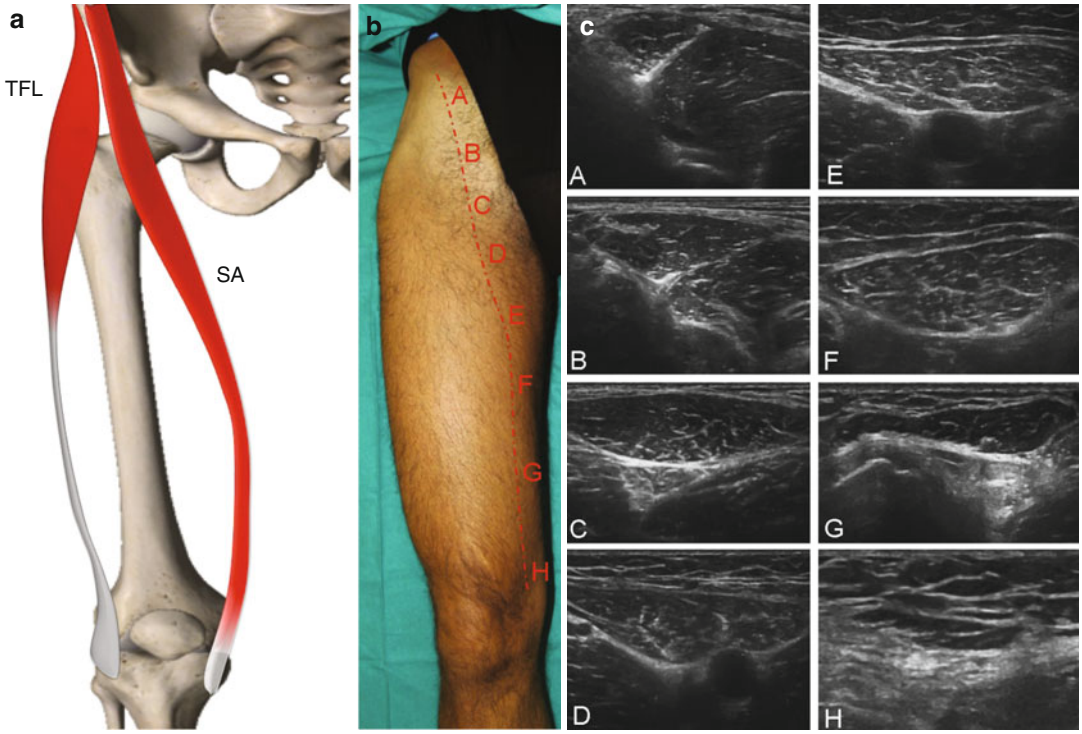

Fig. 7.5 (**a**) Anatomical scheme of tensor fasciae latae (*TFL*) and sartorius (*SA*) muscles. (**b**) US probe path to explore SA muscle from proximal to distal insertion; (**c**) US axial scans demonstrate SA muscle belly at different level of the thigh (**A–H**)

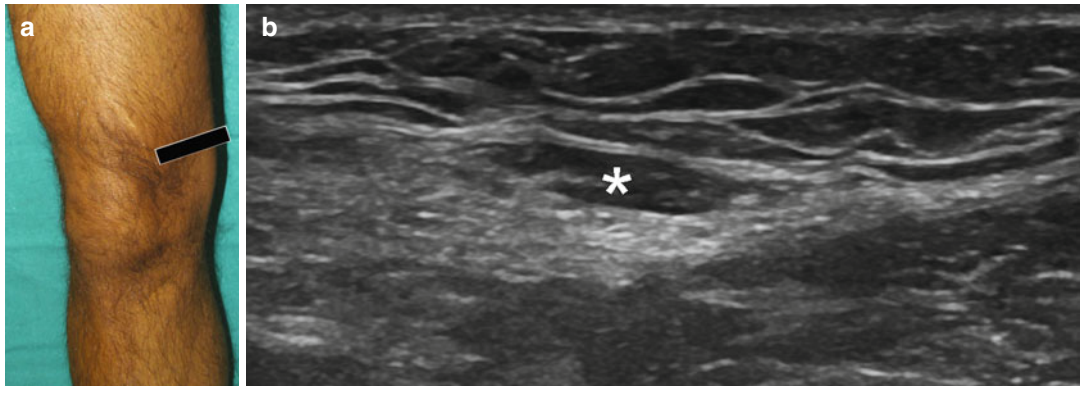

Fig. 7.6 (**a**) Probe position to explore the myotendinous junction on axial plane. (**b**) US axial scan of myotendinous junction of sartorius muscle (*)

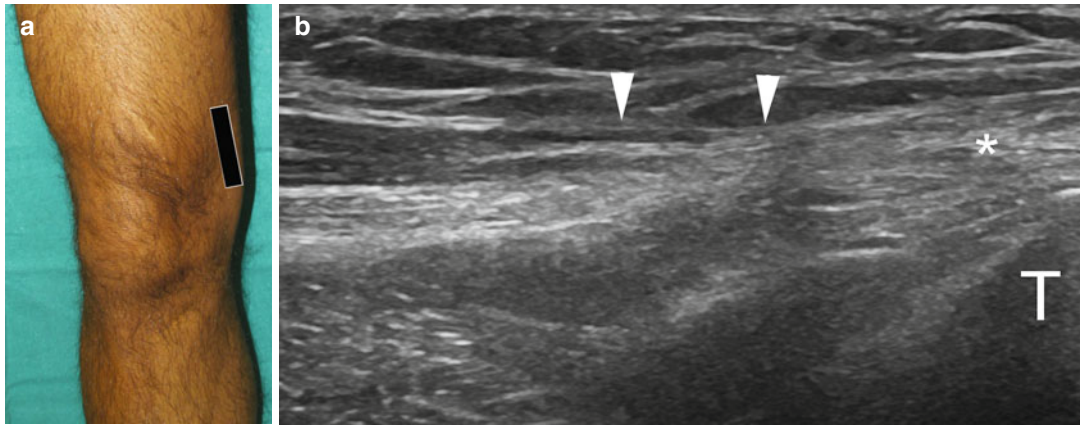

Fig. 7.7 (**a**) US probe position to explore the myotendinous junction on longitudinal plane. (**b**) US longitudinal scan of myotendinous junction (*arrowheads*) of sartorius muscle and tendon (*). *T* tibial shaft

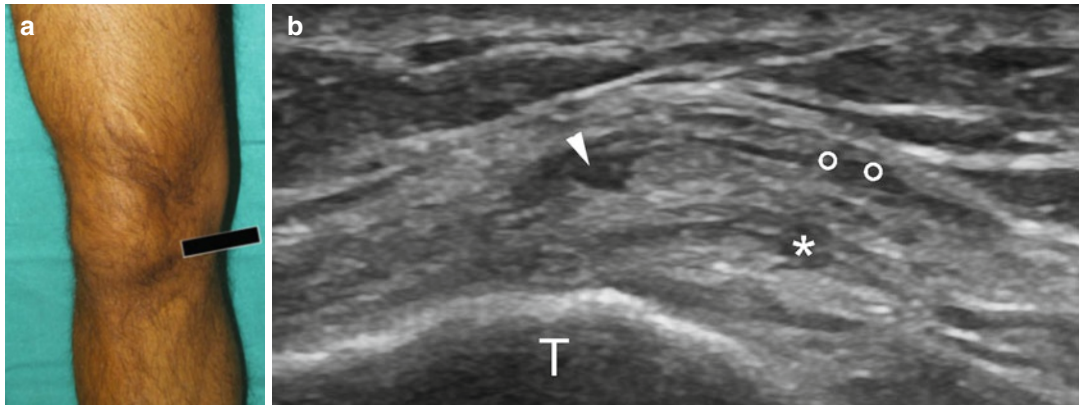

Fig. 7.8 US probe position (**a**) and US axial plane (**b**) to explore the distal insertion of the SA muscle (*circles*) on the surface of the tibia medial to the tibial tuberosity, just anterior to the gracilis (*) and the semitendinosus tendons (*arrowhead*). *T* tibial shaft

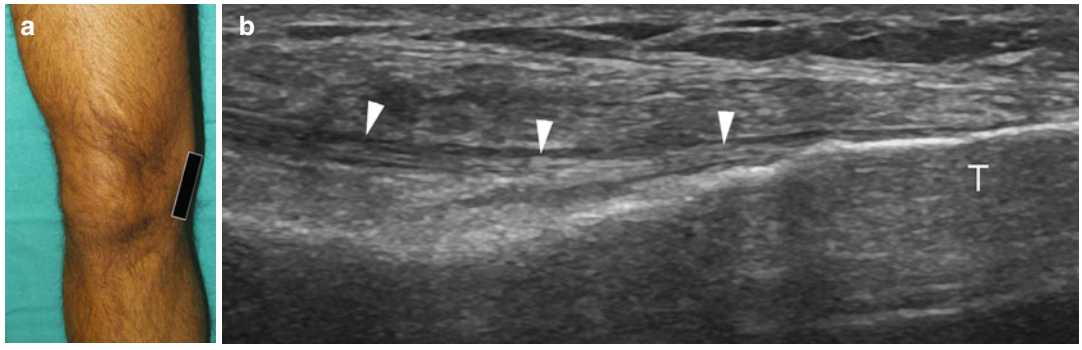

Fig. 7.9 US probe position (**a**) and US longitudinal plane (**b**) to explore the pes anserinus (*arrowheads*). *T* tibial shaft

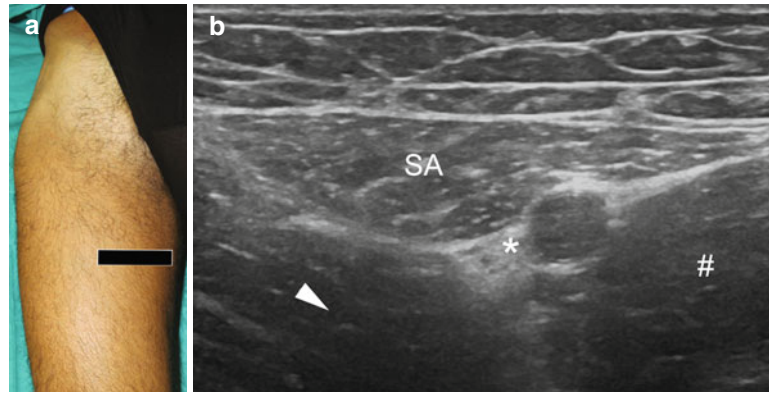

Fig. 7.10 (**a**) Patient and US probe position for the assessment of the proximal third of the sartorius muscle (*SA*) on an axial scan plane; (**b**) US axial scan: in the proximal third of the thigh SA is in a superficial position, coursing under the fascia and in strict relationship with the femoral vascular bundle (*). *Arrowhead* vastus medialis, # adductor longus

7.1.3 Summary Table

Muscle	Origin	Insertion	Action	Innervation
Sartorius	Anterior-superior iliac spine and the region just below it	Anteromedial margin of the superior aspect of the tibial shaft	Flexion, abduction and lateral rotation of the thigh at the hip; flexion of the knee	Femoral nerve

7.2 Tensor Fasciae Latae

7.2.1 Anatomy Key Points

The tensor fasciae latae muscle is located in a very superficial position, just under the fascia on the anterolateral aspect of the hip (Fig. 7.1). It arises from the lateral aspect of the anterior-superior iliac spine and descends with its short belly over the anterolateral aspect of the proximal thigh. Then, it converge in the anterior edge of the fascia lata which is a fibrous lamina covering the lateral aspect of the thigh. This structure is also referred to as the 'iliotibial tract' and courses superficially along the lateral aspect of the thigh, from the lateral edge of the iliac crest down to its insertion into Gerdy's tubercle at the anterolateral aspect of the proximal tibial epiphysis.

7.2.2 Ultrasound Examination Technique

Start the US evaluation placing the probe on the anterosuperior iliac spine (ASIS), with a transverse orientation. The US image shows the 'pseudothyroid' typical aspect, with the iliac cortex simulating the trachea, and the sartorius (medially) and the tensor fasciae latae (laterally) origins simulating thyroid lobes (Fig. 7.3).

Proceed laterally and caudally following the tensor fasciae latae muscle belly, which courses superficially on the anterolateral aspect of the proximal thigh (Fig. 7.11).

Note that, this muscle has a more echogenic appearance than the others, due to a large amount of fatty tissue among its fascicles. At its proximal portion, tensor fasciae latae covers the gluteus medius muscle belly; more distally, it courses over the vastus lateralis muscle, whose fibres can be seen arising from the deep portion of the image and lateral to the rectus femoris proximal portion (Fig. 7.12).

In a scanning plane corresponding to the greater trochanter, turn the probe by 90° and follow the distal portion of the muscle converging in the antero-inferior aspect of the fascia lata and continuing into the iliotibial tract (Fig. 7.13).

At this level, when scanning patients suffering for hip trauma, remember also to investigate the superficial anatomical planes between the fascia and the subcutaneous tissue that are commonly distended by fluid (Morel-Lavallée syndrome).

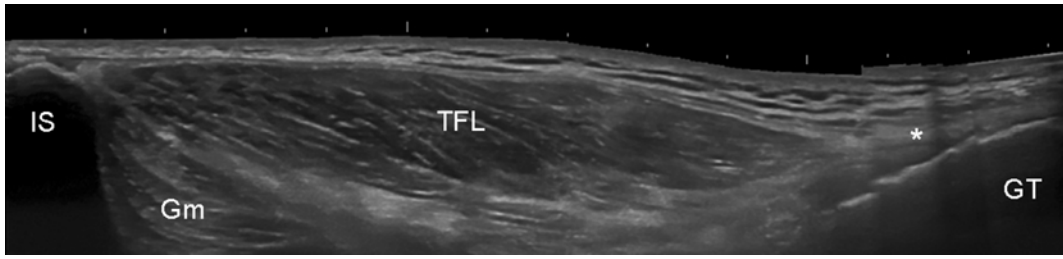

Fig. 7.11 Extended field of view; the longitudinal US scan shows the course of the tensor fasciae latae muscle (*TFL*) from the anterior-superior iliac spine (*IS*), passing over the gluteal muscles (*Gm*) to continue into the iliotibial tract (*asterisk*) at the level of the greater trochanter (*GT*)

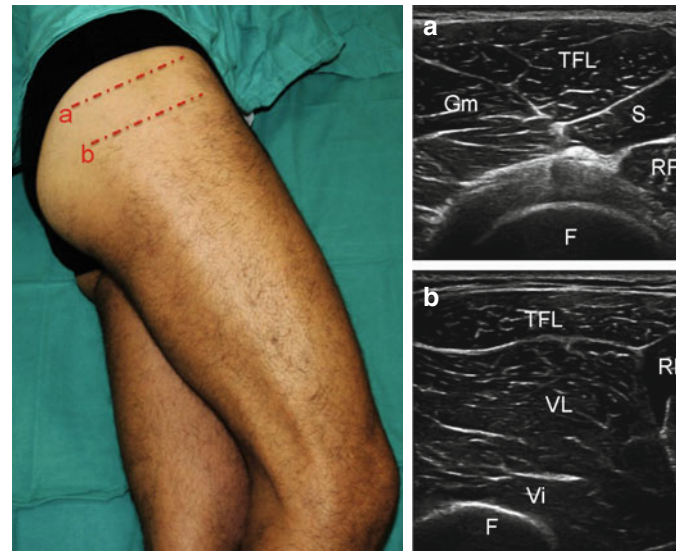

Fig. 7.12 Probe position over the lateral hip on different planes for the evaluation of the tensor fasciae latae muscle. (**a**) Corresponding more proximal US axial scan: gluteus medius muscle (*Gm*), tensor fasciae latae (TFL) muscle, sartorius muscle (S), rectus femoris muscle (*RF*) and femoral head (*F*) covered by the hip joint capsule. (**b**) Corresponding more distal US axial scan: vastus lateralis muscle (*VL*), vastus intermedius muscle (*VI*), tensor fasciae latae muscle (*TFL*), sartorius muscle (*S*), rectus femoris muscle (*RF*) and femur (*F*)

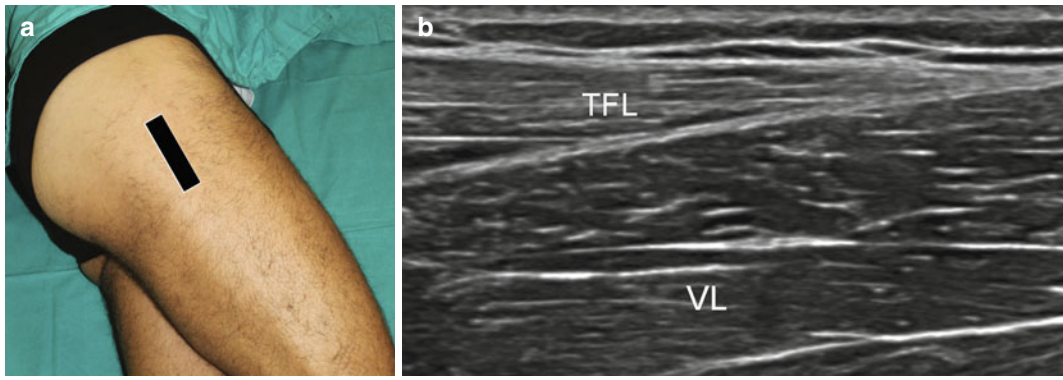

Fig. 7.13 (**a**) Probe position over the lateral hip for the evaluation of the tensor fasciae latae muscle. (**b**) Longitudinal-oblique US scan over the distal portion of the tensor fasciae latae muscle (*TFL*): see the tensor fasciae latae fibres in a superficial position and the muscular fibres of the vastus lateralis (*VL*) passing just deep to it

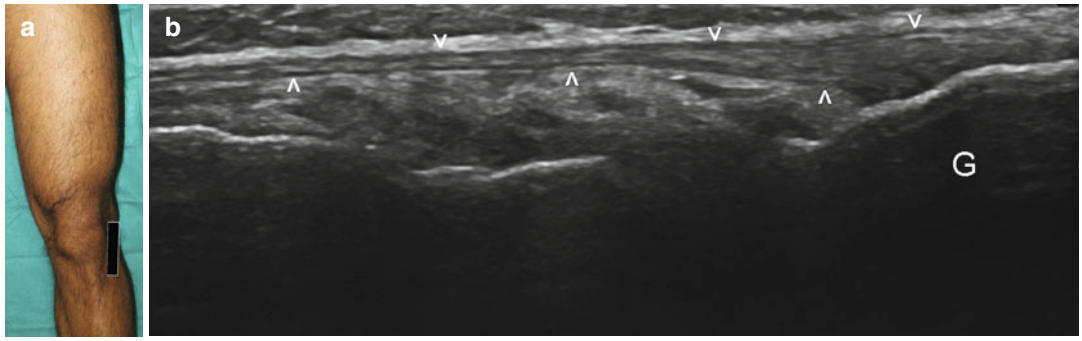

Fig. 7.14 (**a**) Probe position over the anterolateral knee for the evaluation of the iliotibial tract insertion. (**b**) Corresponding longitudinal-oblique US scan: the image shows the distal portion of the iliotibial tract (*arrowheads*) inserting onto the Gerdy's tubercle of the tibia (G)

Complete the examination following this hyperechoic fibrous band over the lateral aspect of the thigh, over the vastus lateralis muscle, till its distal insertion on the Gerdy's tubercle on the anterolateral aspect of the proximal tibia (Fig. 7.14).

Pay particular attention to the distal portion of the iliotibial tract, at the passage over the knee, where the band may come in conflict with the lateral condyle of the femur in the so-called runner's knee.

Dynamic manoeuvres may help to investigate clinical symptoms as in the snapping hip syndrome or in the iliotibial tract friction syndrome. In the former condition, the patient lies on the examination table in contralateral decubitus. Flex and externally rotate the adducted and internally rotated patient hip with the US probe placed over the lateral aspect of the greater trochanter. The iliotibial tract, tensor fasciae latae or gluteus medius tendon slides back and forth across the greater trochanter. This normal action becomes a snapping hip syndrome when one of these connective tissue bands thickens and catches with motion. The underlying bursa may also become inflamed, causing a painful external snapping hip syndrome. Transverse US scan easily depict the impingement of the posterior border of the fascia lata (or the anterior portion of the gluteus maximus) over the osseous prominence of the greater trochanter.

The iliotibial band friction syndrome could be evaluated moving the patient knee forward in extension and backward in flexion: the transverse US scan over the lateral condyle of the femur shows the impingement between such structure and the pre-insertional portion of the iliotibial tract.

7.2.3 Summary Table

Muscle	Origin	Insertion	Innervation	Action
Tensor fasciae latae	Anterior-superior iliac spine	Gerdy's tubercle of the tibia	Superior gluteal nerve	Abduction and flexion of the thigh; also tightens the iliotibial tract

Suggested Reading

Armfield DR, Kim DH-M, Towers JD, Bradley JP, Robertson DD (1973) Anserina bursitis – a treatable cause of knee pain in patients with degenerative arthritis. Calif Med 119:8–10

Asinger DA, el-Khoury GY (1998) Tensor fascia lata muscle tear: evaluation by MRI. Iowa Orthop J 18:146–149

Bianchi S, Martinoli C (2009) US of the musculoskeletal system. Springer, Berlin

Drake RL, Vogl W, Mitchell AWM (2012) Gray's basic anatomy. Churchill Livingstone, Elsevier Inc., Edinburgh

Huang BK, Campos JC, Michael Peschka PG et al (2013) Injury of the gluteal aponeurotic fascia and proximal iliotibial band: anatomy, pathologic conditions, and MR imaging. Radiographics 33(5):1437–1452

Imani F, Rahimzadeh P, Abolhasan Gharehdag F, Faiz SH (2013) Sonoanatomic variation of pes anserine bursa. Korean J Pain 26(3):249–54

Jaffer U, Najefi A, Nott D (2014) Management of infected femoral artery pseudoaneurysm repair: rectus abdominis flap as second-line management after sartorius flap failure. Surg Infect (Larchmt). doi:10.1089/sur.2012.187

McNally EG (2005) Practical musculoskeletal ultrasound. Elsevier, Philadelphia

Mendis MD, Wilson SJ, Hayes DA, Watts MC, Hides JA (2014) Hip flexor muscle size, strength and recruitment pattern in patients with acetabular labral tears compared to healthy controls. Man Ther 19(5):405–10

Mike Benjamin M (2009) The fascia of the limbs and back – a review. J Anat 214(1):1–18

Mojallal A, Boucher F, Shipkov H, Saint-Cyr M, Braye F (2014) Superficial femoral artery perforator flap: anatomical study of a new flap and clinical cases. Plast Reconstr Surg 133(4):934–944

Ohishi T, Suzuki D, Yamamoto K, Banno T, Ushirozako H, Koide Y, Matsuyama Y (2014) Snapping knee caused by medial meniscal cyst. Case Rep Orthop 151580. doi:10.1155/2014/151580. Epub 2014 Apr 13

Paparo F, Sconfienza LM, Muda A et al (2010) High-resolution ultrasound (HRUS) evaluation of neurovascular and muscular structures of the Hunter canal. doi:10.1594/ecr2010/C-2339

Silvestri E, Muda A, Sconfienza LM (2012a) Normal ultrasound anatomy of the musculoskeletal system. Springer, Milan/New York

Silvestri E, Muda A, Sconfienza LM (2012b) Normal ultrasound anatomy of the musculoskeletal system: a practical guide. Springer, Milan

Stoller DW (2007) Stoller's atlas of orthopaedics and sports medicine. Lippincott Williams & Wilkins, Philadelphia

Weinrauch P, Kermeci S (2013) Ultrasonography-assisted arthroscopic proximal iliotibial band release and trochanteric bursectomy. Arthrosc Tech 2(4):e433–e435

Iliopsoas

8

Emanuele Fabbro and Alessandro Muda

8.1 Anatomy Key Points

The iliopsoas muscle complex is composed of two muscles with different areas of origin and same distal insertion: psoas major muscle and iliacus muscle (Fig. 8.1).

Psoas major originates proximally from the lower spine, in particular from the lateral aspect of the vertebral bodies and transverse processes of T12–L5 and the intervening intervertebral discs. The iliacus is a broad muscle of the lateral pelvis which has a wide origin from the iliac crest, the iliac fossa, the ala of the sacrum and the sacroiliac and iliolumbar ligaments; then it runs downward in the iliac fossa and, just cranially to the inguinal ligament, joins with the psoas major fibres forming the iliopsoas muscle. It passes below the inguinal ligament (together with the femoral nerve on its anteromedial aspect) into the so-called lacuna musculorum, which represent the lateral compartment of the femoral triangle; then it passes around the iliopubic ramus and courses anteromedial to the hip joint to insert distally onto the lesser trochanter of the femur through its conjoint tendon. Common femoral artery and vein pass just medially to the fibres of the iliopsoas muscle in the so-called lacuna vasorum space (which constitute the medial compartment of the femoral triangle). Further, sited medial to the iliopsoas and deep to the femoral vessels is the pectineus muscle, which constitute the floor of the femoral triangle.

The iliopsoas bursa is located anteriorly between the joint capsule and the posterior surface of the iliopsoas muscle. This is the largest synovial bursa of the human body, which communicates with the joint space in 15 % of cases.

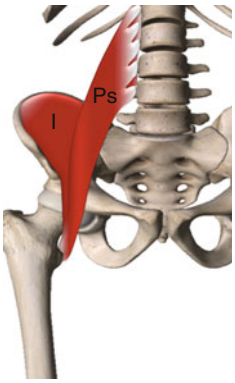

Fig. 8.1 Anatomical scheme of the ilipsoas muscle: *I* iliac muscle, *Ps* psoas major muscle

E. Fabbro
Dipartimento di Radiologia,
Università degli studi di Genova, Genoa, Italy
e-mail: emanuele.fabbro@gmail.com

A. Muda (✉)
Dipartimento di Radiologia,
IRCCS Ospedale San Martino IST, Genoa, Italy
e-mail: alessandro.muda@tiscali.it

E. Silvestri et al., *Ultrasound Anatomy of Lower Limb Muscles: A Practical Guide*,
DOI 10.1007/978-3-319-09480-9_8, © Springer International Publishing Switzerland 2015

Focus On

The *femoral triangle* (or Scarpa's triangle) is a connective tissue space located anteriorly in the proximal thigh. Its boundaries are the inguinal ligament, the medial border of the sartorius muscle, and the superior-lateral border of the adductor longus muscle (respectively superior, lateral and medial margins). Pectineus and adductor longus muscles compose the floor of this space, and the fascia lata (and the cribriform fascia at the saphenous opening) composes the roof of the triangle (Fig. 8.2). The femoral triangle could be divided into two compartments: a lateral compartment, the 'lacuna musculorum', which contains the iliopsoas muscle and the femoral nerve and a medial compartment, and the 'lacuna vasorum', which houses the common femoral artery and, lateral to it, the femoral vein.

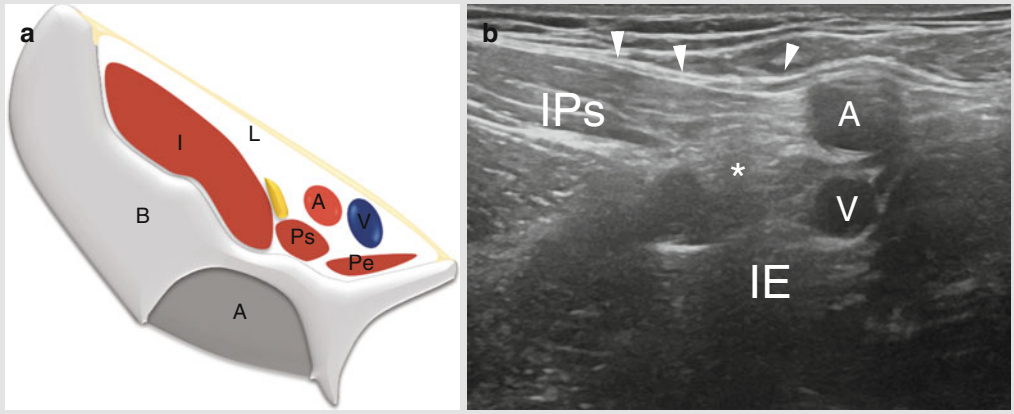

Fig. 8.2 (**a**) Anatomical scheme illustrating the femoral triangle. (**b**) US axial scan of the femoral triangle. *IE* ileopectineal eminence, *A* common femoral artery, *V* common femoral vein, * femoral nerve, *IP* Iliopsoas, *arrowheads* inguinal ligament

8.2 Ultrasound Examination Technique

The iliopsoas muscle is evaluated with the patient lying supine on the table with the leg extended and the hip slightly extrarotated (Fig. 8.3).

Palpate the anteroinferior iliac spine and position the probe just medially to it in a transverse plane. At this level, the US image shows, from lateral to medial, the hyperechoic cortex of the iliac bone with the attachment of the rectus femoris tendon, the fibres of the iliac muscle, the fibres of the psoas major muscle and finally the femoral neurovascular bundle (Fig. 8.4).

Maintaining a transverse orientation, it is possible to follow the iliopsoas muscle moving the transducer from cranial to caudal positions: on the US image, the myotendinous junction of the iliopsoas muscle can be progressively seen forming by the two distinct muscular bellies until the hyperechoic fibrillar oval structure of the tendon appears in a postero-medial eccentric position (Fig. 8.5).

At this level, turn the probe by 90° and follow the tendon along its long axis until its insertion on the lesser trochanter. Due to the curvilinear course of the iliopsoas tendon before the enthesis, anisotropy may significantly affect the visualization of tendon attachment over the lesser trochanter. Anisotropy can be reduced by positioning the patient in flexion, abduction and maximal external rotation of the thigh and by

pressing on the distal edge of the probe in order to correctly visualize also the distal portion of the tendon (Fig. 8.6).

The longitudinal US scan shows the cortex of the femoral head covered by the articular cartilage and the anterior joint capsule (normally the anterior joint recess is a virtual space); the acetabulum is located proximally, covered by the iliopsoas tendon and the rectus femoris muscle fibres. At this level, it is important to evaluate the presence of the iliopsoas bursa, which intervenes between the tendon and the anterior capsule on the medial hip and could be seen when distended by fluid (Fig. 8.7).

Further, dynamic scans may be useful to assess internal snapping hip. The patient is asked to move the hip in the frog leg position and then to return it to the normal supine position: oblique transverse US images obtained over the tendon can demonstrate the impingement between the iliopectineal eminence and the tendon which moves abruptly in a medial direction causing the snap.

Fig. 8.3 Lower limb position to evaluate the iliopsoas muscle

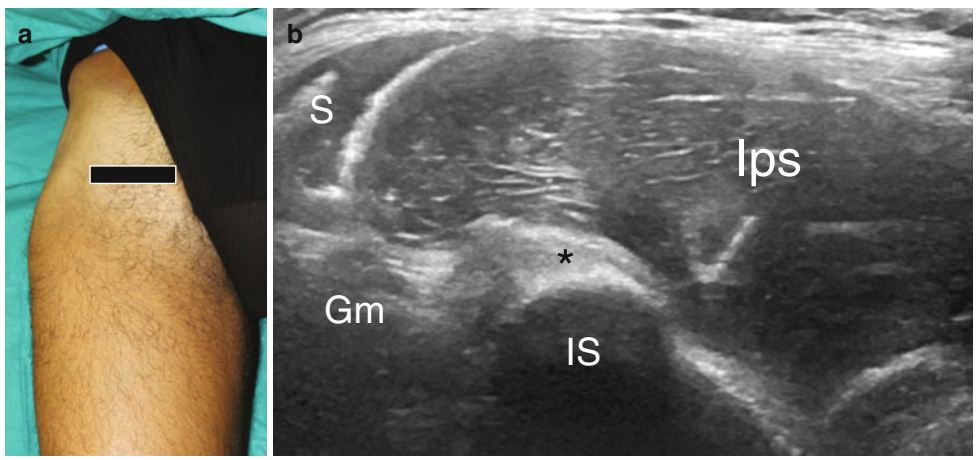

Fig. 8.4 (**a**) Probe position over the anterior hip for the evaluation of the iliopsoas muscle. (**b**) Corresponding US axial scan: this image shows the relationship between the anterior-inferior iliac spine (*IS*) and the iliopsoas muscle (*Ips*); on the left, the muscular fibres of the sartorius (*S*) and gluteus medius muscle (*Gm*) can be seen

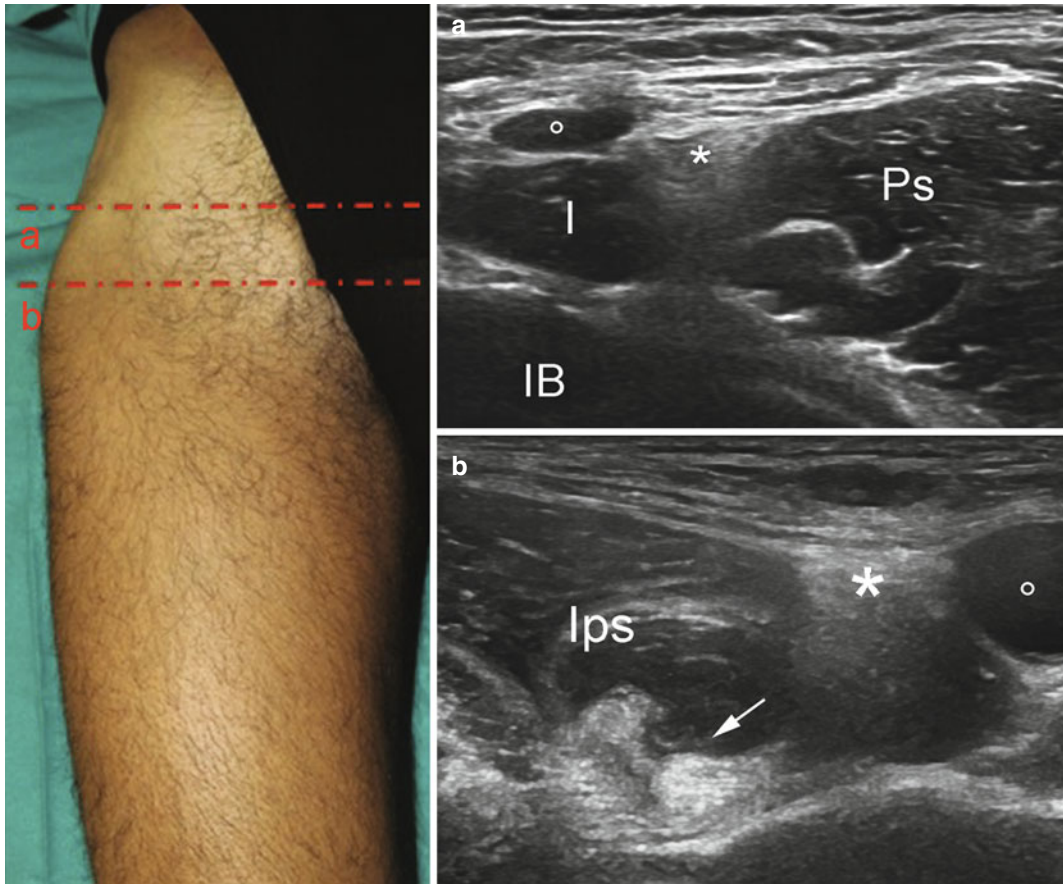

Fig. 8.5 Probe position over the anterior hip at different transverse planes for the evaluation of the iliopsoas muscle. (**a**) Cranial US axial scan showing the distinct muscle bellies of the iliac (*I*) and psoas major (*Ps*) muscles, respectively, on the left and on the right of the image, coursing in the lateral pelvis over the iiac bone (*IB*); at this level, the femoral neurovascular bundle with the femoral artery (*circle*) and nerve (*asterisk*) can be seen between the two converging muscular bellies. (**b**) Caudal US axial scan which shows the iliopsoas muscle belly (*Ips*) with its tendon in the typical eccentric position (*arrow*); at this level, the femoral neurovascular bundle can be seen on the medial aspect of the iliopsoas muscle, entering the femoral triangle

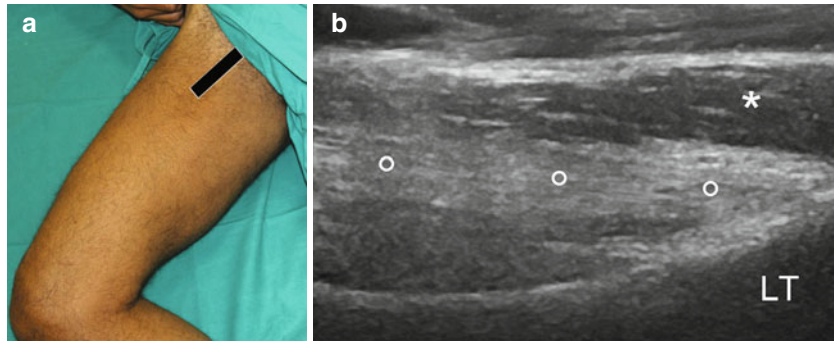

Fig. 8.6 (**a**) Patient position in flexion, abduction and maximal external rotation (**b**) US longitudinal scan showing the distal iliopsoas tendon (*circles*) inserting on the lesser trochanter (*LT*) and some fibres of the adductor longus muscle passing close to it. Press the probe over the skin and position along the tendon course to obtain a proper US scan

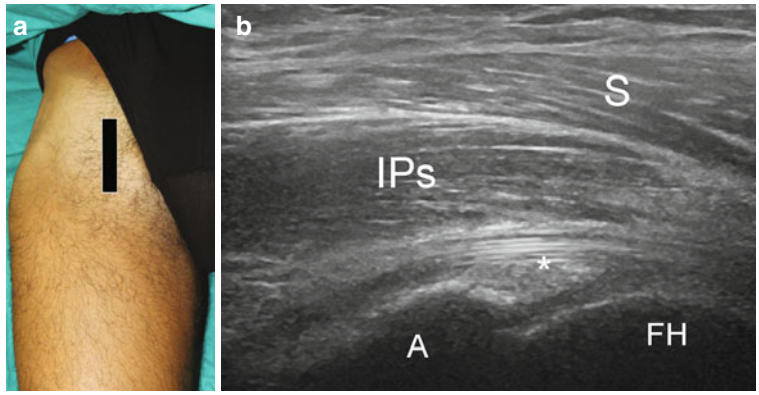

Fig. 8.7 (**a**) Probe position in a longitudinal scan, over the anterior aspect of the hip joint for the evaluation of the iliopsoas muscle. (**b**) Corresponding US longitudinal scan: this image shows the relationship between the iliopsoas muscle fibres (*IPs*), seen in a longitudinal plane, and the underlying joint capsule (*asterisk*), acetabulum (*A*) and femoral head (*FH*); sartorius muscular fibres (*S*) can be seen in a superficial position, passing over the iliopsoas muscle at this level

8.3 Summary Table

Muscle	Origin	Insertion	Innervation	Action
Psoas major	Lateral aspect of the vertebral bodies and transverse processes from T12 to L5	Lesser trochanter of the femur (conjoint tendon with iliacus)	Lumbar plexus: L2 and L3	Strongest flexor of the thigh and a flexor of the trunk when the thigh is flexed; also rotates the thigh laterally and stabilizes the pelvis
Iliacus	Iliac crest, iliac fossa, ala of the sacrum and sacroiliac and iliolumbar ligaments	Lesser trochanter of the femur (conjoint tendon with psoas major)	Femoral nerve (L2, L3, L4)	

Suggested Reading

Balconi G (2011) US in pubalgia. J Ultrasound 14(3): 157–166

Fantino O, Borneand J, Bordet B (2012) Conflicts, snapping and instability of the tendons. Pictorial essay. J Ultrasound 15(1):42–49

Lee KS, Rosas HG, Phancao JP (2013) Snapping hip: imaging and treatment. Semin Musculoskelet Radiol 17(3):286–294

Shu B, Safran MR (2011) Case report: bifid iliopsoas tendon causing refractory internal snapping hip. Clin Orthop Relat Res 469(1):289–293

Silvestri E, Muda A, Sconfienza LM (2012) Normal ultrasound anatomy of the musculoskeletal system: a practical guide. Springer, Milan

Stoller DW (2007) MRI in orthopaedics and sports medicine, 3rd edn. WoltersKluwer/Lippincott, Philadelphia

Quadriceps

9

Davide Orlandi and Giulio Ferrero

Four muscle bellies form the quadriceps muscle group, occupying the anterior compartment of the thigh: the rectus femoris, the vastus lateralis, the vastus medialis and the vastus intermedius muscles (Fig. 9.1).

The origin of the four bundles varies for each of them, while caudally the tendons of these muscles merge to form the quadriceps tendon, taking a common insertion onto the superior pole of the patella.

The quadriceps acts as a powerful extensor of the leg on the thigh. Moreover, the rectus femoris muscle, with its insertion onto the hip, also contributes to hip flexion; the vastus medialis and lateralis play a secondary role in stabilizing the patella.

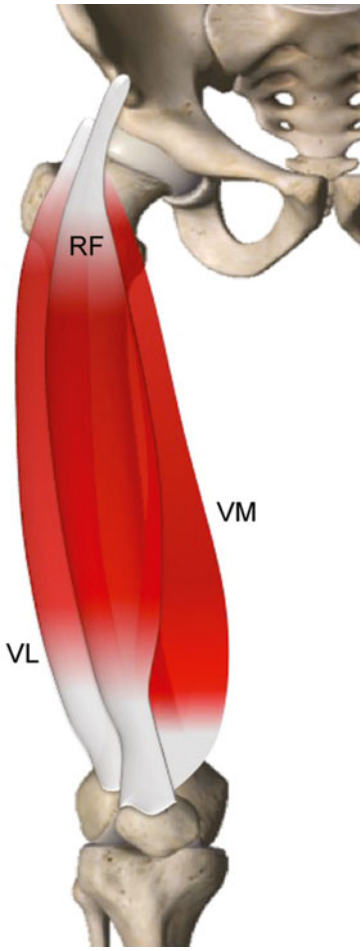

Fig. 9.1 Anatomical scheme of the quadriceps group: *RF* rectus femoris muscle, *VM* vastus medialis muscle, *VL* vastus lateralis muscle. The vastus intermedius muscle lies deep to the RF muscle

D. Orlandi (✉) • G. Ferrero
Dipartimento di Radiologia,
Università degli studi di Genova, Genoa, Italy
e-mail: my.davideorlandi@gmail.com;
giulio.ferrero@gmail.com

E. Silvestri et al., *Ultrasound Anatomy of Lower Limb Muscles: A Practical Guide*,
DOI 10.1007/978-3-319-09480-9_9,

9.1 Rectus Femoris

9.1.1 Anatomy Key Points

The *rectus femoris* is a long fusiform biarticular muscle, forming the anterior superficial portion of the quadriceps muscle group. In respect to the vastus lateralis, vastus medialis and vastus intermedius muscles, the rectus femoris is the most commonly involved in strain injuries and also has the most complex anatomy.

The muscle fibres originate from the hip through a complex proximal insertion, consisting of three separate tendons (Fig. 9.2). The *direct tendon* (or straight head) arises from the anterior inferior iliac spine (AIIS); the *indirect tendon* arises slightly more inferiorly and posteriorly from the supero-lateral aspect of the acetabular rim; the *reflected tendon* (or reflected head) is the smallest and anchors the insertional complex of the rectus femoris, reflecting into the anterior capsule of the hip joint, in the proximity of the greater tuberosity. Each tendon nearly retains a separate identity (with 10–20 % intermingling of fibres) and continues in a specific aponeurosis.

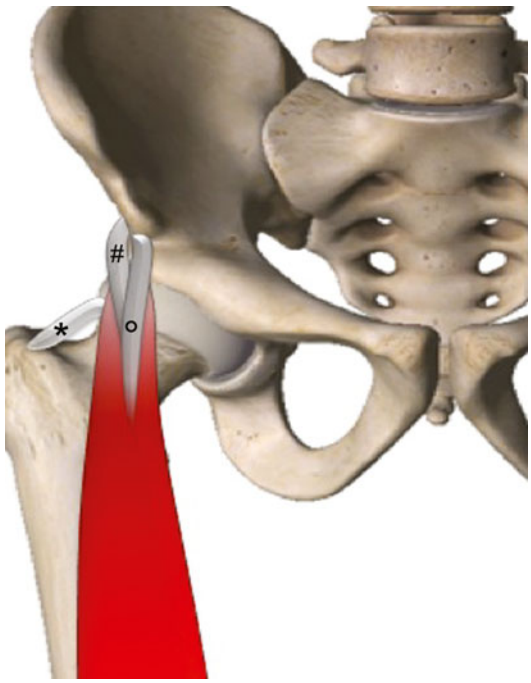

Fig. 9.2 Anatomical scheme of the rectus femoris proximal insertion: (°) direct tendon, (#) indirect tendon, (*) reflected tendon

The strict relationship between the acetabulum and the above-mentioned tendons justifies the frequent association among strain injuries of the rectus femoris muscle, which are common in young athletic patients, and a concomitant tear of the acetabular labrum.

The rectus femoris muscle has a complex internal structure consisting of different muscle fibres and fibrous-aponeurotic components. Proximally, two aponeurosis can be distinguished, the superficial and the central aponeurosis. The *superficial aponeurosis* represents the continuation of the direct tendon within the muscle substance and is oriented on a coronal plane; it extends in the cranial third of the muscle belly and blends with the anterior fascia. The *central aponeurosis* is primarily connected to the indirect tendon and is oriented on a sagittal plane; it is located in the cranial two-thirds of the muscle belly. The inferior surface of the superficial aponeurosis gives origin to the outer muscle fibres, while the inner fibres expand from the lateral and medial side of the central aponeurosis. For this reason, the outer portion of the rectus femoris muscle has a unipennate appearance, while the inner one appears bipennate, so that the rectus femoris muscle is overall composed of a small inner bipennate component surrounded by a large unipennate muscle. Both the outer and inner muscle fibres run caudally to insert into the *deep distal aponeurosis* that

arises from the posterior surface of the distal two-thirds of the muscle and continues distally in the quadriceps tendon. This particular tendinous and "muscle within a muscle" architecture is responsible of unusual patterns of muscle tears that differ from what is typically encountered in other muscles.

The distal myotendinous junction is located between the midline and distal third of the thigh. It continues the distal tendon that blends with the tendons of the vastus lateralis, vastus medialis and vastus intermedius muscles, forming the superficial layer of the quadriceps tendon. The most superficial tendinous fibres of the rectus femoris overcome the patella to reach the tibial tuberosity, contributing to the formation of the patellar tendon.

The descending branch of the lateral femoral circumflex artery furnishes the vascular supply of the rectus femoris muscle; the posterior division of the femoral nerve provides its innervation.

Fig. 9.3 Lower limb position to evaluate the rectus femoris muscle

9.1.2 Ultrasound Examination Technique

The patient lies supine, with the lower limb extended in a neutral position (Fig. 9.3).

Place the probe on the anterior superior iliac spine (ASIS) in an axial position in order to visualize the proximal insertions of the sartorius (medial) and tensor fasciae latae (lateral) muscles as shown in Fig. 7.3.

Then, move the transducer caudally to reach the anterior inferior iliac spine (AIIS), the key bony landmark to identify the rectus femoris proximal insertion (Fig. 9.4). The direct tendon of the rectus femoris can be seen above the AIIS cortex and deep to the iliopsoas muscle.

Pay particular attention when assessing the attachment point of the direct tendon onto the AIIS in young patients. As the growth plate is not completely fixed, this structure is frequently involved in avulsion fracture secondary to strain injuries.

Rotate the transducer by 90° to evaluate the direct tendon on the longitudinal plane (Fig. 9.5). Deep to the hyperechoic band representing the direct tendon, note the shadow determined by the change in orientation of the indirect tendon that descends externally and obliquely toward the upper rim of the acetabulum (Fig. 9.6).

In order to better assess the indirect tendon, ask the patient to put the examined leg over the other leg in a cross-legged position (Fig. 9.7a), and then swipe the probe laterally on an axial

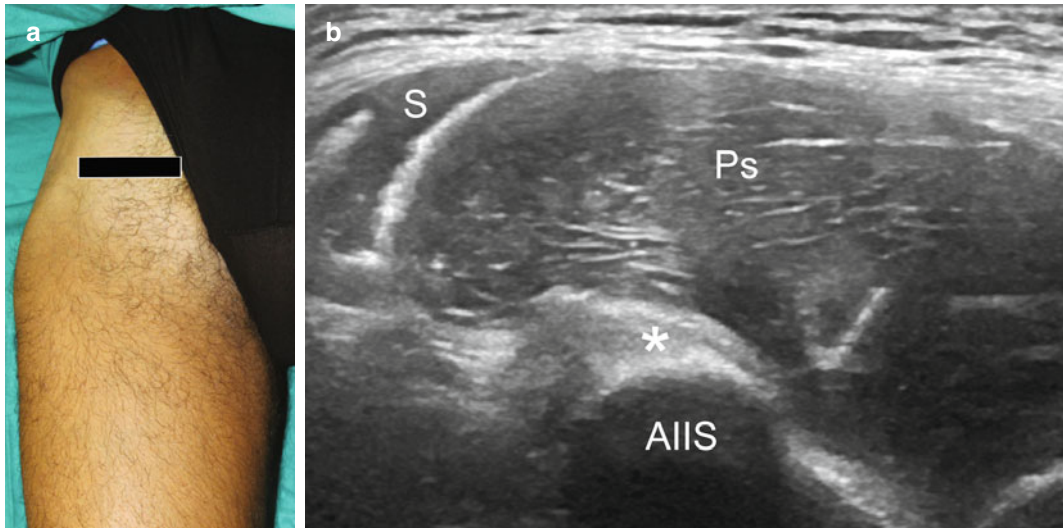

Fig. 9.4 (**a**) Probe position (*axial plane*) to visualize the rectus femoris proximal insertion onto the anterior inferior iliac spine (AIIS). (**b**) US axial scan at AIIS level shows the proximal insertion of the rectus femoris muscle. The direct tendon has an oval hyperechoic shape (*) just above the thin hyperechoic band of the AIIS bony cortex and under the iliopsoas muscle (*Ps*). *S* sartorius muscle

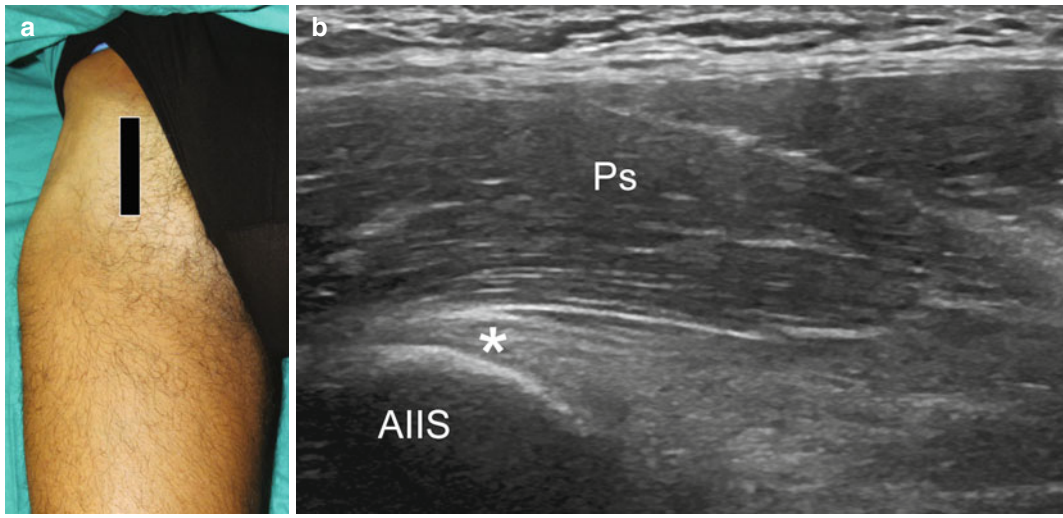

Fig. 9.5 (**a**) Probe position to evaluate the direct tendon of the rectus femoris muscle on the longitudinal plane. (**b**) US longitudinal scan of the direct tendon insertion (*) onto the AIIS. *Ps* iliopsoas muscle

plane, exposing the indirect tendon on its long axis (Fig. 9.7b).

Then, move the transducer medially to reach the anterior inferior iliac spine (AIIS), and then shift the probe caudally to reach the proximal myotendinous junction on its longitudinal plane (Fig. 9.8). Rotating the probe by 90°, complete the evaluation with an axial scan.

Continue the examination exploring the muscle belly and its aponeurotic components on axial scans that provide panoramic views (Fig. 9.9). The exam should be performed from

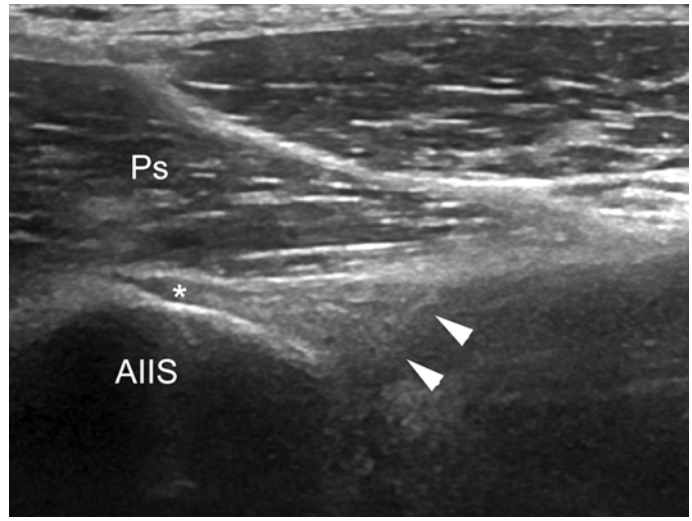

Fig. 9.6 US longitudinal scan shows the direct (*) and indirect (*white arrowheads*) tendon of the rectus femoris muscle. Identify the hypoechoic appearance of the indirect tendon caused by the change in orientation of its fibres (anisotropy), which runs obliquely and externally compared with that of the direct tendon

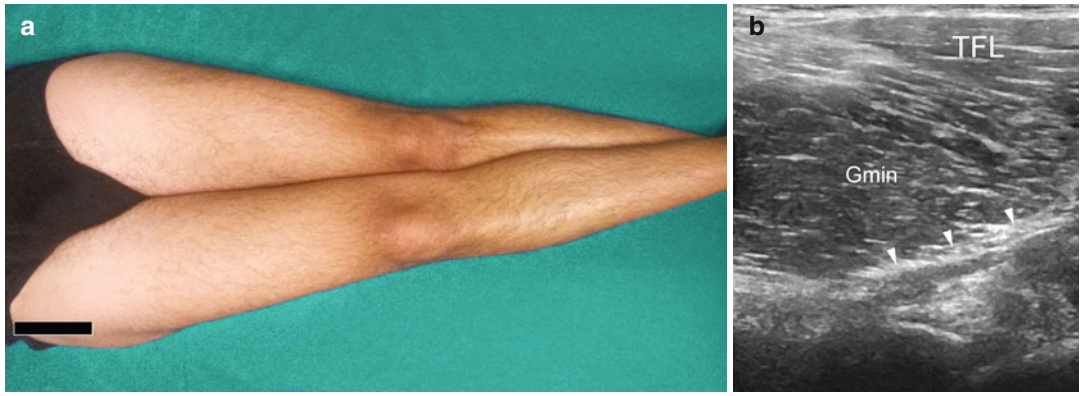

Fig. 9.7 (**a**) Probe position (*axial plane*) to visualize the indirect tendon of the rectus femoris muscle on its long axis. The patient is in a cross-legged position with the examined leg above the other one. (**b**) US axial scan shows the indirect (*white arrowheads*) tendon of the rectus femoris muscle on its long axis. *TFL* tensor fasciae latae, *Gmin* gluteus minimus

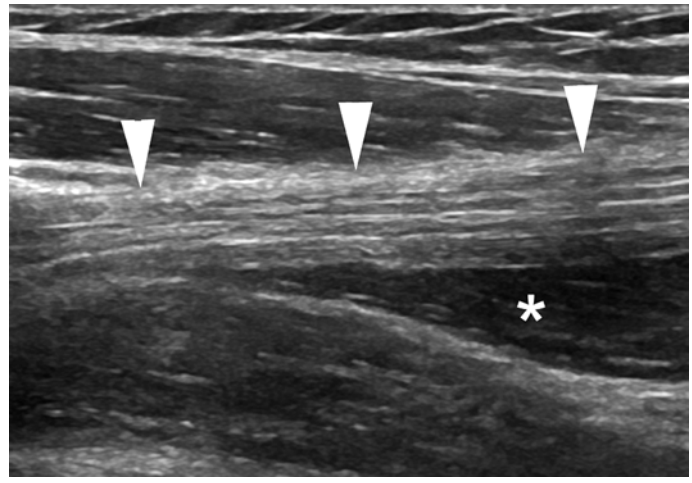

Fig. 9.8 US longitudinal scan shows the proximal myotendinous junction (*white arrowheads*) of the rectus femoris muscle (*)

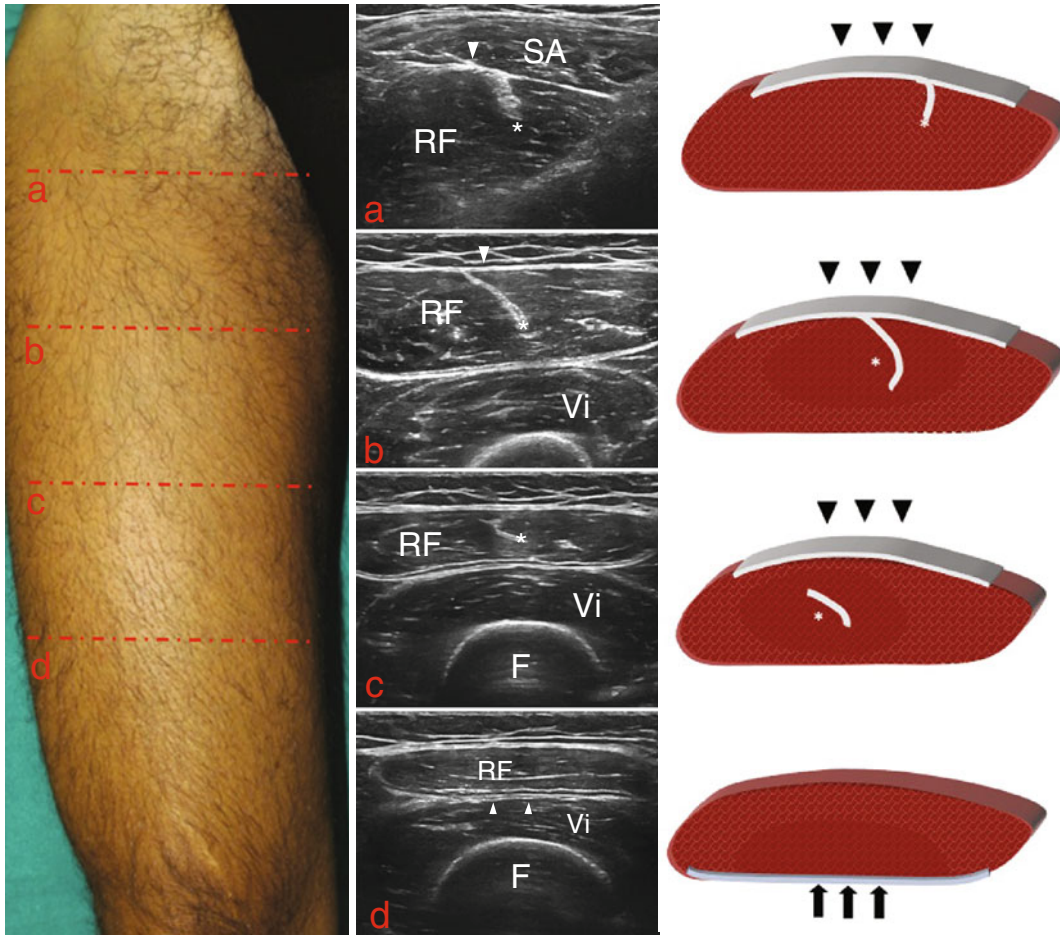

Fig. 9.9 Anatomical schemes correlated to US axial scans at different levels of the rectus femoris muscle and its aponeurotic components. (**a**) Proximal third of the rectus femoris muscle (*RF*). The superficial aponeurosis (*white arrowhead*) is seen as a thin hyperechoic band, just under the sartorius muscle (*SA*); the central aponeurosis (*) appears as a thin hyperechoic structure located within the medial aspect of the muscle. (**b**, **c**) Proximal and distal middle third of the rectus femoris muscle (*RF*). The central aponeurosis (*) becomes flattened, with a typical "comma-shaped" appearance, parallel to the sagittal plane with its long axis and located within the anterior central aspect of the muscle. *Vi* vastus intermedius muscle, *F* femur. (**d**) Distal third of the rectus femoris muscle (*RF*). The deep aponeurosis (*white arrowheads*) is seen as an hyperechoic band, arising from the posterior surface of the muscle belly, located between the rectus femoris and the vastus intermedius (*Vi*) muscles. *F* femur

the proximal myotendinous junction up to the distal myotendinous junction (Fig. 9.10). Look at the superficial aponeurosis at the proximal third and the central aponeurosis at the proximal two-thirds of the muscle belly.

If a strain injury is suspected, perform an accurate examination of the region surrounding the central aponeurosis because it is the most commonly involved in traumatic tears. Indeed, the majority of rectus femoris injuries occur at the deep intramuscular myotendinous junction, while myofascial junction injuries, at the periphery of the muscle, are less frequent.

Rotating the probe by 90°, scan the distal myotendinous junction on its longitudinal plane (Fig. 9.11); then, shift the probe cranially to examine the rectus femoris muscle belly on its major axis (Fig. 9.12).

Complete the examination with the quadriceps tendon analysis (as shown below).

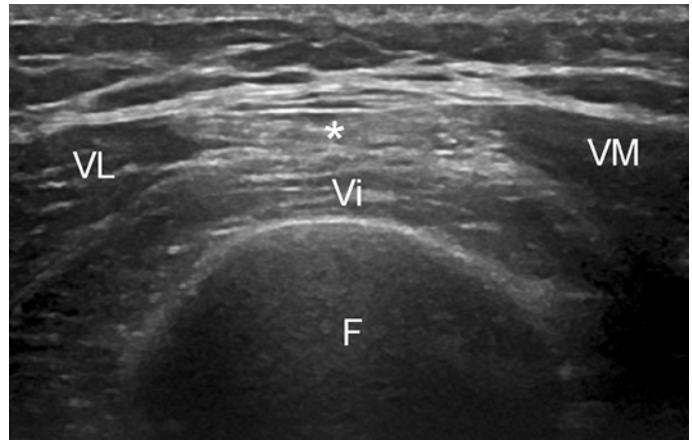

Fig. 9.10 US axial scan of the rectus femoris distal myotendinous junction (*). *VL* vastus lateralis muscle, *VM* vastus medialis muscle, *Vi* vastus intermedius muscle, *F* femur

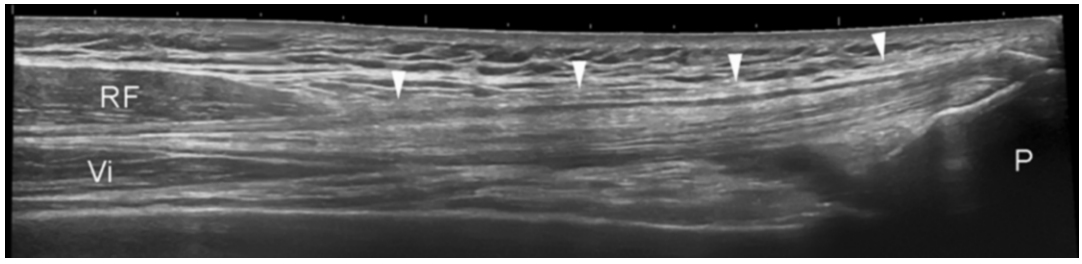

Fig. 9.11 Extended field-of-view of the rectus femoris distal myotendinous junction (*white arrowheads*). *RF* rectus femoris muscle belly, *Vi* vastus intermedius muscle, *P* patella

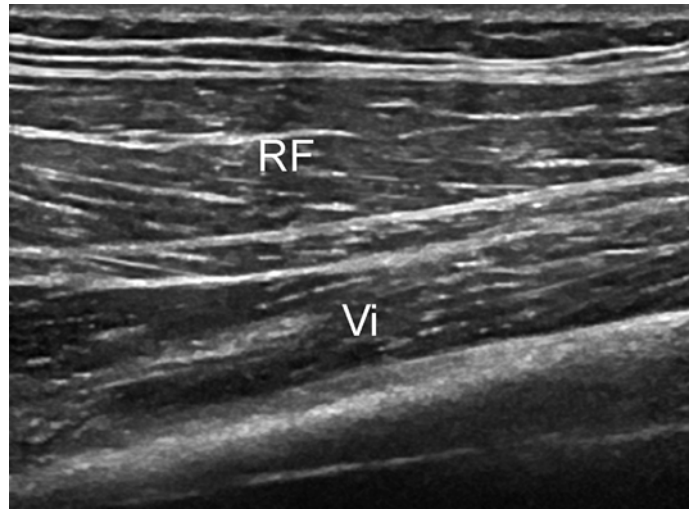

Fig. 9.12 US longitudinal scan of the rectus femoris muscle belly (*RF*). Vi vastus intermedius muscle

9.2 Vastus Muscles

9.2.1 Anatomy Key Points

The *vastus lateralis* (VL) muscle (Fig. 9.13), the largest of the quadriceps femoris bellies, has a multiple origin from the superior intertrochanteric line of the femur, the antero-inferior margin of the greater trochanter, the gluteal tuberosity, the lateral linea aspera and the lateral intermuscular septum. The proximal tendon of the vastus lateralis muscle has a close relationship with the insertional tendon of the gluteus minimum muscle with which it partly bends.

The vastus lateralis muscle belly forms a broad and flattened mass on the femoral shaft lateral to the vastus medialis muscle, deep to rectus femoris muscle and anterior to the biceps femoris muscle. Its lateral surface is covered by the tensor fascia latae muscle (at the proximal third of the thigh) and the ilio-tibial tract (at the distal two-thirds of the thigh).

The distal tendon of the vastus lateralis, together with the vastus medialis tendon, forms the intermediate layer of the quadriceps tendon. In addition, some fibres of the vastus lateralis reach directly the lateral margin of the patella (lateral patellar retinaculum).

The *vastus medialis* (VM) muscle is thicker and less wide than the vastus lateralis. It takes its origin from the entire medial linea aspera, the inferior intertrochanteric line of the femur and the medial intermuscular septum.

The muscle belly covers the medial aspect of the femur, at the same level of the vastus lateralis, placing deep to rectus femoris and anterior to the adductor muscles. At the middle third of the thigh, it is overcome superficially by the sartorius muscle.

The distal tendon of the vastus medialis, together with that of the vastus lateralis, forms the intermediate layer of the quadriceps tendon. Some fibres of the vastus medialis attach directly onto the medial margin of the patella (medial patellar retinaculum).

The *vastus intermedius* (VI) muscle is the deepest of the vastus muscles, lying in direct contact with the femoral diaphysis, largely covered by the vastus lateralis and medialis muscles. It has an extensive proximal insertion onto the inferior and lateral linea aspera (as the vastus lateralis), the anterior and lateral femoral shaft and the lateral intermuscular septum.

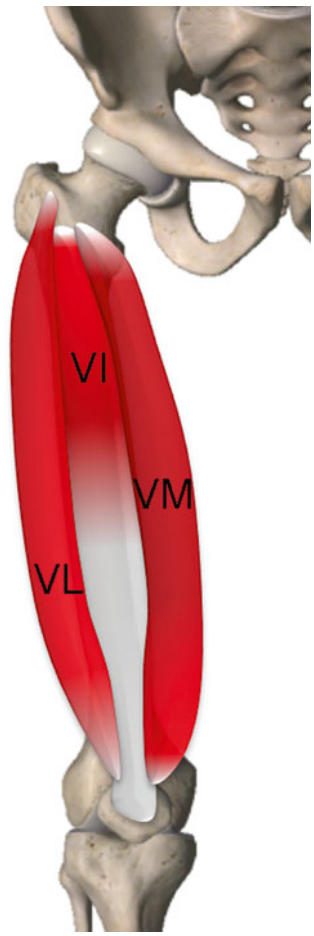

Fig. 9.13 Anatomical scheme of the vastus muscle group: *VM* vastus medialis muscle, *VL* vastus lateralis muscle, *VI* vastus intermedius muscle

The vastus intermedius distal tendon contributes to form the deep layer of the quadriceps tendon.

9.2.2 Ultrasound Examination Technique

The patient lies supine with the lower limb extended on the examination table (Fig. 9.14).

Place the probe in the axial plane on the anterior inferior iliac spine (AIIS), the main bony landmark used to identify the proximal insertion of the rectus femoris muscle, as shown in Fig. 9.4. Then, shifting the probe caudally, visualize its proximal myotendinous junction and muscle belly, as show in Fig. 9.9b.

From this position, shift the probe laterally to image the *vastus lateralis* muscle belly at its proximal third (Fig. 9.15a). The vastus lateralis has a wide proximal insertion on the proximal and lateral femoral shaft not clearly detectable on US examination.

Continue the exam moving the probe caudally along the anterolateral surface of the thigh to examine the vastus lateralis muscle belly in its full extension (Fig. 9.15b), up to the distal myotendinous junction, located at the distal third of the thigh (Fig. 9.16).

Rotate the probe by 90° to visualize the vastus lateralis distal myotendinous junction and tendon on their long axis (section "quadriceps tendon evaluation").

Shifting the probe cranially, complete the US examination imaging the vastus lateralis muscle belly on the longitudinal plane (Fig. 9.17).

As described before, also for the *vastus medialis* muscle examination, the rectus femoris muscle must be considered the main anatomic landmark, so start the examination placing the probe in the axial plane to visualize the rectus femoris muscle belly, as shown in Fig. 9.9a.

Shifting the probe medially on the axial plane, the vastus medialis muscle appears anterior to the adductors, medial to the rectus femoris and superficial to the vastus intermedius muscles (Fig. 9.18). Similar to the vastus lateralis muscle, the tendinous origin of the vastus medialis is not clearly identifiable on US examination.

Fig. 9.14 Lower limb position for vastus muscles evaluation

Move the probe caudally, along the anteromedial thigh, to examine the vastus medialis muscle belly on the axial plane, at different levels (Fig. 9.19).

Note the close relationship of the vastus medialis muscle with the superficial femoral neurovascular bundle for almost its entire course. The course of the femoral bundle, located medially to the vastus medialis, can be used as a helpful anatomical landmark (Fig. 9.20).

The vastus medialis muscle belly extends more distally than the vastus lateralis and the vastus intermedius muscles, descending in proximity of the superior pole of the patella (Fig. 9.21).

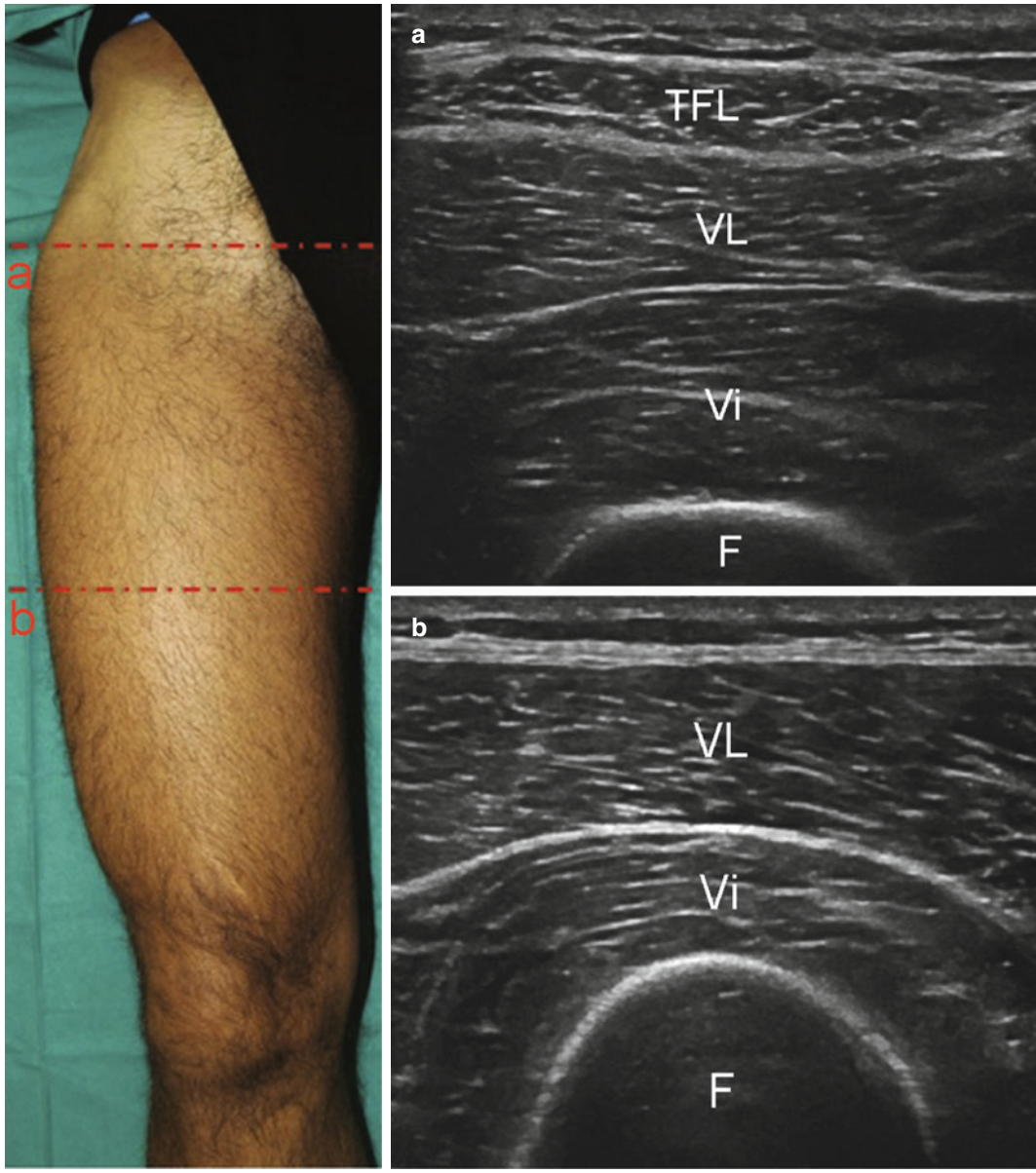

Fig. 9.15 Probe position to evaluate the vastus lateralis muscle on the axial plane. (**a**) US axial scan at the proximal third of the anterolateral thigh: the vastus lateralis (*VL*) muscle belly is identifiable deep to the tensor fasciae latae (*TFL*) and superficial to the vastus intermedius (*Vi*) muscles. (**b**) US axial scan at the middle and distal third of the thigh: the vastus lateralis (*VL*) lies in a superficial position, just under the subcutaneous tissue. *Vi* vastus intermedius muscle. *F* femur

At the distal third of the thigh, visualize its distal myotendinous junction and tendon on the axial plane (Fig. 9.22).

Rotate the probe by 90° to evaluate the distal myotendinous junction and tendon also in the longitudinal plane (Fig. 9.23).

Starting from the position shown in Fig. 9.9a, the *vastus intermedius* muscle belly is seen deep to rectus femoris muscle in direct contact with the anterior surface of the femoral shaft (Fig. 9.24). The identification of the femoral cortex on the deep portion of the image helps to find the exact scan.

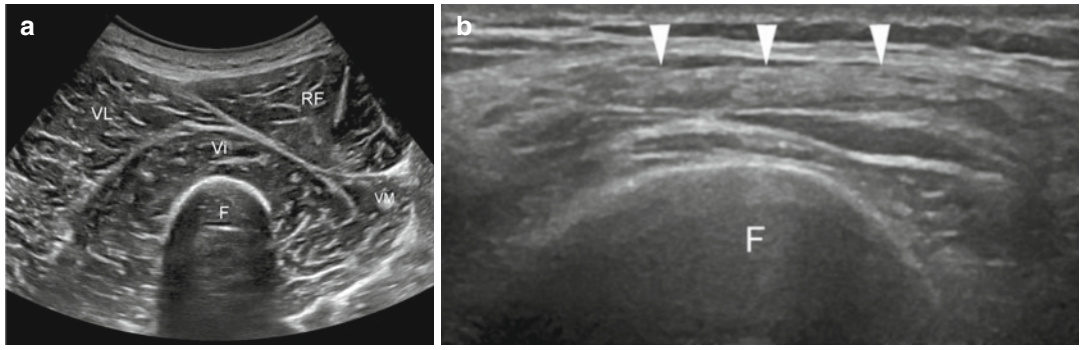

Fig. 9.16 (**a**) US axial scan at the middle third of the anterolateral thigh, using a convex-array probe that allows a more panoramic view. The vastus lateralis muscle (*VL*) is imaged lateral to the rectus femoris (*RF*) and superficial to the vastus intermedius muscles (*Vi*). *VM* vastus medialis muscle, *F* femur. (**b**) US axial scan of the distal myotendinous junction of the vastus lateralis muscle (*white arrowheads*). *F* femur

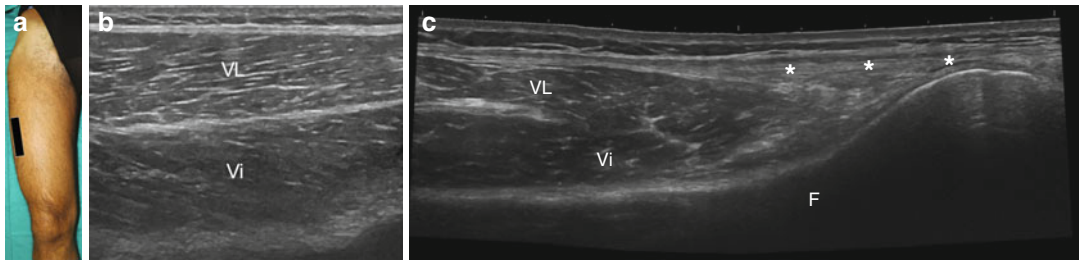

Fig. 9.17 (**a**) Probe position to evaluate the vastus lateralis muscle on the longitudinal plane. (**b**) US longitudinal scan of the vastus lateralis muscle belly (*VL*). (**c**) Extended field-of-view of the vastus lateralis and vastus intermedius muscles along the lateral thigh; *Vi* vastus intermedius muscle; (*), ilio-tibial band

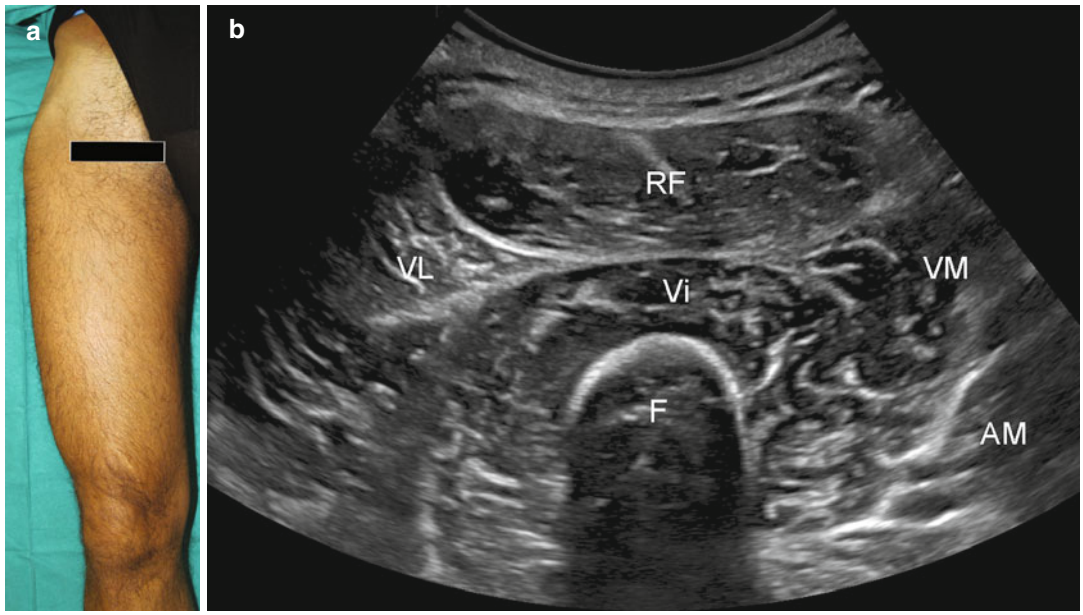

Fig. 9.18 (**a**) Probe position to evaluate the vastus medialis muscle on the axial plane. (**b**) Panoramic axial scan of the anteromedial muscles of the thigh. *RF* rectus femoris muscle, *VL* vastus lateralis muscle, *VM* vastus medialis muscle, *Vi* vastus intermedius muscle, *AM* adductor magnus muscle, *F* femur

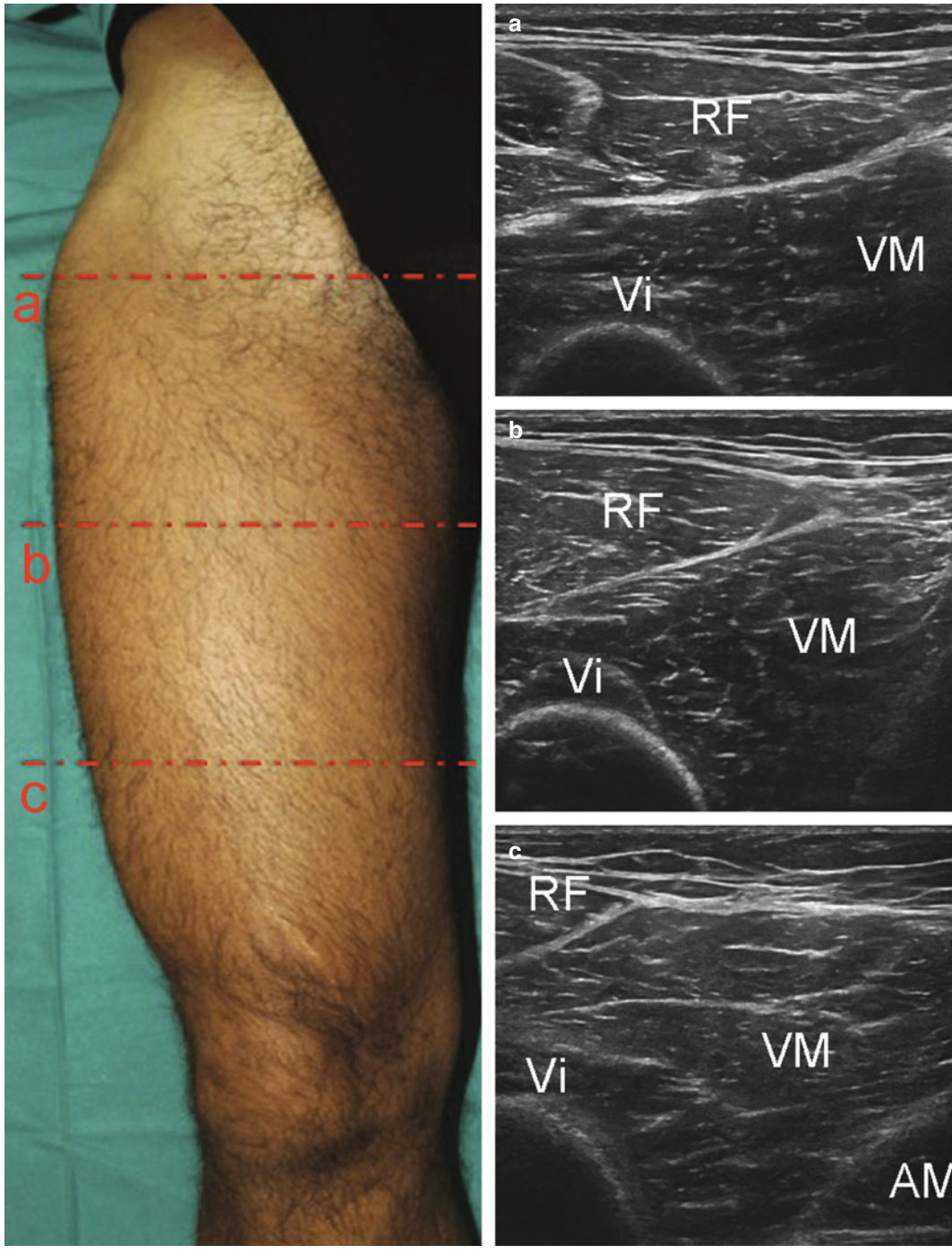

Fig. 9.19 Probe position to evaluate the vastus medialis muscle belly at different levels on the axial plane. US axial scan of the vastus medialis (*VM*) muscle belly at the proximal (**a**), middle (**b**) and distal (**c**) third of the anteromedial thigh. *RF* rectus femoris muscle, *Vi* vastus intermedius muscle, *AM* adductor magnus muscle

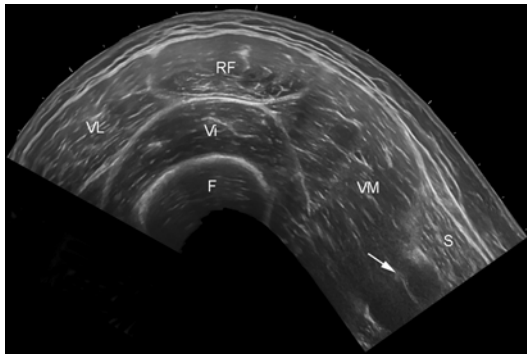

Fig. 9.20 Extended field-of-view of the vastus medialis (*VM*) muscle belly at the middle third of the anteromedial thigh. Look at the superficial neurovascular bundle (*white arrow*). *RF* rectus femoris muscle, *VL* vastus lateralis muscle, *VM* vastus medialis muscle, *Vi* vastus intermedius muscle, *S* sartorius muscle, *F* femur

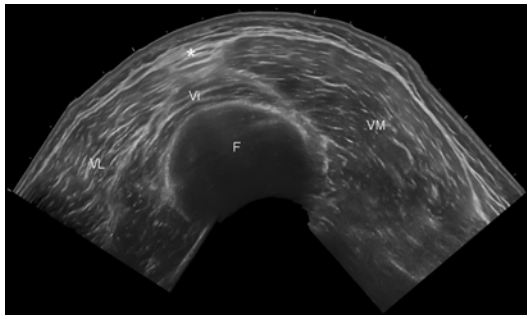

Fig. 9.21 Extended field-of-view of the vastus medialis (*VM*) muscle belly at the distal third of the thigh. The vastus medialis shows a large muscle belly while the vastus lateralis (*VL*) and the vastus intermedius (*Vi*) muscles start to decrease in size to become tendinous. *Asterisk*, rectus femoris distal tendon fibres

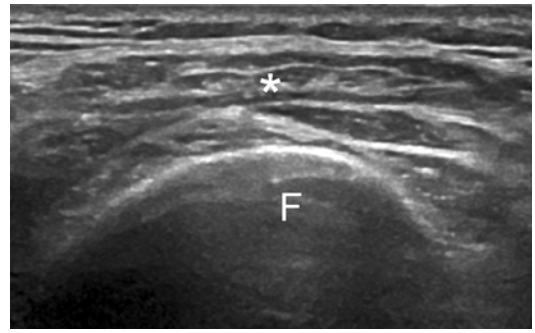

Fig. 9.22 US axial scan of the vastus medialis distal myotendinous junction (*). *F* femur

Move the probe caudally, along the central anterior thigh, to visualize the entire muscular mass.

In patients with significant muscle mass, such as obese patients or athletes, the use of low-frequency-convex array probes may help to obtain an appropriate depiction of the deeper aspect of the muscle.

At the distal third of the thigh, identify the distal myotendinous junction on an axial plane, up to the distal tendon where the vastus intermedius muscle fibres fit into the deep lamina of the quadriceps tendon (Fig. 9.25).

Rotate the probe clockwise by 90 ° and get a longitudinal scan of the distal tendon and the myotendinous junction (Fig. 9.26).

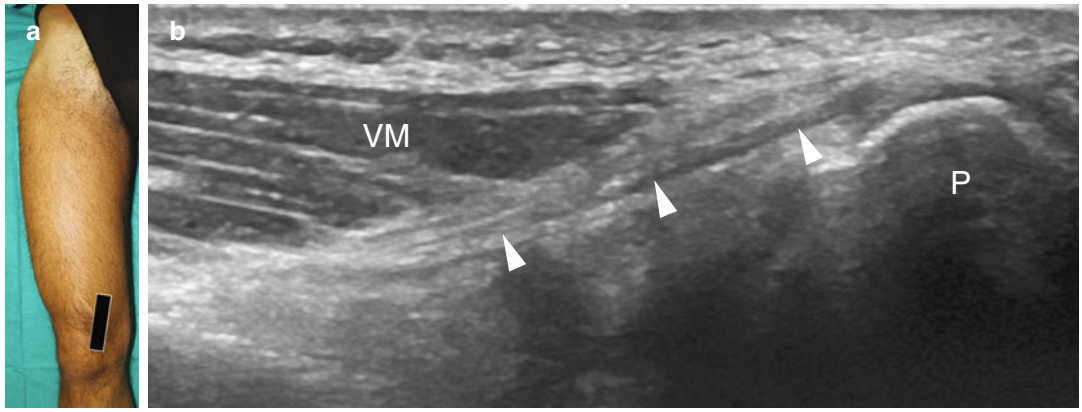

Fig. 9.23 (**a**) Probe position to evaluate the vastus medialis distal myotendinous junction on the longitudinal plane. (**b**) US longitudinal scan of the vastus medialis (*VM*) distal myotendinous junction. *White arrowheads*, vastus medialis distal tendon; *P* patella

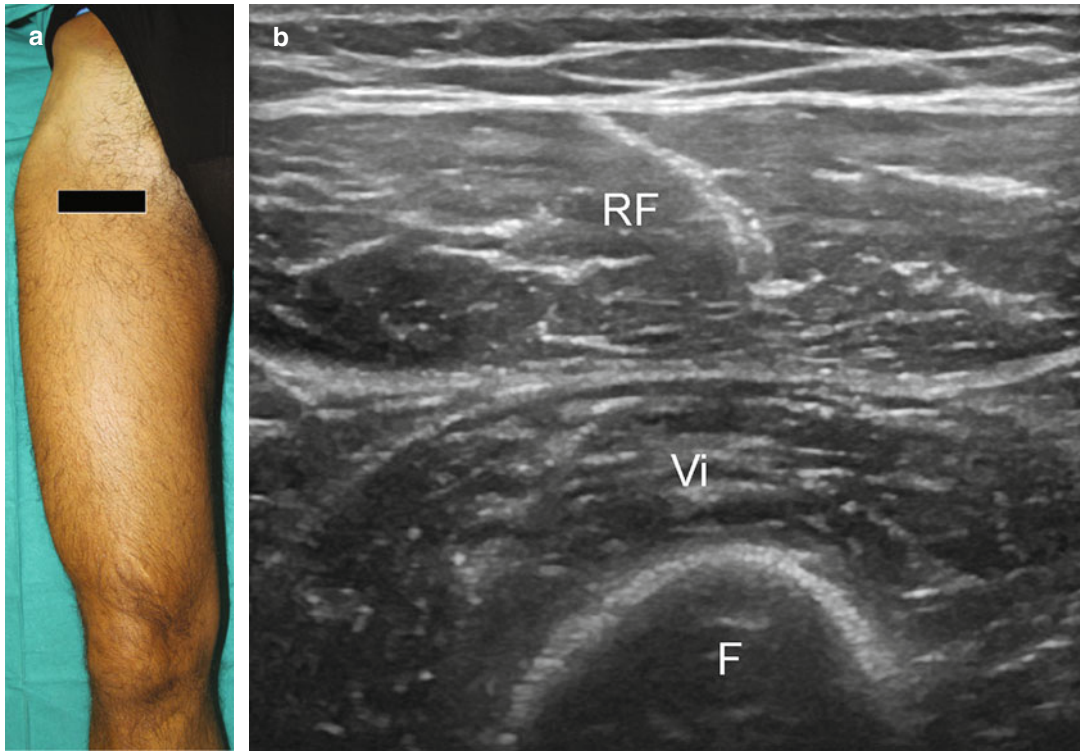

Fig. 9.24 (**a**) Probe position to evaluate the vastus intermedius muscle on the axial plane. (**b**) US axial scan of the vastus intermedius muscle belly. *Vi* vastus intermedius muscle, *RF* rectus femoris muscle, *F* femur

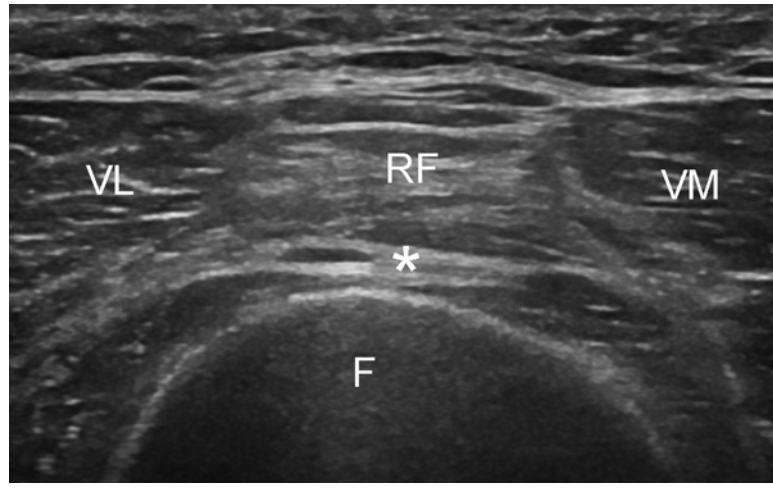

Fig. 9.25 US axial scan of the vastus intermedius distal myotendinous junction (*). *RF* rectus femoris muscle, *VL* vastus lateralis muscle, *VM* vastus medialis muscle, *F* femur

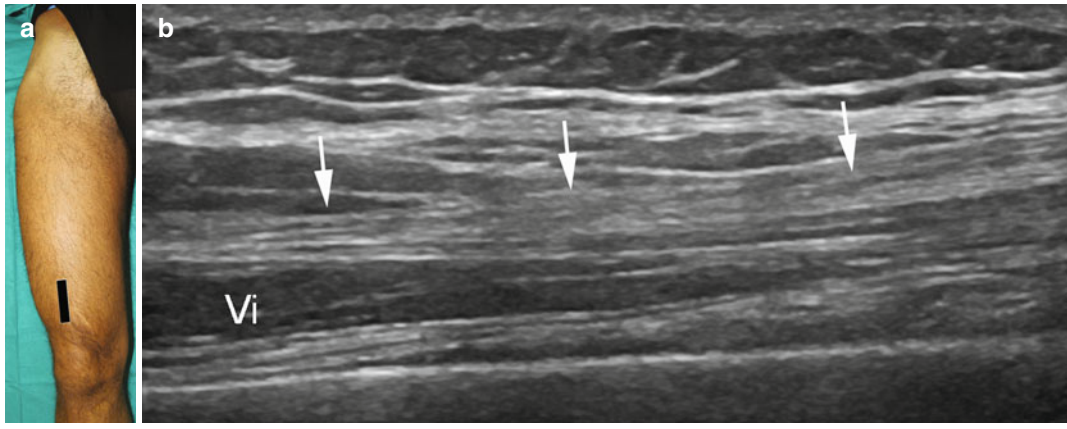

Fig. 9.26 (**a**) Probe position to evaluate the vastus intermedius distal myotendinous junction on the longitudinal plane. (**b**) US longitudinal scan of the vastus intermedius distal myotendinous junction (*white arrows*). *Vi* vastus intermedius muscle

9.2.3 Summary Table

Muscle	Origin	Insertion	Nerve supply	Action
Rectus femoris	AIIS (direct tendon), supero-lateral aspect of the acetabular rim (indirect tendon), anterior capsule of the hip joint (reflected)	Superior pole of the patella (superficial lamina of the quadriceps tendon), tibial tuberosity (patellar tendon)	Femoral nerve	Extension of the knee Flexion of the hip
Vastus lateralis	Superior intertrochanteric line of the femur, antero-inferior margin of the greater trochanter, gluteal tuberosity, lateral linea aspera, the lateral intermuscular septum	Superior pole of the patella (intermediate lamina of the quadriceps tendon)	Femoral nerve	Extension of the knee
Vastus medialis	Medial linea aspera, inferior intertrochanteric line of the femur, medial intermuscular septum	Superior pole of the patella (intermediate lamina of the quadriceps tendon)	Femoral nerve	Extension of the knee
Vastus intermedius	Inferior and lateral linea aspera, anterior and lateral femoral shaft, lateral intermuscular septum	Superior pole of the patella (deep lamina of the quadriceps tendon)	Femoral nerve	Extension of the knee

9.3 Quadriceps Tendon

9.3.1 Anatomy Key Points

The distal insertions of the vastus muscles converge with the rectus femoris muscle to form an apparently unique tendinous structure, the quadriceps tendon.

The *quadriceps tendon* is a multilayered fibrous band that attaches onto the superior pole of the patella. It has a trilaminar appearance because three different layers constitute it: the superficial one contains the fibres from the rectus femoris muscle; the intermediate lamina is formed by the vastus medialis and lateralis fibres melted together; the deep layer contains the vastus intermedius distal tendinous fibres. These distinct layers are separated by fibroadipose bands of tissue that allow gliding movements during quadriceps muscle activation.

9.3.2 Ultrasound Examination Technique

The patient lies supine with the knee flexed at about 30°–45° to straighten the tendon.

Place the probe on a longitudinal plane with the distal edge on the superior pole of the patella and evaluate the quadriceps tendon on its major axis (Fig. 9.27a–c).

Then complete the examination with axial scans (Fig. 9.27c). Pay attention to the quadriceps tendon features: usually, it appears quite irregular because of the orientation of the converging fibres coming from the three different layers (rectus femoris, vastus medialis and lateralis, vastus intermedius muscles).

Extended field-of-view systems are particularly well suited to illustrate the distal myotendinous junctions and the tendon in a panoramic image.

Fig. 9.27 (**a**) Probe position to evaluate the quadriceps tendon on the longitudinal plane. (**b**) US longitudinal scan shows the typical hyperechoic multilayered appearance of the quadriceps tendon. The superficial lamina of the quadriceps tendon is formed by the rectus femoris fibres (*white arrowheads*); the intermediate layer is constituted by the fibres of the vastus lateralis and medialis; the vastus intermedius contribute to the formation of the deep lamina (*void arrowheads*). (*) suprapatellar recess; *P* patella. (**c**) US axial scan shows the oval hyperechoic appearance of the quadriceps tendon (*). (°), articular cartilage; *T* femoral trochlea

Suggested Reading

Hart JM, Pietrosimone B, Hertel J, Ingersoll CD (2010) Quadriceps activation following knee injuries: a systematic review. J Athl Train 45(1):87–97

Lee JC, Healy J (2004) Sonography of lower limb muscle injury. AJR 182:341–351

Pasta G, Nanni G, Molini L, Bianchi S (2010) Sonography of the quadriceps muscle: examination technique, normal anatomy and traumatic lesions. J Ultrasound 13:76–84

Razek AAKA, Fouda NS, Elmetwaley N, Elbogdady E (2009) Sonography of the knee joint. J Ultrasound 12:53–60

Waligora AC, Johanson NA, Hirsch BE (2009) Anatomy of the quadriceps femoris and extensor apparatus of the knee. Clin Orthop Relat Res 467:3297–3306

Adductors, Gracilis, and Pectineus

10

Angelo Corazza and Enzo Silvestri

10.1 Adductors and Pectineus Muscles

10.1.1 Anatomy key points: Adductors

The *adductor muscles* are composed of the adductor longus, brevis, and magnus muscles (Fig. 10.1).

The main function of these muscles is to adduct and to rotate internally the thigh and to stabilize the hip joint. The adductor longus can also flex the extended thigh, while the adductor magnus extends the thigh at the hip joint level.

The *adductor longus* muscle is the most anterior muscle in the adductor group and originates from the anterior pubis, just lateral to the pubic symphysis.

It is a slender and triangular muscle, lateral to adductor brevis and magnus muscles and medial to the vastus medialis muscle. The muscle belly of adductor longus

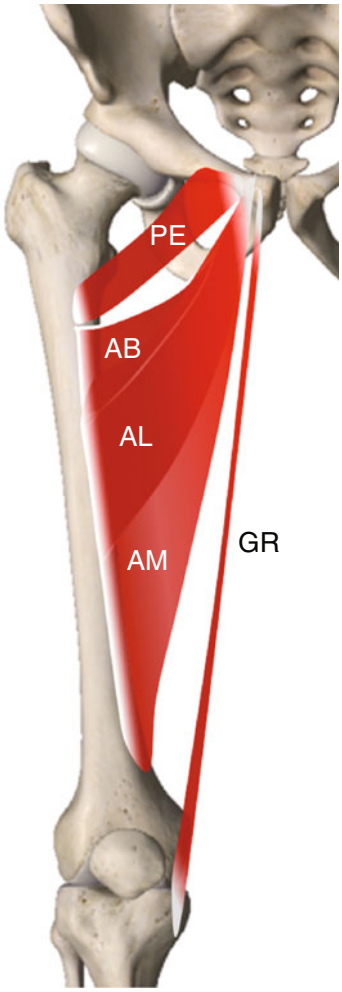

Fig. 10.1 Anatomical scheme of medial thigh muscles. *PE* pectineus, *GR* gracilis, *AL* adductor longus, *AB* adductor brevis, *AM* adductor magnus

A. Corazza
Dipartimento di Radiologia,
Università degli studi di Genova, Genoa, Italy
e-mail: angelcoraz@libero.it

E. Silvestri (✉)
Struttura Complessa di Diagnostica
per Immagini ed Ecografia Interventistica,
Ospedale Evangelico Internazionale, Genoa, Italy
e-mail: silvi.enzo@gmail.com

E. Silvestri et al., *Ultrasound Anatomy of Lower Limb Muscles: A Practical Guide*,
DOI 10.1007/978-3-319-09480-9_10, © Springer International Publishing Switzerland 2015

becomes progressively thinner caudally, and its fibers run downwards and laterally to attach to the middle third of *linea aspera* of femur, anterior to adductor magnus and brevis and posterior to vastus medialis insertions.

Linea aspera is a rough crest of bone running down the posterior shaft of the femur in its middle third.

The *adductor brevis* muscle is a short and triangular-shaped muscle; the upper aspect of its belly is posterior to pectineus, while its lower aspect is posterior to adductor longus muscle. It originates from the lateral part of the front of the body of the pubis and from the inferior pubic ramus. It distally attaches between the lesser trochanter and the superior end of linea aspera, anteriorly to adductor magnus insertion.

Finally, the largest and the most posterior of adductor muscle group is the *adductor magnus* muscle. It is a large triangular-shaped muscle with a thick medial margin that originates from the femoral surface of the ischiopubis ramus and the lateral part of the inferior surface of the ischial tuberosity. It lies anteriorly to semimembranosus and semitendinosus muscles and posteriorly to adductor longus and brevis muscles.

This muscle has two different components: the adductor and the hamstring part. The adductor portion attaches with a wide aponeurosis on the medial margin of the linea aspera of the femur; the hamstring part attaches by a rounded tendon to adductor tubercle on top of the medial condyle of femur.

Some of these fibers continue vertically downwards fusing with the medial collateral ligament of the knee. The most anterior ischiopubic fibers course from linea aspera to the greater trochanter medially to the insertion of the gluteus maximus.

The two bellies converge distally forming the roof of the adductor canal, a conical-shaped pathway that contains the femoral vessels, saphenous nerve, and fibrous tissue.

10.1.2 Anatomy Key Points: Pectineus

The *pectineus* muscle is a flat and quadrangular-shaped muscle; it is located in the upper and medial aspect of the thigh deep in the groin. It lies between iliopsoas and adductor longus muscles. These three muscles form the floor of the femoral triangle of Scarpa.

The pectineus muscle consists of two layers: the superficial and the deep one. It arises from the pectin pubis (pectineal line of the pubis) and from the surface of bone in front of it, between the iliopectineal eminence and pubic tubercle. Some fibers also come from the fascia covering the anterior surface of the muscle.

It runs vertically downward, backward, and lateral and inserts into the posterior surface of the femur, along the line of the lesser trochanter to the linea aspera. This line is called the pectineal line of the femur.

The pectineus muscle is in relation anteriorly with the pubic portion of the fascia lata, which separates it from the femoral artery and vein and internal saphenous vein and posteriorly with the capsule of the hip joint and with the obturator externus and adductor brevis muscles.

The femoral nerve provides the main innervation of the pectineus muscle although it may sometimes receive additional innervation for its deep portion from the obturator nerve called the accessory obturator nerve.

10.1.3 Ultrasound Examination Technique

The patient is supine, with the thigh abducted and externally rotated and the knee bent (frog leg position) (Fig. 10.2).

Holding the transducer in a longitudinal position localize the anterior surface of the pubis,

which can be considered an important bony landmark for US examination. Then identify the insertional components of the adductor muscles and three muscle layers: from the most superficial to the deepest, the adductor longus, the adductor brevis, and the adductor magnus (Fig. 10.3). The myotendinous junction of the adductor longus is seen with its triangular hypoechoic shape and its tendon results eccentric to muscle belly.

With the probe always in the same position, pay attention to the profile of the pubic symphysis because a bone surface irregularity could represent a direct sign of osteitis pubis.

Shift the transducer cranially to evaluate the tendon of rectus abdominis muscle, which is in direct continuity with the adductor longus tendon. Therefore a single continuous structure, termed the common adductor–rectus abdominis origin, forms a critical anatomic and biomechanical structure, playing an important role as dynamic stabilizer of the pubic symphysis (Fig. 10.4).

The long-axis US plane is useful for determining an avulsion injury of the tendon of the adductor muscles especially of the adductor longus tendon and less frequently of the adductor brevis tendon.

Rotate the transducer by 90° to evaluate the adductor insertions on axial plane and move down the transducer to detect and evaluate the course of each muscle belly (Fig. 10.5).

Three muscle layers are recognized on axial planes: the superficial one is represented by the adductor longus (lateral) and the gracilis (medial) muscles, the intermediate by the adductor brevis muscle, and the deepest by the adductor magnus muscle (Figs. 10.6 and 10.7).

Swipe the transducer distally on an axial scan to distinguish each muscle belly. Femoral neurovascular bundle, placed between the vastus intermedius, the sartorius, and the adductor longus muscles, should be used as an important landmark: the adductor muscles lie medially to the femoral artery and vein (Fig. 10.8).

Following the course of the adductor longus muscle, its cross-sectional area progressively decreases until its distal insertion on the middle third of the *linea aspera* (Fig. 10.9).

Fig 10.2 Lower limb position (frog leg position) to evaluate the adductor muscles

US are not able to distinguish the thin distal tendon because it is positioned too deep.

Continue the exam with an axial scan of the adductor brevis muscle performed at the upper third of the thigh. At this level, it lies superolaterally to adductor longus muscle. Caudally it becomes deeper than adductor longus muscle.

With axial scans, also evaluate the adductor magnus muscle that appears as a large muscle deep and posterior to adductor longus (Fig. 10.10).

Ultrasound allows a reliable assessment of the proximal components of adductor muscles; conversely the distal insertion of these muscles is hard to examine because of the deep location and the anatomical intrinsic complexity.

Also color Doppler examination may be useful to evaluate the femoral vessels patency, representing a crucial part of ultrasound examination of the medial compartment of the thigh.

Conclude the examination of the adductor muscles performing axial or longitudinal scan during isometric contraction, which is useful to evaluate even small muscular injuries.

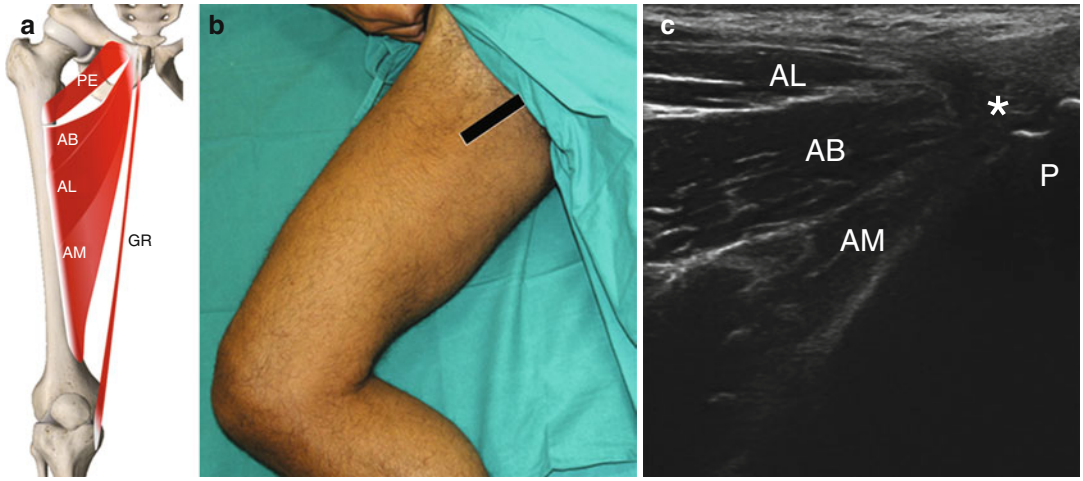

Fig. 10.3 (**a**) Anatomical scheme of medial thigh compartment muscles. (**b**) Probe position to evaluate the proximal insertion of adductor muscles (*) in the anterior surface of the pubis on the sagittal plane. *PE* pectineus, *AB* adductor brevis, *AL* adductor longus, *AM* adductor magnus, *GR* gracilis. (**c**) US sagittal scan: note the three muscle layers represented from superficial to deepest by adductor longus (*AL*), adductor brevis (*AB*), and adductor magnus (*AM*) muscles

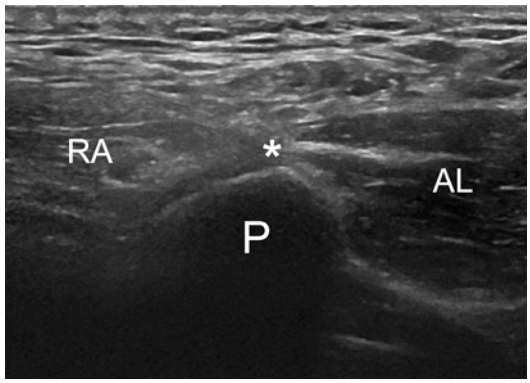

Fig. 10.4 US longitudinal scan at level of pubic symphysis (*P*) that shows the anatomical relationship (*) between the tendon of the adductor longus (*AL*) and the tendon of the rectus abdominis (*RA*)

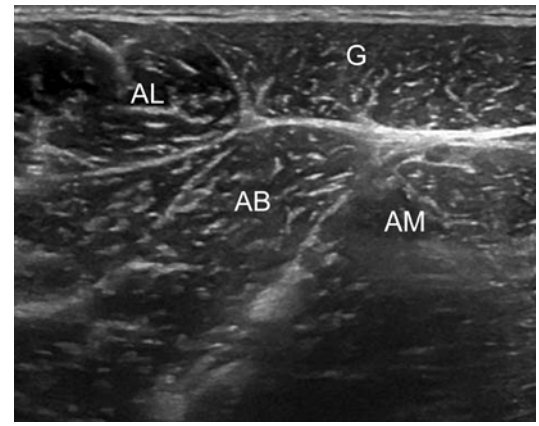

Fig. 10.5 US axial scan at proximal third of the thigh that shows the anatomical relationship between the adductor longus (*AL*), adductor brevis (*AB*), adductor magnus (*AM*), and gracilis (*G*) muscles

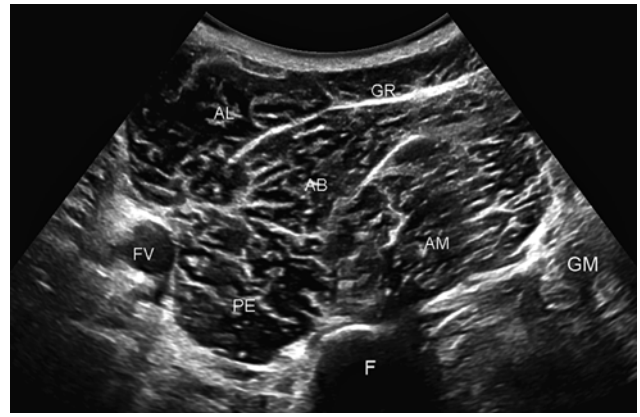

Fig. 10.6 US axial scan performed with a convex probe at proximal third of the thigh, showing a panoramic view of muscular anatomy of the medial compartment. *AL* adductor longus muscle, *AB* adductor brevis muscle, *AM* adductor magnus muscle, *GM* gluteus maximus muscle, *GR* gracilis muscle, *F* femur, *FV* superficial femoral vascular bundle

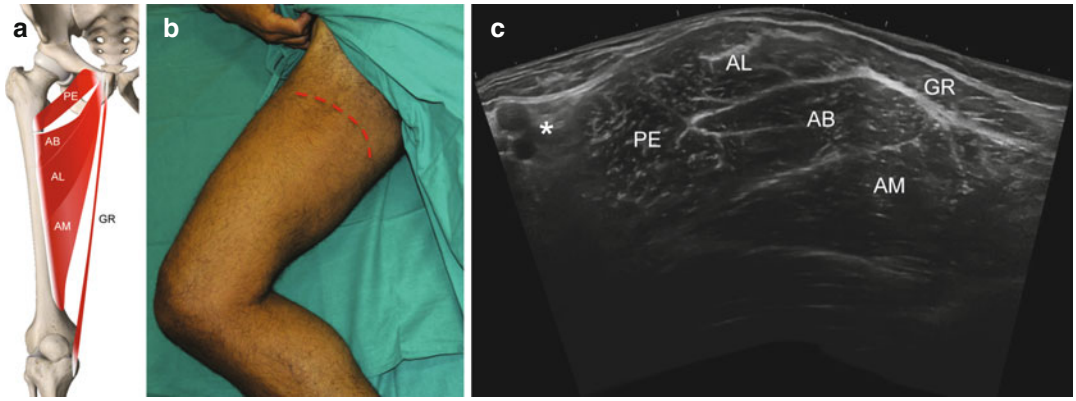

Fig. 10.7 Anatomical scheme correlated to EFV US axial scan at the proximal third of the thigh showing the anatomical relationship among the pectineus (*PE*), adductor longus (*AL*), adductor brevis (*AB*), adductor magnus (*AM*), and gracilis (*GR*). At this level the most superficial muscles are *AL* and *GR*; *AB* lies just deeper to *AL*; *AM* appears as a large muscle posterior and deeper to *AB*. Note the superficial femoral neurovascular bundle (*)

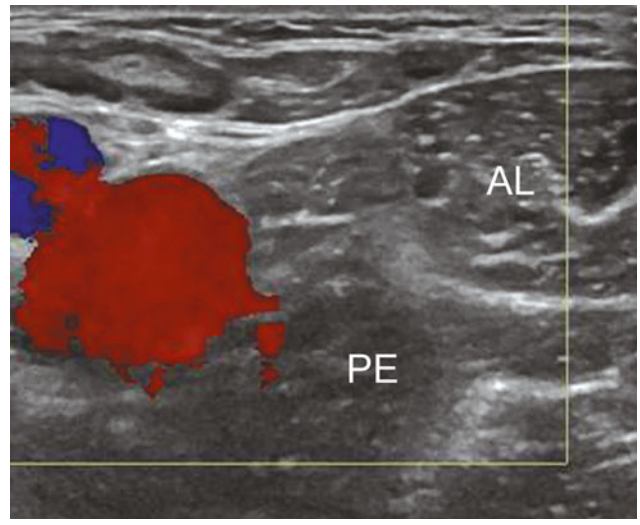

Fig. 10.8 US axial scan with color Doppler at level of the femoral vascular bundle. The adductor longus (*AL*) and the pectineus (*PE*) muscles lie medial to the femoral vascular bundle

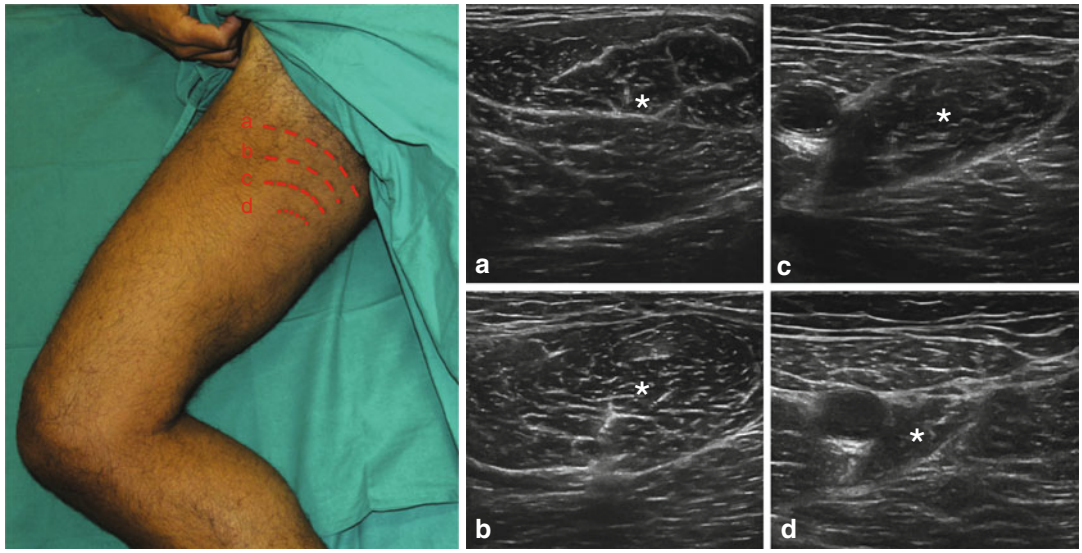

Fig. 10.9 Anatomical scheme correlated to US axial scans at different levels (**a**–**d**) of the adductor longus muscle (*). Note that muscle cross-sectional area progressively decreases

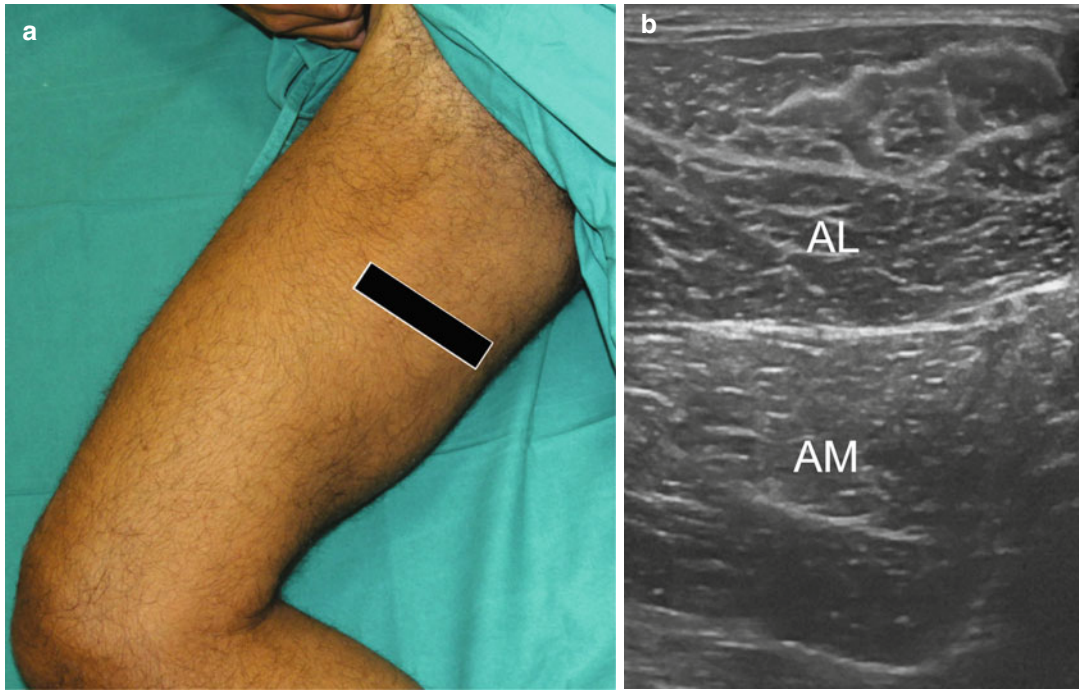

Fig. 10.10 At middle third of the thigh (**a**) US axial scan (**b**) that shows the anatomical relationship between the adductor longus (*AL*), adductor magnus (*AM*) muscles

10.2 Gracilis Muscle

10.2.1 Anatomy Key Points

The *gracilis* muscle, as its name implies, is a long, slim, strip-like muscle. It is the most superficial adductor muscle and lies on the medial aspect of the thigh and the knee.

Gracilis muscle adducts and flexes the thigh at the hip joint and aids the flexion of the knee.

It originates by a thin aponeurosis from the front of the body and the inferior ramus of the pubis.

It runs vertically downwards between semimembranosus posteriorly and sartorius anteriorly, and its belly develops a fusiform shape at its middle third.

The gracilis muscle becomes tendinous above the knee and inserts into the anteromedial surface of the superior aspect of the tibial shaft. This distal attachment is located anteriorly to the semitendinosus and blends with the posterior aspect of the sartorius insertion. A few fibers of the lower part of the tendon continue into the deep fascia of the leg.

Crossing both hip joint and knee joint, it is the only two-joint adductor muscle.

Gracilis, sartorius, and semitendinosus tendons, which are conjoined proximally on the medial side of the tibia, form the *pes anserine*. These three tendons are separated from the medial collateral ligament by the pes anserinous bursa, which is a fluid-filled vesicle. It secretes synovial fluid in order to reduce friction between tissues and also works as a cushion for bones, tendons, and muscles. The inflammation of the bursa does not appear suddenly but rather progresses over a period of time.

10.2.2 Ultrasound Examination Technique

Continue the exam visualizing the gracilis muscle in short axis from proximal to distal insertion (Figs. 10.11 and 10.13).

Place the probe with an axial scan at upper third of the thigh and identify the gracilis muscle belly superficial and medial to adductor muscles, just below the subcutaneous tissue. Follow it up to the anteromedial aspect of the superior tibial shaft where the gracilis tendon inserts.

Then turn the probe by 90° to evaluate the myotendinous junction and the distal attachment of gracilis tendon on the anteromedial aspect of the tibia on its long axis (Figs. 10.12, 10.16, and 10.17).

10.3 Pes Anserinus

10.3.1 Anatomy Key Points

The common attachment of the sartorius, gracilis, and semitendinous tendons, on the anteromedial aspect of the proximal tibia, forms a structure that resembles the natatory membrane of the goose; therefore, it has been called “goosefoot” or, from the Latin, “pes anserinus” (Fig. 10.14). The main function of these muscles is to flex the knee but also to aid the internal rotation of the tibia, protecting the knee against valgus stress.

The *anserinus bursa* is located deep to pes anserina tendons and superficial to the insertion of the tibial collateral knee ligament. Usually, this bursa does not communicate with the knee but sometimes can communicate with the subtendinous bursa of sartorius.

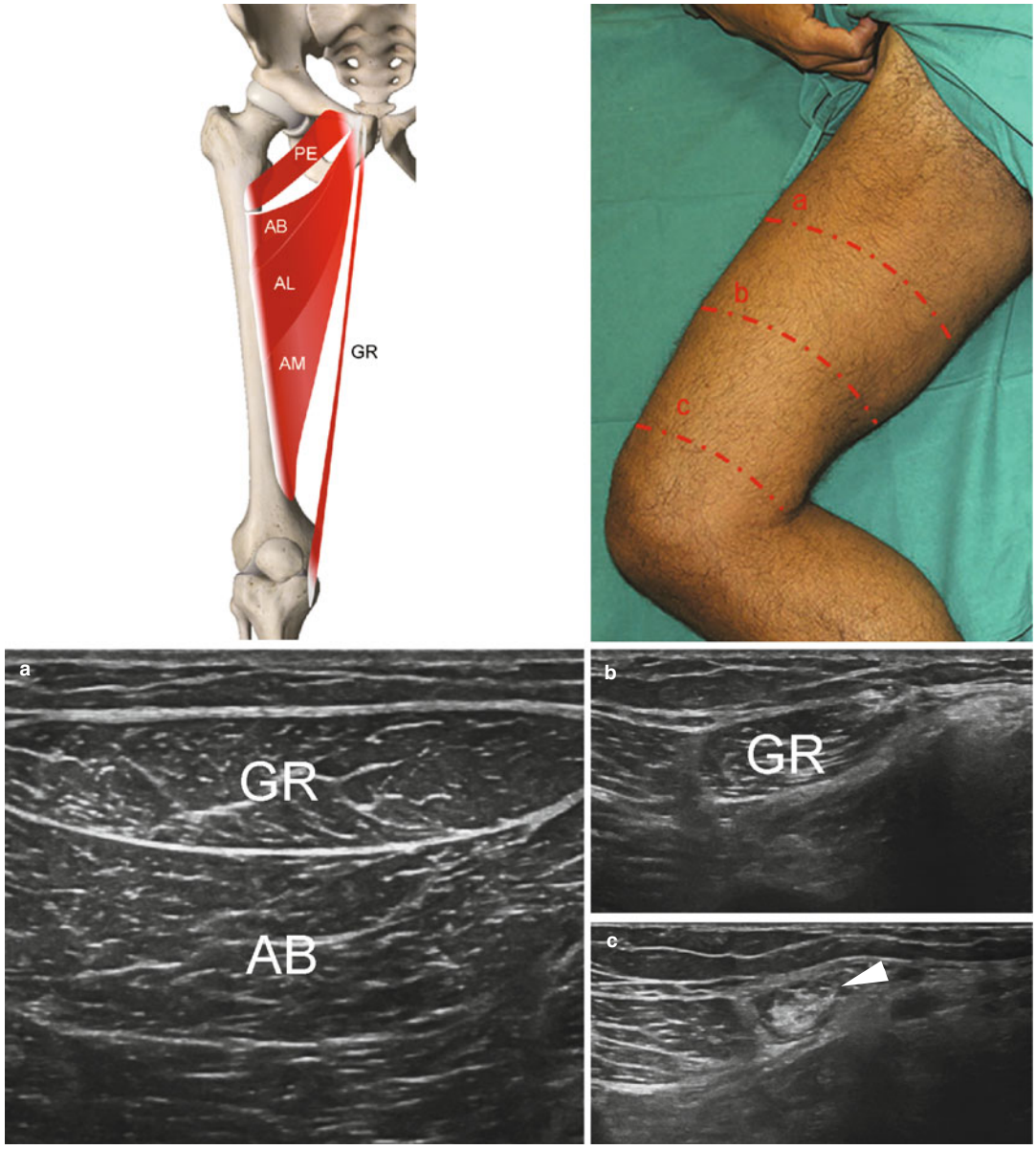

Fig. 10.11 Anatomical scheme, probe position and US axial scans at different levels of the gracilis muscle (*GR*). Cross-sectional area progressively decreases from the proximal third of the thigh to the distal myotendinous junction (*arrowhead*) (**a**–**c**). *AB* adductor brevis muscle

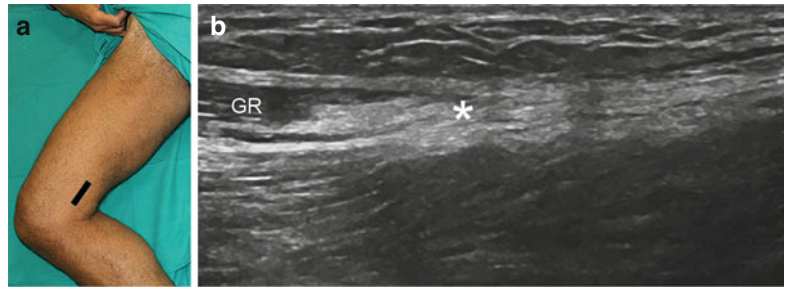

Fig. 10.12 (**a**) US probe position to assess the myotendinous junction and the distal insertion of gracilis (*GR*) muscle on longitudinal plane. (**b**) US longitudinal scan of gracilis (*GR*) muscle myotendinous junction (*)

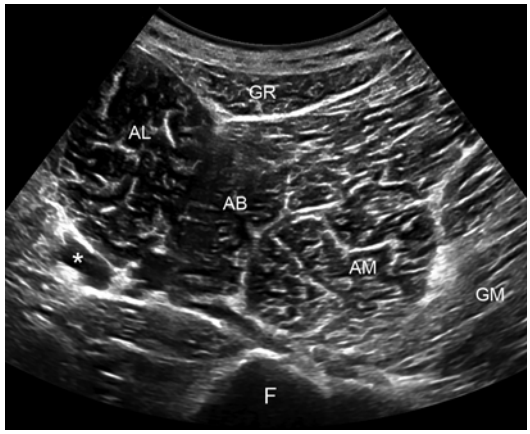

Fig. 10.13 US axial scan performed with convex probe at proximal third of the thigh showing a panoramic view of muscular anatomy of the medial compartment. *AL* adductor longus muscle, *AB* adductor brevis muscle, *AM* adductor magnus muscle, *GM* gluteus maximus muscle, *GR* gracilis muscle, *F* femur, * superficial femoral vascular bundle

10.3.2 Ultrasound Examination Technique

US is an excellent imaging technique to evaluate superficial soft tissues, such as tendons and *bursae*.

For examination of *pes anserine* tendons, the patient lies supine and rotates the leg externally with the knee flexed about 30° (Fig. 10.15).

Place the transducer on the medial aspect of the obliquely oriented knee, over the long axis of the medial collateral ligament. Then, move the transducer caudally following the medial collateral ligament (Fig. 10.16). Distally, rotate the transducer forward to visualize the "goosefoot" tendons (sartorius, gracilis, and semitendinosus) in their short axis (Fig. 10.17).

These tendons are very close to each other at the level of the tibial insertion, so they cannot be easily distinguished from each other with ultrasound.

Fig. 10.14 Anatomical scheme of pes anserinus. *SA* sartorius muscle, *GR* gracilis muscle, *ST* semitendinosus muscle

Fig 10.15 Lower limb position to evaluate the *pes anserinus*

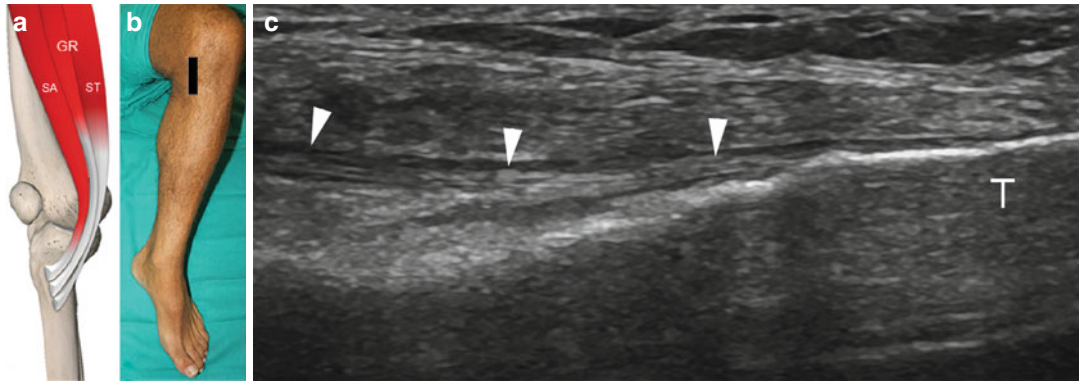

Fig. 10.16 (**a**) US probe position to evaluate the *pes anserinus* on longitudinal plane. (**b**) Anatomical scheme of pes anserinus. *SA* sartorius muscle, *GR* gracilis muscle, *ST* semitendinosus muscle. (**c**) US longitudinal scan shows the distal insertion of the *pes anserinus* tendons (*arrowheads*) on the surface of the tibia (*T*) medial to the tibial tuberosity

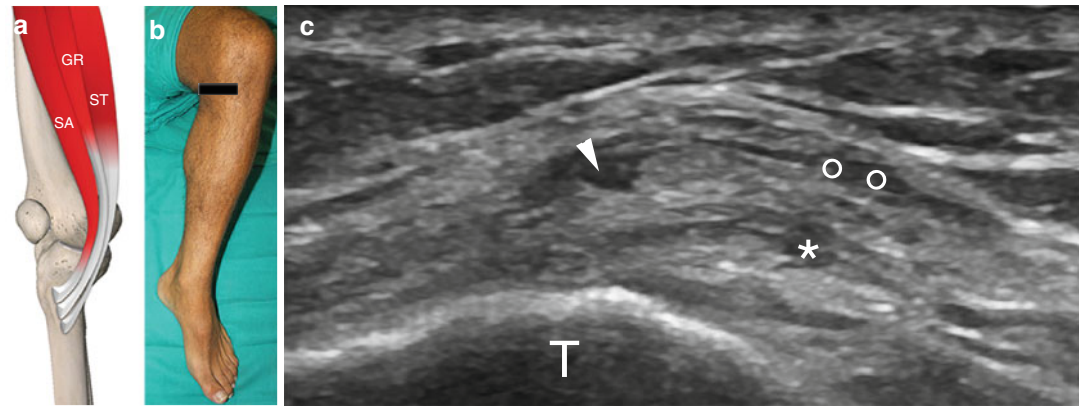

Fig. 10.17 (**a**) US probe position to evaluate the *pes anserinus* on axial plane. (**b**) Anatomical scheme of pes anserinus. *SA* sartorius muscle, *GR* gracilis muscle, *ST* semitendinosus muscle. (**c**) US axial scan shows the distal insertion of the *pes anserinus* tendons on the surface of the tibia (*T*) medial to the tibial tuberosity. *circles sartorius tendon*, *arrowhead* gracilis tendon, * semitendinosus tendon

Complete the examination with the measurement of the thickness of the pes anserine insertion (mean normal value ≤2,5 mm), the intratendinous and subcutaneous fat features, and the physiological absence of fluid collection in the bursa, which results to be virtual in normal conditions.

10.4 Hunter's Canal

Focus On

The adductor canal, or Hunter's canal (Fig. 10.18), was firstly described by John Hunter in 1786; it is an aponeurotic-fibromuscular tunnel delimitated by the vastus medialis muscle anterolaterally, adductor longus and magnus muscles posteriorly, and sartorius muscle medially and by a strong aponeurosis that extends between the adductors across the vessels, to vastus medialis (vastoadductor membrane) anteromedially. This aponeurotic tunnel, located in the middle third of the thigh, runs from the apex of the femoral triangle (Scarpa's triangle) to a passage in adductor magnus. The femoral vessels leave the adductor canal to reach the popliteal fossa.

Two different entrapment syndromes are related to compression of the neurovascular bundle inside the adductor canal: the vascular one presents as a claudication syndrome, while the nervous one brings on the compression of the saphenous nerve at the adductor hiatus resulting in pain on the medial aspect of the knee. The muscular hypertrophy may play an important role in the pathophysiological compressive mechanism.

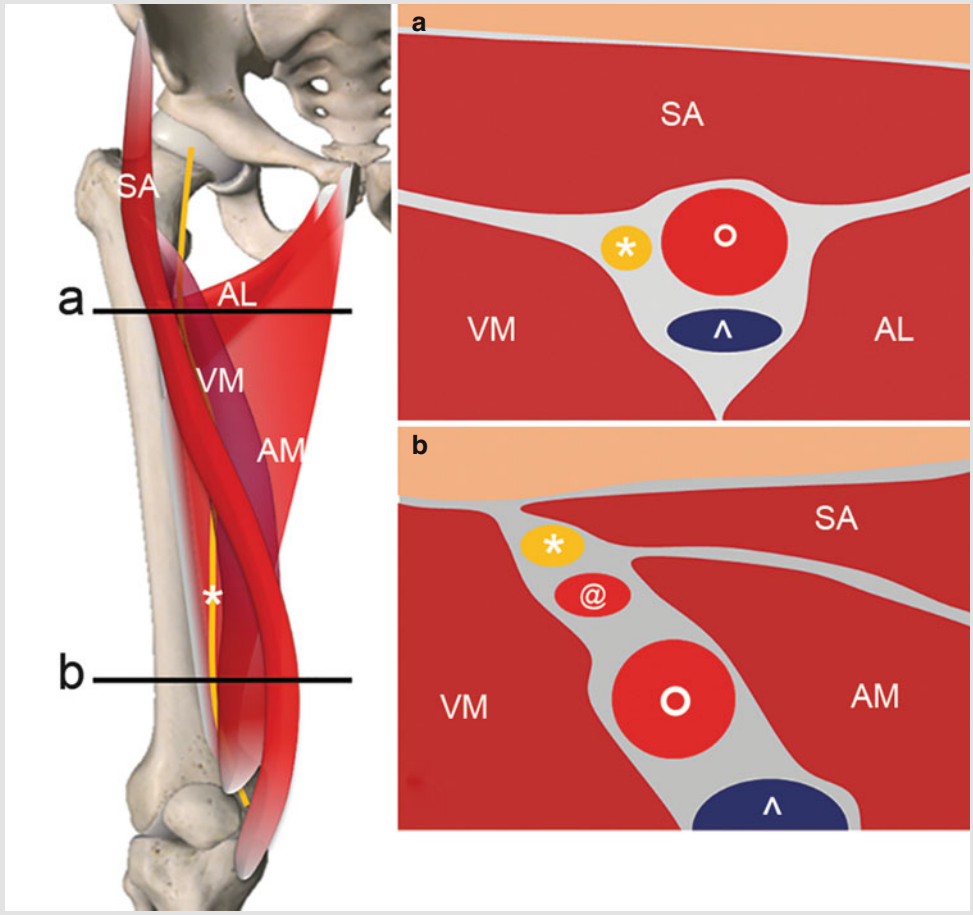

Fig. 10.18 Anatomical scheme of Hunter's canal with focus on the proximal (**a**) and distal part (**b**). *SA* sartorius muscle, *AL* adductor longus muscle, *AM* adductor magnus, *VM* vastus medialis muscle, * saphenous nerve, ° femoral artery, ^ femoral vein, @ descending genicular artery

10.4.1 Ultrasound Examination Technique

High-end ultrasound machine equipped with high-resolution transducers are required for the evaluation of Hunter's canal and its neurovascular content.

The patient lies supine with the thigh abducted and externally rotated and the knee bent (frog leg position) (Fig. 10.1).

Place the linear probe on an axial plane at level of crural region, at the apex of the Scarpa's triangle, where the sartorius muscle crosses anteriorly the superficial femoral artery: a superficial vessel in relation with the deep fascia of sartorius muscle.

Move the transducer caudally to reach the superficial femoral artery, branch of the common femoral artery, when it enters in the adductors' canal (Fig. 10.19).

The examination continues with exploration of proximal part of Hunter's canal: the saphenous nerve, the largest cutaneous branch of the femoral nerve, is lateral to the superficial femoral artery; the femoral vein is posterior to the artery. The saphenous nerve presents a fascicular echostructure, with a hyperechoic oval structure, surrounded by a rim of hypoechoic perineural fat. Note the typical "honeycomb" appearance of the saphenous nerve. The adductor longus muscle is the posterior wall of Hunter's canal (Fig. 10.20).

From this position, shift the probe caudally to follow the neurovascular bundle in the second part of the adductor canal where the posteriormedial wall is represented by adductor magnus muscle: the saphenous nerve becomes progressively more anterior to the superficial femoral artery (Fig. 10.21).

Then, move the transducer caudally on the anteromedial aspect of the distal third of the thigh to reach the origin of the descending genicular artery from the superficial femoral artery, which represents a precise landmark to identify the distal end (hiatal region) of the adductor canal. At this level the femoral artery and vein are deeper than saphenous nerve (Fig. 10.22).

Rotate the transducer by 90° to evaluate the descending genicular artery on its longitudinal plane.

The coronal oblique US scan shows the relation between descending genicular artery and adductor magnus rounded tendon, which forms the medial wall of the adductor canal hiatus.

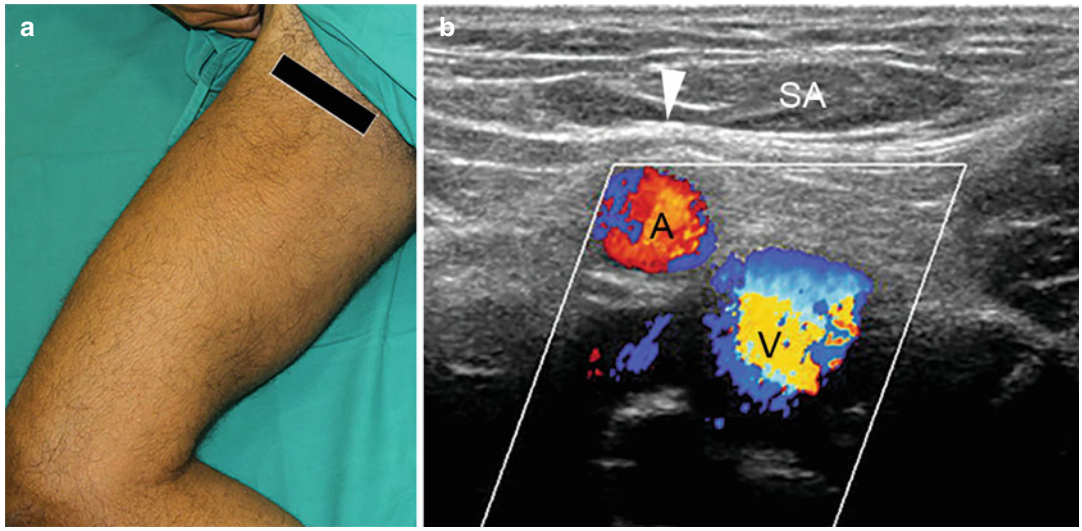

Fig. 10.19 (**a**) US probe position on the crural region at the apex of the femoral triangle. (**b**) color Doppler axial scan. The deep fascia (*arrowhead*) of sartorius muscle (*SA*) is in relation with the anterior aspect of the superficial femoral artery wall (*A*). *V* femoral vein

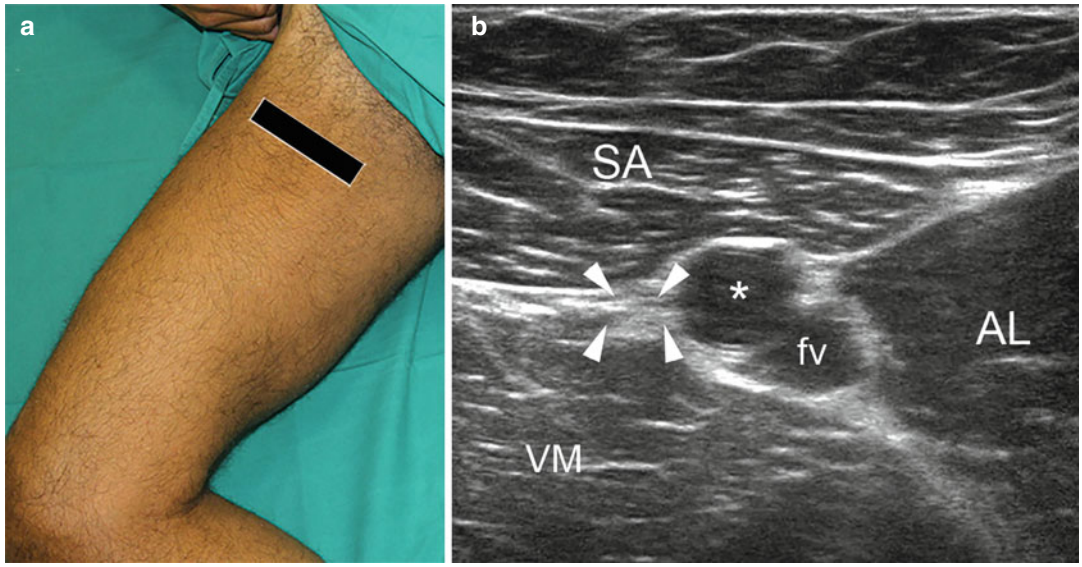

Fig. 10.20 (**a**) US probe position on the anteromedial aspect of the thigh. (**b**) Axial oblique US scan showing the neurovascular bundle inside the proximal third of the adductor canal. The saphenous nerve (*arrowheads*) is lateral to the femoral artery (*); the femoral vein (*fv*) is posterior. The posterior wall is represented by adductor longus muscle (*AL*). Note the "honeycomb" echostructure of the saphenous nerve, adjacent to the arterial wall. *SA* sartorius muscle, *VM* vastus medialis muscle

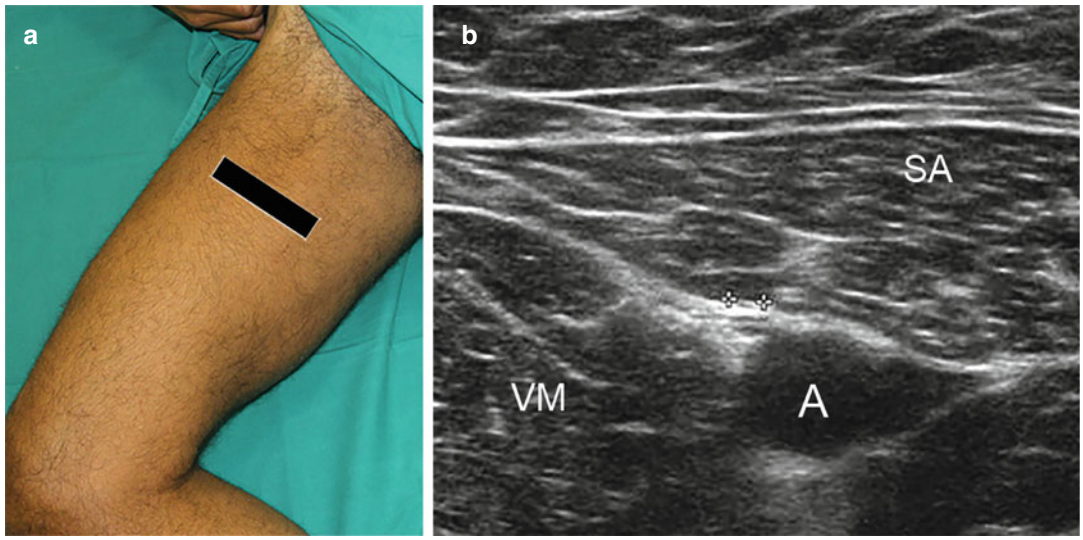

Fig. 10.21 (**a**) US probe position on the anteromedial aspect of the thigh. (**b**) Axial oblique US scan showing the neurovascular bundle inside the middle third of the adductor canal. The saphenous nerve (*calipers*) moves from a lateral position to the femoral artery (*A*) to an anterior position to this vessel near the hiatal region. The saphenous nerve may be identified on axial US scans between the anterior surface of the arterial wall and the deep fascia of sartorius (*SA*) muscle. *VM* vastus medialis muscle

At this level, use the adductor tubercle of the medial femoral condyle as a bony landmark to identify the rounded tendon of adductor magnus that presents a fibrillar echostructure. Slight cranially the probe, always in the coronal oblique scan plane, to visualize the myotendinous junction of the tendon itself. The superficial femoral vessels are lateral to the myotendinous structure (Fig. 10.23).

The color Doppler module may aid the detection of the neurovascular bundle at all levels of the Hunter canal.

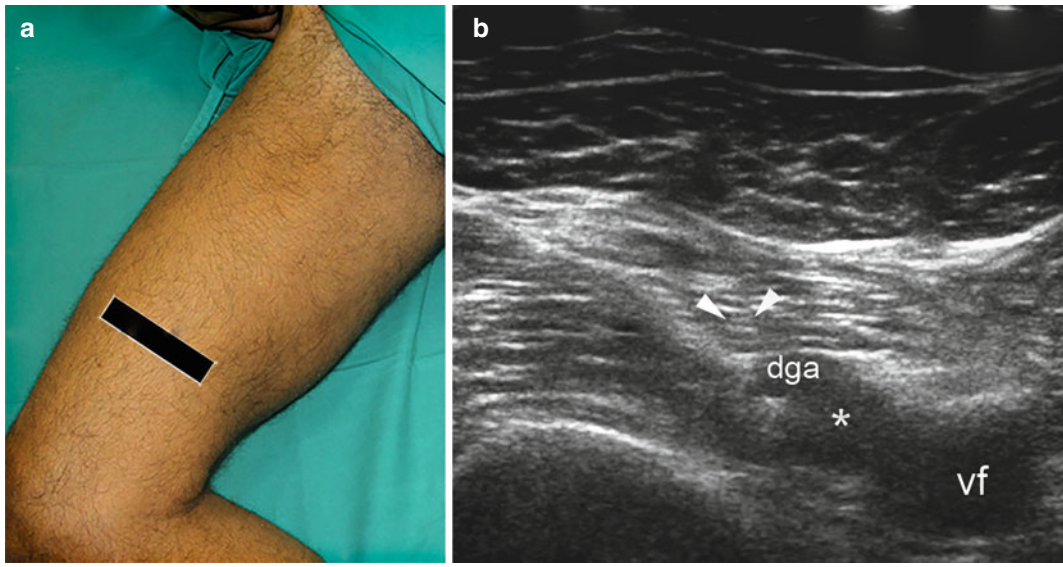

Fig. 10.22 (**a**) US probe position on the anteromedial aspect of the distal third of the thigh. (**b**) Axial US scan showing the neurovascular bundle inside the middle third of the adductor canal. Femoral vessels (* femoral artery, *fv* femoral vein) and saphenous nerve (*arrowheads*) diverge at this level. The saphenous nerve is adjacent to the descending genicular artery (*dga*), which may not be confused with a large, more proximal, muscular branch of the femoral artery to vastus medialis

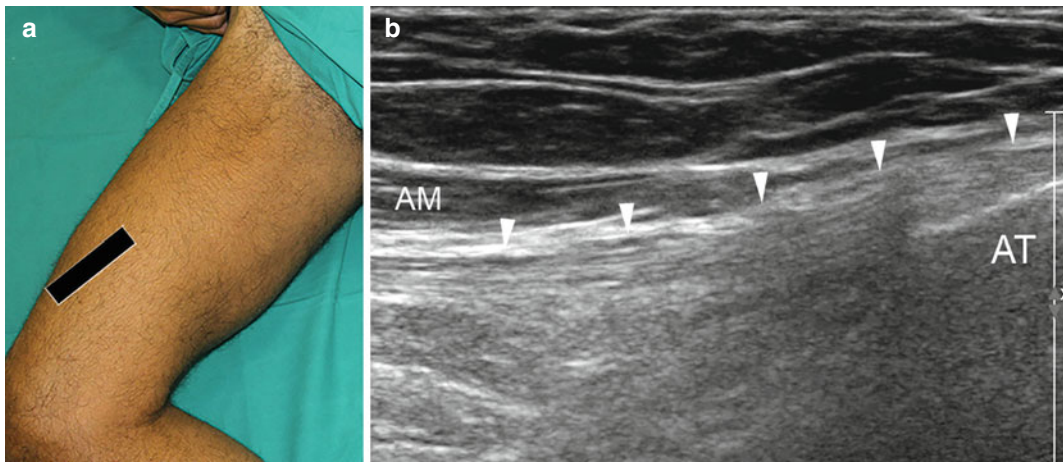

Fig. 10.23 (**a**) US probe position on the medial femoral condylar region. (**b**) Coronal oblique US scan at the adductor tubercle (*AT*) of the medial femoral condyle; the adductor magnus rounded tendon (*arrowheads*) shows the typical fibrillar pattern. *AM* adductor magnus muscle

10.5 Summary Table

Muscle	Origin	Insertion	Action	Nerve supply
Gracilis	Inferior ramus of pubis; ramus of ischium body and inferior ramus of the pubis	Anteromedial surface of the superior part of the shaft of the tibia	Adduction of the thigh; flexion of the leg	Obturator nerve
Adductor longus	Anterior pubis	Middle third of linea aspera of femur	Adduction of the thigh and assistance in lateral rotation	Obturator nerve
Adductor brevis	Body of the pubis and inferior pubic ramus	Linea aspera of femur	Adduction of the thigh and assistance in lateral rotation	Obturator nerve
Adductor magnus	Femoral surface of the ischiopubis ramus and inferior surface of the ischial tuberosity	Linea aspera of femur; adductor tubercle of femur	Adduction of the thigh and assistance in lateral rotation. Hamstring part extends thigh	Obturator nerve and tibial part of sciatic
Pectineus	Pectineal line and the surface of bone between the iliopectineal eminence and pubic tubercle	Pectineal line	Flexion and adduction of the thigh and assistance in medial rotation	Femoral nerve and accessory obturator nerve

Suggested Reading

Bianchi S, Martinoli C (2007) US of the musculoskeletal system. Martinoli, Berlin/New York: Springer

de Souza RR, de Carvalho CA, König B Jr (1978) Topographical anatomy of adductor canal: form, limits and constitution of its walls. Rev Paul Med 92(1–2):6–9

Drake RL, Vogl W, Mitchell A (2005) Grey's anatomy. Elsevier/Churchill Livingstone: Drake, Edinburgh

Gilmore J (1998) Groin pain in the soccer athlete: fact, fiction, and treatment. Clin Sports Med 17:787–793

Hunter LY, Louis DS, O'connor GA (1979) The saphenous nerve: its course and importance in medial arthrotomy. Am J Sports Med 7(4):227–230

Paparo F, Sconfienza LM, Muda A, Grillo G, Lacelli F, Silvestri E (2008) High-resolution ultrasound (HRUS) evaluation of neurovascular and muscular structures of the Hunter canal. Skeletal Radiol 37:575–596

Scholten FG, Mali WP, Hillen B, van Leeuwen MS (1989) US location of the adductor canal hiatus: morphologic study. Radiology 172(1):75–78

Silvestri E, Muda A, Sconfienza LM (2012) Normal ultrasound anatomy of the musculoskeletal system. Silvestri, Milan/New York: Springer

Stoller DW (2007) Stoller's Atlas of orthopaedics and sports medicine. Lippincott Williams & Wilkins: Stoller, Philadelphia

Tschirch FTC, Schmid MR, Pfirrmann CWA et al (2003) Prevalence and size of meniscal cysts, ganglionic cysts, synovial cysts of the popliteal space, fluid filled bursae, and other fluid filled collections in asymptomatic knees on MR imaging. AJR Am J Roentgenol 180:1431–1436

Tyler TF, Silvers HJ, Gerhardt MB, Nicholas SJ (2010) Groin injuries in sports medicine. Sports Health 2:231–236

Valenti A, Frizziero A, Bressan S, Zanella E, Giannotti E, Masiero S (2012) Insertional tendinopathy of the adductors and rectus abdominis in athletes: a review. Muscles Ligaments Tendons J 2(2):142–148

Vitiello FS (1975) Anatomical and surgical notes on the morphology of Hunter's canal. Minerva Med 66(15): 706–710

Gluteal and Piriformis

11

Alice Arcidiacono and Alessandro Muda

11.1 Gluteal Muscles

11.1.1 Anatomy Key Points

Gluteal muscles are composed by three structures disposed into two layers: gluteus maximus superficially and gluteus medius and gluteus minimus more deeply (Fig. 11.1).

Gluteus maximus is the largest and most superficial of gluteus muscles; it is a thick flat sheet of muscle that forms the contour of the buttock. It arises from the gluteal line on the posterior border of the ilium, from the side of lower sacrum and coccyx, from the sacrotuberous ligament and from the aponeurosis of the erector spinae. Gluteus maximus fibres cover superficially the entire area comprised among the ilium, the sacrum and the ischium, to reach the iliotibial tract and the femur laterally: the whole upper portion of the muscle and the superficial fibres of the lower portion attach to the posterior portion of the fascia lata; the lower, deep portion of the muscle inserts on the gluteal tuberosity on the posterior aspect of the proximal femoral metaphysis, between the vastus lateralis and the adductor magnus attachments and under the quadratus femoris insertion (Fig. 11.2a).

Gluteus medius is a deep muscle of the posterior hip: its posterior third is located deep to the gluteus maximus muscle, whereas its anterior two thirds result more superficial, just below the fascia lata. Gluteus medius originates from the posterior two thirds of the iliac wing and then courses laterally and downwards. It inserts into the posterior aspect of the greater trochanter of the femur with its more posterior portion and onto the inferolateral aspect of the greater trochanter with its middle-anterior portion (Fig. 11.2b).

Gluteus minimus is the deepest gluteal muscle; it takes origin from the anterior third of the posterior iliac wing and, with its fibres, comes laterally and downwards to attach onto the anterior facet of the greater trochanter of the femur (Fig. 11.2c).

Several synovial bursae are disposed around the greater trochanter and are detectable when distended by fluid: the trochanteric bursa, which is the largest and is

A. Arcidiacono
Dipartimento di Radiologia,
Università degli studi di Genova, Genova, Italy
e-mail: alice.arcidiacono@hotmail.com

A. Muda (✉)
Dipartimento di Radiologia,
IRCCS Ospedale San Martino IST, Genoa, Italy
e-mail: alessandro.muda@tiscali.it

E. Silvestri et al., *Ultrasound Anatomy of Lower Limb Muscles: A Practical Guide*,
DOI 10.1007/978-3-319-09480-9_11,

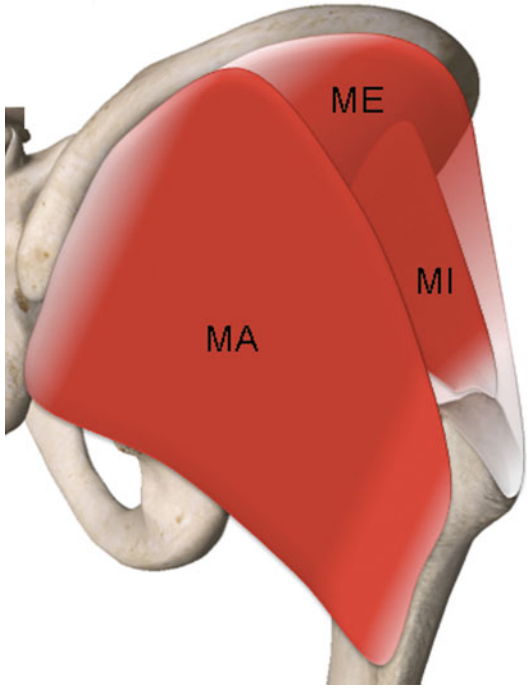

Fig. 11.1 Anatomical scheme of the gluteal muscles: *MA* gluteus maximus, *ME* gluteus medius, *MI* gluteus minimus

located in a plane between the gluteus maximus and the tendon of the gluteus medius and the trochanter; the subgluteus maximus bursa, which is located between the gluteus maximus tendon attachment and the femur; the subgluteus medius bursa, which is located between the gluteus medius tendon insertion and the trochanter; and the subgluteus minimus bursa, sited anteromedially to the gluteus minimus tendon attachment.

11.1.2 Ultrasound Examination Technique

The patient lies on the table in lateral decubitus.

Start the evaluation of the gluteal region palpating the lateral aspect of the hip and find the bony prominence of the greater trochanter of the femur (Fig. 11.3).

Place the probe with a transverse orientation over the anterior-superior aspect of the trochanter: the US image shows the typical 'rotator cuff appearance' of the tendinous insertions of the gluteal muscles covered by the muscular fibres of the gluteus maximus. Such a definition is due to some analogies with the deltoid muscle in the shoulder, which lies over the rotator cuff tendons (Fig. 11.4).

Proceeding from anterior to posterior along the hyperechoic cortex of the femur are three different hyperechoic fibrillar structures: the tendon of the gluteus minimus (inserting onto the anterior facet of the trochanter), the anterior portion of the gluteus medius tendon (inserting on the lateral aspect of the trochanter) and the thicker posterior portion of the tendon of the gluteus medius (on the posterolateral aspect of the trochanter), covered by gluteus maximus muscular fibres.

Then rotate the probe by 90° and slide the transducer from anterior to posterior to assess each tendon along its long axis, in order to avoid anisotropic effects (Fig. 11.5).

Fascia lata, which courses between gluteus maximus posteriorly and tensor fasciae latae anteriorly, could be used as an important anatomic landmark during the US examination. It is indeed detectable on the US image as a hyperechoic layer of fibrous tissue standing just below the subcutaneous fat: remember that gluteus medius and gluteus minimus course under that fascia (Fig. 11.6).

Further, gluteal muscles can be followed proximally from the greater trochanter to their individual origins. With the patient in lateral decubitus, place the probe on the greater trochanter as for the tendinous attachments evaluation, then move it cranially with a transverse-oblique orientation towards the anterosuperior iliac spine: in this way the anterior portion of the gluteus medius (superficially and posterior) and the gluteus minimus (anteriorly and deep) can be followed (Fig. 11.7).

To evaluate the gluteus medius, position the patient in a lateral-oblique decubitus (slightly prone) and move the probe from the greater trochanter up to the iliac crest: the relatively

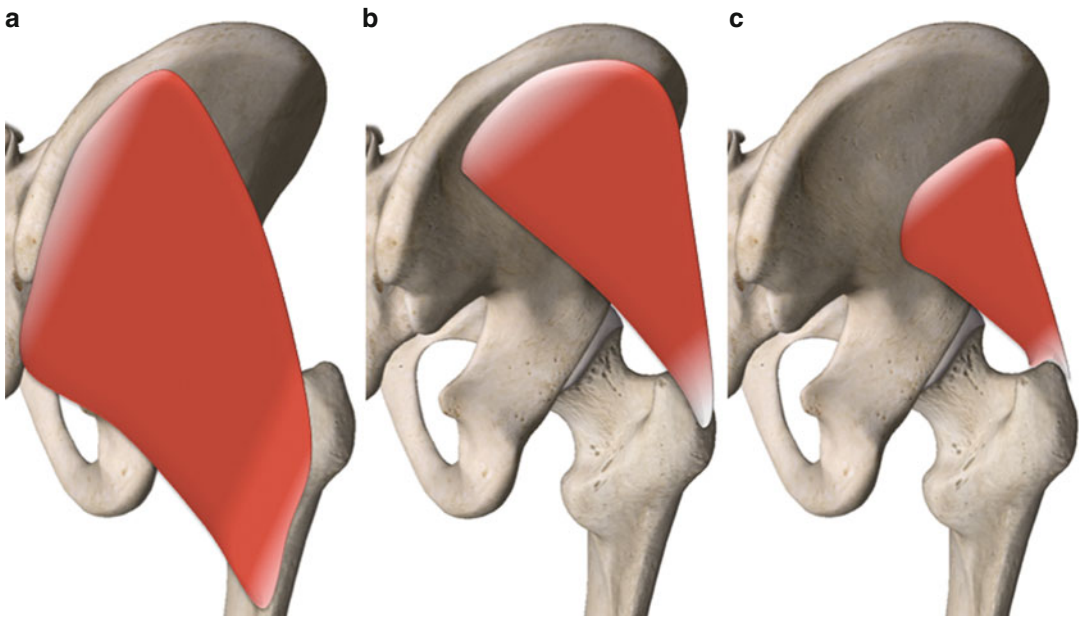

Fig. 11.2 Anatomical scheme of the (**a**) gluteus maximus, (**b**) gluteus medius and (**c**) gluteus minimus muscles

Fig. 11.3 Lower limb position to evaluate (**a**) the gluteus medius and minimus and (**b**) gluteus maximus

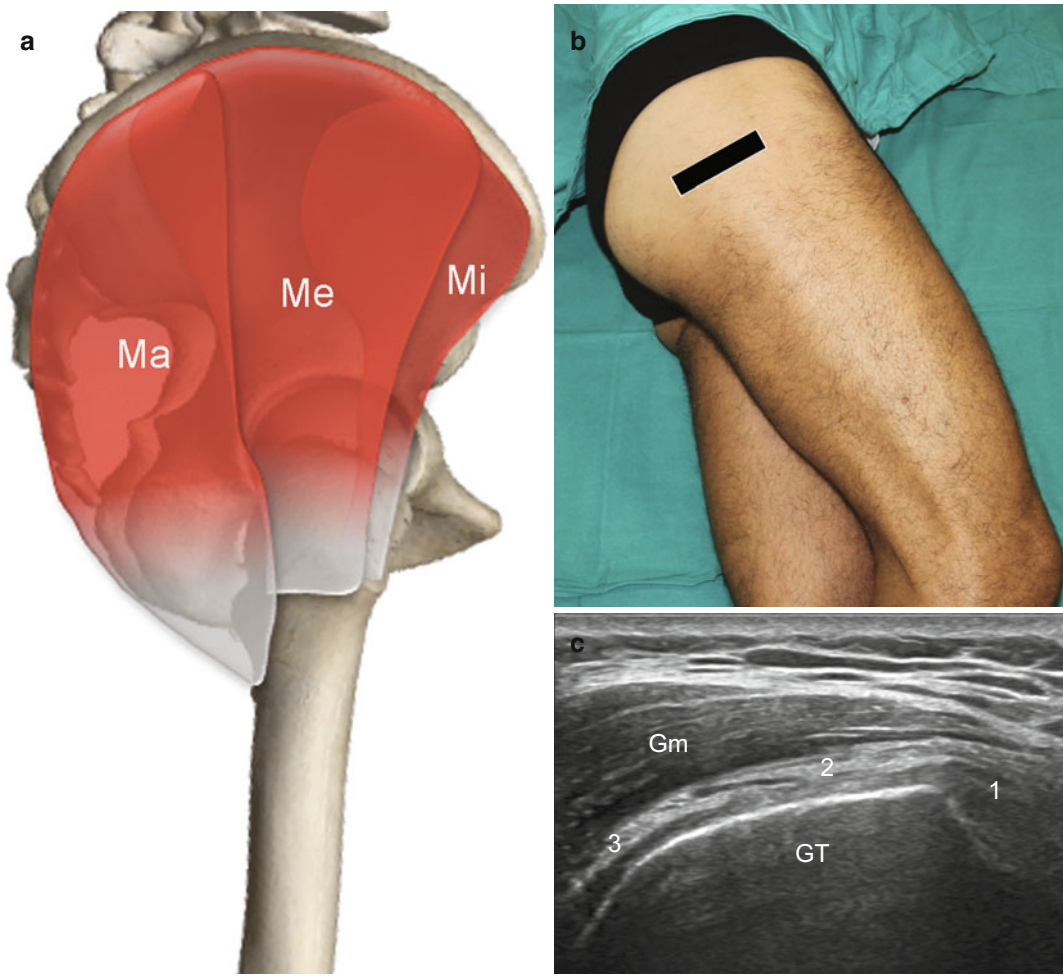

Fig. 11.4 (**a**) Anatomical scheme of the gluteal muscles: lateral view; *Ma* gluteus maximus, *Me* gluteus medius, *Mi* gluteus minimus. (**b**) Probe position over the lateral hip for the evaluation of the gluteal muscles. (**c**) Corresponding US axial scan over the greater trochanter: the image shows the "cuff-like" appearance of gluteal muscles insertions on the greater trochanter (*GT*); the gluteus minimus tendon (*1*) attaches on the anterior aspect of the trochanter, gluteus maximus tendon (*3*) inserts on the posterior inferior aspect of the proximal femur and covers the trochanter with its muscular fibres (*Gm*), gluteus medius tendon (*2*) is positioned in the middle

hypoechoic muscular bundles of the gluteus medius, covered by the fascia lata, can be seen up to its proximal portion (Fig. 11.8).

Gluteus maximus must be evaluated within the patient in the prone position.

Place the transducer under the posterior edge of the iliac crest, just medially to the posterior superior iliac spine, and move obliquely towards the femoral metaphysis (keep the posterior aspect of the greater trochanter as an anatomic reference) following the muscular bundles of the gluteus maximus until their attachment on the gluteal tuberosity.

Remember that all the muscular fibres running superficially in the area comprised among the posterior iliac crest, sacrum, coccyx, ischium, proximal femur, and fascia lata, belong to the gluteus maximus.

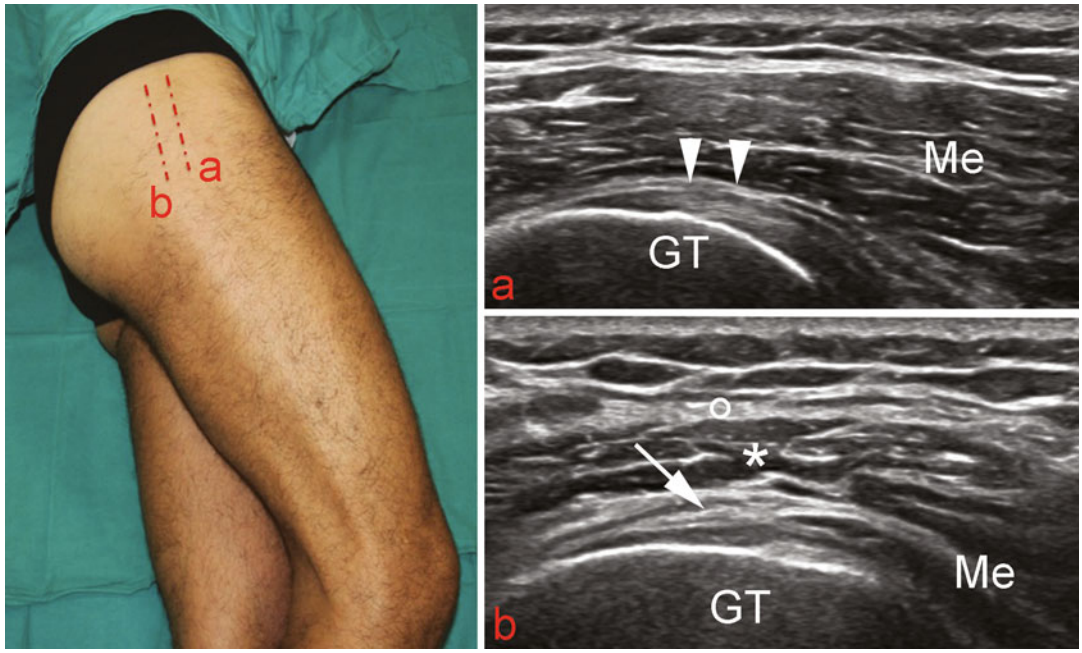

Fig. 11.5 Probe position at different levels over the lateral hip for the evaluation of the gluteal muscles on longitudinal planes. (**a**) More anterior US longitudinal scan: this image shows the relationship between the greater trochanter (*GT*) and the gluteus minimus tendon (*arrowheads*); superficial to it the gluteus medius fibres (*Me*) can be seen. (**b**) More posterior US longitudinal scan: this image shows the relationship between the greater trochanter (*GT*) and the gluteus medius tendon (*arrow*) and muscle (*Me*); superficial to it the fascia lata (*circle*) can be seen with its hyperechoic fibrillar structure, inside the surrounding fat tissue (*asterisk*)

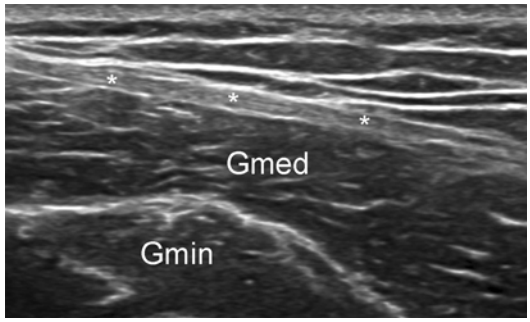

Fig. 11.6 Longitudinal-oblique US scan over the lateral hip which shows the relationship between gluteus medius (*Gmed*) and minimus (*Gmin*) and fascia lata (*asterisks*): the fascia passes just over those gluteal muscles bellies on the posterior aspect of the hip, ranging from the gluteus medius to the tensor fasciae latae muscle in posterior-to-anterior view

Along its distal posterior portion, gluteus maximus is in close relationship with an important anatomic structure: the sciatic nerve.

Place the probe in a transverse-oblique orientation keeping the ischial tuberosity on the medial side and the femur on the lateral as bony landmarks: a fascicular hyperechoic oval structure can be seen passing just below the relatively hypoechoic gluteus maximus muscle belly (Fig. 11.9).

Rotating the probe by 90° is possible to evaluate the nerve on its long axis and, in particularly slender subjects, the underlying muscular bellies of the superior gemellus, obturator internus, inferior gemellus and quadratus femoris (oblique cranial-to-caudal arrangement); unfortunately, detailed assessment is limited and dependent to patient habitus.

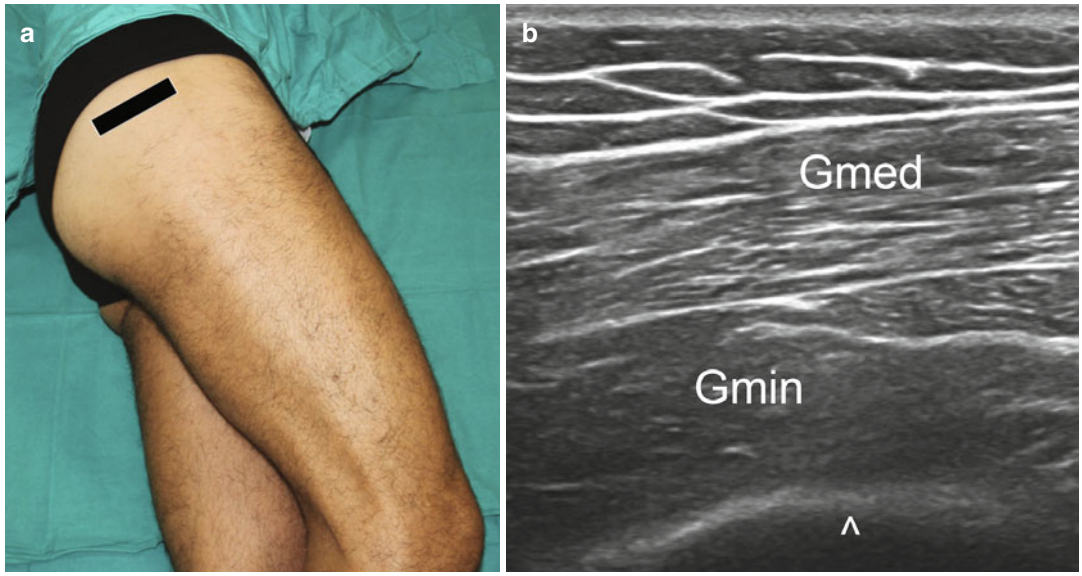

Fig. 11.7 (**a**) Probe placement over the lateral hip, cranial to the greater trochanter; (**b**) Corresponding US axial scan of the lateral hip, showing the gluteus medius (*Gmed*) and minimus (*Gmin*) bellies coursing over the iliac bone sited deeply

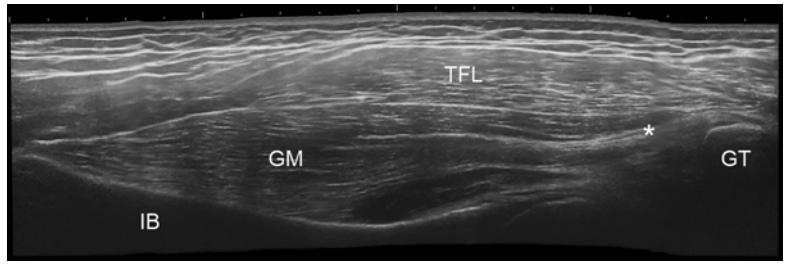

Fig. 11.8 Extended field of view. US longitudinal scan showing the entire course of the gluteus minimus muscle (*GM*) and tendon (*) from the external aspect of the iliac bone (*IB*) to the greater trochanter (*GT*); the more fatty muscular belly of the tensor fasciae latae (*TFL*) can be seen just superficial to them

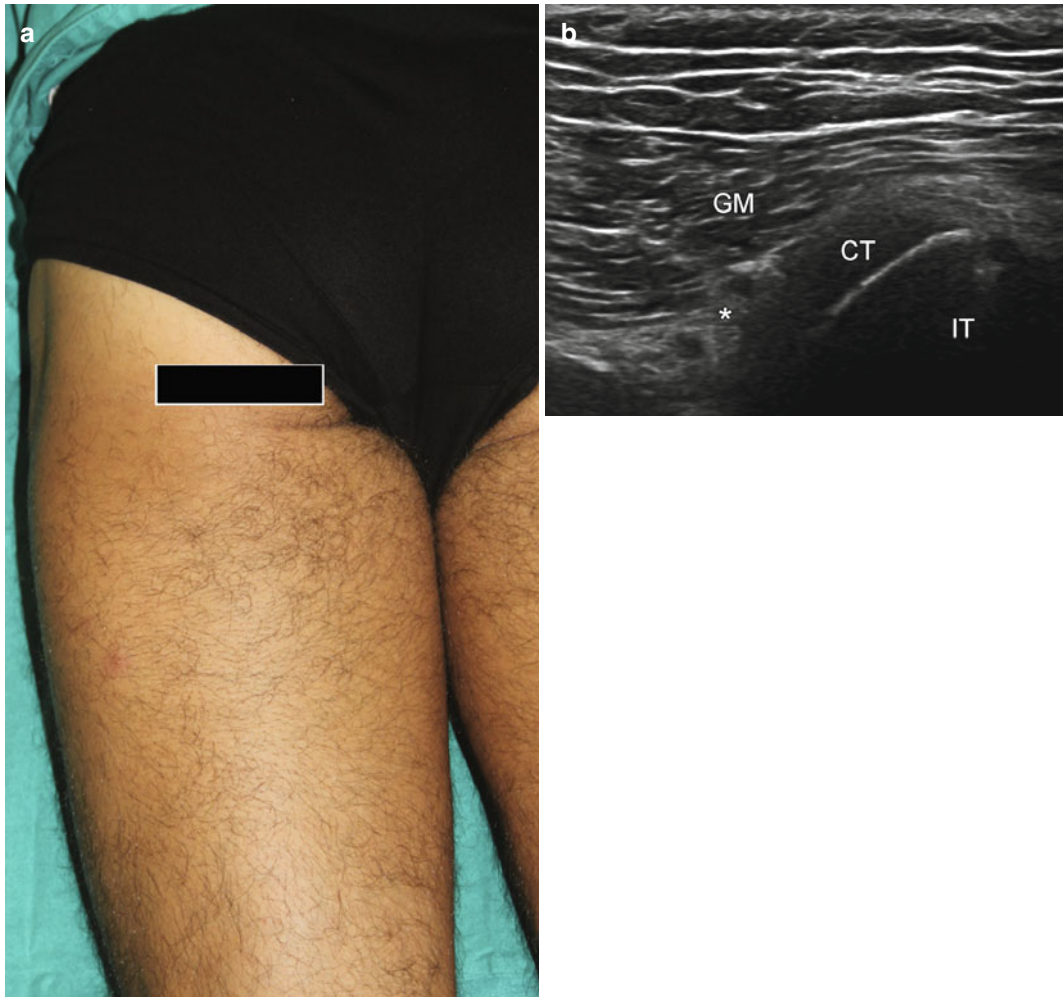

Fig. 11.9 (**a**) Probe position over the lateral hip for the evaluation of the gluteus maximus muscle. (**b**) Corresponding US transverse-oblique scan over the ischial tuberosity (*IT*): the image shows this important bony landmark, covered by the anisotropic fibres of the hamstrings conjoint tendon (*CT*) and, superficially, the muscular fibres of the gluteus maximus covering the entire area. The *asterisk* indicates the sciatic nerve with its fascicular hyperechoic structure, passing just laterally to the *IT* and deeply to the *GM*

11.1.3 Summary Table

Muscle	Origin	Insertion	Innervation	Action
Gluteus maximus	Posterior iliac crest, posterior iliac wing, sacrum, coccyx, sacrotuberous ligament, aponeurosis of the erector spinae	Fascia lata, gluteal tuberosity of posterior proximal femur	Inferior gluteal nerve (L5, S1, S2)	Major thigh extensor muscle; abductor and external rotator of the thigh; antigravitary function
Gluteus medius	Posterior two thirds of the iliac wing	Posterior and inferolateral aspect of the greater trochanter	Superior gluteal nerve (L4, L5, S1)	Abductor of the thigh; medial rotator of the thigh
Gluteus minimus	Anterior third of the posterior iliac wing	Anterior facet of the greater trochanter		

11.2 Piriformis Muscle

11.2.1 Anatomy Key Points

Piriformis is a pyramidal muscle located on posterior aspect of hip joint, inferiorly to gluteus medius. It arises from the anterolateral surface of sacrum, leaves the posterior pelvis trough the greater sciatic foramen along with the sciatic nerve (just above it), and inserts on the superomedial aspect of the greater trochanter (Fig. 11.10). Occasionally its tendon joins with those of the superior and inferior gemellus, and obturator internus muscles, before the insertional area. Piriformis is closely related to the sciatic nerve, which courses deep or through it in most of the population. Sometimes trapping and irritation of sciatic nerve are due to hypertrophy, inflammation and/or anatomic variant of the piriformis muscle, causing the so-called piriformis syndrome.

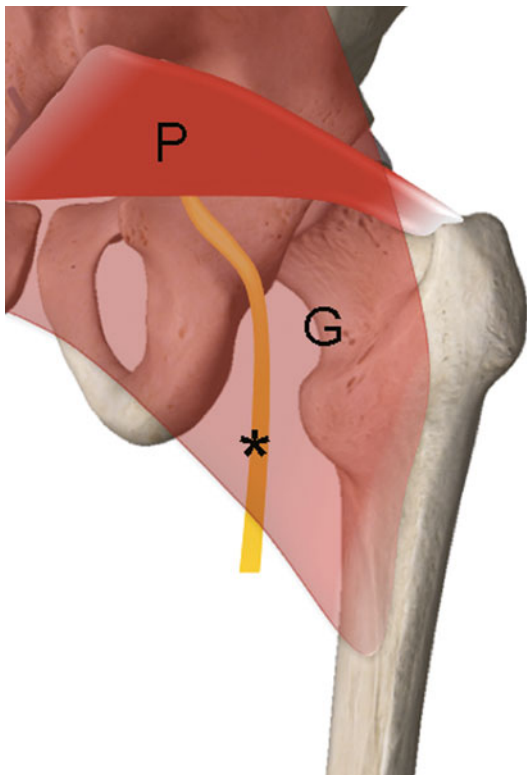

Fig. 11.10 Anatomical scheme of the piriformis muscle (*P*) and its relationship with the gluteus maximus muscle (*G*) and the sciatic nerve (*asterisk*)

11.2.2 Ultrasound Examination Technique

The US evaluation of the piriformis muscle must be performed with the patient lying prone on the examination table, as for the gluteus maximus muscle (see Fig. 11.3b). Placing a pillow or towels under the pelvis may contribute to expose the anatomic area under evaluation. In slender subjects a linear transducer may be used increasing the depth parameter; otherwise, a convex transducer allows the identification of the piriformis muscle.

Keep the lateral border of the sacrum as a bony landmark and place the medial edge of the probe next to it (with a transverse-oblique orientation). The US image shows the gluteus maximus superficially and, just below it, the first extrapelvic portion of the piriformis muscle. The sciatic nerve appears as an oval fascicular structure lying deep in the piriformis muscle and lateral to the inferior gluteal artery (easily seen with colour Doppler imaging): keep such structures as additional anatomical landmarks. Further, with the sciatic nerve in the middle of the US image, turn the probe by 90° and examine the nerve along its long axis.

At this level it is important to evaluate the relationship between the nerve and the piriformis muscle in order to assess possible causes of piriformis syndrome when clinically suspected (Fig. 11.11).

Then, moving the probe laterally, follow the piriformis muscular bundles coursing along the posterior aspect of ilium, then passing on the posterior aspect of the hip joint and inserting to the greater trochanter. Note that the adjacent muscular fibres, which course just caudally to the piriformis muscle and seem to merge together in the distal tendinous portion (occasionally merging into a unique tendon), belong to the gemelli and obturator internus muscles.

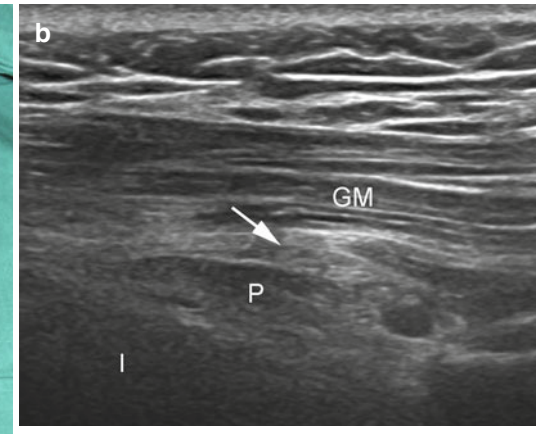

Fig. 11.11 (**a**) Probe position over the posterior hip for the evaluation of the piriformis muscle. (**b**) Corresponding US oblique scan: the image shows the sciatic nerve (*arrow*) coursing through the muscular fibres of the piriformis muscle (*P*), sited over the iliac bone (*I*); superficial to the piriformis muscle, the gluteus maximus (*GM*) fibres can be seen

11.2.3 Summary Table

Muscle	Origin	Insertion	Innervation	Action
Piriformis	Anterolateral surface of the sacrum	Superomedial aspect of the greater trochanter	(L5) S1, S2	External rotation of the thigh

Suggested Reading

Bianchi S, Martinoli C (2007) Ultrasound of the musculoskeletal system. Springer, Berlin

Laurell L, Court-Payen M, Nielsen S et al (2011) Ultrasonography and color Doppler of proximal gluteal enthesitis in juvenile idiopathic arthritis: a descriptive study. Pediatr Rheumatol Online J 9:22

Martinoli C, Garello I, Marchetti A et al (2012) Hip ultrasound. Eur J Radiol 81(12):3824–3831

Martinoli C, Miguel-Perez M, Padua L et al (2013) Imaging of neuropathies about the hip. Eur J Radiol 82(1):17–26

Molini L, Precerutti M, Gervasio A et al (2011) Hip: anatomy and US technique. J Ultrasound 14(2):99–108

O'Neill J (2008) Musculoskeletal ultrasound, anatomy and technique. Springer Science Business Media, New York

Silvestri E, Muda A, Sconfienza LM (2012) Normal ultrasound anatomy of the musculoskeletal system: a practical guide. Springer, Milan

Stecco A, Gilliar W, Hill R et al (2013) The anatomical and functional relation between gluteus maximus and fascia lata. J Bodyw Mov Ther 17(4):512–517

Westacott DJ, Minns JI, Foguet P (2011) The diagnostic accuracy of magnetic resonance imaging and ultrasonography in gluteal tendon tears-a systematic review. Hip Int 21(6):637–645

Hamstrings

12

Davide Orlandi and Luca Maria Sconfienza

The hamstring (ischiocrural) muscle complex consists of three main muscles that share a common origin site from the ischial tuberosity and occupy the entire posterior compartment of the thigh: from lateral to medial, the long head of the biceps femoris muscle, the semitendinosus muscle and the semimembranosus muscle (Fig. 12.1). It also includes the ischiocondylar portion of the adductor magnus muscle, located deeply in the medial compartment.

The hamstrings span two joints, the hip and the knee, and they are primarily extensors of the thigh and flexors of the leg. The long head of the biceps femoris is also responsible for external rotation of the leg with flexed knee, while the semitendinosus and the semimembranosus muscles play a secondary role in internal rotation of the leg with flexed knee.

The short head of the biceps femoris muscle does not cross two joints and is not included in hamstring complex, but it is debated in this chapter for a more comprehensive overview.

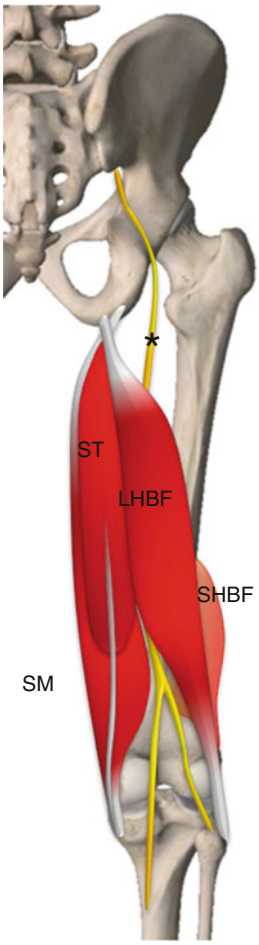

Fig. 12.1 Anatomical scheme of hamstring muscles: *SM* semimembranosus muscle, *ST* semitendinosus muscle, *LHBF* long head of biceps femoris muscle, (*) sciatic nerve. The short head of biceps femoris muscle (*SHBF*), included in the scheme, is not an ischiocrural muscle

D. Orlandi (✉)
Dipartimento di Radiologia,
Università degli studi di Genova, Genoa, Italy
e-mail: my.davideorlandi@gmail.com

L.M. Sconfienza
Unità di radiologia,
IRCCS Policlinico San Donato, Milan, Italy

Dipartimento di scienze biomediche per la salute,
Università degli studi di Milano, Milan, Italy
e-mail: io@lucasconfienza.it

E. Silvestri et al., *Ultrasound Anatomy of Lower Limb Muscles: A Practical Guide*,
DOI 10.1007/978-3-319-09480-9_12, © Springer International Publishing Switzerland 2015

12.1 Anatomy Key Points

12.1.1 Biceps Femoris

The *long head of the biceps femoris* muscle (LHBF) arises from the inferomedial facet of the ischial tuberosity by way of a conjoined tendon with the semitendinosus muscle (Fig. 12.2). The LHBF muscle belly is covered by the gluteus maximus muscle at the root of the thigh and then runs superficially in the posterior thigh, just under the subcutaneous tissue, lateral to the semitendinosus muscle and posterior to the adductor magnus, the vastus lateralis and the short head of the biceps femoris muscles. Along its entire course, the LHBF muscle lies superficial to the sciatic nerve. At the distal third of the thigh, the LHBF diverge from the semitendinosus and the semimembranosus muscles delimiting the popliteal space. At this level the LHBF joins the short head forming a common distal tendon, which attaches onto the lateral aspect of the fibular head. Just prior to the insertion, the distal tendon of the biceps femoris muscle forms a conjoined tendon with the distal component of the lateral collateral ligament of the knee (a *synovial bursa* may be placed between these two fibrous structures). Some tendon fibres also reach the lateral tibial condyle and the distal iliotibial tract. From the apex of the popliteal space to its attachment onto the fibular head, the biceps femoris muscle and tendon course in close relationship with the common peroneal nerve.

The long head of the biceps femoris muscle is supplied by the inferior gluteal artery, perforating arteries and the popliteal artery. It is innervated by the tibial component of the sciatic nerve.

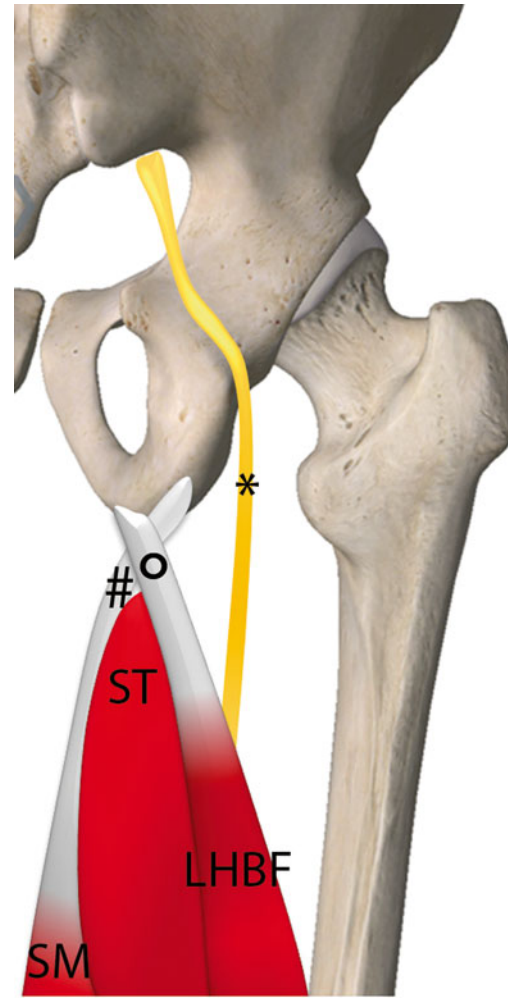

Fig. 12.2 Anatomical scheme of hamstrings proximal insertion: (#), semimembranosus tendon; (°) LHBF-ST conjoined tendon. *LHBF* long head of biceps femoris muscle, *SM* semimembranosus muscle, *ST* semitendinosus muscle, (*), sciatic nerve

The *short head of the biceps femoris* muscle (SHBF) takes its origin from the middle third portion of the lateral linea aspera, the lateral supracondylar line and the intermuscular septum. The muscle belly is placed at the distal thigh, deep to the LHBF. The fibres of the SHBF merge into those of the LHBF, contributing to the formation of the distal tendon, which inserts onto the fibular head.

The SHBF is not part of hamstrings because it does not span two joints.

Sometimes, the SHBF may be absent.

Unlike the long head, the short head of the biceps femoris muscle is innervated by the peroneal division of the sciatic nerve.

12.1.2 Semitendinosus

The *semitendinosus* (ST) is a fusiform polyarticular muscle, which originates from the inferomedial aspect of the ischial tuberosity via a conjoined tendon with the LHBF. Together with the semimembranosus muscle, they are known as medial hamstrings.

The semitendinosus can be considered as a digastric muscle because it shows an internal raphe inside the proximal third of the muscle belly onto which the proximal fibres insert.

Just caudal to the ischial tuberosity, the semitendinosus rapidly becomes bulbous with the LHBF-ST conjoined tendon lying lateral to it and the semimembranosus tendon lying anterior to it. The muscle belly is placed superficially in the posterior thigh, medial to the LHBF, lateral to the semimembranosus and posterior to the adductor magnus muscle.

At the middle-distal third of the thigh, the semitendinosus forms a long thin superficial tendon that posteriorly overcomes the semimembranosus muscle and inserts along the medial aspect of the proximal tibia, forming the pes anserinus complex together with the sartorius and gracilis tendons. As opposed to the semimembranosus muscle, the semitendinosus is entirely tendinous in the distal thigh.

The semitendinosus muscle is supplied by the inferior gluteal artery and perforating arteries. The innervation is represented by the tibial component of the sciatic nerve.

12.1.3 Semimembranosus

The *semimembranosus* (SM) muscle arises from the superolateral surface of the ischial tuberosity by way of an elongated tendon, which runs deep to the proximal semitendinosus muscle belly. The proximal tendon, which has connections with the adductor magnus tendon and the LHBF-ST conjoined tendon, course down running anteromedial to the semitendinosus muscle belly and the LHBF-ST conjoined tendon. Then, it continues in a large coronal-oriented aponeurosis extending in the proximal half of the thigh and giving origin to the muscle fibres.

The semimembranosus muscle belly is almost entirely located in the mid-distal thigh, anteromedial to other hamstrings, posterior to the adductor magnus muscle and posterolateral to the gracilis muscle. It has a closer relationship with the semitendinosus distal tendon, which course superficially.

Unlike the semitendinosus muscle, which is thin and band-like, the semimembranosus muscle is composed of short unipennate and multipennate fibres. Moreover, the semimembranosus, as its name implies, have a thin and wide tendon in the upper thigh, while the semitendinosus is more tendinous distally.

The semimembranosus distal insertion has multiple attachment points, the main two onto the infraglenoid tubercle of the posteromedial proximal tibial condyle (direct tendon) and onto the medial aspect of the proximal tibial epiphysis (indirect tendon). Other tendinous expansions also reach the posterior capsule of the knee joint and the popliteal fascia. The semimembranosus distal tendon is intimately connected with the medial collateral ligament of the knee from which it may be separated by a synovial bursa that sometimes communicate with the femorotibial joint.

Fig. 12.3 Lower limb position to evaluate hamstring complex

The semimembranosus muscle is supplied by gluteal arteries and the *profunda femoris artery* (deep femoral artery). The innervation is provided by the tibial portion of the sciatic nerve.

The patient lies prone with the lower limb extended in a neutral position (Fig. 12.3).

12.2 Ultrasound Examination Technique

Palpate the ischial tuberosity, a key bony landmark for hamstrings evaluation, and place the probe on it in an axial plane to identify ischiocrural proximal insertion (Fig. 12.4). At this level the LHBF-ST conjoined tendon and the semimembranosus tendon cannot be visualized as distinct structures because they are intimately superimposed. The sciatic nerve is located lateral to the ischial tuberosity.

Focus On

The *sciatic nerve*, the longest and largest peripheral nerve in the body, supplies the lower back, the hamstrings, the adductor magnus muscle and, with its terminal branches, the leg. It is composed of two distinct portions, a medial and a lateral fascicle, which continue at the popliteal space as tibial and common peroneal nerve, respectively.

The sciatic nerve exits the greater sciatic foramen of the pelvis, passing between the ventral aspect of the piriformis muscle and the posterior surface of the quadratus femoris muscle. At the upper thigh, the sciatic nerve is placed lateral to the hamstrings attachment on the ischial tuberosity; then, it runs distally the posterior thigh between the adductor magnus muscle (anterior) and the long head of the biceps femoris and semitendinosus muscles (posterior). Reached the apex of the popliteal fossa, where it lies between the biceps femoris (on the lateral side) and the semitendinosus and semimembranosus muscles (on the medial side), it divides into the tibial nerve and the common peroneal nerve.

Shifting the probe just caudally, the semitendinosus is immediately seen as a muscle belly, and the first visible separation of the LHBF-ST conjoined tendon from the semimembranosus tendon can be identified (Fig. 12.5). Remember that the LHBF-ST conjoined tendon has an eccentric position in respect to the semitendinosus muscle belly that extends lateral to the tendon itself.

Note the relationship between the LHBF-ST conjoined tendon and the sciatic nerve.

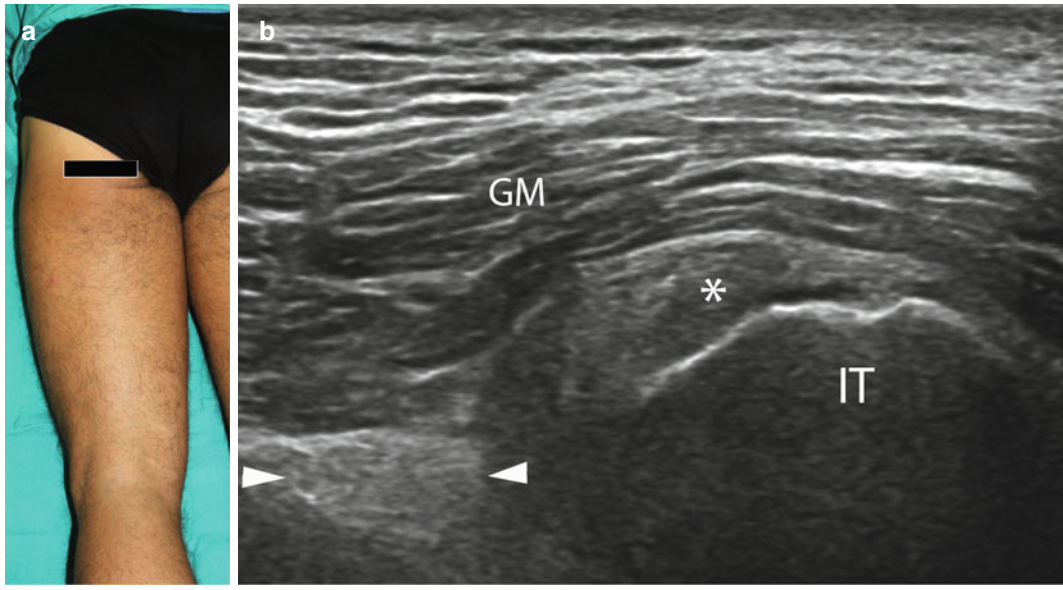

Fig. 12.4 (**a**) Probe position to evaluate hamstrings proximal insertion on the axial plane. (**b**) US axial scan of hamstrings common origin from the ischial tuberosity. The ischial tuberosity (*IT*) is seen as a hyperechoic band, deep to the LHBF-ST conjoined and the SM tendons; these two tendons cannot be separated and are imaged as a unique tendinous structure with a typical fibrillar hyperechoic appearance (*). The sciatic nerve (*white arrowheads*) is visualized as a rounded structure, with a fascicular hyperechoic appearance, lateral to the ischial tuberosity. *GM* gluteus maximus

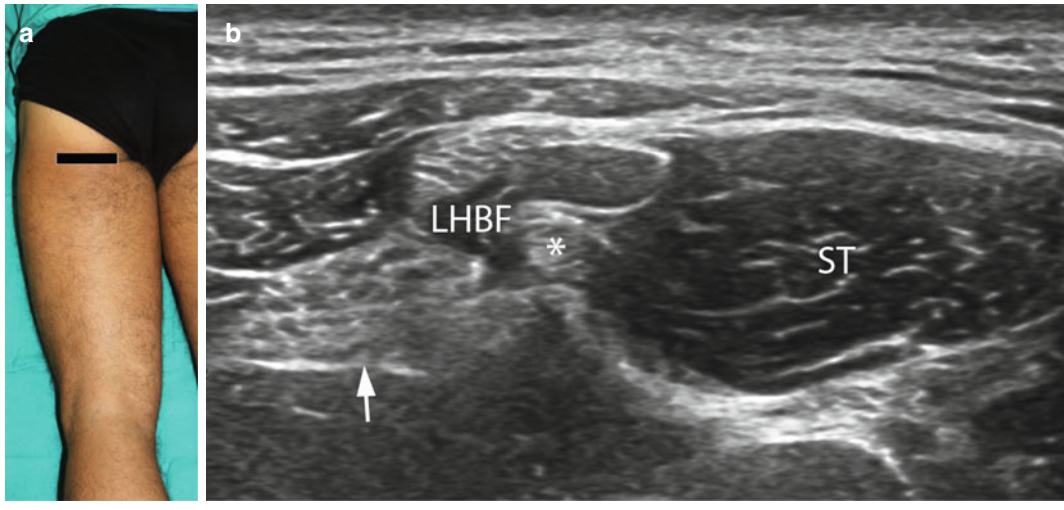

Fig. 12.5 (**a**) Probe position to visualize the LHBF-ST conjoined tendon on an axial plane. (**b**) US axial scan: note the hyperechoic "comma-shaped" appearance of the LHBF-ST conjoined tendon that is placed superficial and lateral to the ST muscle. *White arrow*, sciatic nerve

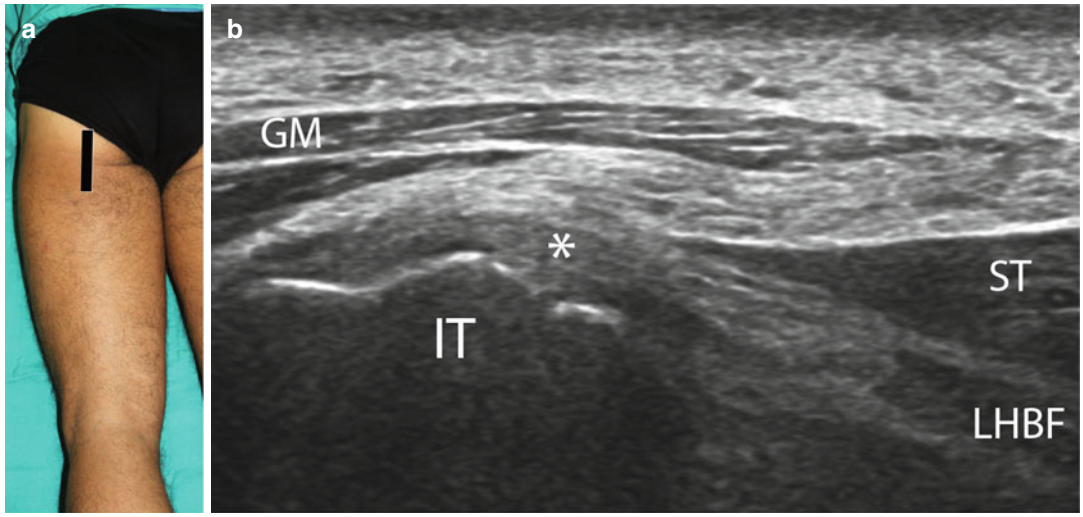

Fig. 12.6 (**a**) Probe position to evaluate the LHBF-ST conjoined tendon on a longitudinal plane. (**b**) US longitudinal scan: *IT* ischial tuberosity, (*) LHBF-ST conjoined tendon, *ST* semitendinosus muscle belly, *LHBF* long head of the biceps femoris muscle belly, *GM* gluteus maximus

Turn the probe by 90° to evaluate the LHBF-ST conjoined tendon on its long axis (Fig. 12.6).

From this position, move the transducer caudally to reach the *LHBF proximal myotendinous junction* (Fig. 12.7). Because this region is often affected by strain injuries during sports, a detailed US evaluation is very important in order to obtain a reliable diagnosis and grading.

Place again the transducer in the axial position shown in Fig. 12.4 and then slightly move the probe laterally and caudally, following the *LHBF* muscle belly along the lateral posterior thigh (Fig. 12.8).

At the distal third, pay attention to the site in which the LHBF fibres merge with the SHBF ones to form a common distal tendon: this is another critical area, frequently involved in strain injuries (Fig. 12.9). This fibres arrangement and the different innervation of the LHBF and the SHBF (the former is supplied by the tibial portion of the sciatic nerve and the latter by the peroneal one) could explain why this muscle has the highest frequency of strain injuries among the hamstring muscles. In this setting the double nerve supply probably determines asynchronies in the coordination and intensity of stimulation of the two heads, resulting in potential tears.

Remember to always evaluate the *biceps femoris distal tendon* up to its insertion onto the fibular head (Fig. 12.10) and then to rotate the transducer by 90° to better visualize the distal myotendinous junction and its tendon on a longitudinal plane (Figs. 12.11 and 12.12). Don't forget the close relationship between the biceps femoris muscle and tendon and the common peroneal nerve in proximity of the fibular head.

Focus On

The *common peroneal nerve* is the smaller of the two terminal branches of the sciatic nerve; at its origin, it courses along the lateral side of the popliteal space, in proximity to the lateral head of the gastrocnemius muscle, posteromedial to the biceps femoris muscle and tendon. Then, the nerve curves anteriorly, turning around the fibular head, to reach the fibular tunnel, in which it lies between the fibula and the proximal tendon of the peroneus longus muscle. At the lateral side of the fibular neck, it enters the anterolateral compartment of the leg and splits in its two terminal branches, the deep and the superficial peroneal nerves.

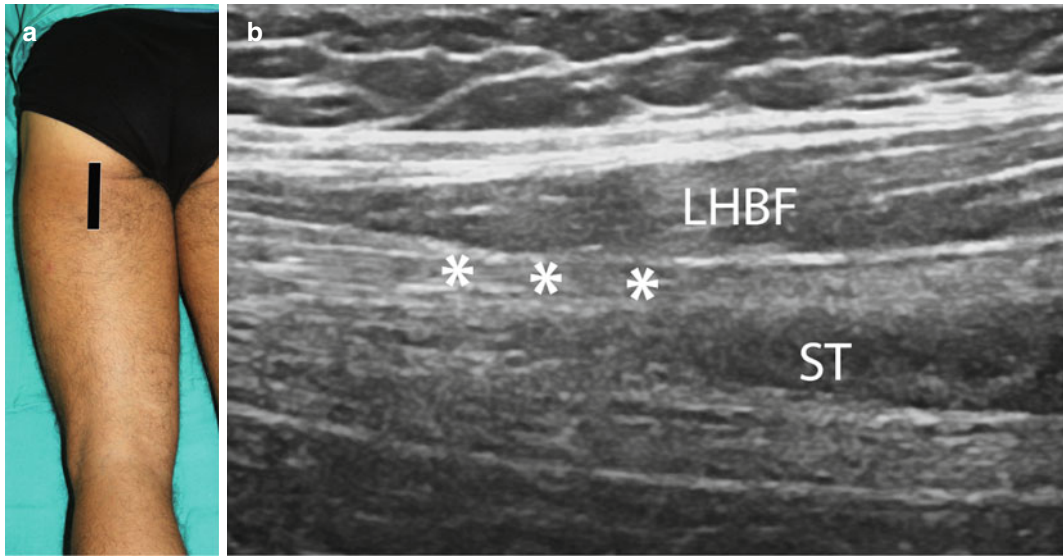

Fig. 12.7 (**a**) Probe position to evaluate the LHBF proximal myotendinous junction on the longitudinal plane (**b**) US longitudinal scan of the long head of biceps femoris proximal myotendinous junction. (*) LHBF-ST conjoined tendon; *LHBF* long head of biceps femoris muscle, *ST* semitendinosus muscle

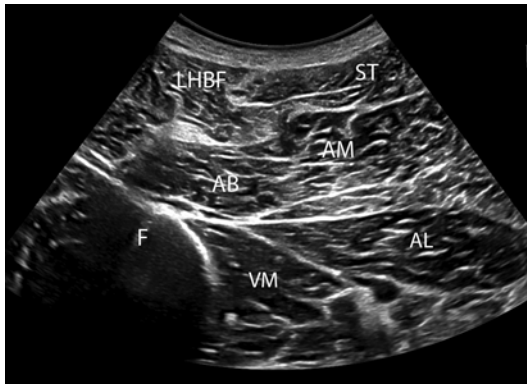

Fig. 12.8 US panoramic scan of the posterior thigh muscles and their relationship with the thigh medial muscles. *LHBF* long head of biceps femoris muscle, *ST* semitendinosus muscle, *AM* adductor magnus muscle, *AB* adductor brevis muscle, *AL* adductor longus muscle, *VM* vastus medialis muscle, *F* femur

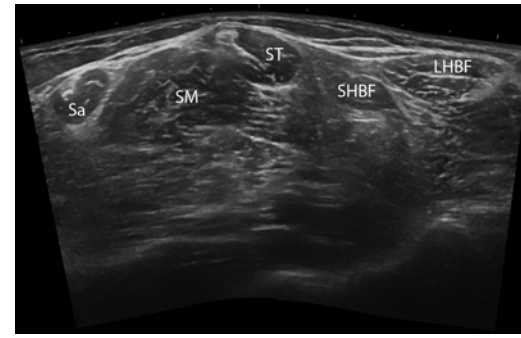

Fig. 12.9 Extended-field-of-view of the posterior thigh. Look at the critical area in which the short head of the biceps femoris fibres (*SHBF*) joint with the long head ones (LHBF). *ST* semitendinosus muscle, *SM* semimembranosus muscle, *Sa* Sartorius muscle

Reposition the probe on the ischial tuberosity, as shown in Fig. 12.4, and then shift it caudally along the central posterior thigh to examine the semitendinosus muscle belly on an axial plane (Fig. 12.13).

At the middle third, the semitendinosus progressively becomes tendinous, while the LHBF and the semimembranosus remain still bulbous (Fig. 12.14).

Move the transducer caudally, from lateral to medial, to follow the semitendinosus long and superficial distal tendon up to its attachment onto the medial proximal tibia, forming the *pes anserinus* complex (Fig. 12.15).

Rotate the probe by 90° to appreciate the distal tendon on the longitudinal plane and move it cranially to reach the *semitendinosus distal myotendinous junction*, best visualized on its long axis (Fig. 12.16). The distal myotendinous

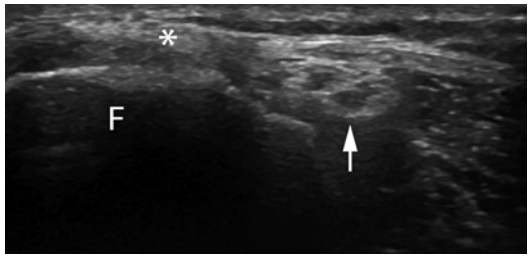

Fig. 12.10 US axial scan of the biceps femoris distal insertion onto the fibular head. (*) biceps femoris distal tendon; *F* fibula. Note the close proximity with the common peroneal nerve (*white arrow*) which courses just posterior and medial to the biceps femoris distal tendon

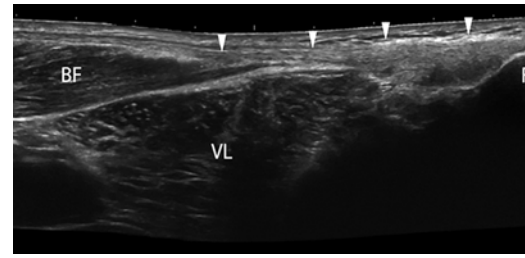

Fig. 12.11 Extended-field-of-view of the biceps femoris distal myotendinous junction (*white arrowheads*). *BF* biceps femoris muscle, *VL* vastus lateralis muscle, *F* fibula

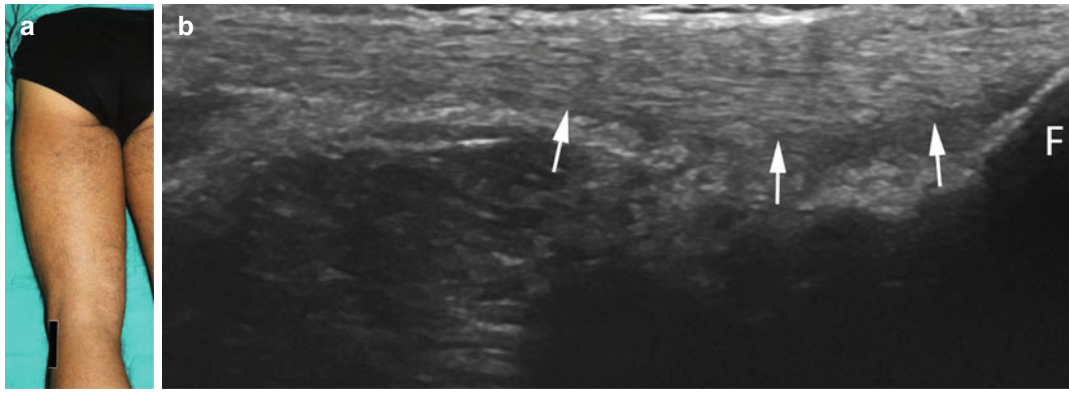

Fig. 12.12 (**a**) Probe position to evaluate the biceps femoris distal insertion onto the fibular head on the longitudinal plane. (**b**) US longitudinal scan of the biceps femoris distal tendon (*arrows*). The biceps femoris distal tendon and the lateral collateral ligament of the knee have a conjoined attachment point onto the tip and the lateral aspect of the fibular head (*F*)

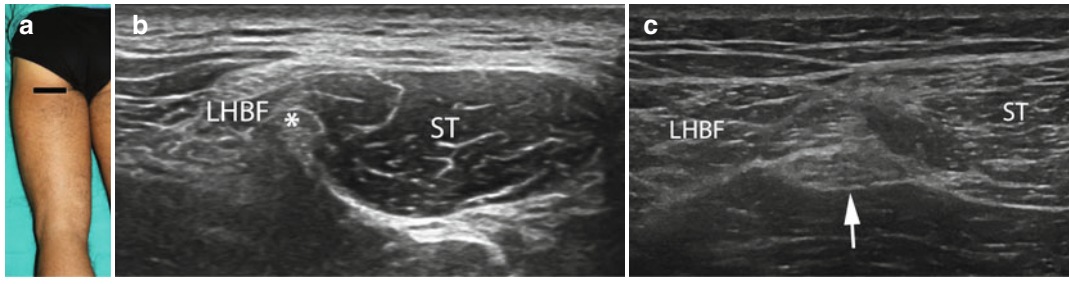

Fig. 12.13 (**a**) Probe position to examine the semitendinosus muscle belly. (**b**) US axial scan of the upper posterior thigh to evaluate the semitendinosus muscle belly. *LHBF* long head of biceps femoris muscle, *ST* semitendinosus muscle, (*) LHBF-ST conjoined tendon. (**c**) US axial scan at the level of the proximal third of the thigh. Note the close proximity of the semitendinosus (medial) and the long head of the biceps femoris (lateral) muscle bellies with the sciatic nerve. *White arrow*, sciatic nerve

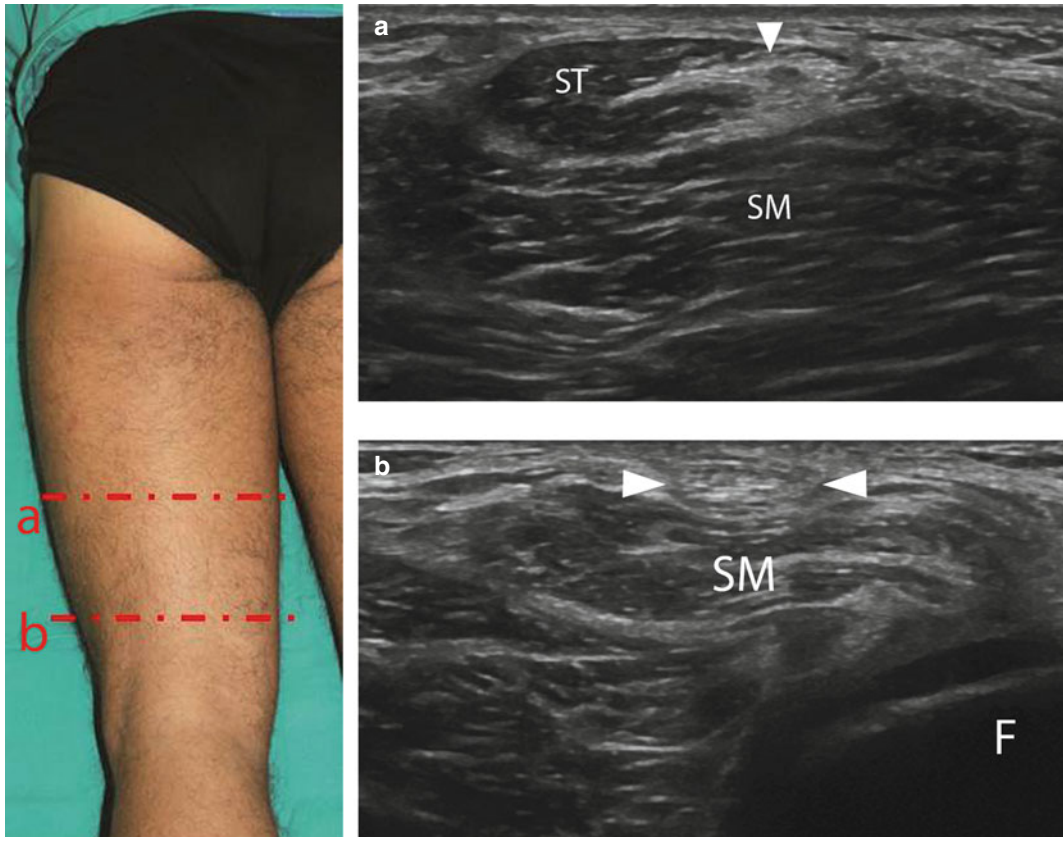

Fig. 12.14 US axial scans of the semitendinosus distal tendon at different levels and its relationship with the semimembranosus muscle belly. (**a**) At the level of the middle third of the posterior thigh, the semitendinosus muscle overcome the semimembranosus and progressively becomes tendinous. *ST* semitendinosus muscle belly, *white arrowhead* distal tendon fibres of the semitendinosus muscle, *SM* semimembranosus muscle. (**b**) At the level of the middle-distal third of the posterior thigh, the semitendinosus distal tendon (*white arrowheads*) lies superficial to semimembranosus muscle belly. *SM* semimembranosus muscle, *F* fibula

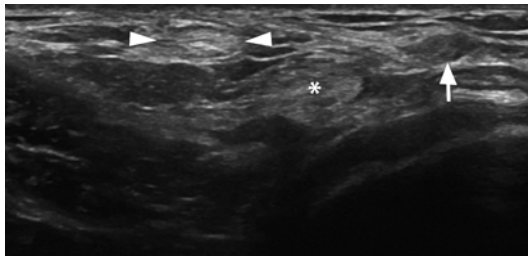

Fig. 12.15 US axial scan of the semitendinosus distal insertion; *white arrowheads*, semitendinosus distal tendon; (*), semimembranosus distal tendon; *white arrow*, gracilis distal tendon

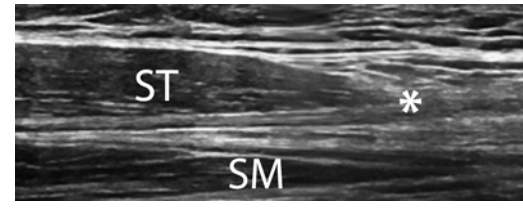

Fig. 12.16 US longitudinal scan of the semitendinosus distal myotendinous junction and tendon (*); *ST* semitendinosus muscle, *SM* semimembranosus muscle

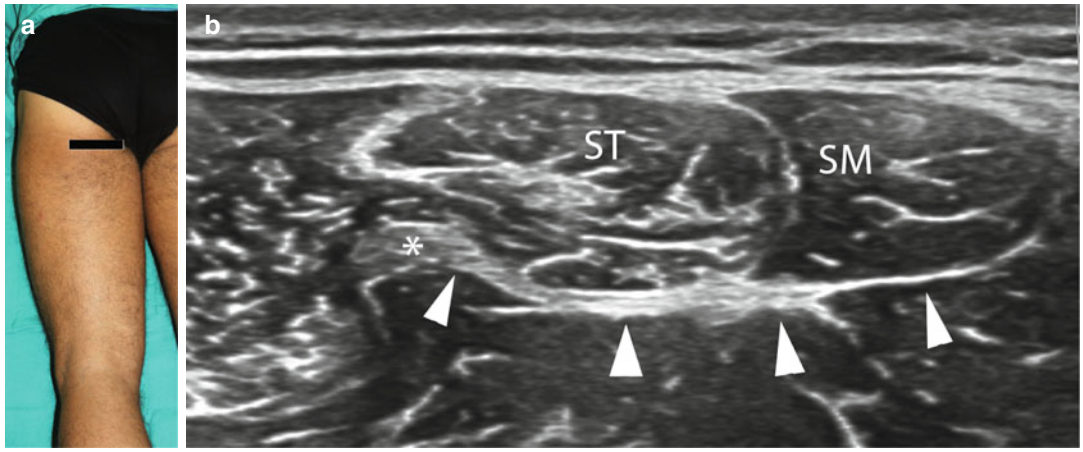

Fig. 12.17 (**a**) Probe position to examine the semimembranosus muscle belly on the axial plane. (**b**) US axial scan of the semimembranosus proximal tendon (*) and its aponeurosis (*white arrowheads*). *ST* semitendinosus muscle, *SM* semimembranosus muscle

junction is often affected in semitendinosus muscle injuries.

Also for the semimembranosus muscle, the ischial tuberosity represents the main landmark to start the US evaluation. From the position shown in Fig. 12.4, shift the probe caudally to obtain the image shown in Fig. 12.5 and move it just medially: the *semimembranosus proximal tendon* can be visualized deep and medial to the ST muscle belly (Fig. 12.17). Note the large aponeurosis, connected to the medial aspect of the tendon, from which the muscle fibres arise.

Slightly move the probe medially and caudally along the medial posterior thigh to examine the proximal myotendinous junction, placed at the level of the mid-third of the thigh, and the semimembranosus muscle belly on the axial plane (Fig. 12.18). Note the typical triangular appearance of the proximal semimembranosus due to its fibres arrangement. Pay particularly attention to the sites in which the semimembranosus fibres attach to the large aponeurosis because traumatic tears often occur at this level.

Distally the semimembranosus increases in size and, at the distal third, progressively becomes tendinous.

Remember to always follow the *semimembranosus distal tendon* up to its insertion onto the posteromedial proximal tibia (Fig. 12.19).

Then, rotate the probe by 90° to evaluate the *semimembranosus distal myotendinous junction* and tendon best imaged on the longitudinal plane (Fig. 12.20).

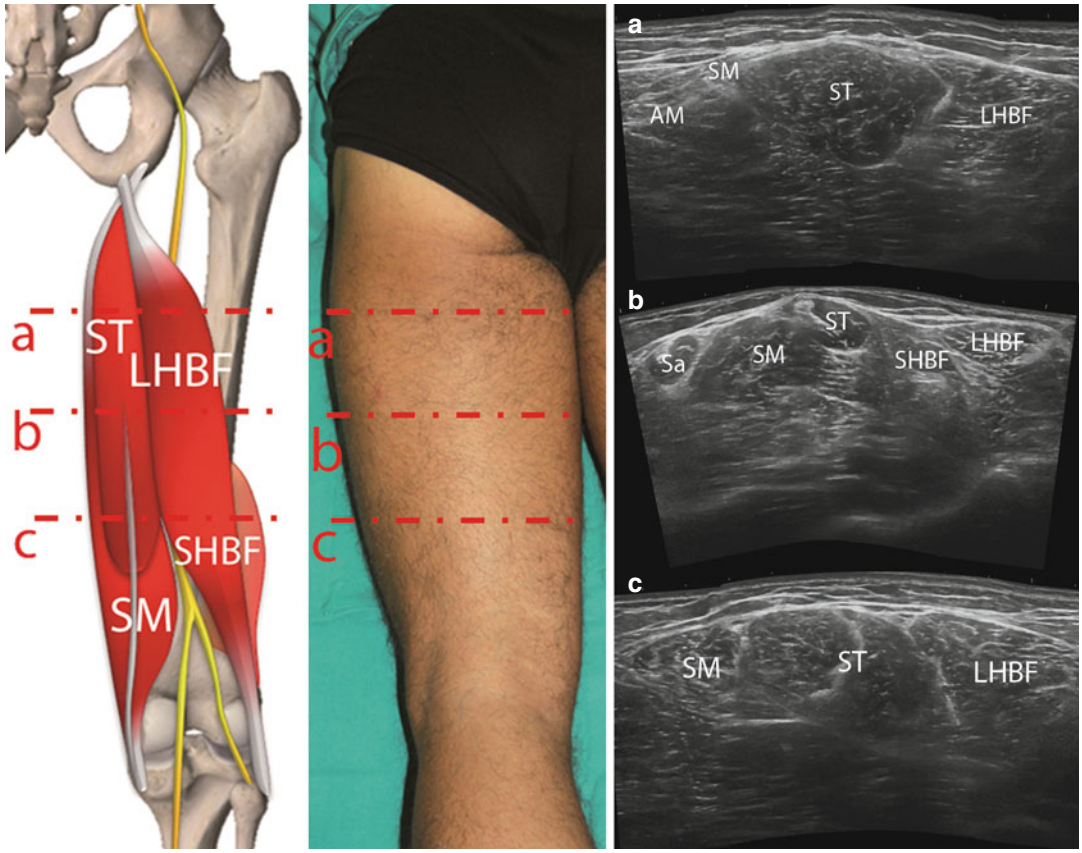

Fig. 12.18 Anatomical scheme of hamstrings correlated to extended-field-of-view axial scans of the semimembranosus muscle belly at different levels, proximal (**a**), middle (**b**) and distal (**c**) third of the posterior thigh. *SHBF* short head of the biceps femoris, *LHBF* long head of the biceps femoris, *ST* semitendinosus muscle, *SM* semimembranosus muscle, *Sa* sartorius muscle, *AM* adductor magnus

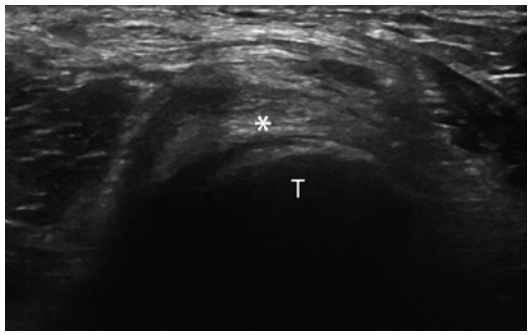

Fig. 12.19 US axial scan of the semimembranosus distal tendon (*). *T* tibia

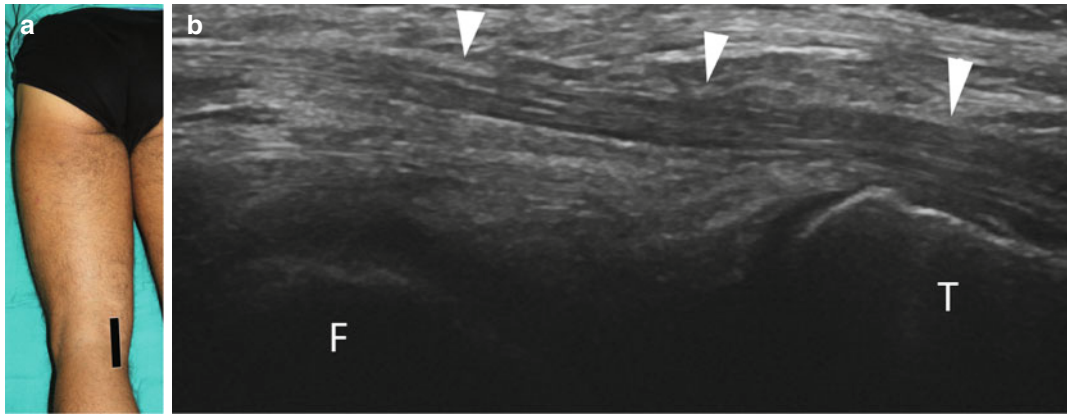

Fig. 12.20 (**a**) Probe position to examine the semimembranosus distal tendon on the longitudinal plane (**b**) US longitudinal scan of the semimembranosus distal tendon insertion (*arrowheads*) onto the posteromedial proximal tibia (*T*). *F* medial femoral condyle onto the posteromedial proximal tibia

12.3 Summary Table

Muscle	Origin	Insertion	Nerve supply	Action
Long head of the biceps femoris	Inferomedial facet of the ischial tuberosity (conjoint tendon with the semitendinosus)	Fibular head (conjoined tendon with the lateral collateral ligament), lateral tibial condyle, iliotibial tract	Tibial portion of the sciatic nerve	Extension of the thigh Flexion of the leg External rotation of the leg with flexed knee
Semitendinosus	Inferomedial facet of the ischial tuberosity (conjoint tendon with the long head of the biceps femoris)	Medial aspect of the proximal tibia (pes anserinus)	Tibial portion of the sciatic nerve	Extension of the thigh Flexion of the leg Internal rotation of the leg with flexed knee
Semimembranosus	Superolateral facet of the ischial tuberosity	Posteromedial (direct tendon) and medial (indirect tendons) aspect of the proximal tibia, posterior capsule of the knee joint, popliteal fascia	Tibial portion of the sciatic nerve	Extension of the thigh Flexion of the leg Internal rotation of the leg with flexed knee
Short head of the biceps femoris	Lateral linea aspera, lateral supracondylar line, intermuscular septum	Fibular head (conjoined tendon with the lateral collateral ligament), lateral tibial condyle, iliotibial tract	Peroneal portion of the sciatic nerve	Flexion of the leg External rotation of the leg with flexed knee

Suggested Reading

Koulouris G, Connell D (2005) Hamstring muscle complex: an imaging review. RadioGraphics 25:571–586
Lee JC, Mitchell AWM, Healy JC (2012) Imaging of muscle injury in the elite athlete. Br J Radiol 85:1173–1185
Maffulli N, Chan O, Del Buono A, Best TM (2012) Acute muscle strain injuries: a proposed new classification system. Knee Surg Sports Traumatol Arthrosc 20:2356–2362
Mariani C, Caldera FE, Kim W (2012) Ultrasound versus magnetic resonance imaging in the diagnosis of an acute hamstrings tear. Am Academy Phys Med Rehab 4:154–155
Martinoli C, Bianchi S (2007) Ultrasound of the musculoskeletal system. Springer, Berlin

Part III

Leg Muscles

Popliteus

13

Riccardo Sartoris and Enzo Silvestri

13.1 Anatomy Key Points

Popliteus is a thin, triangular muscle sited at the posterior aspect of the knee; it arises from the posterior medial aspect of the proximal tibia, passes downwards and medially to the tibial surface and inserts with its tendon on the lateral epicondyle of the femur into the homonymous bony groove. Popliteus tendon passes through the joint capsule of the knee and runs beneath the proximal part of the lateral collateral ligament (which inserts on the lateral femoral epicondyle just cranial to the popliteal sulcus) to reach its insertion in its groove (Figs. 13.1 and 13.2). Because of its structure and attachments, the popliteus muscle-tendon unit is known as the major dynamic stabilizer of the posterolateral corner: in particular it is involved in maintaining dorsolateral stability, stabilizing the lateral meniscus and balancing the neutral tibial rotation.

13.2 Ultrasound Examination Technique

Start the US examination with the patient lying prone on the table with the leg extended.

Place the transducer over the posterior aspect of the proximal tibia with a transverse-oblique scan. Identify the posterior hyperechoic cortex of the fibula; just superficial to it, you can find a very thin oval muscular structure running upwards and laterally: it is the popliteus muscle belly.

Rotate the probe by 90° obtaining a long axis of the muscle with the proximal edge of the probe pointing at the lateral epicondyle of the femur (Figs. 13.3 and 13.4).

Hence follow the fibrillar tendon structure as it enters the knee joint capsule, runs adjacent the posterior horn of the lateral meniscus and inserts into the popliteal groove on the lateral femoral epicondyle. Due to its curvilinear course and depending on the incidence of the US beam, anisotropy may be evident in the popliteus tendon.

R. Sartoris
Dipartimento di Radiologia,
Università degli studi di Genova, Genoa, Italy
e-mail: riccardo.sartoris@hotmail.it

E. Silvestri (✉)
Struttura Complessa di Diagnostica
per Immagini ed Ecografia Interventistica,
Ospedale Evangelico Internazionale, Genoa, Italy
e-mail: silvi.enzo@gmail.com

E. Silvestri et al., *Ultrasound Anatomy of Lower Limb Muscles: A Practical Guide*,
DOI 10.1007/978-3-319-09480-9_13, © Springer International Publishing Switzerland 2015

Fig. 13.1 Anatomical scheme of the popliteus muscle. *P* popliteus

Fig. 13.2 Lower limb position to evaluate the popliteus muscle

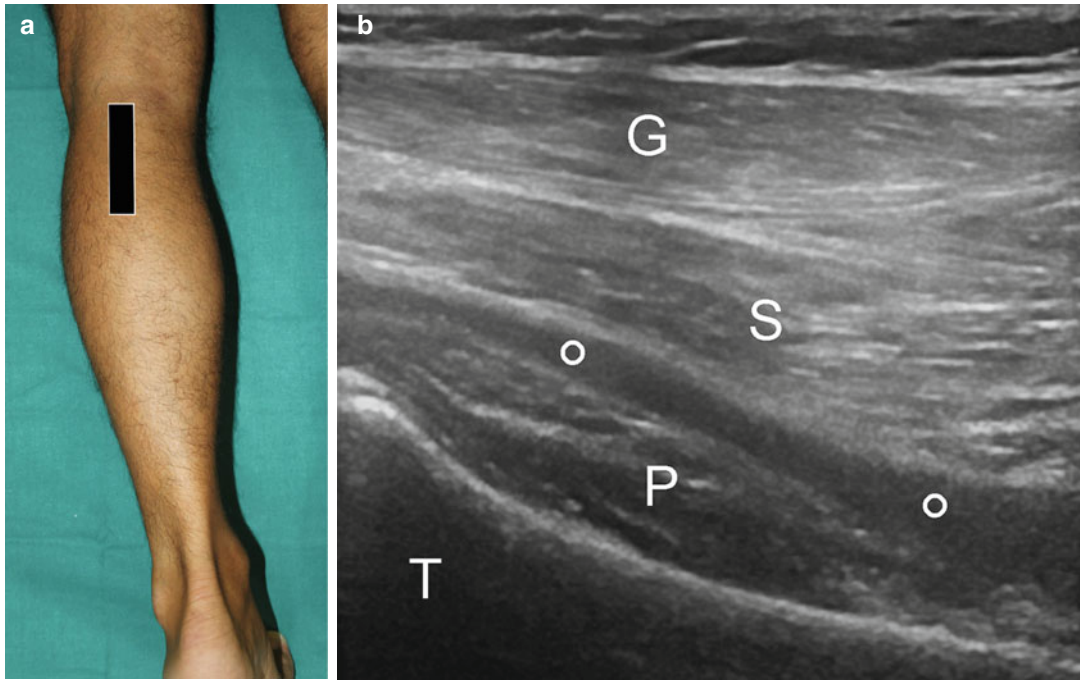

Fig. 13.3 (**a**) Probe position over the posterior knee. (**b**) Corresponding US longitudinal scan over the midline of the posterior aspect of the proximal tibia (*T*): the image shows this important bony landmark, covered by the muscular fibres of the popliteus; popliteal vessels (*circles*) can be used as an anatomical landmark to identify the popliteus muscle. Superficial to it, the fibres of the soleus muscle (*S*) and gastrocnemius muscle (*G*) can be appreciated

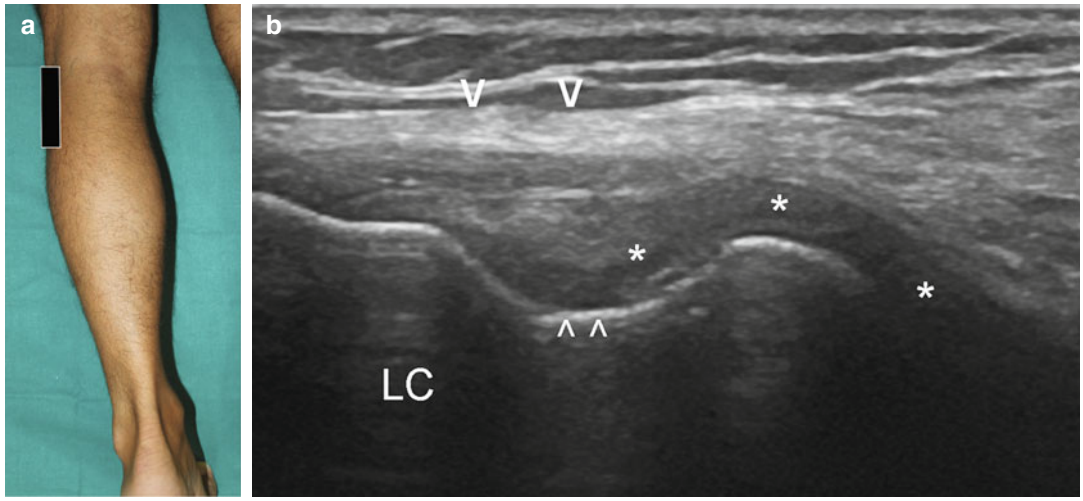

Fig. 13.4 (**a**) Probe position over the posterolateral knee for the evaluation of the popliteus muscle. (**b**) Corresponding US transverse-oblique scan over the posterolateral aspect of the lateral femoral condyle (*LC*): the image shows the hypoechoic fibres of the popliteus tendon (*asterisks*) arising from the popliteal groove (*smaller arrowheads*); in a more superficial position, the hyperechoic lateral collateral ligament of the knee (*greater arrowheads*) can be seen. Note the anisotropic popliteus tendon appearance due to its curvilinear course at this level

Occasionally, the tendon may contain an internal ossicle or sesamoid called "cyamella": remember not to misidentify it as an avulsed bone fragment.

13.3 Summary Table

Muscle	Origin	Insertion	Innervation	Action
Popliteus	Posteromedial aspect of proximal tibia	Lateral epicondyle	Tibial nerve	Major dynamic stabilizer of the knee Minor flexor of the knee; also internal rotator of the tibia

Suggested Reading

Alessi S, Depaoli R, Canepari M et al (2012) Baker's cyst in pediatric patients: ultrasonographic characteristics. J Ultrasound 15(1):76–81

English S, Perret D (2010) Posterior knee pain. Curr Rev Musculoskelet Med 3(1–4):3–10

Hwang K, Lee KM, Han SO et al (2010) Shape and innervation of popliteus muscle. Anat Cell Biol 43(2):165–168

Mansfield CJ, Beaumont J, Tarnay L et al (2013) Popliteus strain with concurrent deltoid ligament sprain in an elite soccer athlete: a case report. Int J Sports Phys Ther 8(4):452–461

Mariani PP, Margheritini F (2009) Partial isolated rupture of the popliteus tendon in a professional soccer player: a case report. Sports Med Arthrosc Rehabil Ther Technol 1:18

Royall NA, Farrin E, Bahner DP et al (2011) Ultrasound-assisted musculoskeletal procedures: a practical overview of current literature. World J Orthop 2(7):57–66

Peroneal

14

Silvia Perugin Bernardi and Alessandro Muda

14.1 Anatomy Key Points

The lateral compartment of the leg is composed by the peroneus brevis and peroneus longus muscles. These muscles are separated from the anterior and posterior compartment muscles, respectively, by the anterior and posterior crural intermuscular septum of the deep fascia.

The peroneus longus is a large superficial muscle and, as its name implies, has a longer tendon than the deeper peroneus brevis. It arises from the lateral aspect of the superior tibiofibular joint and from the proximal two thirds of the lateral fibular shaft. Its origin extends up onto the head of the fibula, with a small gap just below it where the deep peroneal nerve passes through. The peroneus brevis arises from the distal portion of the lateral aspect of the fibula and runs caudally to continue in its flat tendon at a lower level than the peronueus longus.

At the ankle level, the tendons of the peroneus longus and brevis pass behind the lateral malleolus with the peroneus longus located posterolaterally and the peroneus brevis located anteromedially. These structures run in close relationship to the adjacent posterior calcaneofibular ligament, which lies just below them. In addition, at this level, the superior and inferior retinacula hold the tendons firmly adherent to the lateral malleolus bony surface.

Along their proximal extent, peroneal tendons have a common synovial sheath which splits distally to follow the different courses of the tendons: the peroneus brevis runs forward to insert on the base of the fifth metatarsal; the peroneus longus tendon runs around the cuboid and inserts on the base of the first metatarsal and on the medial cuneiform (Fig. 14.1).

In addition to the peroneus longus and brevis muscles, the peroneus quartus muscle is an accessory muscle of the lateral distal leg, which occasionally is present. Despite its variability in origin and insertion, it may originate from the peroneus brevis muscle (or from the fibula or from distal fibers of the peroneus longus).

S. Perugin Bernardi
Dipartimento di Radiologia, Università degli studi di Genova, Genoa, Italy
e-mail: silvia.perugin@gmail.com

A. Muda (✉)
Dipartimento di Radiologia, IRCCS Ospedale San Martino IST, Genoa, Italy
e-mail: alessandro.muda@tiscali.it

E. Silvestri et al., *Ultrasound Anatomy of Lower Limb Muscles: A Practical Guide*,
DOI 10.1007/978-3-319-09480-9_14,

Then it passes posteromedial or medial to the peroneal tendons and inserts onto the retrotrochlear eminence of the calcaneus (alternatively onto the fifth metatarsal bone and the cuboid).

Fig. 14.2 Lower limb position to evaluate the peroneal muscles

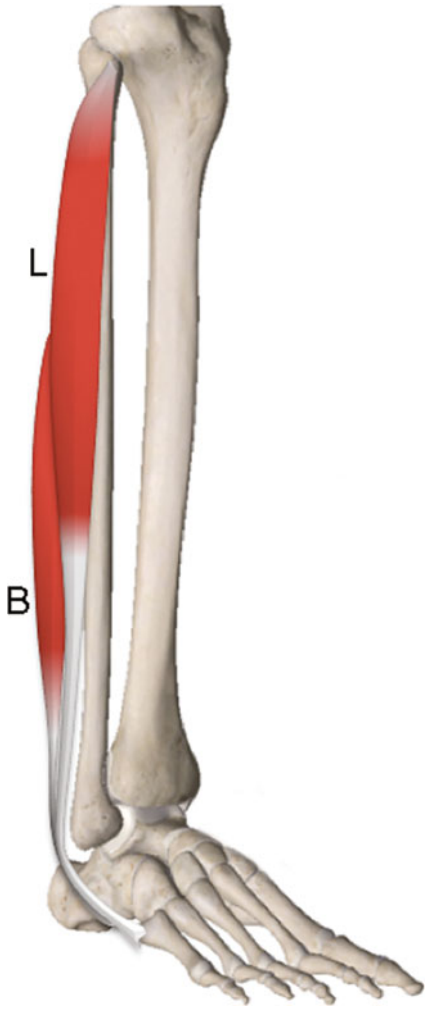

Fig. 14.1 Anatomical scheme of the peroneal muscles: *L* peroneus longus, *B* peroneus brevis

14.2 Ultrasound Examination Technique

Ultrasound evaluation of the peroneal muscles must be performed with the patient in the same position as for the anterior compartment (supine with about 20–45° knee flexion) with the foot inverted in order to expose the lateral aspect of the lower leg and of the ankle; alternatively, the patient can lie obliquely with the medial aspect of the foot on the table (Fig. 14.2).

Start the US examination by manually palpating the head of the fibula and place the transducer with a transverse orientation above its lateral aspect; at this level, the US image shows the cranial portion of the peroneus longus muscle, which lies just superficially to the hyperechoic cortex of the fibula (Fig. 14.3).

Moving the probe caudally, the peroneus longus muscle can be followed along the lateral aspect of the fibula: at the middle third of the leg, it continues into its flat tendon arising in the external portion of the muscle (Fig. 14.4).

More caudally, transverse scans demonstrate the peroneus longus tendon, which progressively becomes oval, overlying the external aspect of the peroneus brevis muscle. The peroneus brevis muscle originates at the level of the musculotendinous junction of the peroneus longus and could be followed with transverse scans starting at the midshaft of the fibula: here the peroneus brevis lies just superficially to the cortex and posterior to the peroneus longus musculotendinous junction.

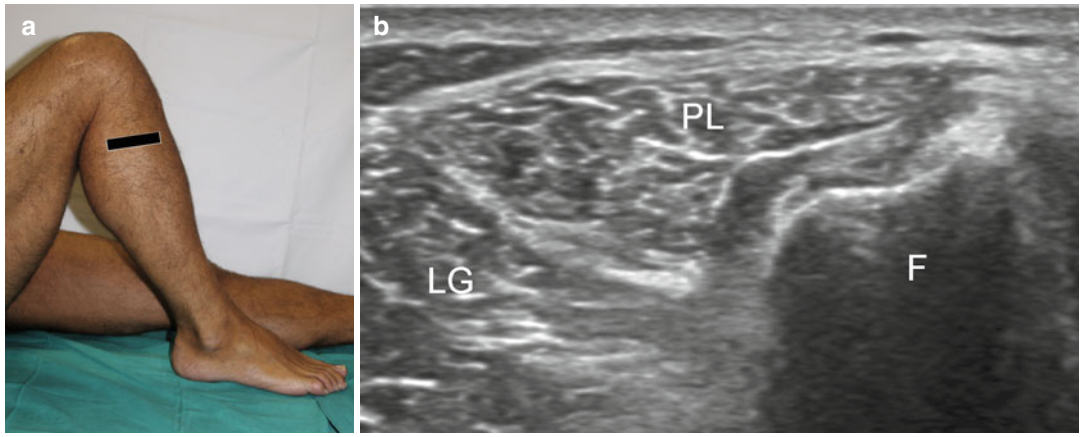

Fig. 14.3 (**a**) Probe position over the proximal lateral leg for the evaluation of the peroneal muscles. (**b**) Corresponding US transverse scan: the image shows the proximal third of the fibula on the right (*F*) and, superficial to it, the muscle belly of the peroneus longus (*PL*); this scan also illustrates the relationship between the peroneus longus and the lateral gastrocnemius (*LG*) posteriorly

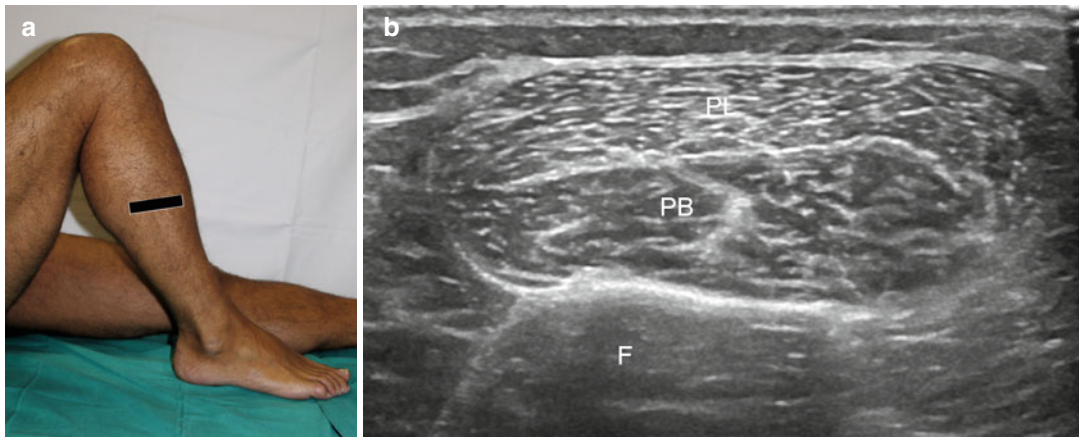

Fig. 14.4 (**a**) Probe position over the intermediate lateral leg for the evaluation of the peroneal muscles. (**b**) Corresponding US transverse scan: the image shows the middle third of the fibula on the bottom (*F*) and, superficial to it, the muscle bellies of the peroneus brevis (*PB*) and longus (*PL*)

Moving downward, the peroneus brevis muscle belly courses over the lateral aspect of the distal fibula, deep into the peroneus longus tendon, and continues with its musculotendinous junction just proximal to the ankle. Sometimes, clear differentiation between these two muscles may be difficult: in these cases, the operator will start the examination distally at the ankle level, moving the transducer upward in order to identify the respective muscle bellies (Fig. 14.5).

Once the muscle bellies are completely evaluated on their transverse plane, the operator can rotate the probe by 90° and complete the US examination on the longitudinal axis (Fig. 14.6).

At the ankle level, place the transducer in a transverse-oblique position with the medial edge of the probe lying on the lateral malleolus: the corresponding US image demonstrates the peroneus brevis lying anteromedially to the peroneus longus, both running in a common synovial sheath. Then, the probe must be moved,

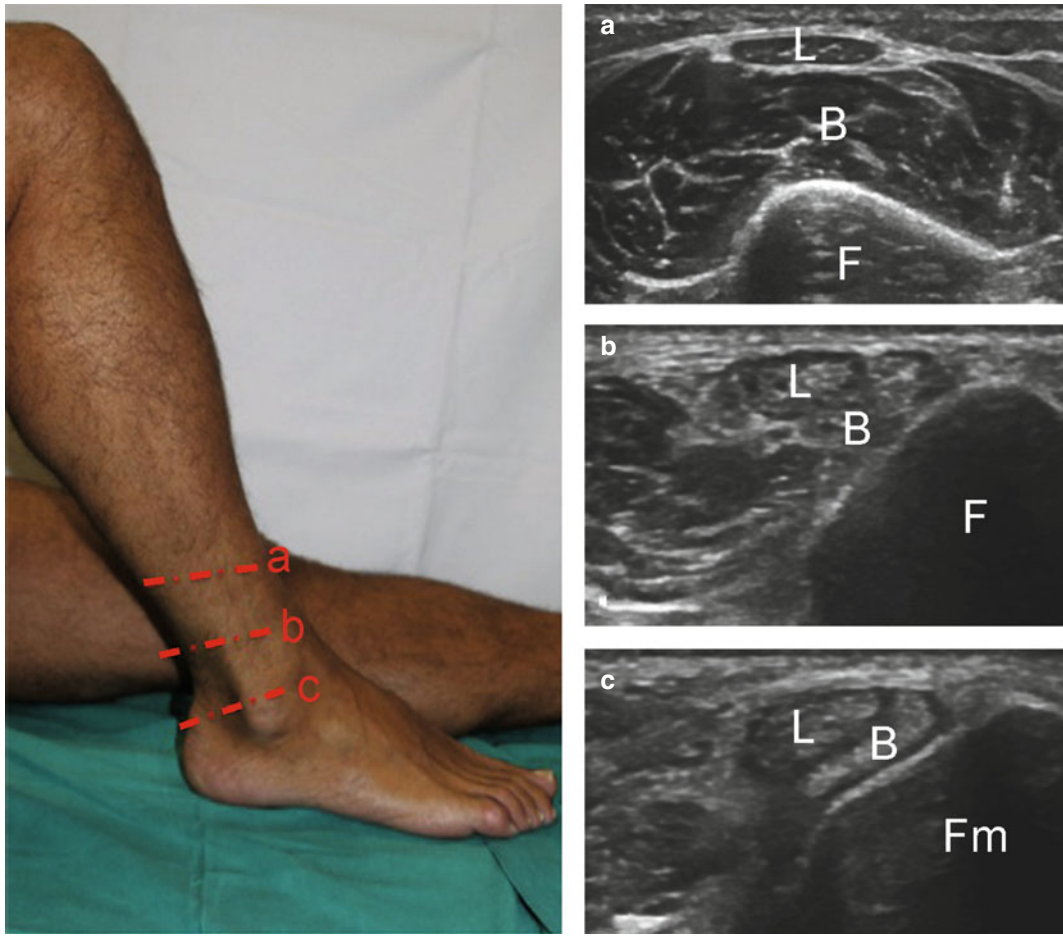

Fig. 14.5 Probe position at different levels over the distal lateral leg for the evaluation of the peroneal muscles and tendons. (**a**) US transverse scan at a more cranial level: the muscle belly of the peroneus brevis (*B*) over the fibula (*F*) and, superficial to it, the myotendinous junction of the peroneus longus (*L*) can be seen. (**b**) US transverse scan at an intermediate level: at this level, the peroneus brevis tendon is arising from the peripheric portion of its muscle belly (*B*); the peroneus longus tendon courses superficial to it. (**c**) US transverse scan at a more caudal level: at this level, the peroneus longus (*L*) and brevis (*B*) tendons are clearly identified together over the fibular malleolus (*Fm*) with their typical oval and semilunar shape

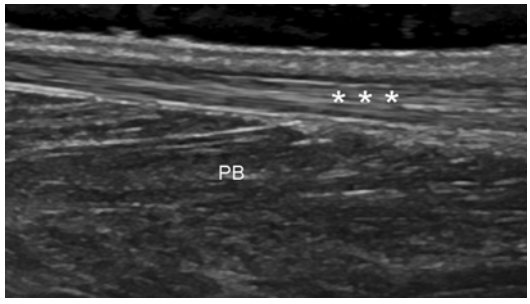

Fig. 14.6 US longitudinal scan of the distal third of the lateral leg, which shows the muscle belly of the peroneus brevis (*PB*) coursing in the distal third of the leg along with the tendon of the peroneus longus muscle (*asterisks*), just superficial to it

keeping its medial edge as fixed a possible, following a curvilinear line that turns around the lateral malleolus. The peroneus brevis tendon has a typical crescent appearance and is located deep into the peroneus longus tendon, which has a typical oval shape. At the level of the lateral malleolus, a common accessory tendon, the peroneus quartus, may be present posteromedially as a tendon or muscle. Note that it is important to recognize this as a separate tendon rather than a split tear of the peroneal tendons.

Distally to the lateral malleolus, the tendons run anteroinferiorly and, reaching the peroneal

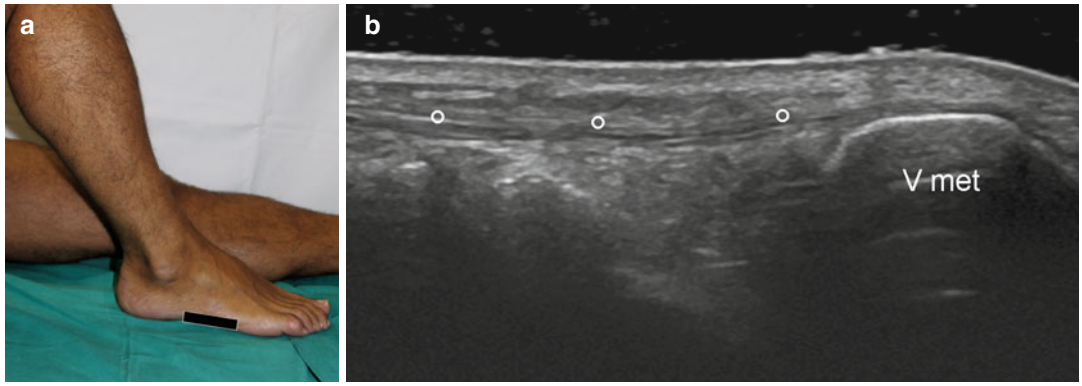

Fig. 14.7 (**a**) Probe position over the inferolateral aspect of the midfoot. (**b**) Corresponding US oblique scan showing the peroneus brevis tendon (*circles*) insertion on the base of the fifth metatarsal bone (V met)

tubercle of the calcaneus, takes two different courses. The peroneus brevis lies on the superior aspect of the peroneal tubercle and the peroneus longus on the inferior one, each of them with its own synovial sheath.

At this level, rotate the probe by 90° and follow the tendon courses along their long axis: the peroneus brevis tendon takes a straight course, inserting onto the lateral margin of the base of the fifth metatarsal; the peroneus longus tendon runs around the cuboid bone to the plantar aspect of the foot and inserts on the medial cuneiform and on the base of the fifth metatarsal (Fig. 14.7).

After ankle sprain, it is mandatory to evaluate the peroneus brevis until its insertion on the fifth metatarsal, which, particularly in young subjects, is a common tendon-bone avulsion site.

Occasionally, the tendons may contain an internal ossicle or sesamoid: remember not to misidentify it as an avulsed bone fragment.

The US exam of peroneal tendons should be completed with dynamic evaluation. It is important to evaluate the tendons at the level of the lateral malleolus during passive and active flexion of the foot in order to assess for tendon subluxation.

The transducer must be placed next to the malleolus obtaining an axial scan of the tendons while the patient everts and dorsiflexes the foot. Remember not to apply too much pressure, which may prevent subluxation.

14.3 Summary Table

Muscle	Origin	Insertion	Innervation	Action
Peroneus longus	Lateral aspect of the superior tibiofibular joint and upper half of the lateral surface of the fibula	Plantar surface of the base of the first metatarsal and medial cuneiform	Superficial fibular nerve	Evert the foot; participate in plantar flexion
Peroneus brevis	Middle-distal third of the lateral aspect of the fibula	Dorsolateral aspect of the base of the fifth metatarsal	Same as above	Same as above
Peroneus quartus (accessory)	Peroneus brevis (most frequent)	Retrotrochlear eminence of the calcaneus (most frequent)	Same as above	Lifts lateral edge of the foot and assists hindfoot pronation

Suggested Reading

Bianchi S, Martinoli C (2007) Ultrasound of the musculoskeletal system. Springer, Berlin

Bianchi S, Martinoli C, Demondion X (2007) Ultrasound of the nerves of the knee region: technique of examination and normal US appearance. J Ultrasound 10(2):68–75

Hayashi D, Hamilton B, Guermazi A et al (2012) Traumatic injuries of thigh and calf muscles in athletes: role and clinical relevance of MR imaging and ultrasound. Insights Imaging 3(6):591–601

O'Neill J (2008) Musculoskeletal ultrasound, anatomy and technique. Springer Science Business Media, New York

Palmanovich E, Laver L, Brin YS et al (2011) Peroneus longus tear and its relation to the peroneal tubercle: a review of the literature. Muscles Ligaments Tendons J 1(4):153–160

Peetrons P (2002) Ultrasound of muscles. Eur Radiol 12:35–43

Silvestri E, Muda A, Sconfienza LM (2012) Normal ultrasound anatomy of the musculoskeletal system: a practical guide. Springer, Italia

Triceps Surae

15

Davide Orlandi and Angelo Corazza

15.1 Anatomy Key Points

15.1.1 Gastrocnemius

The *gastrocnemius* is the largest and most superficial muscle of the calf (Fig. 15.1). The proximal portion of the muscle is formed by two heads, a medial and a lateral one, which arises respectively from the back of the medial and lateral condyles of the femur. They course downwards, posterior to the popliteal fossa, composing the superficial layer of the posterior leg compartment, and merge at the middle-distal third of the leg forming the gastrocnemius tendon. This large flat tendon joins with the underlying soleus muscle tendon to form the calcaneal tendon or Achilles tendon.

Frequently, there is a sesamoid bone in the head of the gastrocnemius tendon, adjacent to the lateral femoral epicondyle, called 'fabella'.

15.1.2 Soleus

The *soleus muscle* is a broad flat muscle, sited in the superficial portion of the posterior compartment of the leg, deep to the gastrocnemius muscle (Fig. 15.1). It is separated from the underlying muscles of the deep portion of the posterior compartment by the deep transverse fascia of the leg. The soleus muscle arises postero-medially from a linear area which runs along the medial edge of the middle third of the tibia up to the posterior edge of the upper third of the tibia, and from a small area on the back of the upper portion of the fibula. Between the fibular and tibial origins of the soleus, there is an arch of fibrous tissue: popliteal vessels and the tibial nerve pass deep into that arch. At the midcalf, the soleus muscle continues into its tendon, which arises from the superficial portion of the muscle belly and, together with the gastrocnemius tendon, forms the Achilles tendon.

D. Orlandi (✉) • A. Corazza
Dipartimento di Radiologia,
Università degli studi di Genova, Genova, Italy
e-mail: my.davideorlandi@gmail.com;
angelcoraz@libero.it

E. Silvestri et al., *Ultrasound Anatomy of Lower Limb Muscles: A Practical Guide*,
DOI 10.1007/978-3-319-09480-9_15, © Springer International Publishing Switzerland 2015

Occasionally an accessory soleus muscle may be present as a normal anatomical variation. It may be detected only in early adulthood when it becomes clinically evident due to hypertrophy of the muscle belly. It more frequently arises from the anterior surface of the soleus, tibia or fibula and attaches to the calcaneus or merges directly with the Achilles tendon fibres.

15.1.3 Achilles Tendon

The *Achilles tendon* is the thickest tendon of the body and is formed proximally by the union of the three tenomuscular structures composing the triceps surae complex, and then it courses longitudinally downwards to insert by an enthesis into the posterior aspect of the calcaneus or heel bone (Fig. 15.1). At this level, there are two tendinous annexes sited below the tendon: the Kager's fat pad and the retrocalcaneal bursa; a subcutaneous virtual bursa, the retroachillean bursa, is also present between the tendon and the subcutaneous tissue.

Fig. 15.1 Anatomical illustration of the triceps surae muscle: the scheme shows the relationship between the more superficial gastrocnemius muscle (*GM*), formed by the union of the medial (*M*) and lateral (*L*) head, and the deeper soleus muscle (*S*); they insert on the calcaneus by means of the Achilles tendon (*A*)

15.1.4 Plantaris Gracilis

The *plantaris gracilis muscle* is a vestigial, accessory structure present in most of the population. It has a small muscle belly and a long thin tendon that crosses from the lateral to medial aspect of the calf. It originates from the lateral supracondylar line, just cranial to the lateral head of the gastrocnemius muscle. Its thin muscle belly courses downwards and medially across the popliteal fossa and at the level of the proximal third of the tibia between the popliteus muscle (inferiorly) and the lateral head of the gastrocnemius muscle (superiorly). At this level, the long thin tendon arises from the medial portion of the muscular fibres and courses between the soleus and gastrocnemius muscles, along the medial side of the Achilles tendon, to insert together on the calcaneus or, otherwise, as a single tendon on the medial aspect of the heel (Fig. 15.2).

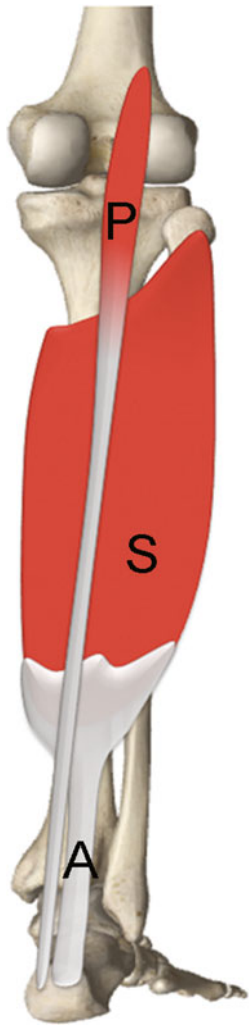

Fig. 15.2 Anatomical scheme of the plantaris (*P*) muscle (the gastrocnemius muscle is not represented to show the underlying structures); *S* soleus muscle, *A* Achilles tendon. In this picture, the most common anatomical variant with the plantaris tendon inserting independently on the medial aspect of the calcaneus is represented

Fig. 15.3 Lower limb position to evaluate the triceps surae muscle

15.2 Ultrasound Examination Technique

US evaluation must be performed with the patient lying prone with the legs extended and the feet projecting over the examination table end (Fig. 15.3).

Start placing the probe onto the posterior aspect of the calcaneus on a transverse plane: at this level, the US image shows the oval hyperechoic shape of the Achilles tendon insertion.

Follow it, maintaining a transverse orientation up to the myotendinous junction, cranial to the calcaneus and under the tendon, the Kager's fat pad can be seen until the tendon merges with the soleus first and then with the gastrocnemius bellies. Note that the fibres of the Achilles tendon present a spiral arrangement from the myotendinous junction to the insertion, with the posterior fibres from the gastrocnemius passing medial to lateral (Fig. 15.4).

Then turn the probe clockwise by 90° and evaluate the tendon on its long axis. The US scan shows the hyperechoic fibrillar structure of the tendon coursing along the superficial portion of

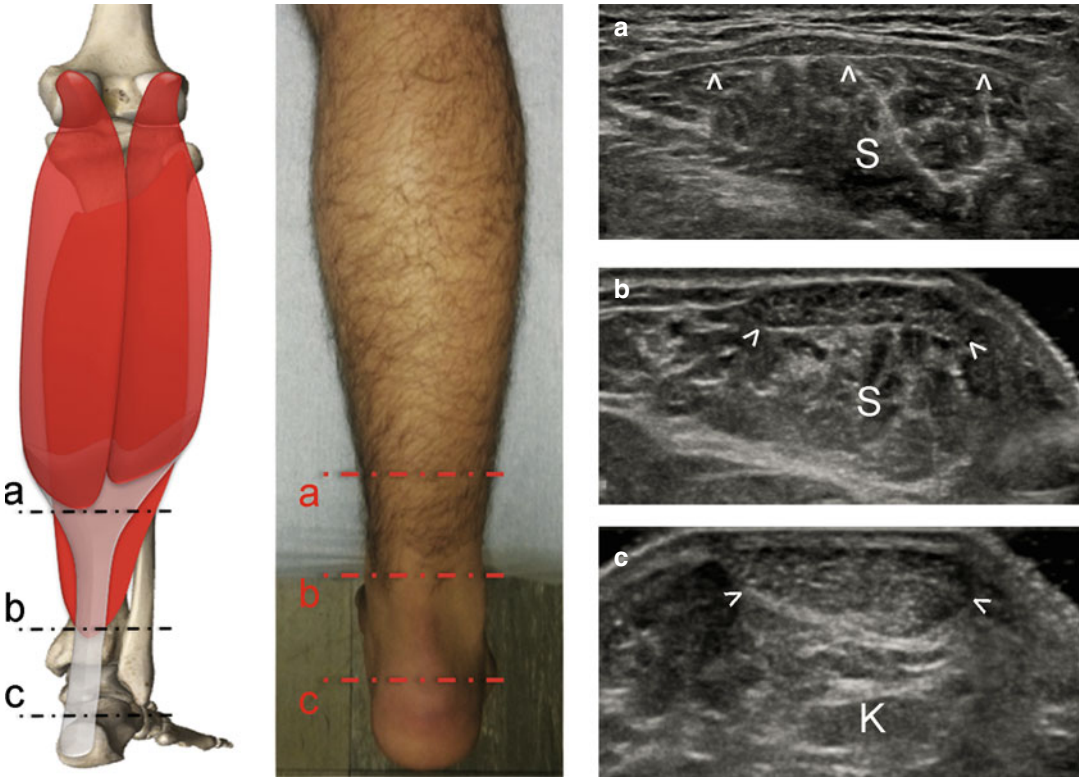

Fig. 15.4 Anatomical scheme and probe position at different levels over the posterior aspect of the distal third of the leg for the evaluation of the Achilles tendon. (**a**) US transverse scan at a more cranial level: the Achilles tendon can be seen as a flat broad fibrillar structure (*arrowheads*) sited superficial to the soleus muscle (*S*); (**b**) US transverse scan at a intermediate level: at this level, the tendon becomes more oval (*arrowheads*); just deep into it, the underlying distal muscular fibres of the soleus (*S*) can still be seen; (**c**) US transverse scan at a more caudal level: at this level, just cranial to the calcaneus, the Achilles tendon is clearly visible with its oval shape (*arrowheads*), coursing over the hyperechoic Kager's fat pad sited below (*K*)

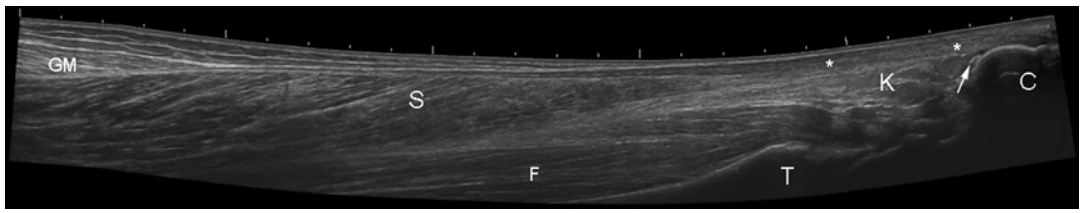

Fig. 15.5 Extended field of view. The longitudinal US image shows the Achilles tendon (*asterisks*) arising proximally from the soleus (*S*) and the gastrocnemius (*GM*) muscles, and inserting onto the posterior aspect of the calcaneus; just deep into the tendon, the hyperechoic Kager's fat pad (*K*) and the retroachillean bursa (*arrow*) can be seen. More deeply, the fibres of the deep flexor muscles of the leg course just over the tibia (*T*)

the image, above the underlying Kager's fat pad: follow it from its insertion on the calcaneus, proximally to its myotendinous junction (Fig. 15.5).

The preinsertional area, due to its decreased vascular supply, is frequently involved in tendinosis processes. At the insertional area, a small hypoechoic area can be seen between the tendon and the calcaneus: it is the retrocalcaneal synovial bursa, which is frequently filled with a small amount of fluid in normal conditions.

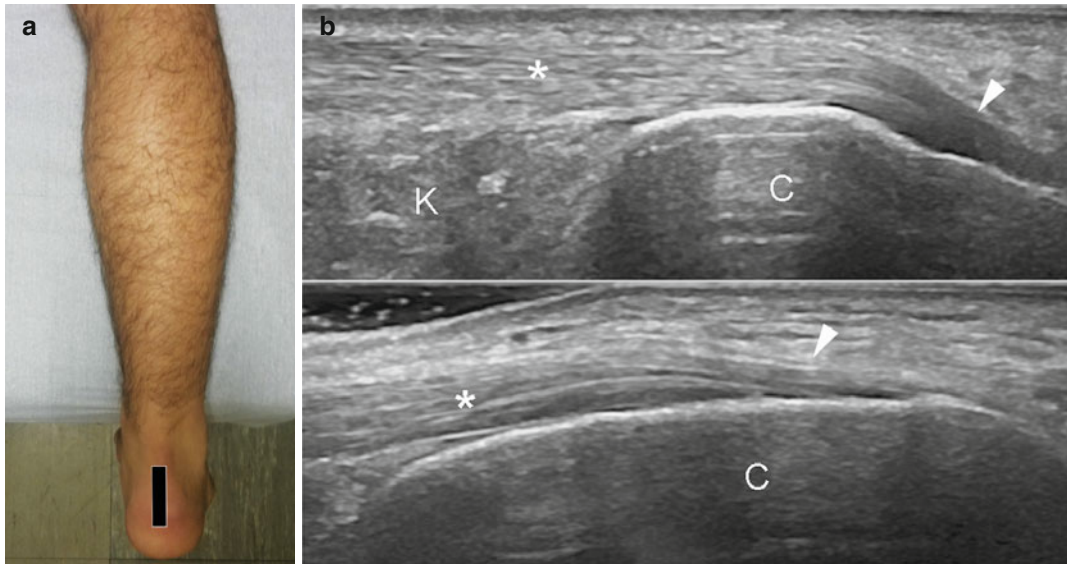

Fig. 15.6 (**a**) Probe position over the posterior aspect of the calcaneus for the evaluation of the Achilles tendon on its long axis. (**b**) *Upper image:* Corresponding US longitudinal scan showing the Achilles tendon (*asterisk*) coursing over the Kager's fat pad and inserting on the posterior aspect of the calcaneus (*C*); the *arrowhead* indicates the insertional area of the tendon which appears hypoechoic due to anisotropy. *Lower image:* Same US longitudinal scan orienting the transducer orthogonal to the course of the insertional fibres of the tendon: in this way, the insertional tendon fibres appear hyperechoic as the rest of the tendon

Despite orthogonal insonation, at this level the insertional fibres are anisotropic and appear hypoechoic due to their oblique orientation at the enthesis: slightly incline the distal edge of the probe on the calcaneus to correctly visualize them (Fig. 15.6).

It is important to reproduce a dynamic manoeuvre: ask the patient to perform plantar-dorsal flexion of the foot in order to evaluate the tenomuscular structures during activity.

Then, move the transducer over the length of the tendon up to the midcalf.

On the US image, the muscular fibres of the soleus, deeply, and gastrocnemius, superficially, appear respectively formed by the contributions from the medial and lateral gastrocnemius aponeurosis and the soleus aponeurosis.

On US image, the soleus muscle can be seen just below the hyperechoic aponeurosis, moving the probe (both with short- and long-axis scans) from the midcalf up to the muscle proximal origin at the upper leg (Fig. 15.7).

Increasing the depth of the US beam, it is possible to visualize the underlying muscular fibres of the flexor hallucis longus, flexor digitorum longus and tibialis posterior, separated from the soleus by the hyperechoic deep transverse fascia.

At the cranial portion of the muscle, between tibial and fibular soleus origins, the popliteal-tibial neurovascular bundle can be seen passing down from the popliteal fossa into the deep posterior compartment of the calf (between soleus, superficially, and deep flexor muscles, deeply).

The gastrocnemius muscle can be followed moving the transducer from the midcalf up to the knee both with longitudinal and transverse orientation (Fig. 15.8).

The US scans show the gastrocnemius fibres composing the superficial muscular layer of the posterior calf, divided into the medial and lateral heads.

An important US scan must be performed in order to study the distal junctional portion of the medial gastrocnemius muscle, which is the most frequent site of traumatic muscle disruption: placing the probe with a longitudinal-oblique orientation on the distal portion of the gastrocnemius

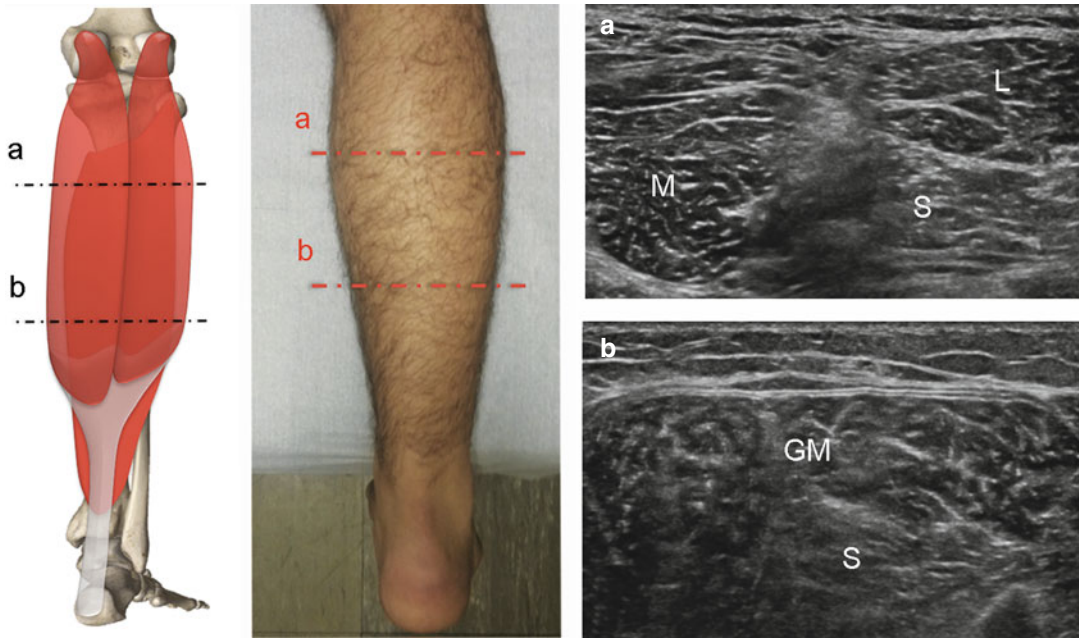

Fig. 15.7 Anatomical scheme and probe position at different levels over the posterior aspect of the proximal-middle third of the leg for the evaluation of the triceps surae muscle. (**a**) US transverse scan on the posterior aspect of the leg at a proximal level showing the lateral (*L*) and medial (*M*) head of gastrocnemius muscles coursing over the proximal portion of the soleus muscle (*S*). (**b**) US transverse scan at a more distal level showing the lateral and medial head of the gastrocnemius merged in one muscle belly (*GM*), over the middle portion of the soleus muscle (*S*)

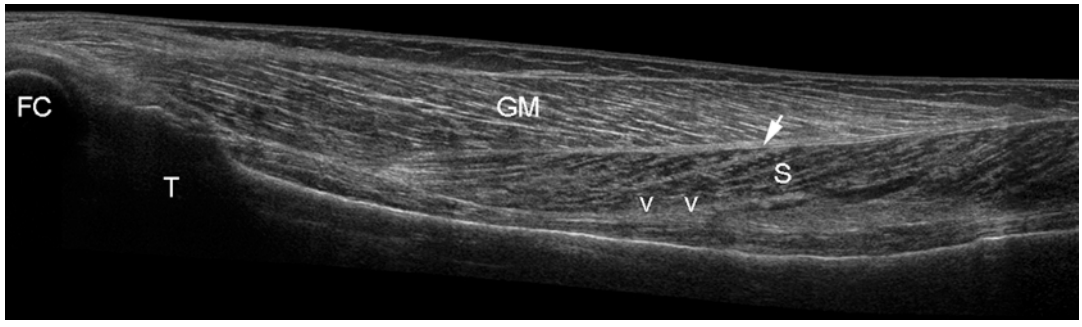

Fig. 15.8 Extended field of view. The longitudinal US image shows the relationships between the gastrocnemius muscle (*GM*) and the soleus muscle (*S*) with their aponeurosis facing each other (*arrow*); the transverse deep fascia of the leg can be seen under to the soleus muscle and over the deep flexor muscles of the leg. *T* tibia, *FC* femoral condyle

medialis muscle belly, find the correct scan as shown in Fig. 15.9.

Complete the gastrocnemius evaluation moving the probe upwards over the knee with a transverse orientation.

At this level, the US image shows the lateral and medial heads of the muscle inserting on the posterior aspect of the respective condyle by means of a superficial aponeurosis.

Rotating the probe on the long axis of the medial head of the gastrocnemius, the insertional area may show the hypoechoic appearance of the medial head gastrocnemius tendon (due to anisotropy), which may simulate fluid in the gastrocnemius-semimembranosus bursa (Fig. 15.10).

Further, note the fibrillar hyperechoic linear structure coursing deep, next to the medial head insertion: it is the descending semimembranosus tendon.

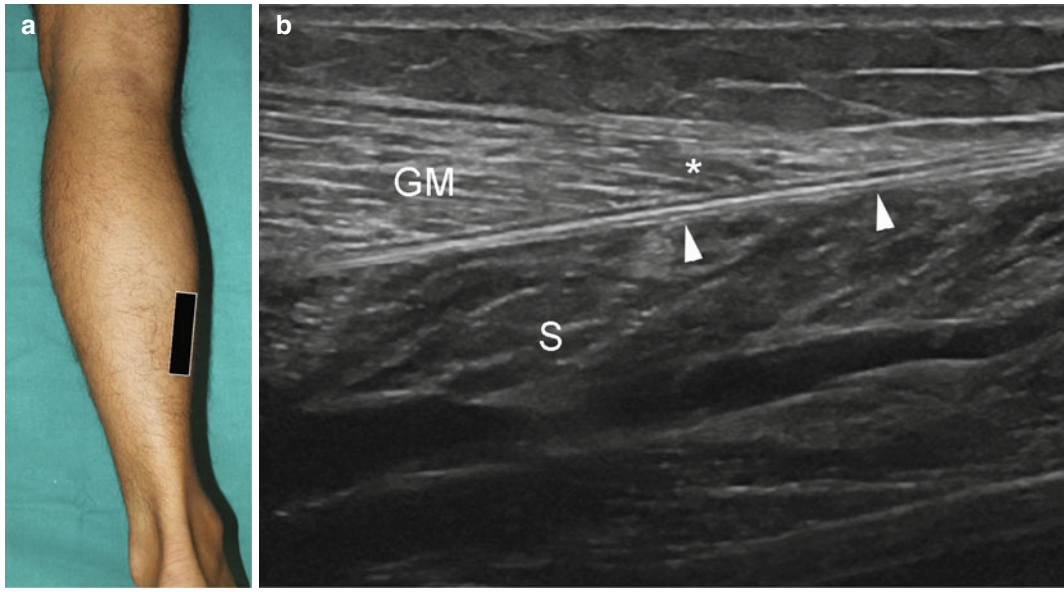

Fig. 15.9 (**a**) Probe position for the evaluation of the gastrocnemius medialis and soleus myotendinous junction. (**b**) Corresponding US longitudinal-oblique scan: the image shows the muscular fibres of the distal portion of the medial gastrocnemius (*GM*) and of the soleus muscle (*S*) inserting respectively on the top and on the bottom of the aponeurosis (*arrowheads*); the *asterisk* indicates the critical area of the triceps surae muscle, most prone to strain, typical for tennis leg injuries

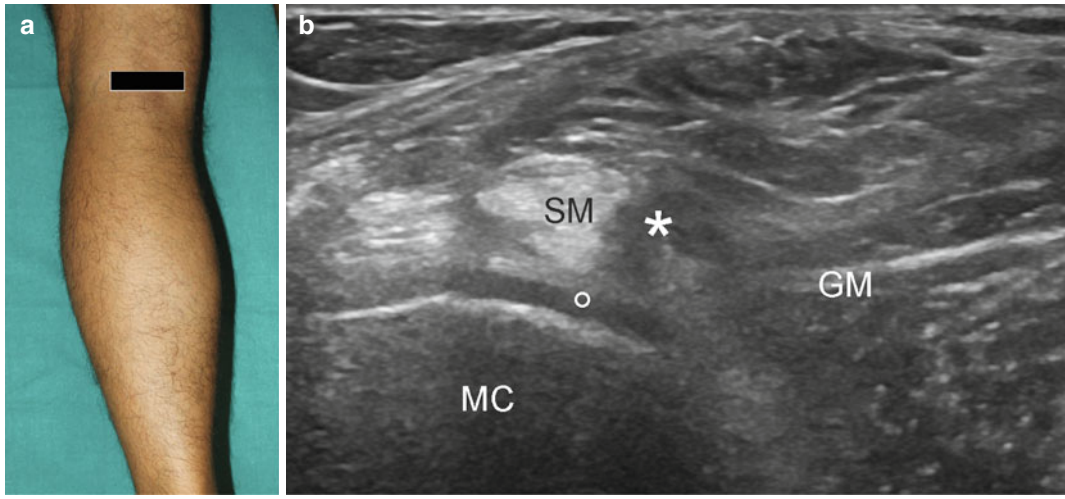

Fig. 15.10 (**a**) Probe position over the posterior knee. (**b**) Corresponding US transverse scan which shows the relationship among the medial condyle of the femur (*MC*), the tendon of the semimembranosus muscle (*SM*), the articular cartilage (*circle*) covered by the joint capsule, the proximal portion of the medial head of the gastrocnemius muscle (*GM*) and the gastrocnemius-semimembranosus bursa (*asterisk*)

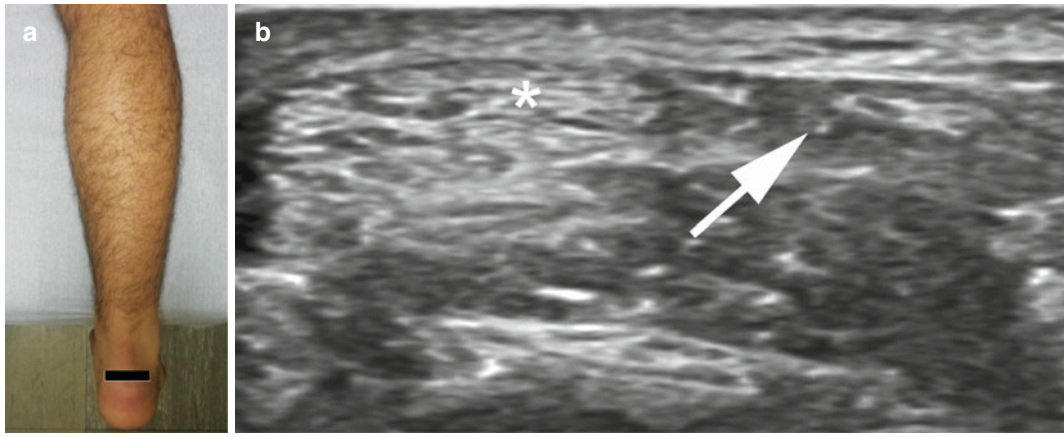

Fig. 15.11 (**a**) Probe position over the posterior aspect of the distal leg for the identification of the plantaris tendon. (**b**) Corresponding US transverse scan which shows the plantaris tendon (*arrow*) as a thin oval hyperechoic structure located just medially to the Achilles tendon (A)

Focus On

The *gastrocnemius-semimembranosus bursa* is a synovial bursa of the knee joint, placed among the semimebranosus tendon, the medial head of gastrocnemius muscle and the posterior aspect of the medial joint capsule. The distension of the gastrocnemius-semimembranosus bursa was also called Baker's cyst and can be evaluated as a mostly hypoechoic (depending on its content) structure with transverse US scans over the posterior aspect of the knee. Placing a towel or a pillow under the ankle helps to get a slight knee flexion (decreasing internal pressure) and to better assess the communication with the joint. Longitudinal scans may contribute to evaluate the cranial or caudal (more common) extent of the cyst.

Moving at the lateral head of the gastrocnemius on the posterior aspect of the lateral femoral condyle a small, a curvilinear ossicle (fabella) with intense posterior shadowing could be seen into the tendon: remember not to confuse the fabella with an intraarticular loose body, a capsular calcification or an osteophyte.

For plantaris muscle evaluation, place the probe on the posterior knee region, using a transverse scan, and move downwards.

On US image, the muscle belly of the plantaris muscle is visualized as a triangular muscular structure between the soleus muscle deeply and the medial and lateral bellies of the gastrocnemius superficially.

Follow the muscle from its proximal attachment on the lateral femoral condyle to the myotendinous junction at the level of the fibular head. Because the tendon forms the medial border of the belly, it is seen on the transverse US scan arising from the medial aspect of the belly.

At the myotendinous junction, rotate the transducer by 90° on the long axis of the tendon and follow it to its distal insertion which could be either on the medial aspect of the calcaneus or directly into Achilles tendon fibres. Otherwise, the tendon is easier to identify distally at the medial border of the Achilles tendon, and followed proximally.

It is very important to assess plantaris muscle presence and insertion, since, in case of complete tears of the Achilles tendon, it may be mistaken for residual intact fibres (Fig. 15.11).

15.3 Summary Table

Muscle	Origin	Insertion	Innervation	Action
Gastrocnemius	Back of the medial and lateral condyles of the femur	Posterior aspect of the calcaneus by the Achilles tendon	Tibial nerve	Plantar flexion of the foot, producing a huge part of the propulsive force involved in walking, running, jumping and standing on the toes; slight flexion of the knee
Soleus	Medial aspect of the middle-distal third of the lateral aspect of the tibia; posterior upper fibula	As above	As above	
Plantaris (most of the population)	Inferior part of the lateral supracondylar line of the femur	Postero-medial aspect of the calcaneus	As above	

Suggested Reading

Armfield DR, Kim DH, Towers JD et al (2006) Sports-related muscle injury in the lower extremity. Clin Sports Med 25:803–842

Ballard DH, Campbell KJ, Hedgepeth KB et al (2013) Anatomic guide and sonography for surgical repair of leg muscle lacerations. J Surg Res 184(1):178–182

Bianchi S, Martinoli C (2007) Ultrasound of the musculoskeletal system. Springer, Berlin

Driessen A, Balke M, Offerhaus C et al (2014) The fabella syndrome – a rare cause of posterolateral knee pain: a review of the literature and two case reports. BMC Musculoskelet Disord 15:100

Gopinath TN, Jagdish J, Krishnakiran K et al (2012) Rupture of plantaris muscle – a mimic: MRI findings. J Clin Imaging Sci 2:19

Lee JC, Healy J (2004) Sonography of lower limb muscle injury. AJR Am J Roentgenol 182(2):341–351

Lee JC, Mitchell AWM, Healy JC (2012) Imaging of muscle injury in the elite athlete. Br J Radiol 85(1016):1173–1185

Megliola A, Eutropi F, Scorzelli A et al (2006) Ultrasound and magnetic resonance imaging in sports-related muscle injuries. Radiol Med 111(6):836–845

Pillen S (2010) Skeletal muscle ultrasound. Eur J Transl Myol 1(4):145–155

Sconfienza LM, Silvestri E, Cimmino MA (2010) Sonoelastography in the evaluation of painful Achilles tendon in amateur athletes. Clin Exp Rheumatol 28(3):373–378

Silvestri E, Muda A, Sconfienza LM (2012) Normal ultrasound anatomy of the musculoskeletal system: a practical guide. Springer, Milan

Spina A (2007) The plantaris muscle: anatomy, injury, imaging, and treatment. J Can Chiropr Assoc 51(3):158–165

Zhou Y, Li JZ, Zhou G et al (2012) Dynamic measurement of pennation angle of gastrocnemius muscles during contractions based on ultrasound imaging. Biomed Eng Online 11:63

Flexor Muscles

16

Emanuele Fabbro, Giulio Ferrero, and Alessandro Muda

The tibialis posterior, flexor digitorum longus and flexor hallucis longus muscles occupy the deep posterior compartment of the leg (Fig. 16.1). They are separated from the superficial posterior muscles by the deep transverse fascia of the leg and from the anterior and lateral muscle compartments by the tibia, the fibula and the interosseous membrane.

16.1 Anatomy Key Points

16.1.1 Tibialis Posterior

The *tibialis posterior* (TP) is a relatively small muscle located in the deep posterior compartment of the leg. Its main actions are plantar flexion and inversion of the foot (it is considered the most powerful supinator of the hindfoot); additionally, it is a primary dynamic stabiliser of the medial longitudinal arch of the foot.

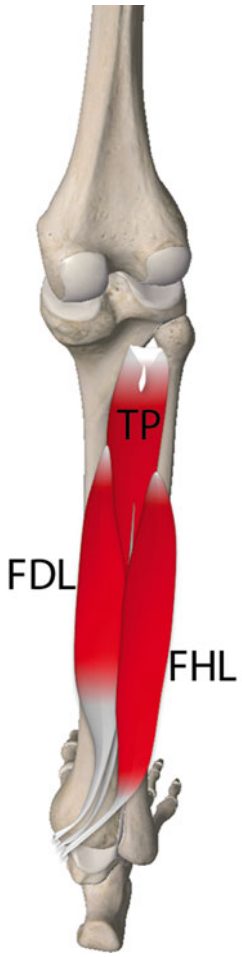

Fig. 16.1 Anatomical scheme of the deep posterior muscles of the leg: *TP* tibialis posterior muscle, *FDL* flexor digitorum longus muscle, *FHL* flexor hallucis longus muscle

E. Fabbro • G. Ferrero
Dipartimento di Radiologia, Università degli studi di Genova, Genoa, Italy
e-mail: emanuele.fabbro@gmail.com; giulio.ferrero@gmail.com

A. Muda (✉)
Dipartimento di Radiologia, IRCCS Ospedale San Martino IST, Genoa, Italy
e-mail: alessandro.muda@tiscali.it

E. Silvestri et al., *Ultrasound Anatomy of Lower Limb Muscles: A Practical Guide*,
DOI 10.1007/978-3-319-09480-9_16,

The tibialis posterior muscle takes its origin from the inner posterior surface of the tibia, from the fibula, just under the proximal tibiofibular joint and from the posterior aspect of the adjacent interosseous membrane. Its superior extremity is bifid and the anterior tibial vessels pass forward between the two attachment points to reach the anterior compartment.

The muscle belly runs posterior to the interosseous membrane, between the flexor digitorum longus (medial) and the flexor hallucis longus (lateral) muscles. Along its entire course, the tibialis posterior muscle has a close relationship with the posterior neurovascular bundle of the leg (formed by the posterior tibial artery and veins and the tibial nerve) that lies between it (anterior) and the soleus muscle (posterior).

The tibialis posterior distal tendon arises from a central aponeurosis that gives a bipennate appearance to the muscle. Then the tendon courses anteriorly to the flexor digitorum longus, under the flexor retinaculum. At this level, the tibialis anterior tendon is the most medial of the three flexor tendons (Fig. 16.2). Distally the tendon turns around the medial malleolus and inserts with different fascicles: the main one attaches onto the navicular tuberosity (with fibrous expansions to the cuboid) and the first cuneiform bone; some fibres also reach the base of the second, third and fourth metatarsal bone.

The vascularisation of the tibialis posterior muscle is supplied by the posterior tibial artery. The innervation is provided by the tibial nerve.

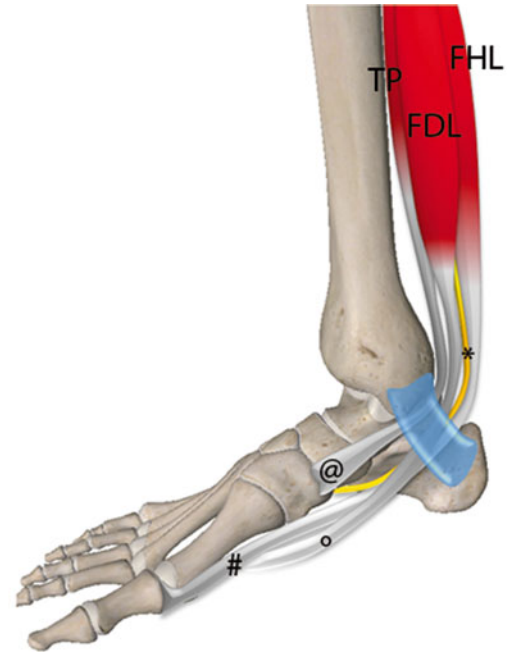

Fig. 16.2 Anatomical scheme of the medial tendons of the ankle: tibialis posterior muscle (*TP*) and tendon (@); flexor digitorum longus muscle (*FDL*) and tendon (°); flexor hallucis longus muscle (*FHL*) and tendon (#); (*), tibial nerve

16.1.2 Flexor Digitorum Longus

The *flexor digitorum longus* (FDL) is the most medial of the deep posterior muscles of the leg. It originates from the posterior surface of the tibia, at the level of the middle third, below the popliteus muscle, the tibial origin of the soleus muscle and medial to the vertical ridge. The muscle belly is located between the posterior aspect of the tibial diaphysis and the ventral surface of the soleus muscle, medial to the tibialis posterior and the flexor digitorum longus muscles. At

the distal third of the leg, it crosses superficial the distal portion of the tibialis posterior muscle and continues in a long distal tendon that grooves the lower end of the tibia and overcomes the tibialis posterior tendon. Then, the flexor digitorum longus tendon passes around the medial malleolus under the flexor retinaculum, between the tibialis posterior and flexor hallucis longus tendons, reaching the plantar aspect of the foot. At this level, it divides into four distinct tendons, each of them inserts onto the base of the distal phalanx of the second to the fifth toe.

The flexor digitorum longus muscle is involved in plantar flexion of the second to the fifth toe; it also contributes to plantar flexion and inversion of the foot.

It is vascularised by the posterior tibial artery and innervated by the tibial nerve.

16.1.3 Flexor Hallucis Longus

The *flexor hallucis longus* (FHL) is a bipennate muscle arising from the posterior diaphysis of the inferior two thirds of the fibula, below the fibular origin of the soleus muscle. The large muscle belly descends down, lateral to the tibialis posterior muscle and medial to the peroneus longus muscle from which it is separated by the posterior crural septum. Then it inclines medially and posteriorly to the lower posterior tibial surface, extending distally to the tibialis posterior and the flexor digitorum longus muscles. The FHL myotendinous junction is located between the medial and lateral tubercle of the posterior process of the talus.

The distal tendon occupies the osteofibrous deep groove on the posterior surface of the talus, then runs down in the tarsal tunnel, behind the medial malleolus under the flexor retinaculum, lateral to the flexor digitorum longus tendon, to attach onto the base of the distal phalanx of the great toe.

Together with the flexor hallucis brevis muscle, the flexor hallucis longus muscle is involved in plantar flexion of the great toe.

The flexor hallucis longus muscle is vascularised by the peroneal branch of the posterior tibial artery and innervated by the tibial nerve.

16.2 Ultrasound Examination Technique

The tibialis posterior, flexor digitorum longus and flexor hallucis longus muscles are sometimes difficult to identify because of their deep position in the posterior leg. US scan of these muscles may require a careful adjustment of the imaging parameters or the use of low-frequency convex-array probes, especially in obese patients or in athletes, in order to obtain a better evaluation of each muscle belly and a panoramic view.

The patient lies seated on the examination table with the knee flexed and the plantar surface of the foot flat on the table, keeping the knee slightly externally rotated to expose the posteromedial aspect of the leg (Fig. 16.3).

Begin the US evaluation at the level of the medial aspect of the ankle joint where the tibialis posterior, flexor digitorum longus and flexor hallucis longus tendons pass behind the medial malleolus, under the flexor retinaculum. Identification of each distal tendon may be helpful to guide the consequent visualisation and differentiation of each muscle belly.

Place the probe on an axial position with the medial extremity on the surface of the medial malleolus, the main bony landmark, to evaluate the relationship among the three flexor tendons (Fig. 16.4). Remember the mnemonic formula "Tom, Dick and a very nervous Harry" (that means *T*ibialis posterior, flexor *D*igitorum longus, AVN bundle and flexor *H*allucis longus) for the order of the three tendons at the level of the ankle joint, from anterior to posterior.

Colour Doppler examination allows to identify the posterior neurovascular bundle (posterior tibial artery and veins and adjacent tibial nerve) and its close relationship with the flexor tendons at the medial malleolus; the posterior neurovascular bundle is shown separating the tibialis posterior and the flexor digitorum longus tendons (medial to it) from the flexor hallucis longus tendon (lateral to it).

Fig. 16.3 Leg position to evaluate the deep posterior flexor muscles

Focus On

The *tibial nerve* is the largest of the two terminal divisions of the sciatic nerve. At the popliteal space, it is located between the medial and the lateral heads of the gastrocnemius muscle and posterior to the popliteal vessels. There, it proceeds down in the same direction of the sciatic nerve, entering the leg at the soleus arcade. The nerve, together with the posterior tibial artery and veins, runs the leg between the superficial and deep posterior muscle compartments. In the proximal two thirds of the leg, it courses in a close relationship with the posterior surface of the tibialis posterior and the flexor digitorum longus muscles, and at the distal third, it curves medially to pass between the Achilles tendon and the medial border of the tibia. At the ankle, the nerve crosses the posterior aspect of the medial malleolus, under the flexor retinaculum, and it divides into the medial and lateral plantar nerves.

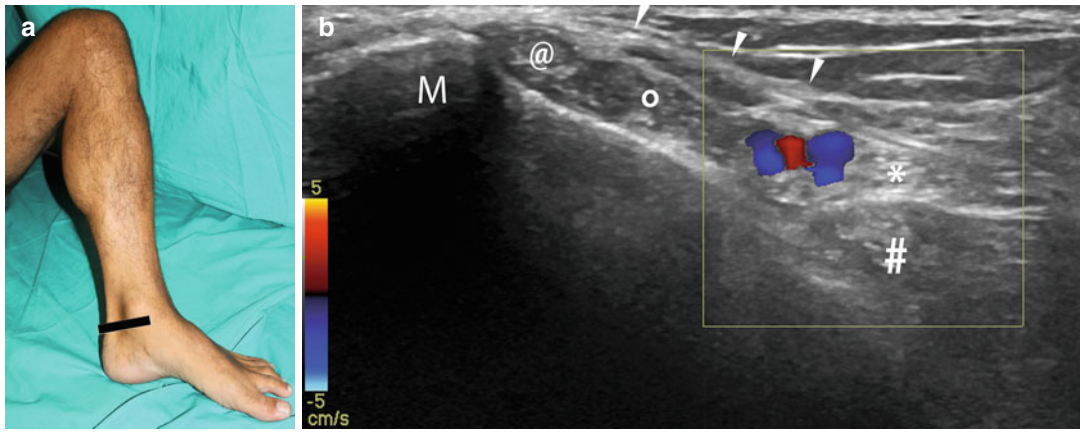

Fig. 16.4 (**a**) Probe position to examine the flexors tendons at the medial malleolus level. (**b**) US axial scan with colour Doppler analysis: the tibialis posterior (@) is the largest and the most anterior tendon lying immediately behind the medial malleolus (*M*). (°) flexor digitorum longus tendon; (#), flexor hallucis longus tendon; arrowheads, flexor retinaculum (*white arrowheads*). Look at the posterior tibial artery (*red*) and veins (*blue*) and the tibial nerve (*)

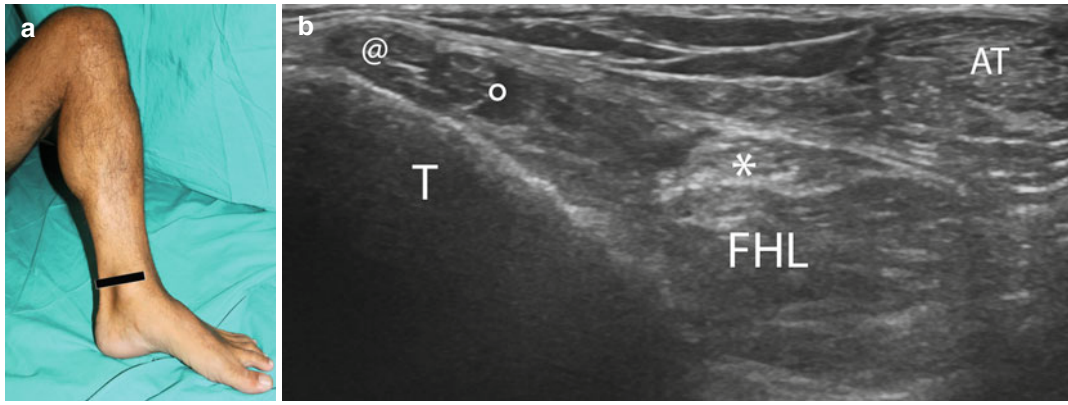

Fig. 16.5 (**a**) Probe position to examine the tibialis posterior, flexor digitorum longus and flexor hallucis longus muscle bellies. (**b**) US axial scan at the level of the tibio-talar joint: the flexor hallucis longus (*FHL*) is already seen as a muscle belly; antero-medial to it, the tibialis posterior tendon (@) and the flexor digitorum longus tendon (°) are visualised. *T* Tibia, *AT* Achilles tendon

Then, move the probe cranially along the posteromedial surface of the leg identifying the proximal myotendinous junction and the belly of each muscle on the axial plane.

Sometimes it may be difficult to differentiate each muscle belly from the others. Use dynamic scans during passive flexion-extension of each toe to distinguish them.

At the tibio-talar joint, the first muscle belly visualised is the flexor hallucis longus because it extends more distally than the others; at this level, the tibialis posterior and the flexor digitorum longus still remain tendinous (Fig. 16.5).

Furthermore, shifting the probe cranially at the distal third of the leg, the tibialis posterior tendon is seen passing under the flexor digitorum longus tendon and the flexor hallucis longus muscle belly, assuming a deep position (Fig. 16.6).

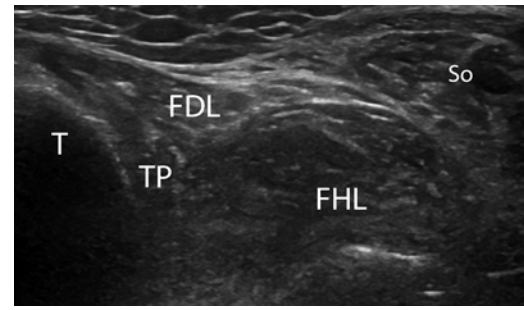

Fig. 16.6 US axial scan at the distal third of the leg. The tibialis posterior tendon has become muscle belly (*TP*) coursing under the flexor digitorum longus tendon and muscle (*FDL*) and the flexor hallucis longus muscle (*FHL*). *T* tibia, *So* soleus muscle

In this setting, the tibialis posterior and the flexor digitorum longus progressively become bulbous: the tibialis posterior muscle is located medial to tibial diaphysis, deep to the flexor digitorum longus (medial) and the flexor hallucis longus (lateral) muscles (Fig. 16.7).

Continue the examination translating the probe cranially, along the posteromedial surface of the leg, following the three muscle bellies until their proximal insertion. A quite variability of the level of the flexor digitorum longus and the flexor hallucis longus proximal insertion, on the tibia and on the fibula respectively, could be seen. However, they usually insert at the middle third of the leg, below the origin of the popliteus and the soleus muscles (Fig. 16.8). In any case, their proximal tendons usually are not clearly identifiable at US examination.

The tibialis posterior muscle continues until the level of the proximal tibiofibular joint, under which it inserts both on the tibia and the fibula.

From the position shown in Fig. 16.7, shift the probe cranially, along the posteromedial

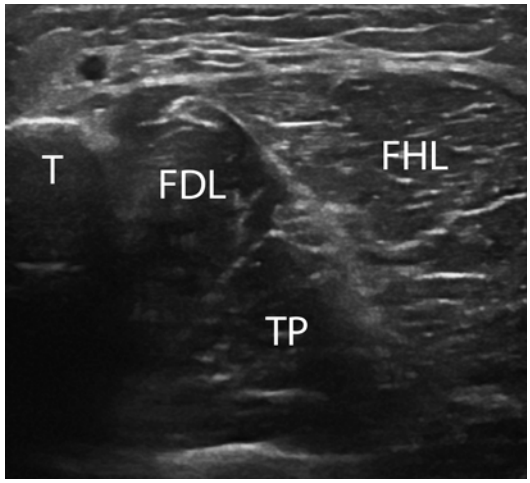

Fig. 16.7 US axial scan demonstrates the relationship of the three flexor muscles. *TP* tibialis posterior muscle, *FDL* flexor digitorum longus muscle, *FHL* flexor hallucis longus muscle. *T* tibia

surface of the leg: the tibialis posterior muscle belly is seen disappearing under the tibial bone (Fig. 16.9).

To accurately evaluate its proximal muscle belly and the proximal insertion, use a posterolateral approach. Place the probe at the same level shown in Fig. 16.9, but on the posterolateral surface of the leg. The tibialis posterior muscle could be seen rising up between the tibia and the fibula, posterior to the interosseous membrane, and then it is possible to follow it up to its proximal tendons (Fig. 16.10). The proximal insertion is difficult to visualise during the US examination because of the deep position of the muscle and the shortness of the two attachment points onto the tibia and the fibula.

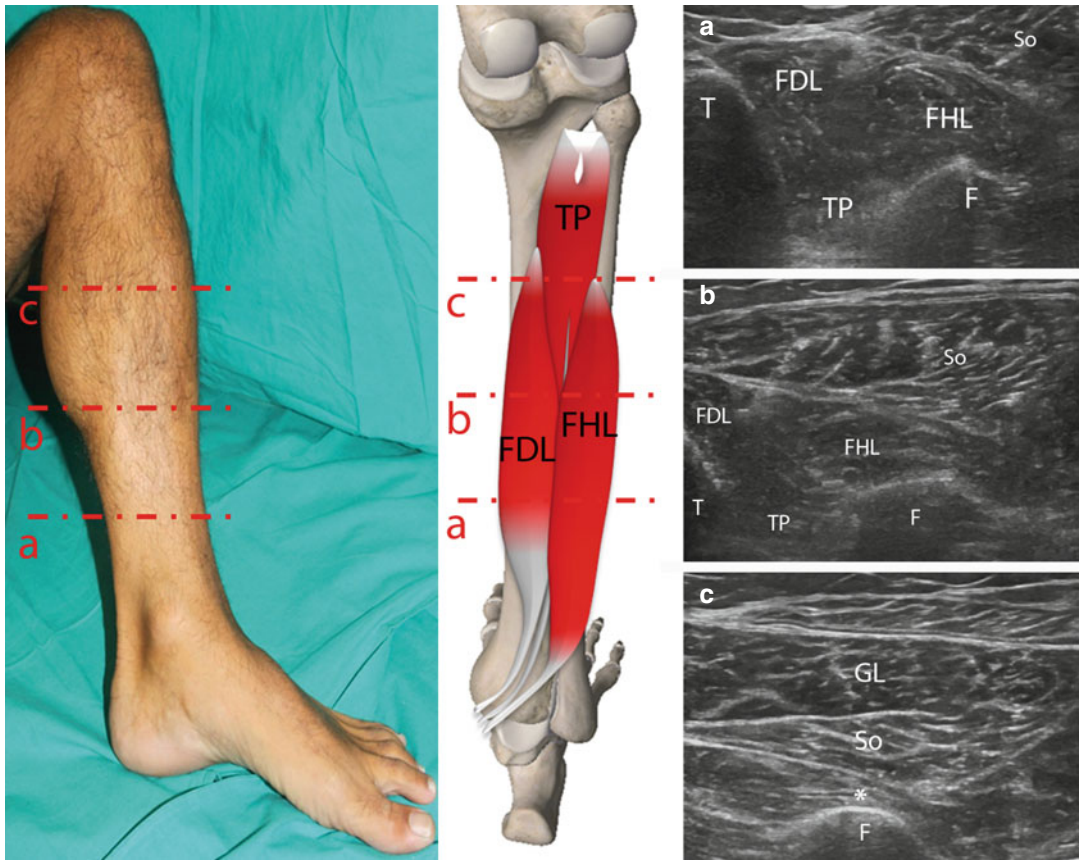

Fig. 16.8 Probe position to evaluate the flexor hallucis longus muscle on the axial plane at different levels. Anatomical scheme of the deep posterior muscles of the leg correlated with US axial scan of the flexor hallucis longus (*FHL*) at different levels (distal (**a**), middle (**b**) and proximal (**c**) third of the leg) up to the proximal insertion (*). *FDL*, flexor digitorum longus, So soleus muscle, *TP* tibialis posterior, *GL* gemellus lateralis muscle, *T* tibia, *F* fibula

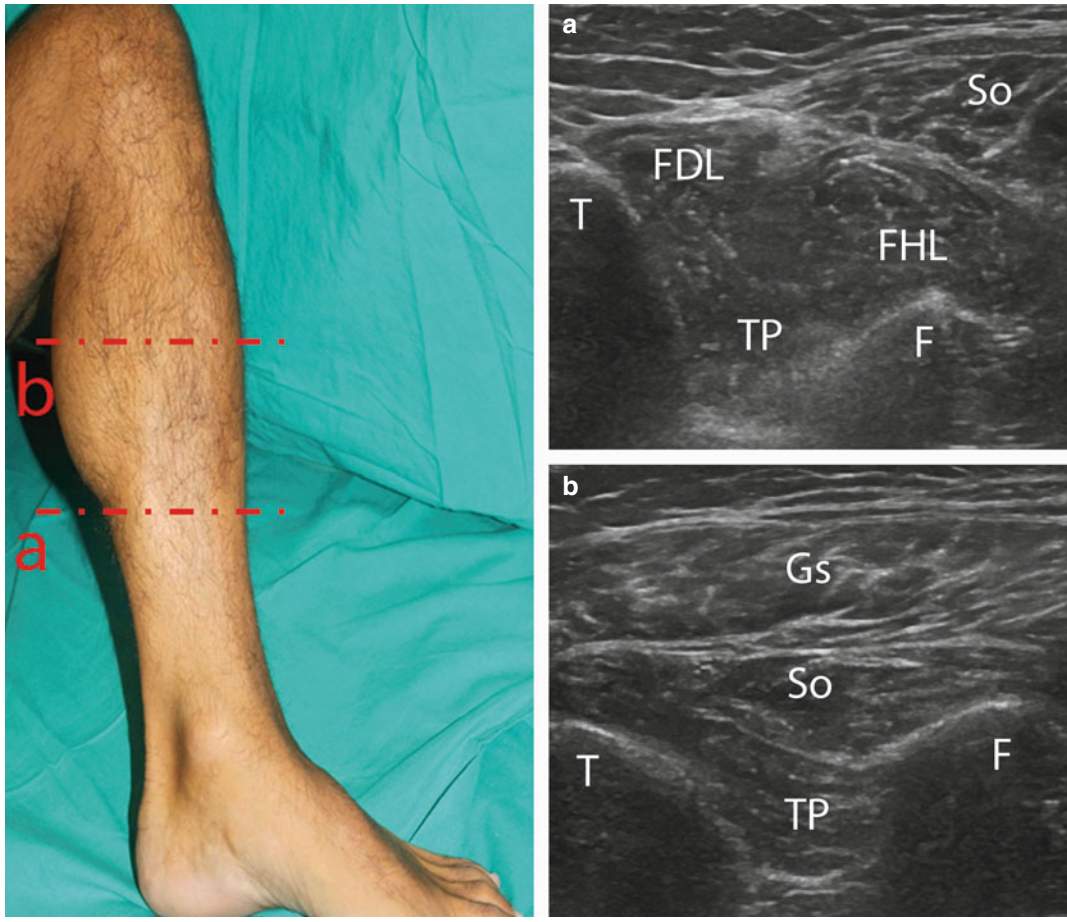

Fig. 16.9 US axial scans of the tibialis posterior muscle at the distal (**a**) and middle (**b**) third of the leg. *TP* tibialis posterior muscle, *FDL* flexor digitorum longus muscle, *FHL* flexor hallucis longus muscle, *So* soleus muscle, *Gs* gastrocnemius muscle, *T* tibia, *F* fibula

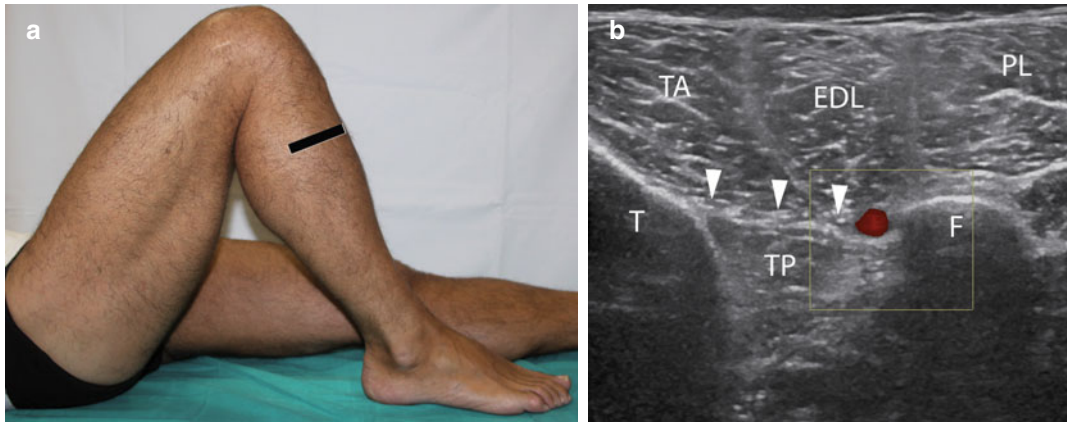

Fig. 16.10 (**a**) Probe position to evaluate tibialis posterior proximal muscle belly on the axial plane. (**b**) US axial scan at the proximal third of the leg. Note the close relationship of the tibialis posterior muscle (*TP*) with the anterior tibial artery and the anterior muscles of the leg. Look at the interosseous membrane (*arrowheads*), seen as a continuous hyperechoic band that courses between the tibia and the fibula, separating the tibialis posterior from the anterior muscles of the leg. *TA* tibialis anterior muscle, *EDL* extensor digitorum longus muscle, *PL* peroneus longus muscle, *T* tibia, *F* fibula

Focus On

The *interosseous membrane* is a thin aponeurotic membrane stretching between the interosseous crest of the tibia and the anteromedial surface of the fibula. It represents a greatly extended surface for muscle origin: the tibialis anterior, extensor digitorum longus and peroneus tertius take partial origin from the anterior surface of this membrane. The tibialis posterior and the flexor hallucis longus take partial origin from its posterior aspect.

In the upper portion, just inferior to the lateral tibial condyle and the head of the fibula, the interosseous membrane shows a concave margin for the passage of the anterior tibial vessels. Distally, is crossed by the anterior peroneal vessels.

The strong oblique fibres of the interosseous membrane run downwards and laterally from the tibia to the fibula and distally continue as the inferior interosseous ligament.

It is an important stabiliser of the tibia and the fibula, the site of muscles attachment, and separates the anterior compartment from the deep posterior compartment of the leg.

Starting from the position shown in Fig. 16.4, rotate the probe by 90° to obtain longitudinal scans of the three flexor tendons. In particular, incline the probe slightly medially to visualise the flexor digitorum longus and the tibialis posterior and slightly laterally to image the flexor hallucis longus tendons (Fig. 16.11). Remember to follow each tendon to reach the proper distal myotendinous junction.

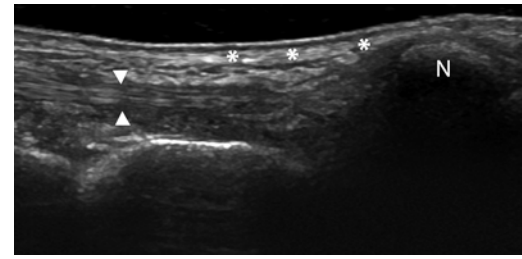

Fig. 16.11 Extended-field-of-view longitudinal scan of the flexor tendons at the level of the medial malleolus: (*), tibialis posterior tendon; (*white arrowheads*), flexor digitorum longus tendon. *N* navicular bone

16.3 Summary Table

Muscle	Origin	Insertion	Nerve supply	Action
Tibialis posterior	Posterior surfaces of the tibia and the fibula, adjacent interosseous membrane	Navicular tuberosity (with expansions to the cuboid), first cuneiform, base of the II, III, IV metatarsal bone	Tibial nerve	Plantar flexion of the foot Inversion of the foot Support to the foot medial arch
Flexor digitorum longus	Posterior surface of the tibia	Bases of the distal phalanges of the II through V toes	Tibial nerve	Plantar flexion of II to V toes Plantar flexion of the foot Inversion of the foot
Flexor hallucis longus	Posterior surface of the fibula	Base of the distal phalanx of the great toe	Tibial nerve	Extension of the thigh Flexion of the leg Internal rotation of the leg with flexed knee

Suggested Reading

Drake RL, Vogl W, Mitchell AWM (2005) Grey's anatomy. Elsevier/Churchill Livingstone, Philadelphia

Lieber RL, Fridén J (2000) Functional and clinical significance of skeletal muscle architecture. Muscle Nerve 23(11):1647–1666

Manaster BJ (2004) Diagnostic and surgical imaging anatomy: musculoskeletal. Amirsys, Salt Lake City

Martinoli C, Bianchi S (2007) Ultrasound of the musculoskeletal system. Springer, Berlin

O'Neill J (2008) Musculoskeletal ultrasound: anatomy and technique. Springer, New York

Stoller DW, Tirman PFJ, Bredella MA (2004) Diagnostic imaging orhtopaedics. Amirsys, Salt Lake City

Extensor Muscles

17

Davide Orlandi and Alice Arcidiacono

The tibialis anterior, extensor hallucis longus and extensor digitorum longus muscles occupy the anterior compartment of the leg (Fig. 17.1). They are separated from the deep posterior muscles by the tibia, the fibula and the interosseous membrane.

17.1 Anatomy Key Points

17.1.1 Tibialis Anterior

The *tibialis anterior* is the largest and most medial muscle of the anterior compartment of the leg.

It is a fusiform muscle, located on the lateral side of the tibia. Its belly is thick and fleshy at its proximal third and becomes thin and fibrous at its distal third forming a strong oval tendon which is led by both extensor retinacula of the foot before its insertion.

The tibialis anterior is a circumpennate muscle with a thick central intramuscular aponeurosis.

It arises from several structures: the lateral femoral condyle, the superior half of the lateral surface of the tibia, the interosseous membrane and the deep surface of the fascia.

The muscular fibres run vertically downwards and end in a tendon, which is eccentric and lies on the anterior aspect of the muscle at the lower third of the leg.

It attaches on the medial and inferior surface of the first cuneiform bone and into the base of the first metatarsal bone.

This muscle overlaps the anterior tibial vessels and deep peroneal nerve in the upper part of the leg.

The blood supply to the tibialis anterior muscle comes from the anterior tibial artery, which originates from the popliteal artery in the posterior compartment of the leg and passes forward into the anterior compartment of the leg trough an aperture in the interosseous membrane. In the proximal third of the leg, the anterior tibial artery lies between the tibialis anterior and extensor digitorum longus muscles; in the middle third between the tibialis anterior and

D. Orlandi (✉) • A. Arcidiacono
Dipartimento di Radiologia, Università degli studi di Genova, Genoa, Italy
e-mail: my.davideorlandi@gmail.com; alice.arcidiacono@hotmail.com

E. Silvestri et al., *Ultrasound Anatomy of Lower Limb Muscles: A Practical Guide*,
DOI 10.1007/978-3-319-09480-9_17, © Springer International Publishing Switzerland 2015

Fig. 17.1 Anatomical scheme of the anterior leg compartment muscles. *TA* tibialis anterior, *EDL* extensor digitorum longus, *EHL* extensor hallucis longus. *EHL* lies in a deeper layer than *TA* and *EDL* and its muscle belly arises more distally

the extensor hallucis longus muscles and at the ankle lies between the tendon of the extensor hallucis longus and the first tendon of the extensor digitorum longus.

The main functions of the tibialis anterior muscle are dorsiflexion of the foot, inversion raising the medial side of the foot off the ground and stabilization of the ankle during walking.

The tibialis anterior tendon together with the extensor hallucis longus and extensor digitorum tendons are anchored to the tibial bony surface by the extensor retinacula, which are canal-like thickenings of the crural fascia or deep fascia of the leg.

The superior extensor retinaculum (transverse crural ligament) lies between the fibula and tibia proximal to the malleoli.

The inferior extensor retinaculum (cruciate crural ligament) presents a Y shape and extends more distally between calcaneus, medial malleolus and plantar aponeurosis.

17.1.2 Extensor Hallucis Longus

The *extensor hallucis longus* muscle is a thin muscle located in the anterior lower leg compartment between the tibialis anterior and the extensor digitorum longus muscles. It arises more distally with respect to the tibialis anterior and the extensor digitorum longus, from the middle third of the anterior surface of the fibula and from the anterior surface of the interosseous membrane. The fibres run downwards, merging into a tendon above the superior extensor retinaculum.

The extensor hallucis longus tendon is eccentric and lies on the anterior aspect of the muscle, passes deep to the superior extensor retinaculum and through the inferior extensor retinaculum inserting into the dorsal aspect of the base of the distal phalanx of the hallux.

In proximity of the metatarsophalangeal joint, a thin prolongation merges from each side of the tendon and covers the dorsal surface of the joint. An expansion

from the medial side of the tendon usually attaches on the base of the proximal phalanx.

In the distal third of the leg, the extensor hallucis longus tendon crosses the tendon of the extensor digitorum longus.

The extensor hallucis longus muscle is innervated by the *deep fibular nerve* and vascularized by the *anterior tibial vessels* which course between it and the tibialis anterior.

The extensor hallucis longus muscle works in synergy with the other extensor of the big toe (the extensor hallucis brevis muscle), pulling the toe upwards and extending the phalanges of the hallux. The extensor hallucis longus also plays a role in the dorsiflexion of the ankle joint.

17.1.3 Extensor Digitorum Longus

The *extensor digitorum longus* muscle lies lateral and deep to the tibialis anterior muscle and medial to the peroneus brevis muscle.

It is a pennate muscle arising from several structures such as the lateral tibial condyle, the upper part of the anterior surface of the shaft of the fibula, the upper part of the interosseous membrane, the deep surface of the fascia cruris and the anterior crural intermuscular septum.

The extensor digitorum longus is serviced by the deep peroneal nerve and the anterior tibial artery, which, in the upper part of the leg, courses between the extensor digitorum and the tibialis anterior muscles.

The extensor digitorum longus fibres course downwards along the anterior aspect of the lower leg and near the ankle turn into a long distal tendon which passes behind the superior and the inferior extensor retinaculum together with the Peroneus tertius, an additional fifth tendon present in about 90 % of the people running towards the lateral foot edge and inserting at the fifth metatarsal bone. The peroneus tertius is a small muscle, laying laterally to the extensor digitorum longus and is considered as a part of it.

The extensor digitorum longus tendon divides into four parts, running towards the corresponding small toe and inserting into the second and third phalanges.

The tendons to the second, third and fourth toes, on the lateral side of the metatarsophalangeal joints, combine with one of the extensor digitorum brevis tendons to form a broad dorsal aponeurosis, which covers the dorsal surface of the proximal phalanx. At the interphalangeal joint, it divides into three slips: the central one is inserted into the base of the middle phalanx and the two laterals are inserted into the base of the distal phalanx.

Variations within the extensor digitorum longus muscle are not uncommon and include attachment also to the hallux.

When the extensor digitorum longus muscle is in contraction, it causes the extension of the lateral four toes and the dorsiflexion of the foot. In addition, it is responsible for a powerful eversion (pronation).

17.2 Ultrasound Examination Technique

The patient is seated on the examination bed with the knee flexed about 20–45°, and the plantar surface of the foot lies flat on the table (Fig. 17.2).

Palpate the tibial tuberosity on the anterior aspect of the tibia, which can be considered an important bony landmark, and place the probe on it in an axial position.

Move the transducer slightly lateral and identify the myotendinous junction of the tibialis anterior near the patellar tendon (Fig. 17.3).

Rotate the probe by 90° to evaluate on a longitudinal plane the proximal attachment of the tibialis anterior tendon on the tibial tuberosity (Fig. 17.4).

Replace the probe in a transverse plane and shift it caudally and lateral to identify the cortical surface of the fibula and the anterior tibial crest in the same scan (Fig. 17.5).

The cortex of the tibia and fibula are identified as continuous hyperechoic lines with posterior shadowing.

The interosseous membrane can be seen as a thin concave hyperechoic layer between the tibial and fibular cortex and opposite to the tibialis posterior muscle.

Power Doppler could be useful in order to identify the anterior neurovascular bundle and the passage of the anterior tibial vessel through the interosseous membrane (Fig. 17.6).

At this level, it is possible to demonstrate the large muscular belly of the tibialis anterior characterized by a thick central aponeurosis (Fig. 17.7).

Fig. 17.2 Leg position to evaluate the anterior leg compartment

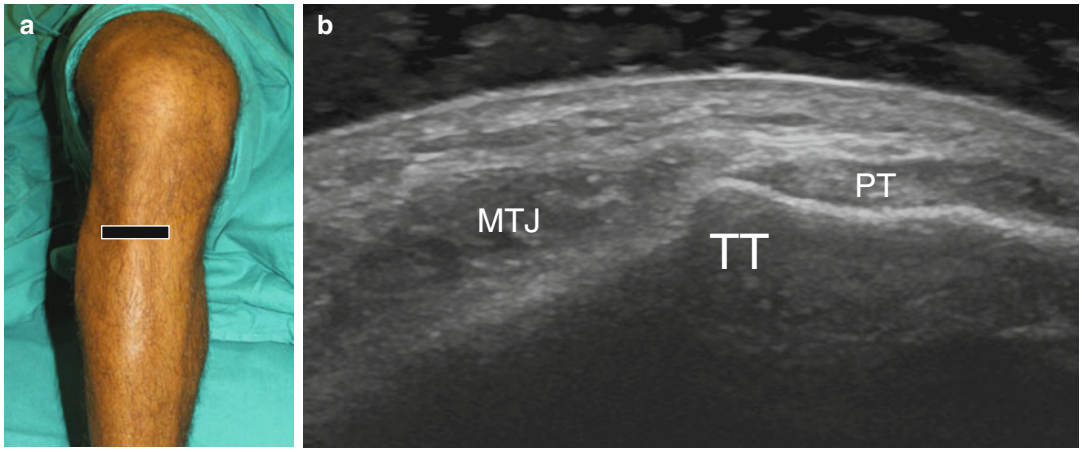

Fig. 17.3 (**a**) Probe position to evaluate the myotendinous junction of the tibialis anterior muscle on axial plane; (**b**) US axial scan: the myotendinous junction (*MJT*) lies lateral to the patellar tendon (*PT*). *TT* tibial tuberosity

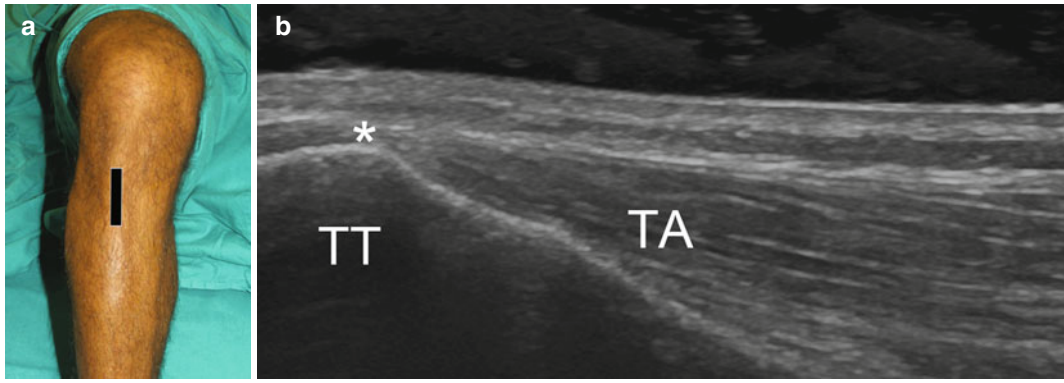

Fig. 17.4 (**a**) Probe position to evaluate the myotendinous junction of the tibialis anterior muscle on longitudinal plane; (**b**) US longitudinal scan shows the myotendinous junction (*) and the proximal insertion of the tibialis anterior (*TA*) on the tibial tuberosity (*TT*)

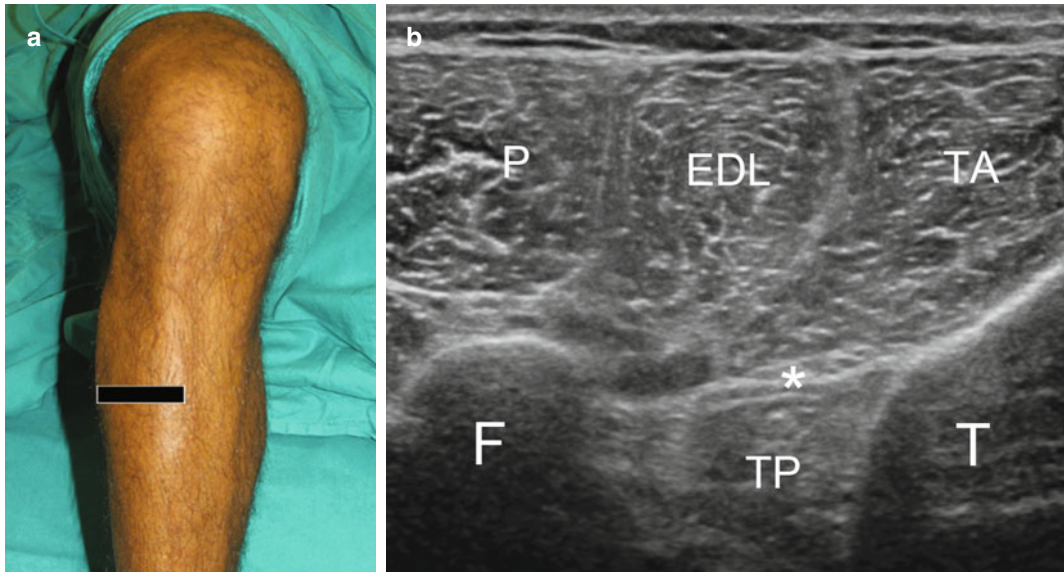

Fig. 17.5 (**a**) Probe position to evaluate the anterior leg compartment at the proximal third of the leg on axial plane. (**b**) US axial scan at the proximal third of the leg illustrates the relationship between the tibialis anterior (*TA*), the extensor digitorum longus (*EDL*) and the peronei muscles (*P*). The interosseous membrane (*) appears as a hyperechoic line, which extends between the tibia (*T*) and the fibula (*F*). *TP* tibialis posterior muscle

This muscle is covered by a thin echogenic fascia (crural fascia) that continues with the anterior fascia of the leg.

A focused evaluation of the integrity of this structure is mandatory if muscle hernia is suspected. A squatting position can be useful to demonstrate the herniation of the muscle and the focal defect of the fascia.

Longitudinal US scan with the probe oriented perpendicular to the skin, in the sagittal plane, is useful to visualize the muscle belly on its long axis. The central aponeurosis appears as a hyperechoic structure that continues from the extra muscular tendon and extends into the muscle dividing in two unipennate halves, above and below the aponeurosis (Fig. 17.8).

At this level, we can measure the muscular thickness and pennation angle (see Chap. 4).

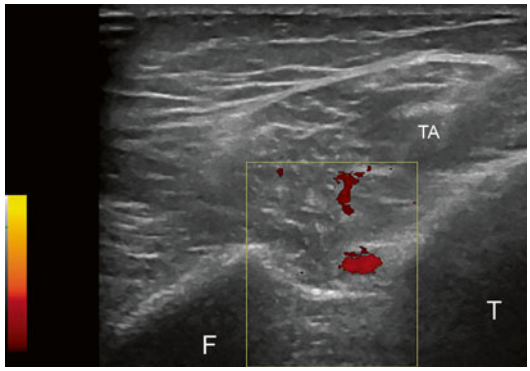

Fig. 17.6 US axial scan at the proximal third of the leg. Power Doppler is useful to identify the anterior tibial artery at the level of the interosseous membrane. *TA* tibialis anterior muscle, *T* tibia, *F* fibula

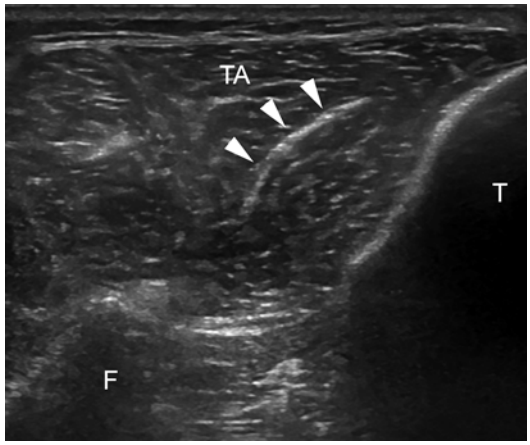

Fig. 17.7 US axial scan at the proximal third of the leg. Note the large muscular belly of the tibialis anterior muscle (*TA*) and the thick central aponeurosis (*arrowheads*). *T* tibia, *F* fibula

Ask the patient to contract the muscle with dorsiflexion of the foot to evaluate the increasing of the pennation angle.

Always remember to move the transducer caudally following the tibialis anterior muscle belly until the myotendinous junction (Figs. 17.9 and 17.10).

Then place the transducer on the proximal middle third of the tibial shaft and shift the probe laterally to examine the extensor digitorum longus muscle belly on an axial scan. In this scan, the extensor digitorum longus muscle is located laterally to the tibialis anterior muscle (Fig. 17.5).

Then move the transducer caudally, always in a transversal plane, until the middle of the leg to visualize the extensor hallucis longus muscle which arises at this level (Fig. 17.11).

If the extensor hallucis longus and the extensor digitorum longus muscles are not well separated, an active or passive muscular contraction can be helpful to distinguish them.

Always remember to move the transducer caudally following the extensor digitorum longus and the extensor hallucis longus muscle bellies until the myotendinous junction (Figs. 17.12 and 17.13).

Rotate the probe by 90° to assess the internal structure of each muscle belly (Fig. 17.14).

Place the transducer over the dorsum of the ankle to examine the extensor tendon group in the axial plane. In this scan, it is possible to visualize, from medial to lateral, the tibialis anterior, the extensor hallucis longus and the extensor digitorum longus tendons. Always examine these structures from the myotendinous junction to their distal insertion (Fig. 17.15).

At this level, also examine the deep peroneal nerve, which runs on the medial side of the anterior tibial artery (Fig. 17.16).

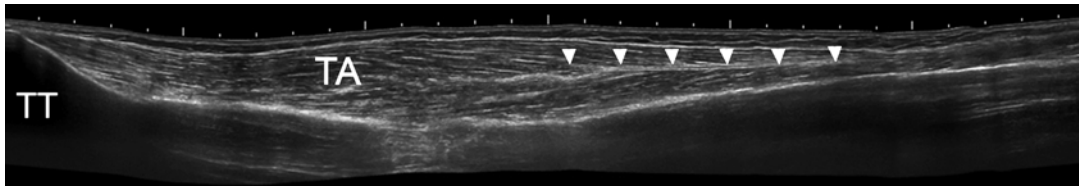

Fig. 17.8 EFV US longitudinal scan of the tibialis anterior muscle (*TA*) from the tibial tuberosity (*TT*). Note the thick central aponeurosis (*arrowheads*) that appears as a hyperechoic structure into the muscular belly

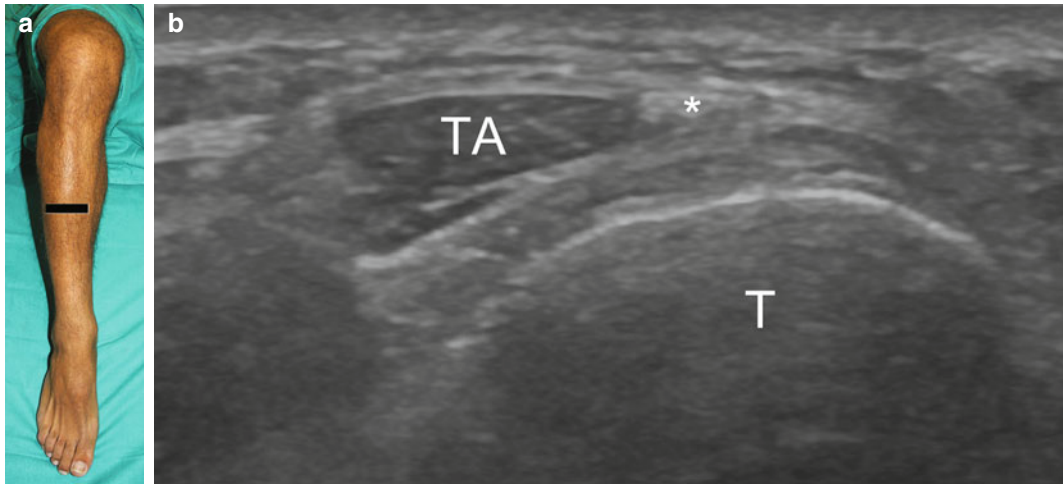

Fig. 17.9 (**a**) Probe position to evaluate the myotendinous junction of tibialis anterior muscle (*TA*) on an axial scan. (**b**) US axial scan of the myotendinous junction (*) of TA. *T* tibia

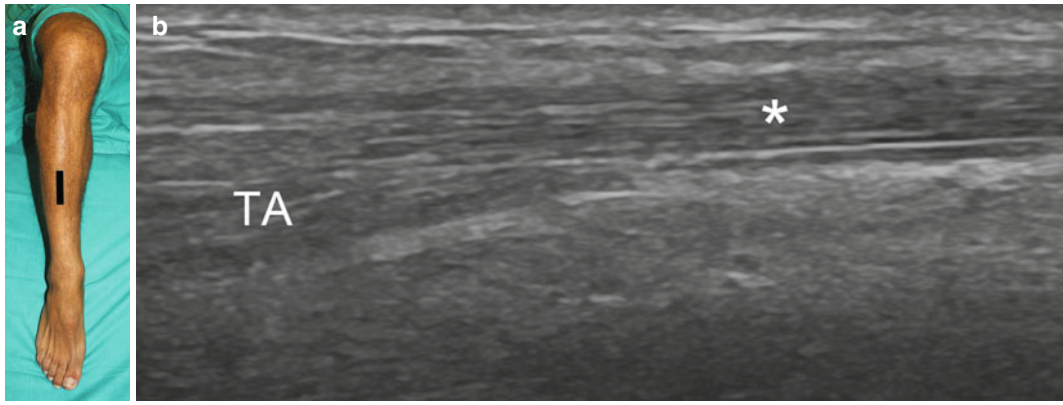

Fig. 17.10 (**a**) Probe position to evaluate the myotendinous junction of the tibialis anterior muscle (*TA*) on a longitudinal scan. (**b**) US longitudinal scan of the myotendinous junction (*) of TA

Focus On

The *deep peroneal nerve (deep fibular nerve)* originates from the common fibular nerve near the neck of the fibula, between the fibula and upper part of the peroneus longus.

The deep fibular nerve travels in the anterior compartment of the leg on the anterior surface of the interosseous membrane.

It passes inferomedially, deep to extensor digitorum longus and, at the middle of the leg, comes in relation with the anterior tibial artery.

It runs initially lateral to the anterior tibial artery, but in proximity of the ankle joint it crosses over to run on the medial side.

At this level, the extensor hallucis longus muscle and tendon and the inferior

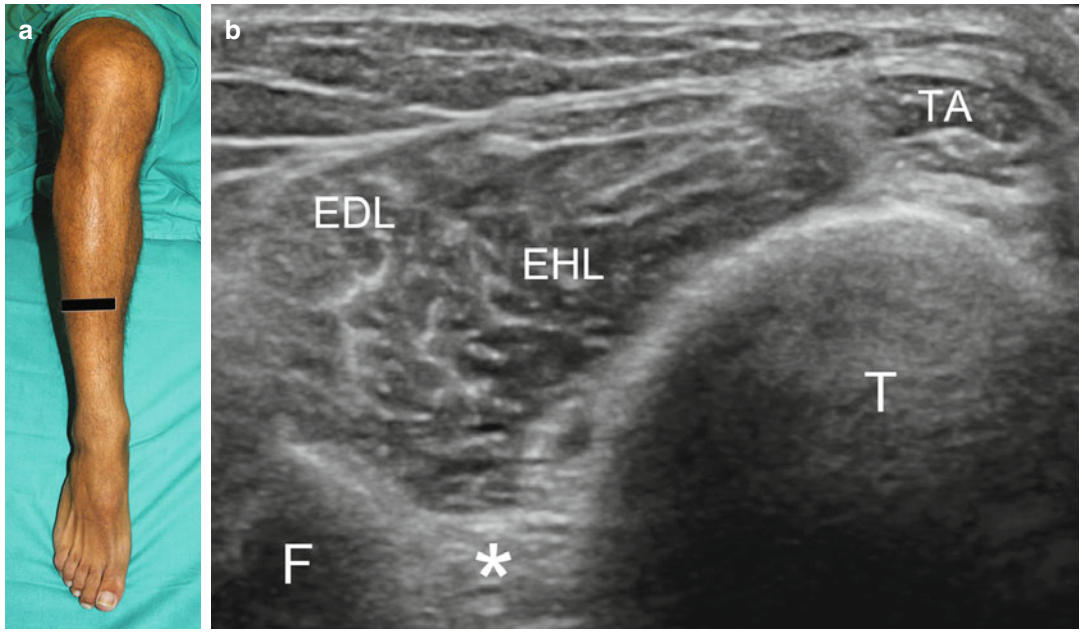

Fig. 17.11 (**a**) Probe position to evaluate the anterior leg compartment at the distal third of the leg on axial plane. (**b**) US axial scan at the distal third of the leg. At this level, the myotendinous junction of the tibialis anterior (*TA*) may be evaluated. The extensor hallucis longus muscle (*EHL*) lies between the myotendinous junction of the tibialis anterior (*TA*) and the extensor digitorum longus muscle (*EDL*) belly. *T* tibia, *F* fibula, * interosseous membrane

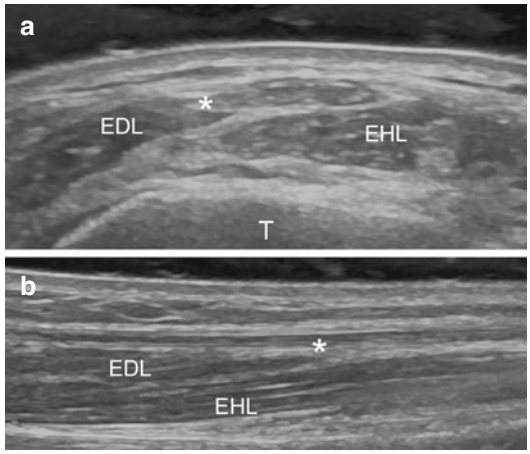

Fig. 17.12 (**a**) US axial scan of the myotendinous junction (*) of the extensor digitorum longus (*EDL*) muscle (**b**) US longitudinal scan of the myotendinous junction (*) of the extensor digitorum longus (*EDL*) muscle. *EHL* extensor hallucis longus muscle

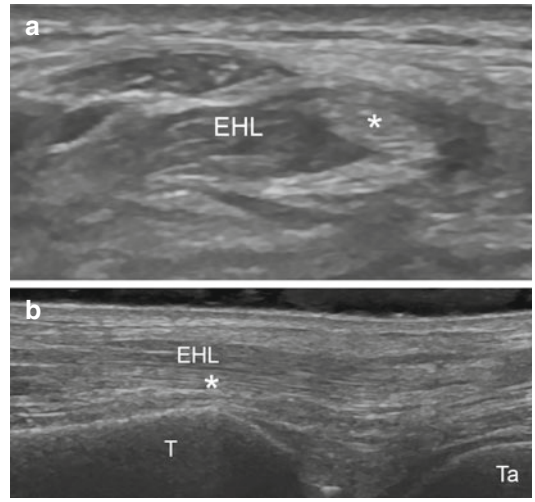

Fig. 17.13 (**a**) US axial scan of the myotendinous junction (*) of the extensor hallucis longus (*EHL*) muscle (**b**) US longitudinal scan of the myotendinous junction (*) of the extensor hallucis longus (*EHL*) muscle. *T* tibia, *Ta* talus

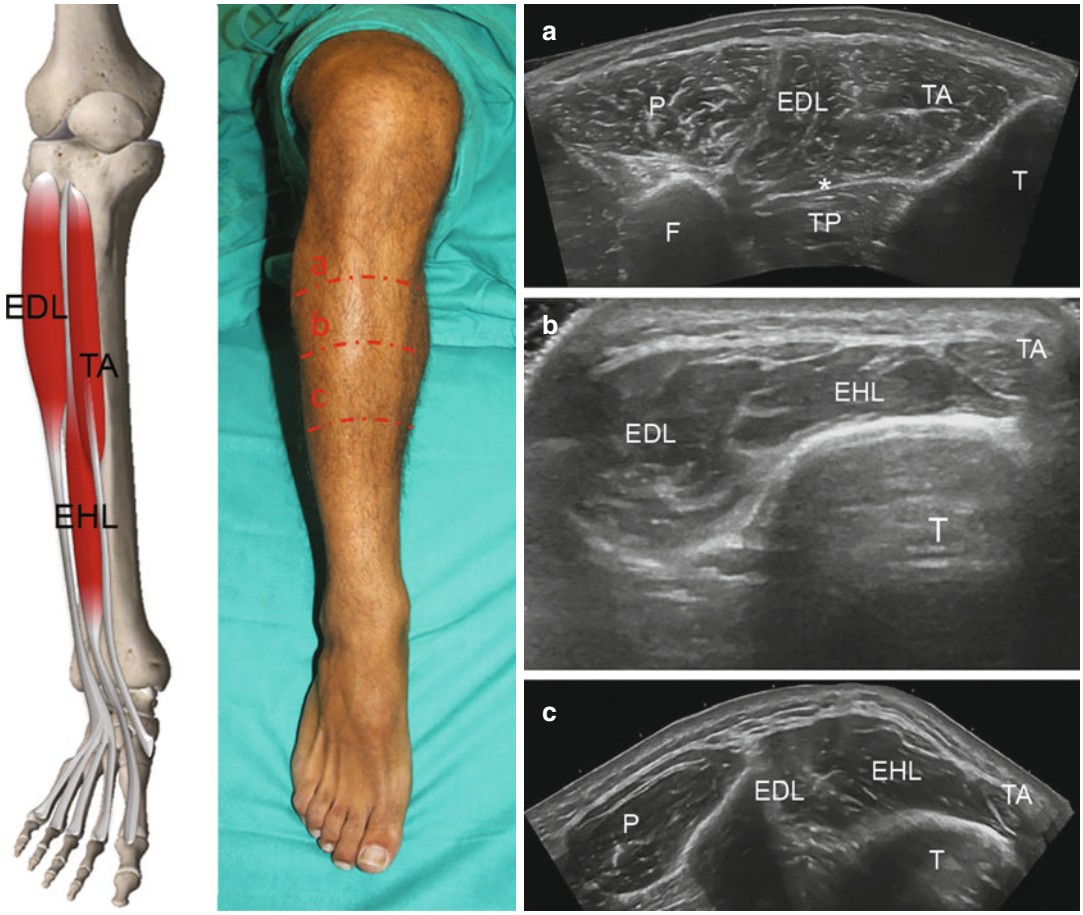

Fig. 17.14 Anatomical scheme correlated to *EFV* US axial scans at different levels of the anterior compartment of leg muscles. (**a**) Proximal anterior compartment. EFV axial scan visualizes the relationship between the peroneus muscles (*P*) and the extensor muscles. The tibialis anterior muscle (*TA*) lies just lateral to the tibial crest and medial to the extensor digitorum longus muscle (*EDL*). The interosseous membrane (*) appears as a hyperechoic layer which separates *TA* from the tibialis posterior muscle (*TP*). (**b**) Middle third of leg anterior compartment. *EFV* axial scan shows *TA* myotendinous junction with its oval tendon anterior to the tibial edge. Note the *EDL* and extensor hallucis longus (*EHL*) muscle bellies. (**c**) Distal anterior compartment of the leg. *EFV* US axial scan evaluates the relationship between the peroneus muscle (*P*) and the extensor muscle at the distal third of the leg. The peroneus brevis and peroneus longus are not well separated. *T* tibia, *F* fibula

extensor retinaculum overly ventrally the nerve that passes through the anterior tarsal tunnel (the space located between the inferior extensor retinaculum and the fascia overlying the talus and the navicular bones).

Just under the inferior extensor retinaculum, the deep peroneal nerve divides into lateral and medial terminal branches.

The lateral terminal branch (external branch) passes across the tarsus anterolaterally and supplies the extensor digitorum brevis and the extensor hallucis brevis muscles. From the enlargement, it gives three small interosseous branches (dorsal interosseous nerves) for the innervation of the tarsal joints and the metatarsophalangeal joints of the second, third and fourth toes.

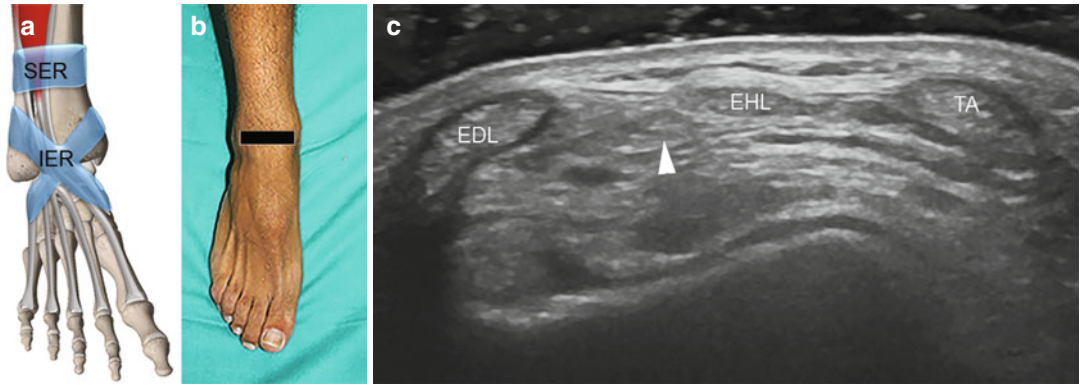

Fig. 17.15 (**a**) Anatomical scheme of the extensor tendon group and extensor retinacula. *SER* superior extensor retinaculum, *IER* inferior extensor retinaculum. (**b**) Probe position to evaluate the extensor tendon group in the axial plane. (**c**) US axial scan of the extensor tendon group. *TA* tibialis anterior tendon, *EDL* extensor digitorum longus tendon, *EHL* extensor hallucis longus tendon, *arrow* deep peroneal nerve

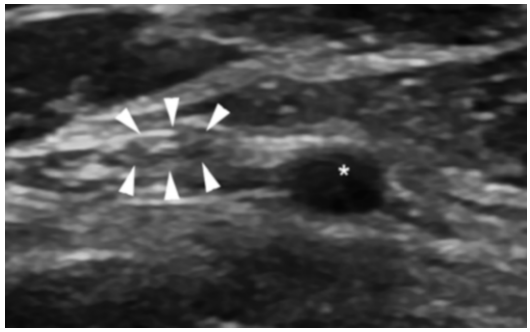

Fig. 17.16 US axial scan of the deep peroneal nerve (*arrowheads*) at the level of the ankle joint. * anterior tibial artery

The medial terminal branch (internal branch) travels medial to the dorsalis pedis artery along the dorsum of the foot. At the first interosseous space, it divides into dorsal digital nerves, which provide sensory innervation to the first webspace and the adjacent dorsum of the foot between the first and second toes.

The deep fibular nerve provides motor innervation to the muscles of the anterior compartment of the leg, the tibialis anterior, extensor digitorum longus, extensor hallucis longus and peroneus tertius muscles.

It also provides sensory innervation to the webspace between the hallux and second digit.

Injury to the deep fibular nerve typically produces loss of dorsiflexion of the foot (foot drop), loss of extension of the toes and loss of sensation in the first webspace.

Complete the examination with dynamics scans in order to evaluate muscles and tendons also during contraction.

Evaluate also the integrity of the superior and inferior extensor retinacula and the relationship between tendons and tibial bony surface at this level (Figs. 17.17 and 17.18).

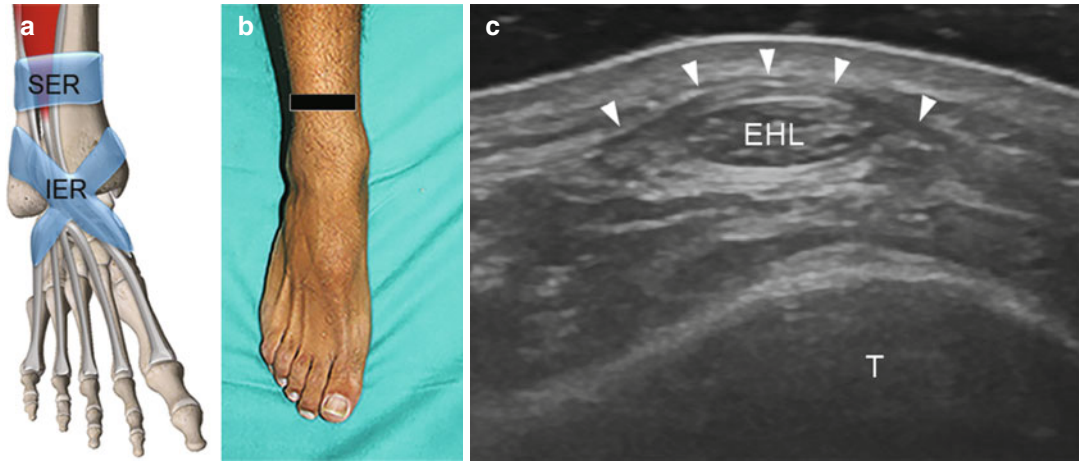

Fig. 17.17 (**a**) Anatomical scheme of the extensor tendon group and extensor retinacula. *SER* superior extensor retinaculum, *IER* inferior extensor retinaculum. (**b**) Probe position to evaluate the superior extensor retinaculum at the level of the extensor hallucis longus tendon. (**c**) US axial scan of the superior extensor retinaculum (*arrowheads*) at the level of the extensor hallucis longus (*EHL*) tendon

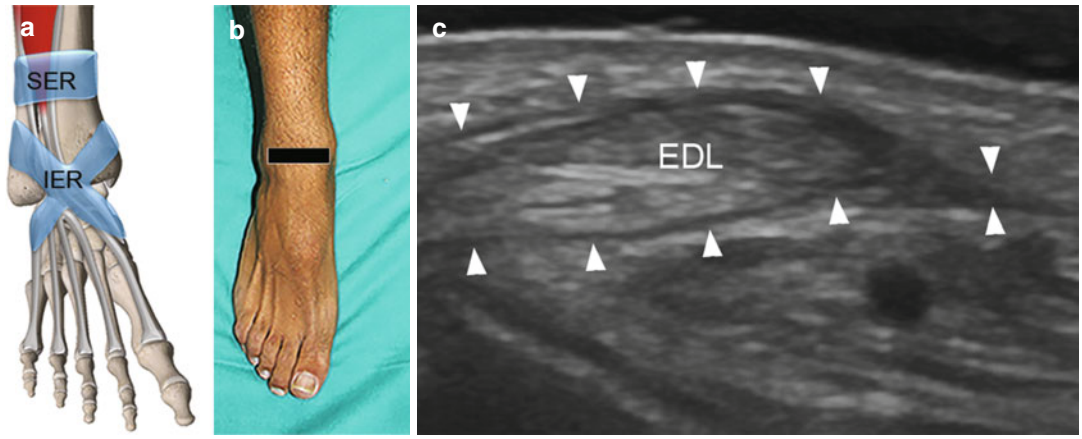

Fig. 17.18 (**a**) Anatomical scheme of the extensor tendon group and extensor retinacula. *SER* superior extensor retinaculum, *IER* inferior extensor retinaculum. (**b**) Probe position to evaluate the inferior extensor retinaculum at the level of the extensor digitorum longus tendon. (**c**) US axial scan of the superior inferior extensor retinaculum (*arrowheads*) at the level of the extensor digitorum longus tendon (*EDL*)

17.3 Summary Table

Muscle	Origin	Insertion	Innervation	Action
Tibialis anterior	Lateral surface of the tibia and neighbouring interosseous membrane in the upper leg	Dorsal aspect of the first metatarsal and medial surface of the medial cuneiform	Deep fibular nerve	Dorsiflexion and inversion of the foot
Extensor hallucis longus	Distal aspect of the fibula and interosseous membrane	Distal phalanx of the first toe	Deep fibular nerve	Extension of the big toe and assists in dorsiflexion of the foot at the ankle
Extensor digitorum longus	Inferior aspect of lateral tibial condyle, anterior surface of the interosseous membrane and medial face of fibula	Distal phalanges of the second through fifth toes	Deep fibular nerve	Extension of toes and dorsiflexion of ankle

Suggested Reading

Bianchi S, Martinoli C (2009) US of the musculoskeletal system. Springer, Berlin

Drake RL, Vogl W, Mitchell AWM (2005) Grey's anatomy. Elsevier/Churchill Livingstone, Philadelphia

Gokhale S (2007) Three-dimensional sonography of muscle hernias. J Ultrasound Med 26:239–242

Jerome JTJ, Varghese M, Thirumagal K (2008) Tibialis Anterior Rupture: a missed diagnosis. Foot Ankle Online J 3(9):2

Lieber RL, Fridén J (2000) Functional and clinical significance of skeletal muscle architecture. Muscle Nerve 23(11):1647–1666

Maganaris CN, Baltzopoulos V, Sargeant AJ (1998) Changes in the tibialis anterior tendon moment arm from rest to maximum isometric dorsiflexion: in vivo observations in man. Clin Biomech 14:661–666

Maganaris CN, Kawakami Y, Fukunaga T (2001) Changes in aponeurotic dimensions upon muscle shortening: in vivo observations in man. J Anat 199:449–456

Nakhostine M, Styf JR, van Leuven S, Hargens AR, Gershuni DH (1993) Intramuscular pressure varies with depth. The tibialis anterior muscle studied in 12 volunteers. Acta Orthop Scad 64(3):377–381

Peer S, Kovacs P, Harpf C, Bodner G (2002) High-resolution sonography of lower extremity peripheral nerves anatomic correlation and spectrum of disease. J Ultrasound Med 21:315–322

Pillen S (2010) Skeletal muscle ultrasound. Eur J Transl Myol 1(4):145–155

Reneman RS (1975) The anterior and the lateral compartmental syndrome of the leg due to intensive use of muscles. Clin Orthop Relat Res 113:69–80

Silvestri E, Muda A, Sconfienza LM (2012) Normal ultrasound anatomy of the musculoskeletal system. Springer, Milan/New York

Stoller DW (2007) Stoller's atlas of orthopaedics and sports medicine. Lippincott Williams & Wilkins, Philadelphia

Styf JR, Korner LM (1987) Diagnosis of chronic anterior compartment syndrome in the lower leg. Acta Orthop Scand 58(2):139–144

Part IV

Sectional Anatomical Tables

Thigh Compartments

18

Enzo Silvestri and Claudio Mazzola

In this chapter we provide a series of images demonstrating cross-sectional anatomy of thigh compartments at different cranio-caudal levels. Every set of images includes a skeleton model that serves as an orientation aid (a), pertinent anatomical scheme (b), and corresponding SE T1w axial MRI scan (c).

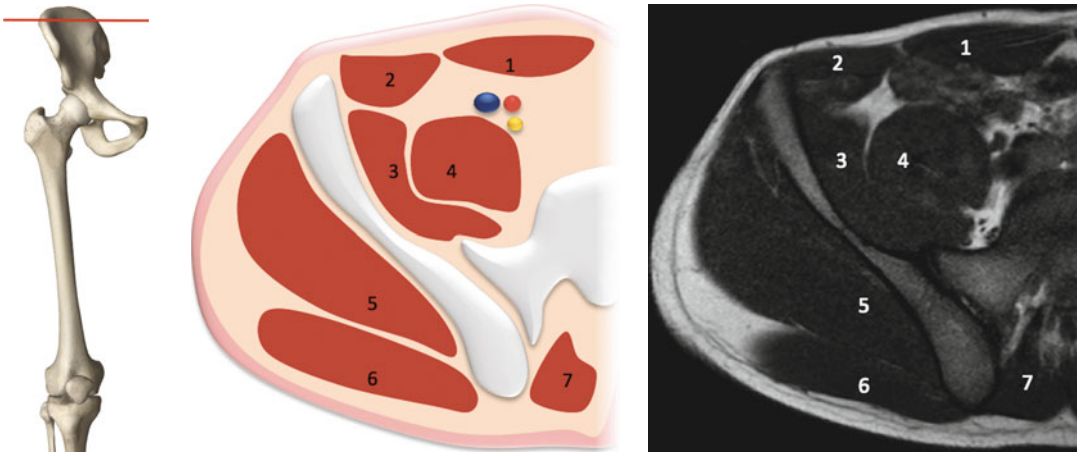

Fig. 18.1 *1* rectus abdomminis; *2* obliquus abdominis; *3* iliacus; *4* psoas major; *5* gluteus medius; *6* gluteus maximus; *7* erector spinae

E. Silvestri (✉)
Struttura Complessa di Diagnostica per Immagini ed Ecografia Interventistica, Ospedale Evangelico Internazionale, Genoa, Italy
e-mail: silvi.enzo@gmail.com

C. Mazzola
Dipartimento di Ortopedia e Chirurgia delle Articolazioni, EO Ospedali Galliera, Genoa, Italy

E. Silvestri et al., *Ultrasound Anatomy of Lower Limb Muscles: A Practical Guide*,
DOI 10.1007/978-3-319-09480-9_18,

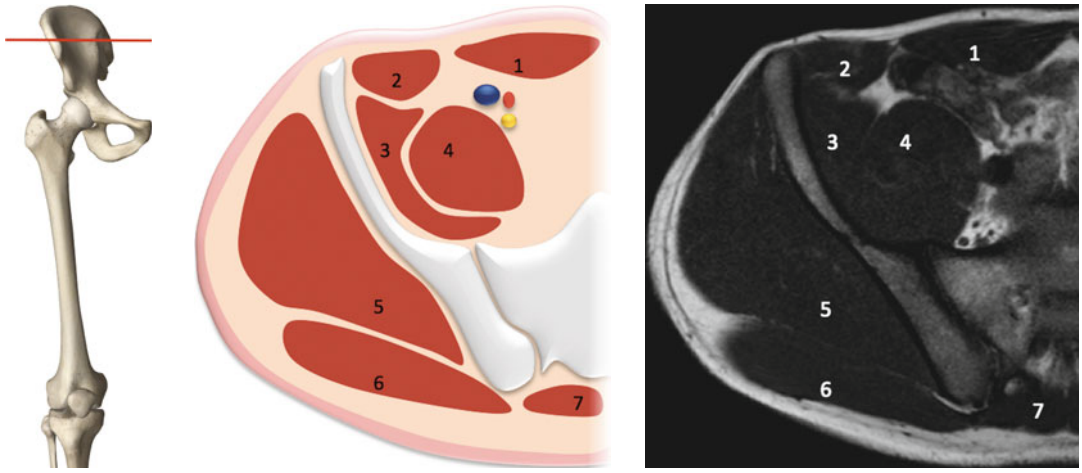

Fig. 18.2 *1* rectus abdomminis; *2* obliquus abdominis; *3* iliacus; *4* psoas major; *5* gluteus medius; *6* gluteus maximus; *7* erector spinae

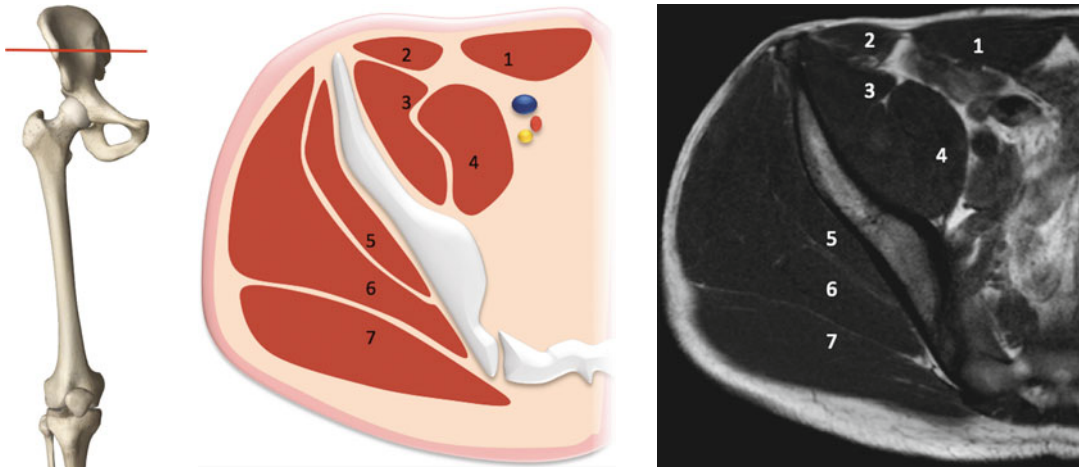

Fig. 18.3 *1* rectus abdomminis; *2* obliquus abdominis; *3* iliacus; *4* psoas major; *5* gluteus minimus; *6* gluteus medius; *7* gluteus maximus

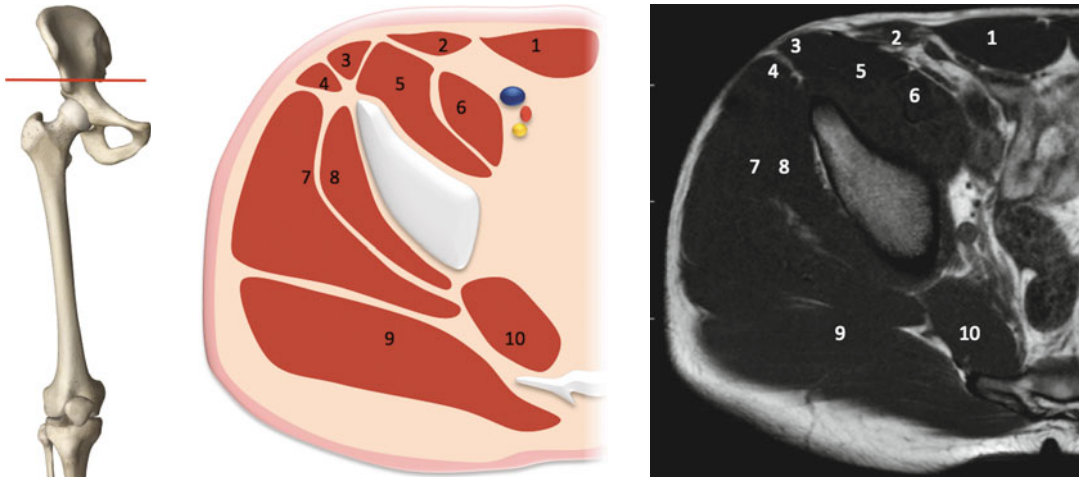

Fig. 18.4 *1* rectus abdomminis; *2* obliquus; *3* sartorius; *4* tensor fasciae latae; *5* iliacus; *6* psoas major; *7* gluteus medius; *8* gluteus minimus; *9* gluteus maximus; *10* piriformis

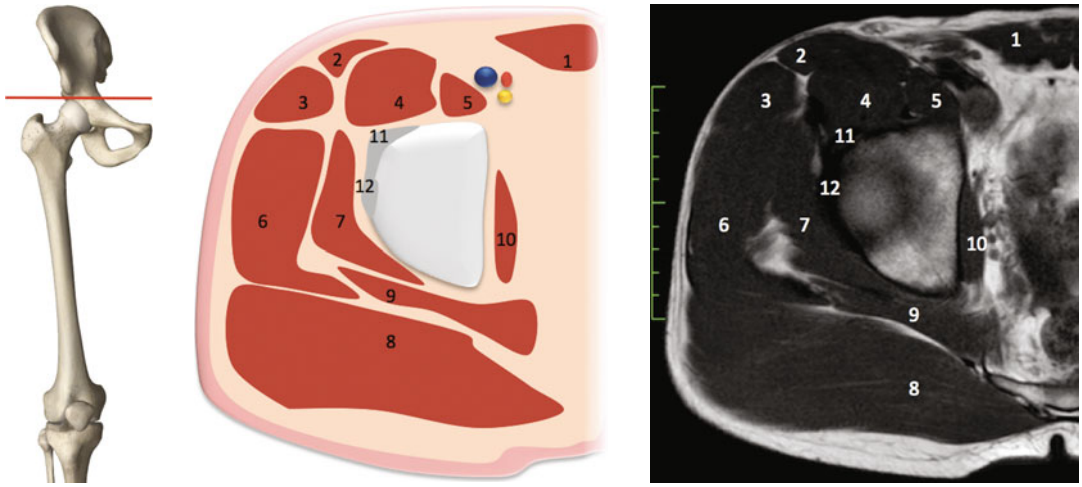

Fig. 18.5 *1* rectus abdominis; *2* sartorius; *3* tensor fasciae latae; *4* iliacus; *5* psoas major; *6* gluteus medius; *7* gluteus minimus; *8* gluteus maximus; *9* piriformis; *10* obturator internus; *11* direct tendon (rectus femoris); *12* indirect tendon (rectus femoris)

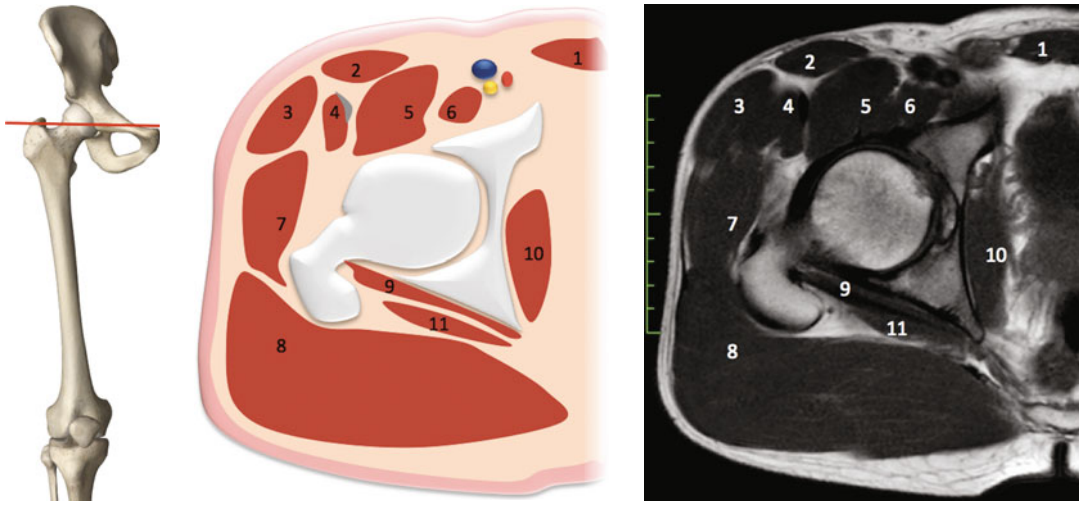

Fig. 18.6 *1* rectus abdominis; *2* sartorius; *3* tensor fasciae latae; *4* rectus femoris; *5* iliacus; *6* psoas major; *7* gluteus medius; *8* gluteus maximus; *9* obturator internus; *10* gemellus superior; *11* piriformis

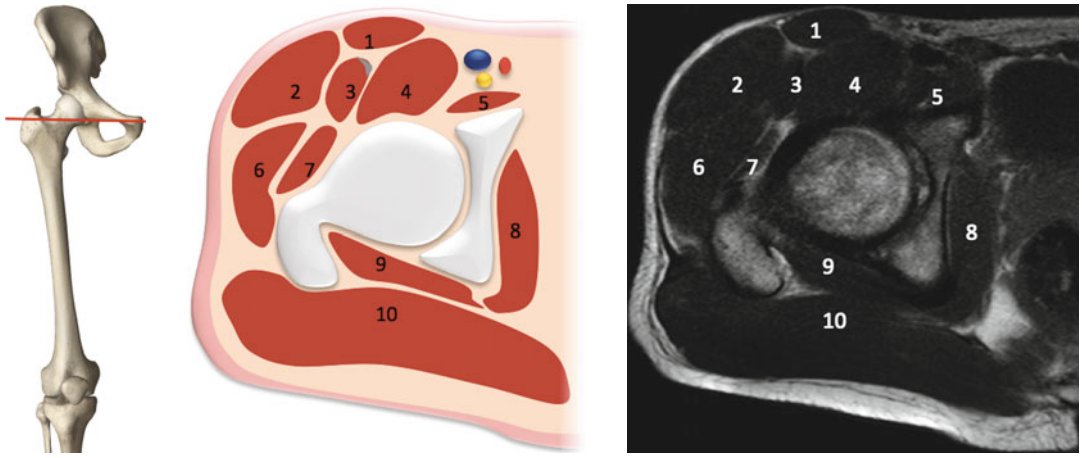

Fig. 18.7 *1* sartorius; *2* tensor fascia lata; *3* rectus femoris; *4* iliopsoas; *5* pectineus; *6* gluteus minimus and medius; *7* vastus lateralis; *8* obturator internus; *9* Gemellus superior; *10* gluteus maximus

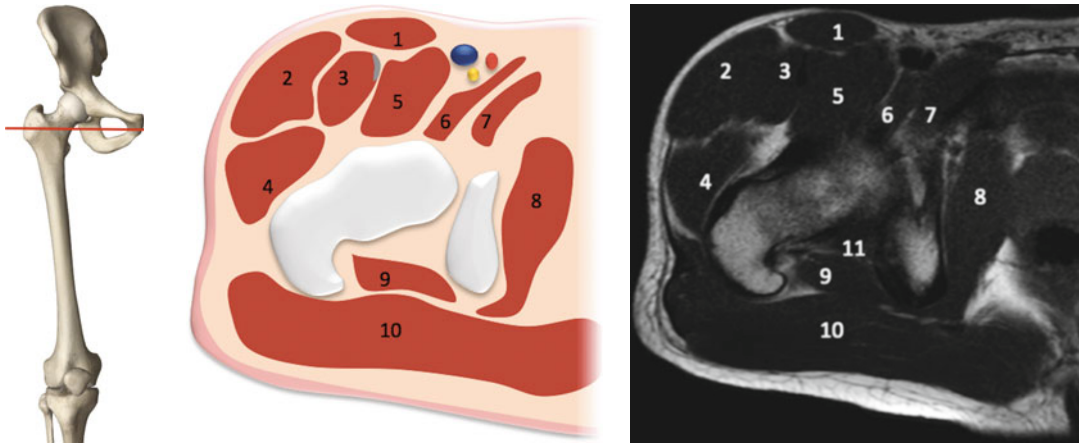

Fig. 18.8 *1* sartorius; *2* tensor fasciae latae; *3* rectus femoris; *4* vastus lateralis; *5* iliopsoas; *6* pectineus; *7* adductor brevis; *8* obturator internus; *9* quadratus femoris; *10* gluteus maximus

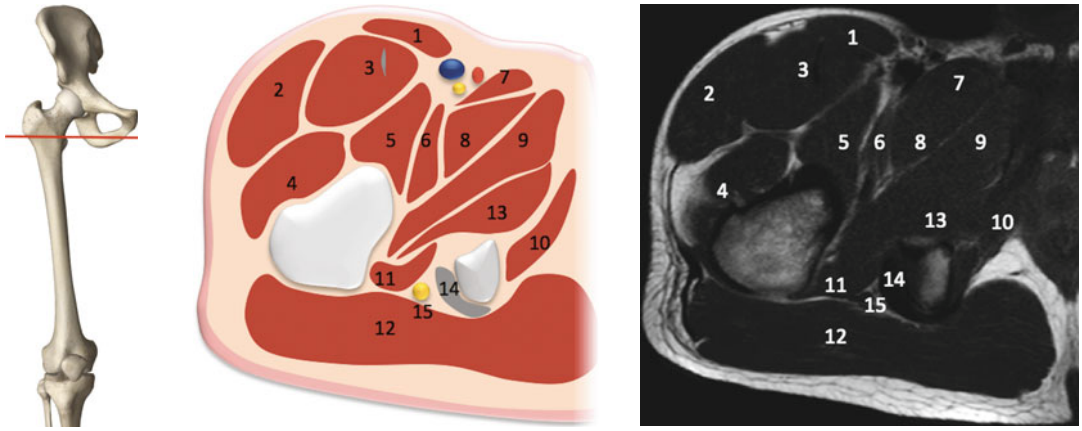

Fig. 18.9 *1* sartorius; *2* tensor fasciae latae; *3* rectus femoris; *4* vastus lateralis; *5* iliopsoas; *6* pectineus; *7* adductor longus; *8* adductor brevis; *9* adductor magnus; *10* obturator internus; *11* quadratus femoris; *12* gluteus maximus; *13* obturator externus; *14* hamstrings proximal tendon insertion; *15* ischiatic nerve

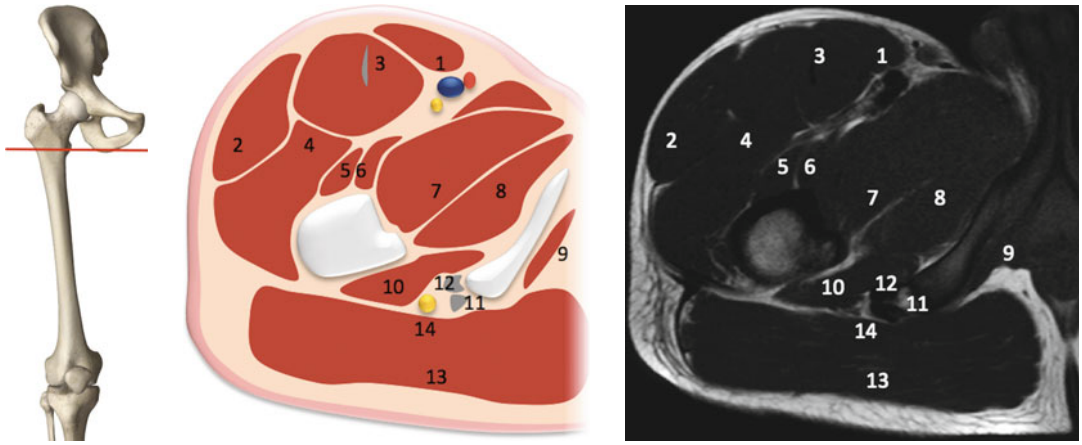

Fig. 18.10 *1* sartorius; *2* tensor fasciae latae; *3* rectus femoris; *4* vastus lateralis; *5* vastus intermedius; *6* pectineus; *7* adductor brevis; *8* adductor magnus; *9* obturator internus; *10* quadratus femoris; *11* hamstrings conjoint tendon; *12* semimembranosus tendon; *13* gluteus maximus; *14* ischiatic nerve

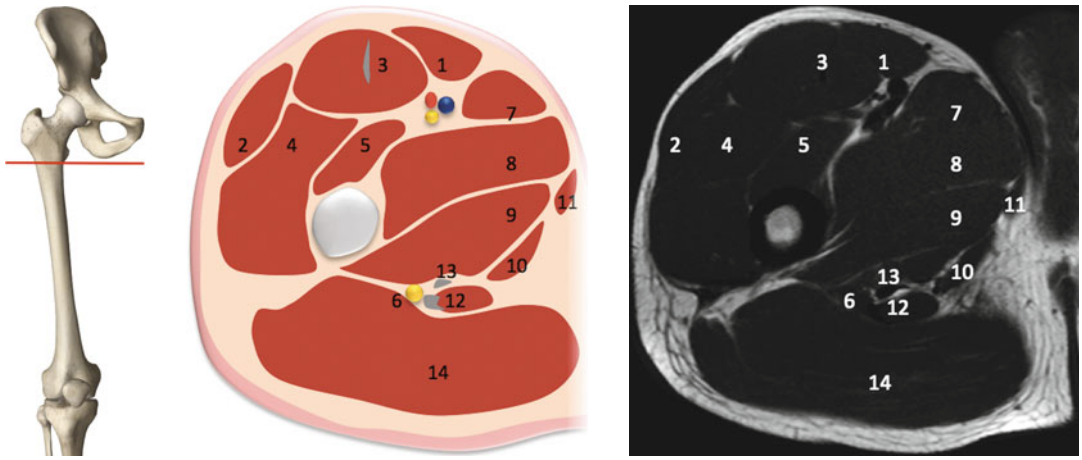

Fig. 18.11 *1* sartorius; *2* tensor fasciae latae; *3* rectus femoris; *4* vastus lateralis; *5* vastus intermedius; *6* ischiatic nerve; *7* adductor longus; *8* adductor brevis; *9* adductor magnus; *10* adductor magnus; *11* gracilis; *12* semitendinosus muscle and conjoint tendon; *13* semimembranosus tendon; *14* gluteus maximus

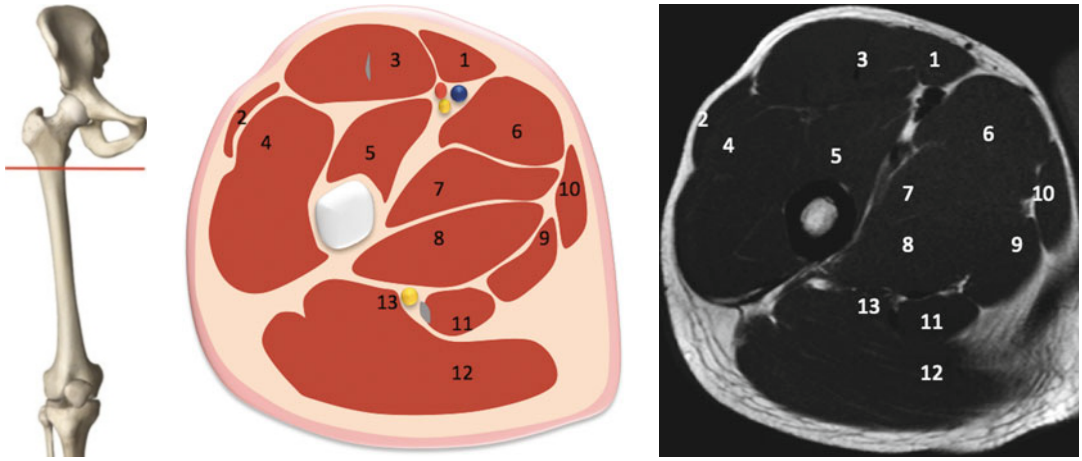

Fig. 18.12 *1* sartorius; *2* tensor fasciae latae; *3* rectus femoris; *4* vastus lateralis; *5* vastus intermedius; *6* adductor longus; *7* adductor brevis; *8* adductor magnus; *9* adductor magnus; *10* gracilis; *11* semitendinosus; *12* gluteus maximus; *13* ischiatic nerve

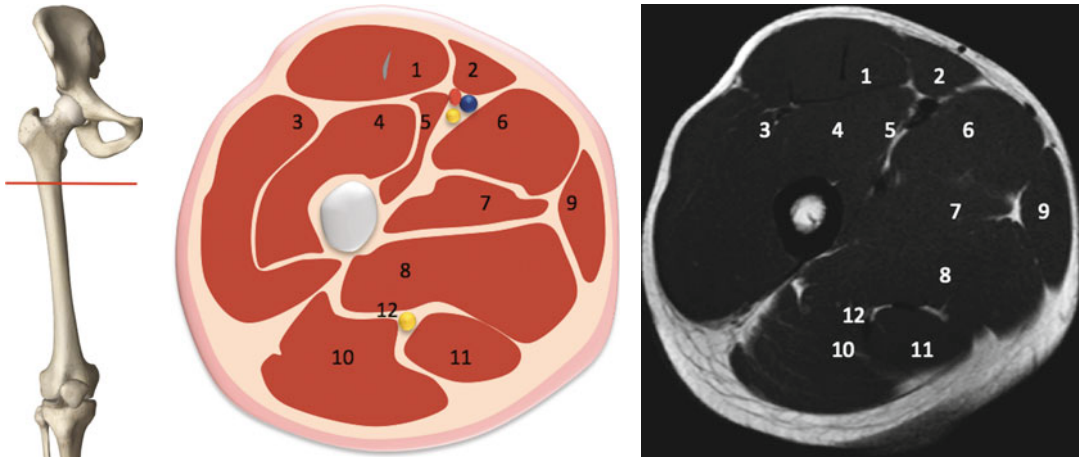

Fig. 18.13 *1* rectus femoris; *2* sartorius; *3* vastus lateralis; *4* vastus intermedius; *5* vastus medialis; *6* adductor longus; *7* adductor brevis; *8* adductor magnus; *9* gracilis; *10* gluteus maximus; *11* semitendinosus; *12* ischiatic nerve

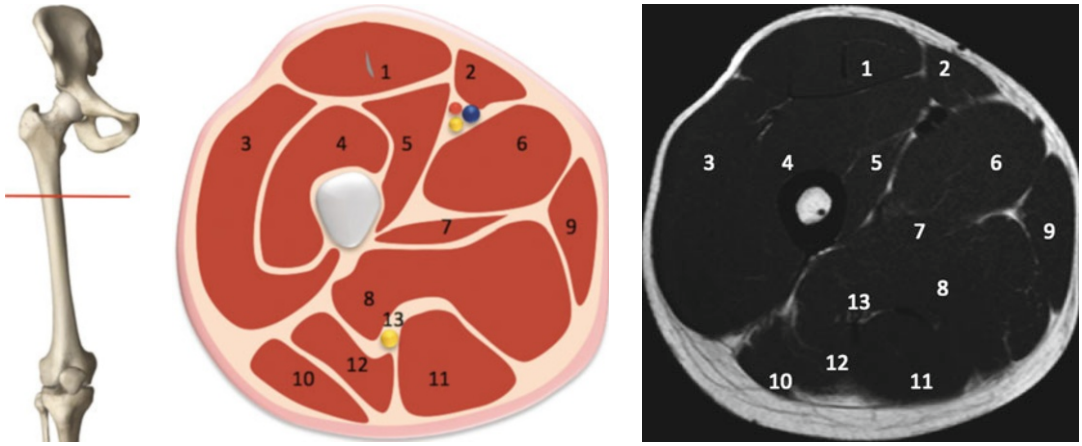

Fig. 18.14 *1* rectus femoris; *2* sartorius; *3* vastus lateralis; *4* vastus intermedius; *5* vastus medialis; *6* adductor longus; *7* adductor brevis; *8* adductor magnus; *9* gracilis; *10* gluteus maximus; *11* semitendinosus; *12* biceps femoris; *13* ischiatic nerve

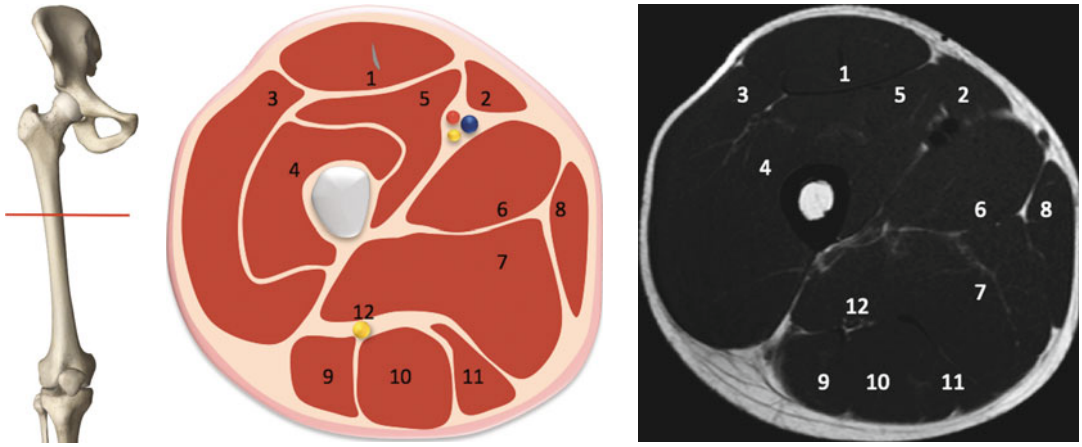

Fig. 18.15 *1* rectus femoris; *2* sartorius; *3* vastus lateralis; *4* vastus intermedius; *5* vastus medialis; *6* adductor longus; *7* adductor magnus; *8* gracilis; *9* biceps femoris; *10* semitendinosus; *11* semimembranosus; *12* ischiatic nerve

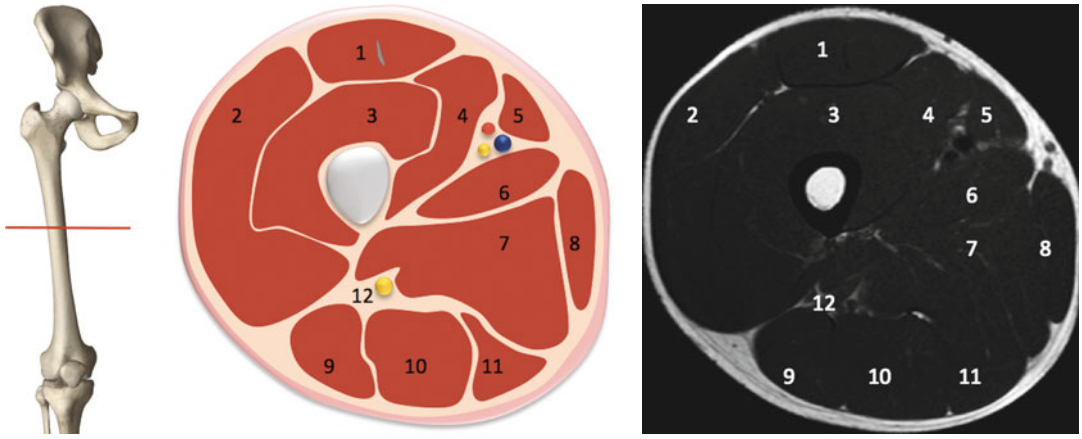

Fig. 18.16 *1* rectus femoris; *2* vastus lateralis; *3* vastus intermedius; *4* vastus intermedius; *5* sartorius; *6* adductor longus; *7* adductor magnus; *8* gracilis; *9* biceps femoris; *10* semitendinosus; *11* semimembranosus; *12* ischiatic nerve

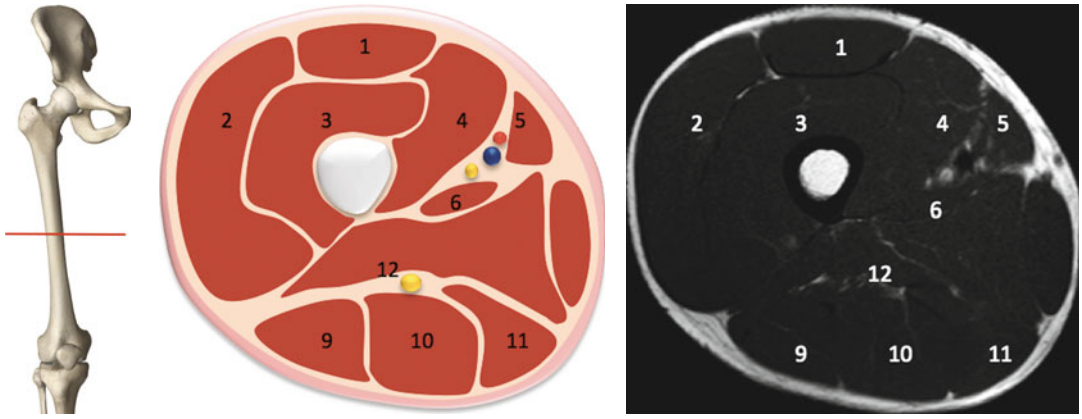

Fig. 18.17 *1* rectus femoris; *2* vastus lateralis; *3* vastus intermedius; *4* vastus intermedius; *5* sartorius; *6* adductor longus; *7* adductor magnus; *8* gracilis; *9* biceps femoris; *10* semitendinosus; *11* semimembranosus; *12* ischiatic nerve

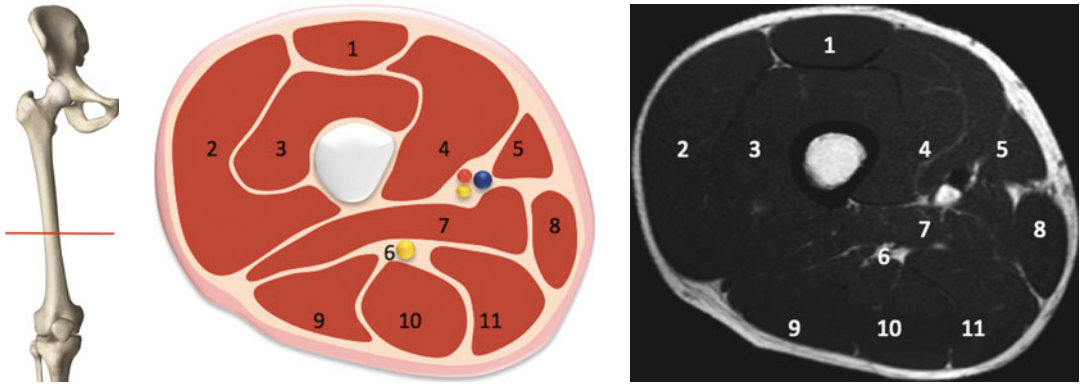

Fig. 18.18 *1* rectus femoris; *2* vastus lateralis; *3* vastus intermedius; *4* vastus medialis; *5* sartorius; *6* ischiatic nerve; *7* adductor magnus; *8* gracilis; *9* biceps femoris; *10* semitendinosus; *11* semimembranosus

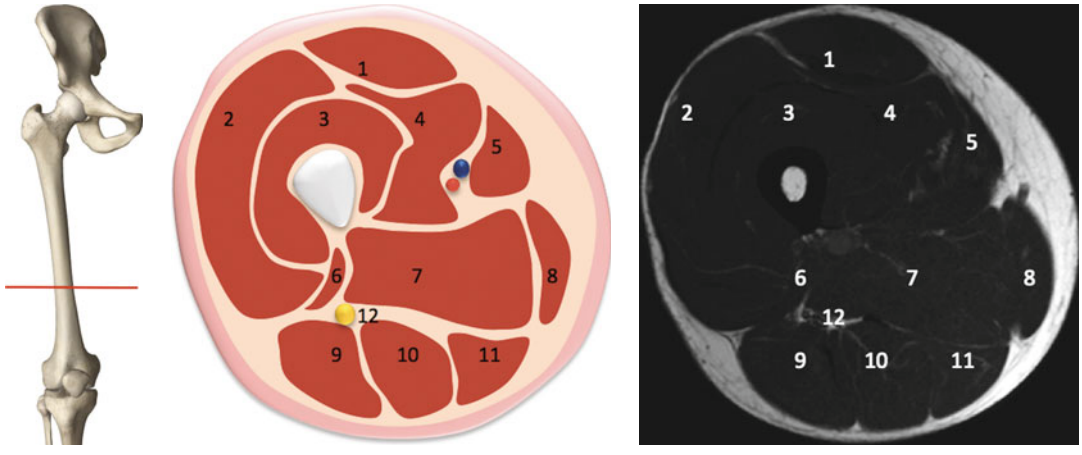

Fig. 18.19 *1* rectus femoris; *2* vastus lateralis; *3* vastus intermedius; *4* vastus medialis; *5* sartorius; *6* biceps femoris (*short head*); *7* adductor magnus; *8* gracilis; *9* biceps femoris (*long head*); *10* semitendinosus; *11* semimembranosus; *12* ischiatic nerve

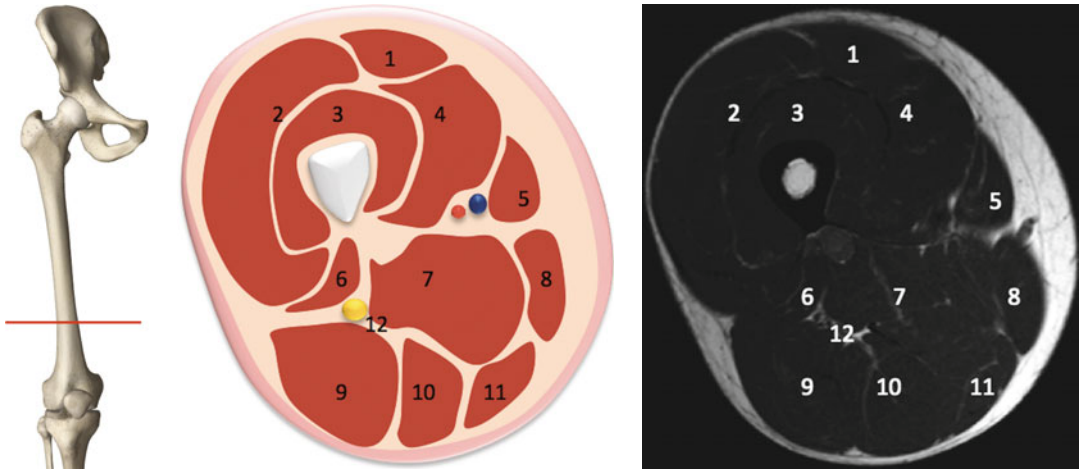

Fig. 18.20 *1* rectus femoris; *2* vastus lateralis; *3* vastus intermedius; *4* vastus medialis; *5* sartorius; *6* biceps femoris (*short head*); *7* adductor magnus; *8* gracilis; *9* biceps femoris (*long head*); *10* semitendinosus; *11* semimembranosus; *12* ischiatic nerve

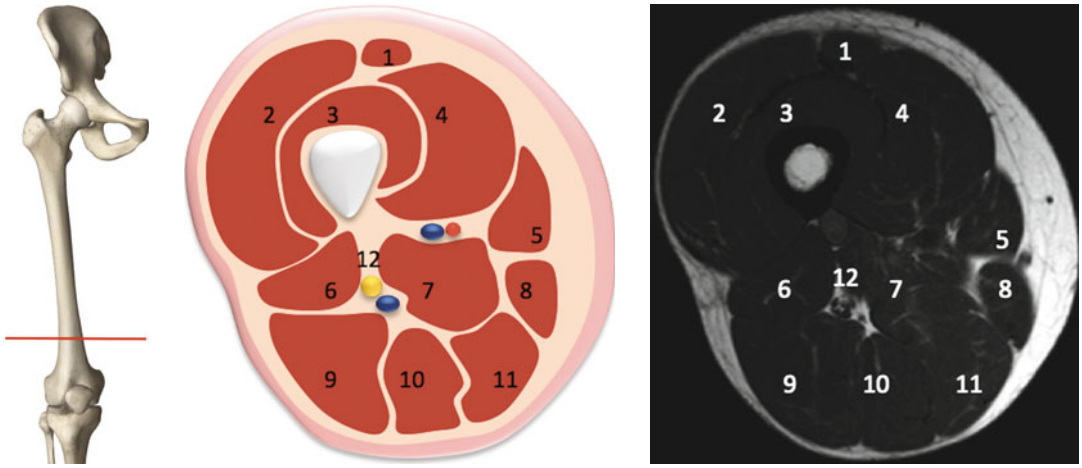

Fig. 18.21 *1* rectus femoris; *2* vastus lateralis; *3* vastus intermedius; *4* vastus medialis; *5* sartorius; *6* biceps femoris (*short head*); *7* adductor magnus; *8* gracilis; *9* biceps femoris (*long head*); *10* semitendinosus; *11* semimembranosus; *12* ischiatic nerve

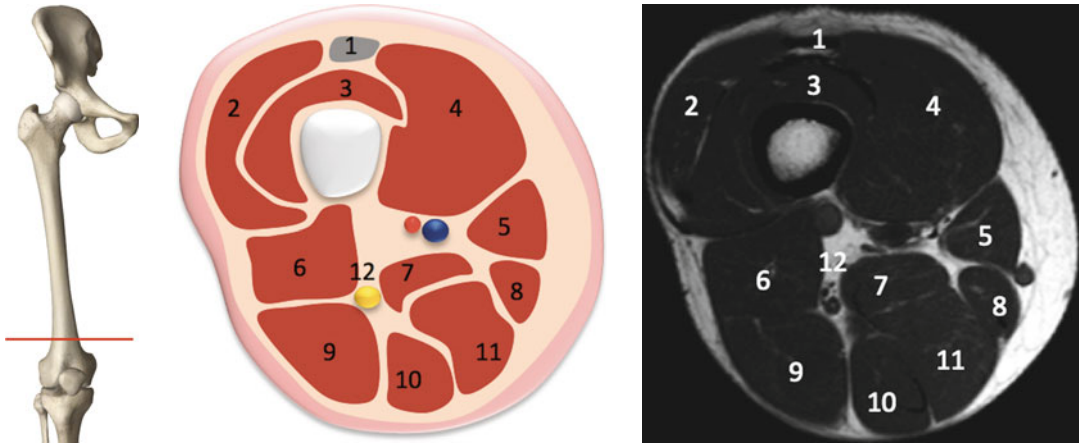

Fig. 18.22 *1* rectus femoris tendon; *2* vastus lateralis; *3* vastus intermedius; *4* vastus medialis; *5* sartorius; *6* biceps femoris (*short head*); *7* adductor magnus; *8* gracilis; *9* biceps femoris (*long head*); *10* semitendinosus; *11* semimembranosus; *12* ischiatic nerve

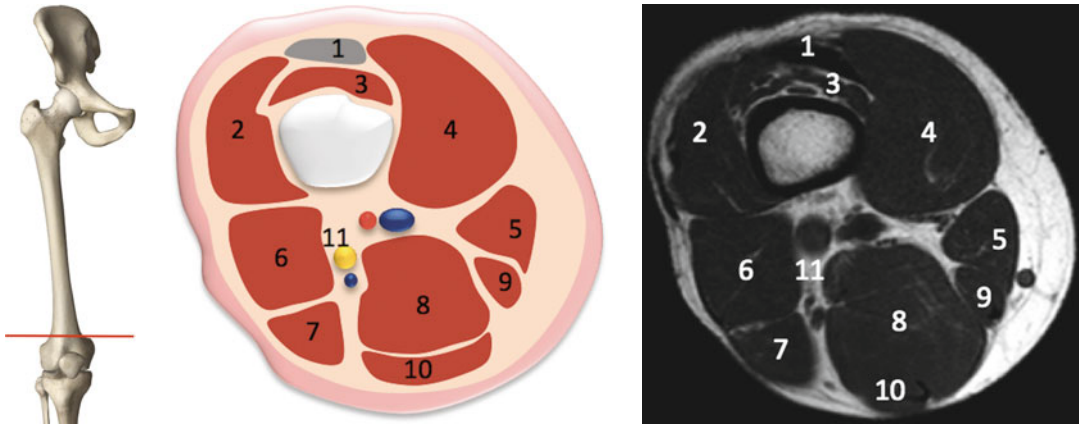

Fig. 18.23 *1* rectus femoris tendon; *2* vastus lateralis; *3* vastus intermedius; *4* vastus medialis; *5* sartorius; *6* biceps femoris (*short head*); *7* biceps femoris (*long head*); *8* semimembranosus; *9* gracilis; *10* semitendinosus; *11* ischiatic nerve

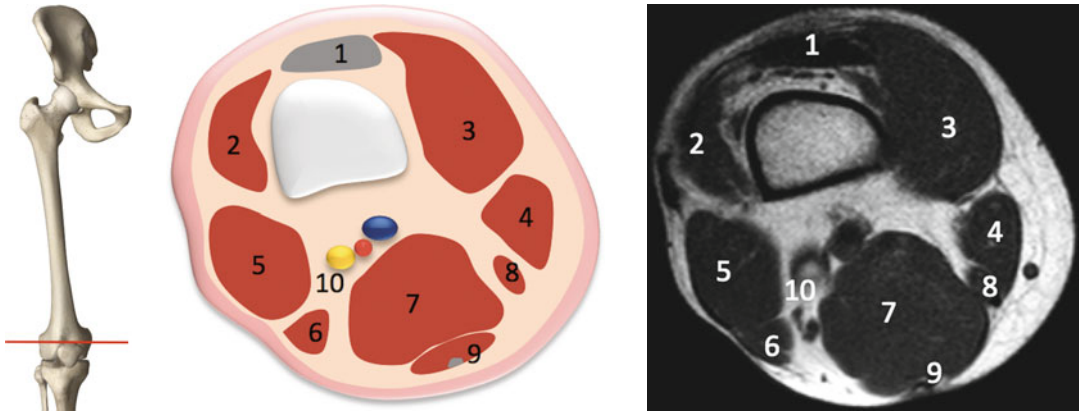

Fig. 18.24 *1* rectus femoris tendon; *2* vastus lateralis; *3* vastus medialis; *4* sartorius; *5* biceps femoris (*short head*); *6* biceps femoris (*long head*); *7* semimembranosus; *8* gracilis; *9* semitendinosus myotendinous junction; *10* ischiatic nerve

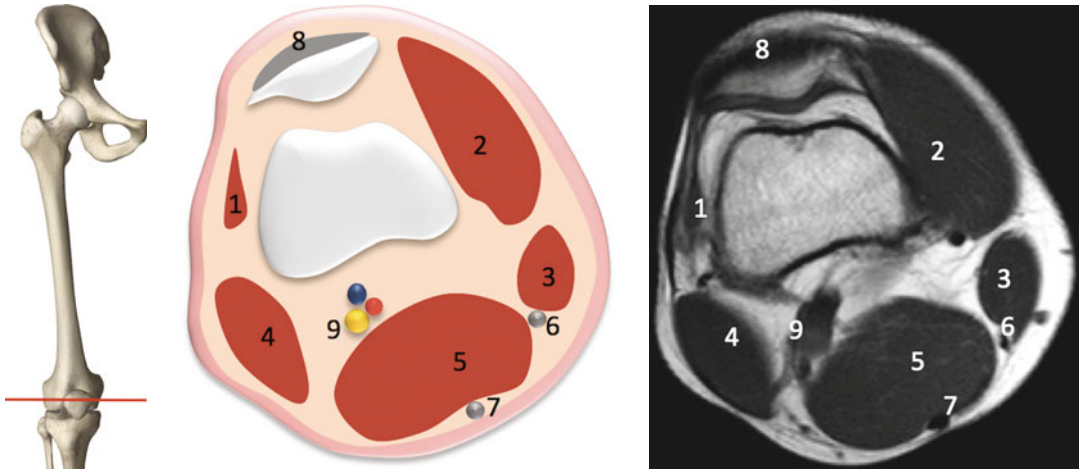

Fig. 18.25 *1* vastus lateralis; *2* vastus medialis; *3* sartorius; *4* biceps femoris; *5* semimembranosus; *6* gracilis tendon; *7* semitendinosus tendon; *8* quadriceps tendon; *9* ischiatic nerve

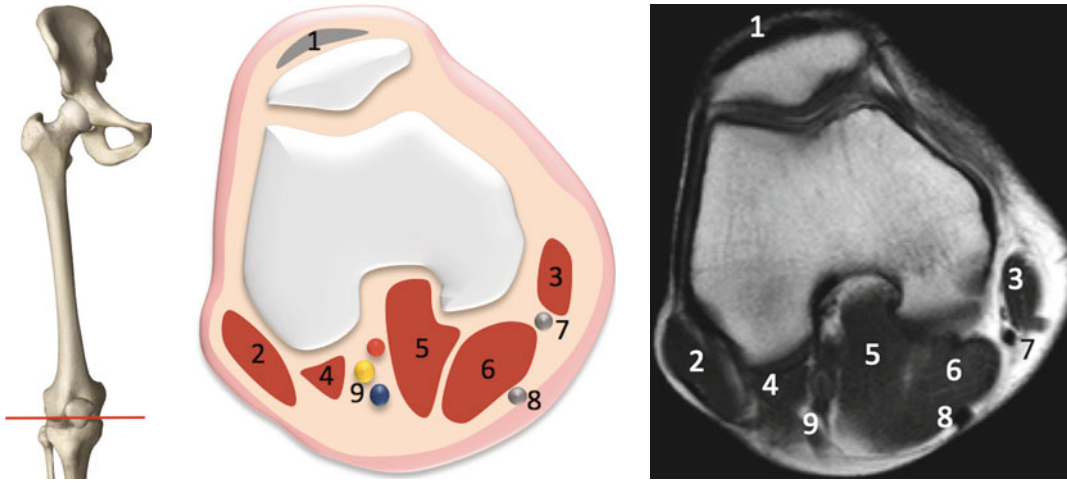

Fig. 18.26 *1* rotuleus tendon; *2* biceps femoris; *3* sartorius; *4* gastrocnemius (*lateral head*); *5* gastrocnemius (*medial head*); *6* semimembranosus; *7* gracilis tendon; *8* semitendinosus tendon; *9* ischiatic nerve

Leg Compartments

19

Alessandro Muda and Amedeo Baldari

In this chapter we provide a series of images demonstrating cross-sectional anatomy of leg compartments at different cranio-caudal levels. Every set of images includes a skeleton model that serves as an orientation aid (a), pertinent anatomical scheme (b), and corresponding SE T1w axial MRI scan (c).

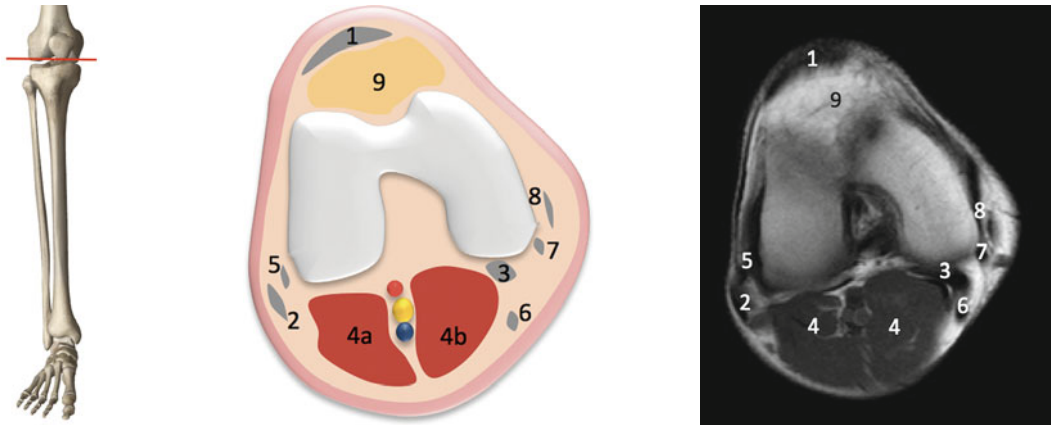

Fig. 19.1 *1* patellar ligament; *2* biceps femoris tendon; *3* semimembranosus tendon; *4* gastrocnemius lateralis (*a*) and medialis (*b*); *5* popliteus tendon; *6* semitendinosus tendon; *7* gracilis tendon; *8* sartorius tendon; *9* Hoffa's fat pad

A. Muda (✉)
Dipartimento di Radiologia,
IRCCS Ospedale San Martino IST, Genoa, Italy
e-mail: alessandro.muda@tiscali.it

A. Baldari
Medical Division, UC Sampdoria Spa, Genoa, Italy

E. Silvestri et al., *Ultrasound Anatomy of Lower Limb Muscles: A Practical Guide*,
DOI 10.1007/978-3-319-09480-9_19, © Springer International Publishing Switzerland 2015

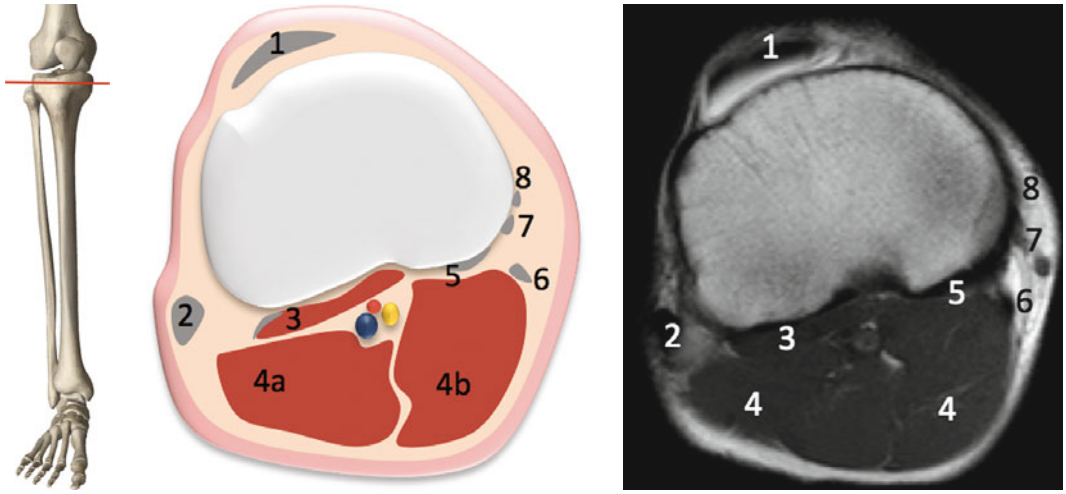

Fig. 19.2 *1* patellar ligament; *2* biceps femoris tendon; *3* popliteus; *4* gastrocnemius lateralis (*a*) and medialis (*b*); *5* semimembranosus tendon; *6* semitendinosus tendon; *7* gracilis tendon; *8* sartorius tendon

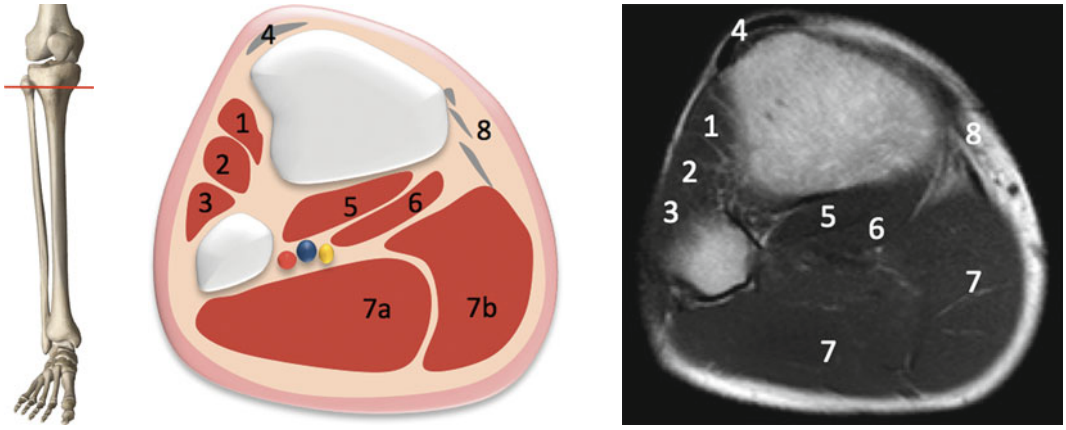

Fig. 19.3 *1* tibialis anterior; *2* extensor hallucis; *3* extensor digitorum; *4* patellar ligament; *5* popliteus; *6* soleus; *7* gastrocnemius lateralis (*a*) and medialis (*b*); *8* pes anserinum

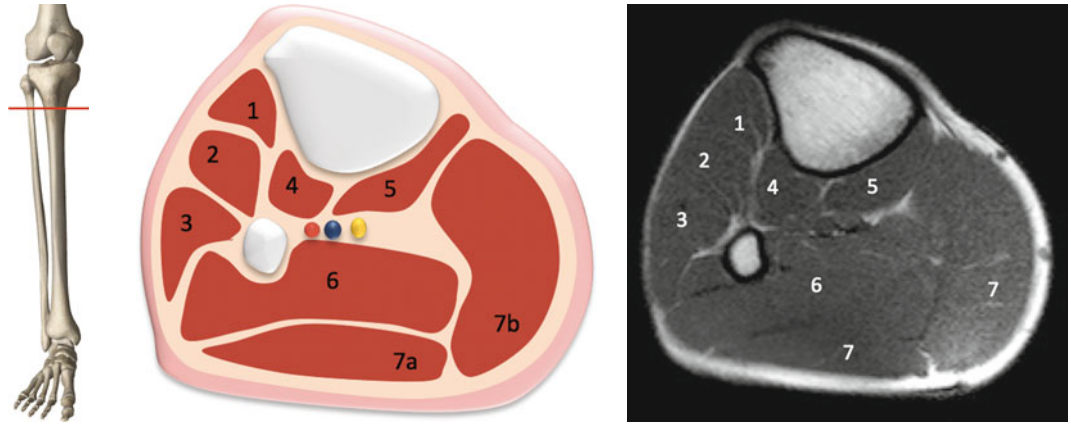

Fig. 19.4 *1* tibialis anterior; *2* extensor digitorum and hallucis; *3* peroneus longus; *4* tibialis posterior; *5* popliteus; *6* soleus; *7* gastrocnemius lateralis (*a*) and medialis (*b*)

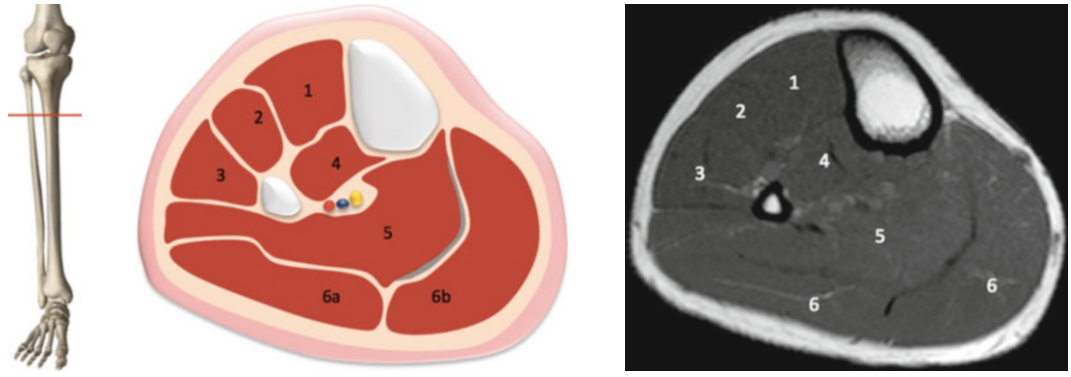

Fig. 19.5 *1* tibialis anterior; *2* extensor digitorum and hallucis; *3* peroneus longus; *4* tibialis posterior; *5* soleus; *6* gastrocnemius lateralis (*a*) and medialis (*b*)

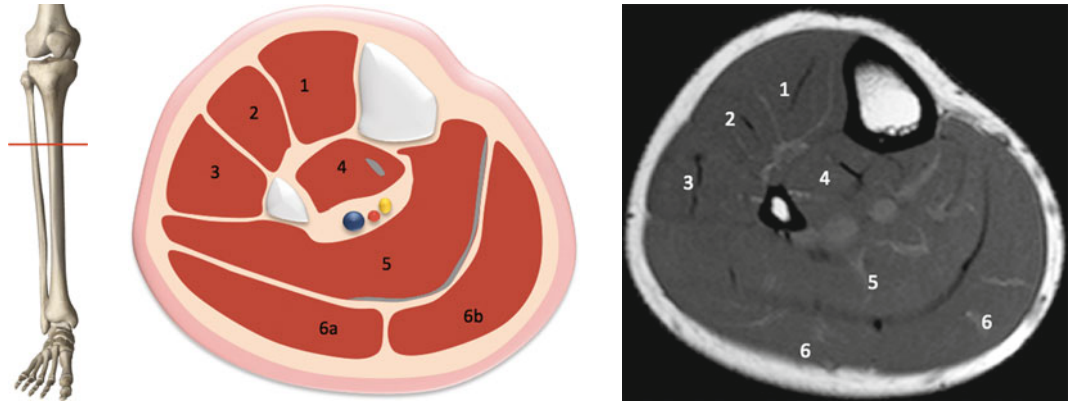

Fig. 19.6 *1* tibialis anterior; *2* extensor digitorum and hallucis; *3* peroneus longus; *4* tibialis posterior; *5* soleus; *6* gastrocnemius lateralis (*a*) and medialis (*b*)

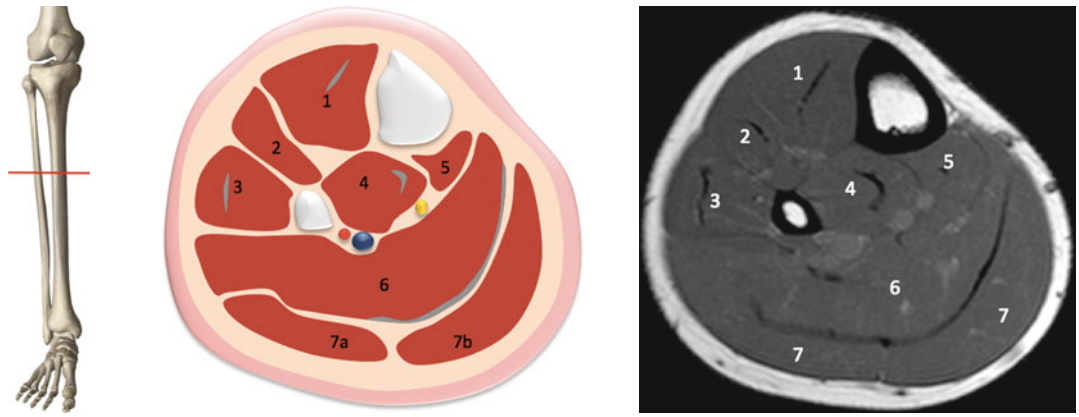

Fig. 19.7 *1* tibialis anterior; *2* extensor digitorum and hallucis; *3* peroneus longus and brevis; *4* tibialis posterior; *5* flexor digitorum longus; *6* soleus; *7* gastrocnemius lateralis (*a*) and medialis (*b*)

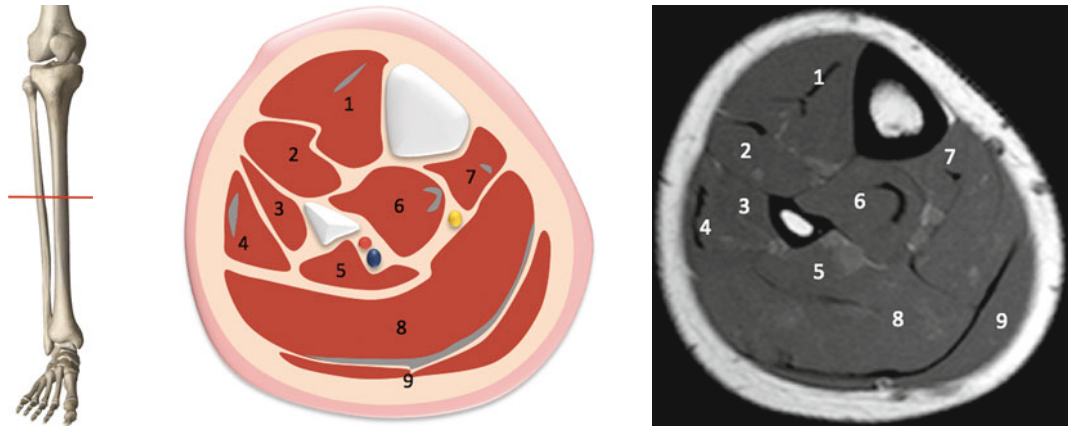

Fig. 19.8 *1* tibialis anterior; *2* extensor hallucis; *3* peroneus longus; *4* peroneus brevis; *6* flexor digitorum longus; *7* tibialis posterior; *8* soleus; *9* gastrocnemius

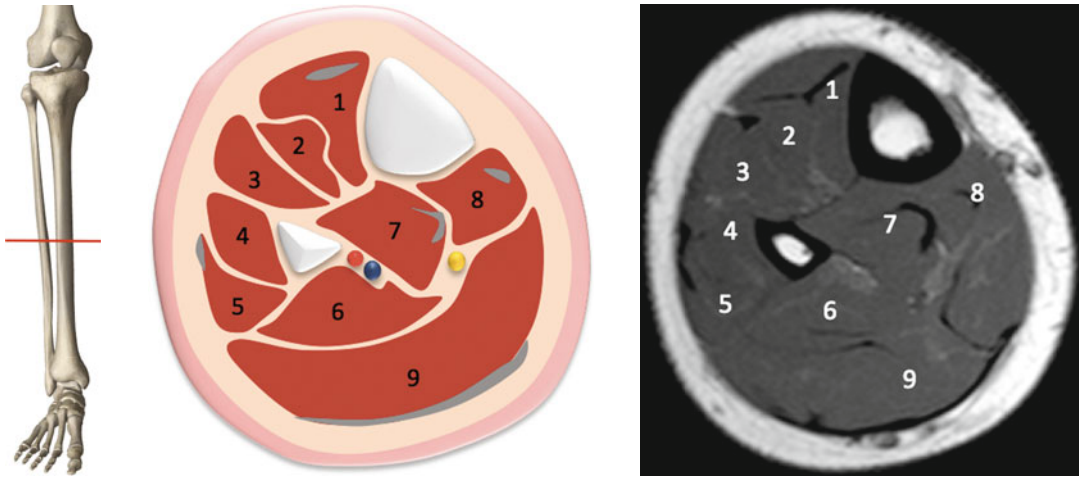

Fig. 19.9 *1* tibialis anterior; *2* extensor hallucis; *3* extensor digitorum longus; *4* peroneus longus; *5* peroneus brevis; *6* flexor hallucis longus; *7* tibialis posterior; *8* flexor digitorum longus; *9* soleus

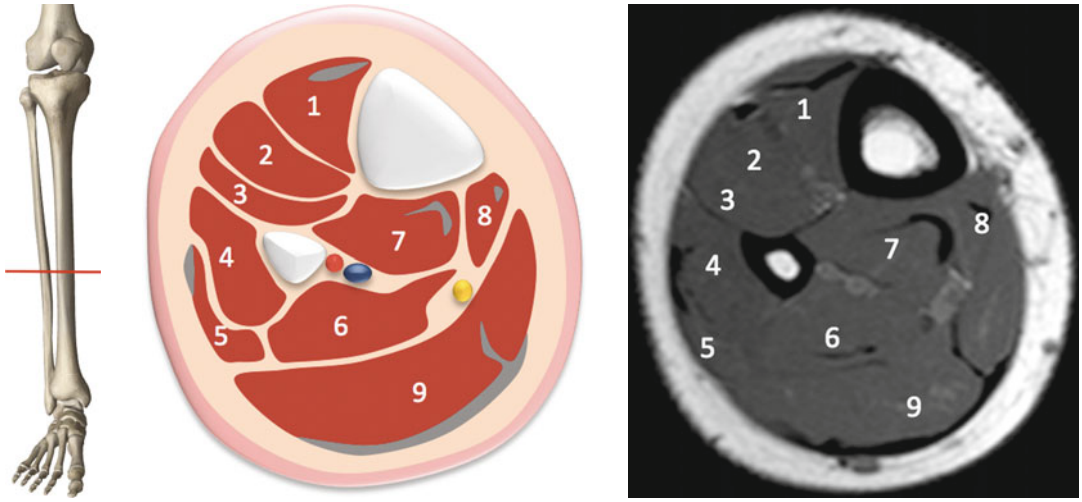

Fig. 19.10 *1* tibialis anterior; *2* extensor hallucis; *3* extensor digitorum longus; *4* peroneus longus; *5* peroneus brevis; *6* flexor hallucis longus; *7* tibialis posterior; *8* flexor digitorum longus; *9* soleus

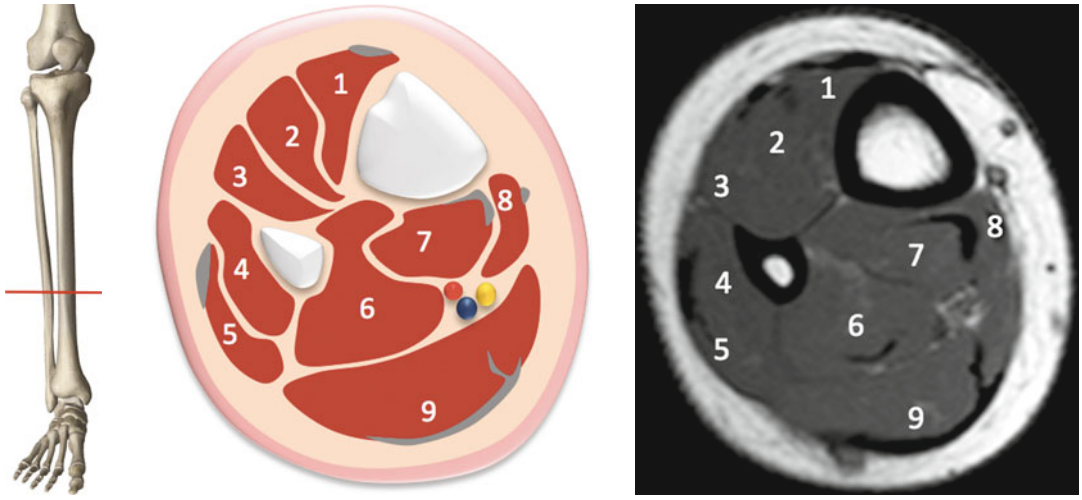

Fig. 19.11 *1* tibialis anterior; *2* extensor hallucis; *3* extensor digitorum longus; *4* peroneus longus; *5* peroneus brevis; *6* flexor hallucis longus; *7* tibialis posterior; *8* flexor digitorum longus; *9* soleus

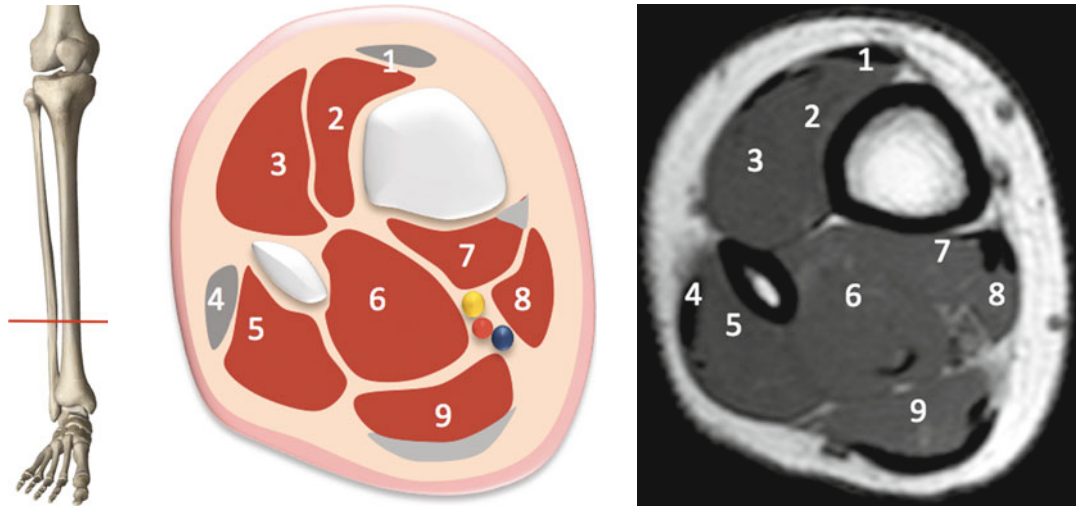

Fig. 19.12 *1* tibialis anterior tendon; *2* extensor hallucis; *3* extensor digitorum longus; *4* peroneus longus tendon; *5* peroneus brevis; *6* flexor hallucis longus; *7* tibialis posterior; *8* flexor digitorum longus; *9* Achilles tendon and soleus

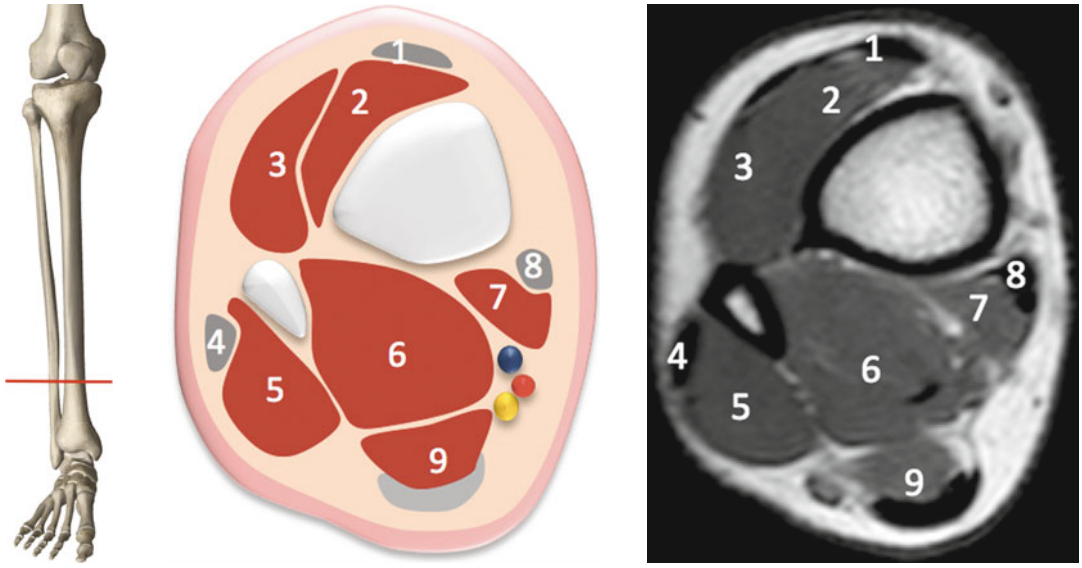

Fig. 19.13 *1* tibialis anterior tendon; *2* extensor hallucis; *3* extensor digitorum longus; *4* peroneus longus tendon; *5* peroneus brevis; *6* flexor hallucis longus; *7* flexor digitorum longus; *8* tibialis posterior tendon; *9* Achilles tendon and soleus

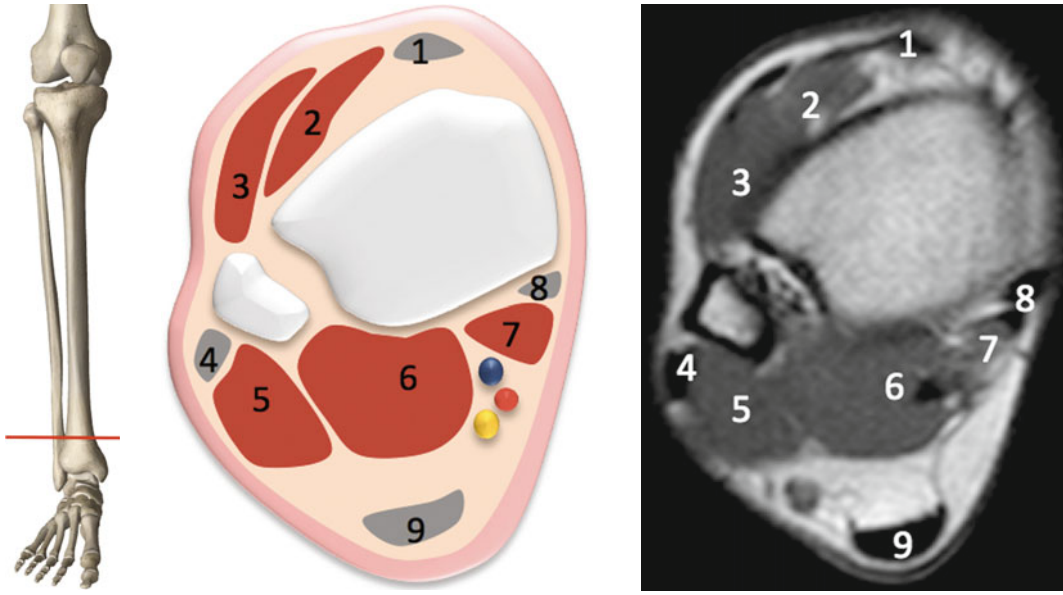

Fig. 19.14 *1* tibialis anterior tendon; *2* extensor hallucis; *3* extensor digitorum longus; *4* peroneus longus tendon; *5* peroneus brevis; *6* flexor hallucis longus; *7* flexor digitorum longus; *8* tibialis posterior tendon; *9* Achilles tendon